Mucosal T cell defence in large animal models of infection



Matthew Edmans

Linacre college, Oxford

Thesis submitted for the degree of

Doctor of Philosophy in clinical medicine

University of Oxford Trinity term 2020

Supervisors:

Dr Elma Tchilian, PhD

Professor Paul Klenerman, MRCP, FRCP, DPhil

Dr Chris Netherton

Mucosal T cell defence in large animal models of infection

Matthew Edmans Linacre college

Submitted for DPhil trinity term 2020

Abstract

The study of cellular immune responses in the mucosa has proven difficult within humans. Capturing the respiratory mucosal immune response is challenging without invasive sampling methods; therefore, research in this area has leant heavily on the use of animal models. Livestock species are naturally infected by a range of diseases which are also major human public health concerns, including influenza in pigs, tuberculosis in cattle and lung disease in sheep. Influenza virus is estimated to cause 1 billion human infections annually with approximately 3- 5 million cases of severe illness and 300-500,000 deaths per year. Pigs make an ideal model for the study of influenza infection as they have comparable size and respiratory anatomy to humans and influenza strains such as the 2009 pandemic H1N1 are endemic in both humans and pigs. The T cell response to influenza has come under renewed investigation in recent years with the potential to target cross reactive T cell epitopes to multiple influenza strains. Additionally, innate like T cells, such as mucosal associated invariant T (MAIT) cells, a prominent T cell population in humans, are being increasingly studied for their role in influenza infection. Here, the kinetic of virus infection and T cell response to H1N1pdm09 influenza is investigated in inbred Babraham pigs and compared to commercial outbred animals. High level of nasal virus shedding continued up to day 4-5 post infection followed by a steep decline and clearance of virus by day 9. The T cell response developed from day 5-6 post infection reaching a peak at 9-14 days. BAL contained the most highly activated CD8 and CD4 T cells actively producing pro-inflammatory cytokines, which likely contribute to the elimination of the virus. The weak response in peripheral blood T cells did not reflect the robust

local immune responses. The immune responses in the Babraham pig were comparable to outbred pigs, validating the Babraham pig as a model for pig immunology. Furthermore, new H1N1pdm09 influenza immunodominant T cell epitopes are described in the Babraham pig which will aid in future studies involving this animal model. Putative MAIT cells have been previously identified in pigs, cattle and sheep by qPCR-based methods though no MAIT cells have been phenotypically described in these species. In this study the MAIT cell population in pigs, cattle and sheep is determined using a variety of methods including functional activation assays and phenotypic assessment utilising species specific and xenogenic tetramers. In pigs the MAIT cell population was at the limits of detection. The absence of MAIT cells identified in pigs precluded the study of MAIT cells in the context of the influenza challenge studies. However, MAIT cells were identified in sheep and cattle and a detailed characterization was therefore performed in cattle. MAIT cells in cattle were highly phenotypically and functionally comparable to MAIT cells described in humans and mice and are activated by disease causing bacteria *in vitro* and *in vivo*. These data and techniques expand the understanding of the T cell response to influenza in pigs, support the use of the Babraham pig as a model for influenza research and enables cattle and sheep to be included as useful models for the study of MAIT cells in these species.

Acknowledgement

I have been privileged to have worked with some exceptional scientists during this DPhil who have been generous with their time and knowledge as well as being friendly, welcoming people.

Firstly, I would like to thank my supervisor's Dr Elma Tchilian and Prof. Paul Klenerman, for their considered guidance and the opportunities they have presented me over the last four years. Also, to my original co-supervisor's Dr Sophie Morgan and Dr Chris Willberg, who both left before the completion of this thesis but generously continued to contribute to my supervision with both scientific input and encouragement. I would also like to thank Dr Chris Netherton for stepping in to be my co-supervisor at Pirbright in my last year and Dr Philipp Hackstein for your advice and helping me pull this thesis together.

Thanks must also go to the incredible collaborators whose input has developed me as a researcher and enabled this thesis. Thanks to Dr Sidonia Eckle (Peter Doherty Institute, Melbourne) for supplying the MR1 tetramer and the careful guidance (from the other side of the world) in the intricacies of their use. Thanks to Dr Lindert Benedictus (University of Utrecht) for donating cattle antibodies, helping during the long week at the Roslin institute collecting cattle samples, and sharing in my excitement at identifying MAIT cells in cattle. Thanks to Professor Mick Baily and colleagues at the University of Bristol for hosting me while we collected samples for the influenza time course study, I miss our discussions at the Langford Inn. Thanks also to Dr Timothy Connelly and his team at the Roslin Institute for hosting me and organising the TCR sequencing of cattle MAIT cells.

Thanks to all the other students and staff at both the Pirbright Institute and the Peter Medawar Building for your camaraderie and advice. Particularly Adam McNee during the long weeks spent at the University of Bristol collecting samples and Veronica Martini who is always so

quick to offer help. Also, Hema Mehta and Joachim Hagel whom I greatly enjoyed talking through ideas with. A special thanks to Samuel Connell and Luke Johnson who offered me a ‘safe house’ when I was working at Pirbright and whose friendship made the last four years great fun, even when experiments failed!

I would also like to thank Linacre College and the Brill Church of England educational endowment fund for financial support.

Most importantly, I would like to thank my incredible partner Rhiannon, for supporting me through the last four years and my son Otis, you are both a constant reminder of what is important in life. Finally, thanks to my parents, who have always been so supportive, I know that my father would have been very proud if he were here today.

Contents

Abstract 1

Acknowledgement 3

Thesis Contributions 11

Abbreviations 12

Chapter 1 Introduction 14

1.1 The immune system 14

1.1.1 The innate immune system 14

1.1.2 The adaptive immune system 16

1.1.3 T cells 16

1.1.4 T cell development 17

1.1.5 CD8 T cells 17

1.1.6 CD4 T cells 18

1.1.7 Large animal models of infectious disease 19

1.2 Influenza 19

1.2.1 Innate response to Influenza 21

1.2.2 Innate cellular responses to Influenza 23

1.2.3 Conventional T cell immunity to Influenza 26

1.2.4 Pig as a model for Influenza 27

1.3 Innate like T cells that bridge the innate and the adaptive immune system 29

1.3.1 Natural killer T (NKT) cells 30

1.3.2 γδ T cells 31

1.4 MAIT cells 32
1.4.1 discovery of a novel innate-like T cell 32
1.4.2 MAIT cell restriction through MR1 33
1.4.3 MAIT cell phenotype 34
1.4.4 MAIT cell tissue distribution 36
1.4.5 MAIT cells in bacterial infection 37
1.4.6 MAIT cells in viral infection 38
1.4.7 Emerging functions of MAIT cells 40
1.4.8 Conservation of MAIT cells between species 41
1.5 Aims of this thesis 43
Chapter 2 Material and methods 44
2.1 Medias and buffers 44
2.2 Compounds used for cellular experiments 44
2.2.1 Mitogenic stimulation 44
2.2.2 Peptides 45
2.2.3 MAIT cell stimulation 45
2.3 Animal experiments 45
2.4 Tissue sampling and processing 45
2.4.1 PBMC 45
2.4.2 tracheobronchial lymph nodes (TBLN) 46
2.4.3 Lung and broncho alveola lavage (BAL) cells 46

2.4.4 Spleen and Ileum....46
2.4.5 Liver....46
2.4.6 Milk....47
2.4.7 All tissues....47
2.5 Bacterial and Virus growth....47
2.5.1 Bacterial growth....47
2.5.2 Virus growth....48
2.5.3 Viral titration Plaque assay....48
2.6 Flow cytometry....48
2.6.1 MR1 tetramer staining....48
2.6.2 Pig SLA tetramer staining....49
2.6.3 Surface staining....49
2.6.4 Intracellular cytokine staining....49
2.6.5 Transcription factor stains....50
2.6.6 Data acquisition and analysis....52
2.7 ELISpot....52
2.8 Cell sorting and depletion....53
2.9 Statistical analysis....53
Chapter 3 Kinetics, magnitude and specificity of conventional T cell responses during H1N1pfm09 infection in outbred and inbred pigs.....54
3.1 Aims and rationale....54
3.2 Chapter specific methods....55

3.3 influenza H1N1pdm09 challenge 55

3.3.1 In vitro influenza stimulation.....56

3.3.2 In vitro Peptide stimulation.....56

3.4 Influenza time course: experimental design viral load and cellular dynamics. 56

3.5 CD8 T cell responses in different tissues during influenza infection in outbred and inbred Babraham pigs. 65

3.6 CD4 response in different tissues during influenza infection in outbred and inbred Babraham pigs. 72

3.7 T cell responses in the BAL of in-contact pigs.....76

3.8 Specificity of influenza response in the inbred Babraham pig 78

3.9 Peptide pool break-down to minimum responding peptides.....85

3.10 Determining which cell type responds to single peptides.....87

3.11 Peptide break-down to minimum epitope.....89

3.12 Further peptide break-down using influenza re-infected animals.....91

3.13 ICS to determine which cell type responds to minimal epitopes.....94

3.14 Discussion.....97

3.15 Summary.....99

Chapter 4 Identification of MAIT cells in different species.....101

4.1 Aims and rationale. 101

4.2 Chapter specific methods.....102

4.2.1 Generation of Sus scrofa and Bos taurus MR1 tetramers.....102

4.2.2 qPCR.....104

4.3 Comparison of MR1 α1- and α2-domains between species. 105

4.4 Generation of pig and cattle MR1 tetramers 110

4.5 Species-specific and mismatched cross-reactive tetramers identify MAIT cells in multiple species 114

4.6 In vitro stimulation with MAIT cell ligands 125

4.7 Further assessment of the MAIT cell population in pigs 127

4.8 Discussion 134

4.9 Summary 135

Chapter 5 Phenotype and response to bacterial infections of cattle MAIT cells 137

5.1 Aims and rationale 137

5.2 Chapter specific methods 138

5.2.1 TCR sequencing 138

5.3 5-OP-RU MR1 tetramer-positive T cells are an expanded population in cattle peripheral blood and express the canonical TRAV1-TRAJ33 MAIT TCR. 141

5.4 Cattle 5-OP-RU tetramer + MAIT cells express the canonical TRAV1-TRAJ33 MAIT TCR and transcription factors associated with MAIT cells 143

5.5 The phenotype of cattle MAIT cells and comparisons of MAIT cells between tissues 149

5.6 Activation of MAIT cells in cattle 159

5.6.1 5-OP-RU and cytokine stimulation of cattle MAIT cells 159

5.6.2 Activation of cattle MAIT cells by bacteria 166

5.7 *In vivo* response of MAIT cells to pathogens in cattle 171

5.8 Discussion 176

Chapter 6 General discussion and future recommendations 179

6.1 Key findings of this thesis 179

6.1.1 Chapter 3. Kinetics, magnitude and specificity of conventional T cell responses during H1N1pfm09 infection in outbred and inbred pigs. 179

6.1.2 Chapter 4 and 5. Identification of MAIT cells in multiple species and characterisation of MAIT cells in cattle 183

6.2 Summary of thesis 188

References 189

Chapter 7 Appendices 207

7.1 Peptides for Epitope identification 207

7.2 TCR sequencing TRAV chain rearrangements 5-OP-RU MR1 tetramer+ T cells 216

Thesis Contributions

All work in this Thesis is my own except for these contributions

Chapter 3

Adam Mcnee (Pirbright institute)

helped with sample processing and plaque assays

Basu Paudyal (Pirbright institute)

Performed some ELISPOT's presented section 3.8 and 3.12

Chapter 4

Sidonia Eckle (Peter Doherty institute Melbourne)

Produced the Tetramer and performed the tetramer characterisation presented in section 4.4

Produced the graphics presented in Figure 4.2 Figure 4.3

Chapter 5

Timothy Connelly, Siddharth Jayaraman, Christina Vrettou (Roslin institute Edinburgh)

Performed the TCR sequencing presented in section 5.4

Lindert Benedictus (Roslin Institute Edinburgh)

Performed some of the phenotyping experiments presented in section 5.5 and generated the *in vivo* data presented in section 5.7

Abbreviations

5-OP-RU	5-(2-oxopropylideneamino)-6-D-ribitylaminouracil
6-FP	6-formylpterin
Ac-6-FP	Acetyl-6-formylpterin
APC	Antigen presenting cell
BAL	Bronchoalveolar lavage
BCG	Bacillus Calmette-Guérin
BM	Babraham
CCR	chemokine receptor
CD	Cluster of differentiation (followed by numbers)
cDNA	complementary deoxyribonucleic acid (DNA)
CFU	colony forming units
ConA	Concanavalin A
CTL	Cytotoxic T lymphocyte
DN	Double negative
DNA	deoxyribonucleic acid
DP	Double positive
DPI	Days post infection
EC50	Effective concentration 50
ELISA	Enzyme-linked immunosorbent assay
ELISpot	enzyme-linked immunospot
EOMES	Eomesodermin 3
FACS	Fluorescence-activated cell sorting
FCS	Foetal calf serum
FMO	Fluorescence minus one
FSC	Forward scatter
GAPDH	Glyceraldehyde 3-phosphate Dehydrogenase
GMFI	Geometric mean fluorescence intensity
HA	Hemagglutinin
HAI	Hemagglutinin inhibition
HLA	Human leucocyte antigen
IAV	Influenza A virus
ICS	Intracellular cytokine staining
IFN	Interferon
IL	Interleukin (followed by number)
iNKT	Invariant natural killer T
IQR	interquartile range
LD	Live/ Dead
M1	Matrix 1
mAb	Monoclonal antibody
MACS	Magnetic associated cellular sorting
MAD	mucosal atomisation device
MAIT	Mucosal associated invariant T (cells)

MDCK	Madin-Darby Canine Kidney
MFI	Median flourescent intensity
MHC	Major histocompatibility complex
MLN	Mesenteric lymph node
MOI	Multiplicity of infection
MR1	Major histocompatibility complex, class I-related protein
M.tb	Mycobacterium tuberculosis
NA	Neuraminidase
NK	Natural killer
NP	Nuclear protein
OB	Outbred
MAMP	Microbial associated molecular pattern
PBMC	Peripheral blood mononuclear cell
PBS	Phosphate-buffered saline
PCR	polymerase chain reaction
PLZF	Promyelocytic leukaemia zinc finger protein 5
PMA	phorbol myristate acetate
PRR	Pattern recognition receptor
RNA	Ribonucleic acid
RORγt	RAR-related orphan receptor gamma
RPM	Revolutions per minute
RT	Reverse transcript
SCC	Single colour control
SD	standard deviation
SEM	standard error of the mean
SFC	Spot forming cell
SLA	swine leucocyte antigen
SNP	Single-nucleotide polymorphism
SSC	side scatter
TB	Tuberculosis
TBLN	tracheobronchial lymph nodes
Tcm	Central memory T cells
TCR	T-cell receptor
Tem	Effector memory T cells
TF	Transcription factor
TFH	T follicuar helper
Th	T helper (followed by number)
TLR	Toll-like receptor
TNF	Tumor necrosis factor
TRA/BV	T cell receptor alpha/beta variable genes
TRAC	T cell receptor constant genes
TRAJ	T cell receptor alpha joining genes

Chapter 1 Introduction

1.1 The immune system

The immune system is a complex arrangement of cellular responses which must identify foreign from self as well as dangerous changes within the organism. This system exists in a delicate balance of destruction of invading pathogens and defective self, whilst preserving healthy cells and non-invasive commensal flora.

The immune system can be broadly divided into two main parts, known as the innate and the adaptive arms. The innate immune system develops immediate though non-specific responses to invading pathogens and may be considered as the first line of defence for the host organism. In contrast, the adaptive immune system is more precise, targeting specific antigens of invading organisms and has the capacity to develop immunologic "memory", which can grant long term protection from re-encountering the same organism. However, compared to the innate, the adaptive immune response is delayed, taking days to become functional (Bachmann et al., 1996).

1.1.1 The innate immune system

The innate immune system developed early during evolution and is found in both invertebrates and vertebrates (Rinkevich, 1999). The innate response includes the physical barriers like the mucosa and cilia, which block and drive potentially hazardous infections away from the mucosal sites. The mucosa also represents an environment inhospitable to microorganisms. For example, members of the collectin family, surfactant protein A and D, show antiviral activity by opsonisation, the formation of viral aggregates and enhancement of phagocytosis. Interestingly, this response is more efficient in pigs than other species (van Eijk et al., 2003). Should these barriers be breached, innate mechanisms can respond rapidly to a variety of

signals which set off a complex chain of events which enables both intracellular immune response and extracellular help from dedicated innate immune cells such as Dendritic cells, Macrophages, NK cells and neutrophils (reviewed in more detail below in the context of influenza infection) as well as the induction of the adaptive immune response.

Pattern recognition receptors (PRR) are innate sensing mechanisms which are ancient in origin. The first identification of PRR was in drosophila (Lemaitre et al., 1996), since then many examples of PRR have been identified spanning the clades of land plants (Saijo et al., 2018) to Mammalia (reviewed in (Suresh and Mosser, 2013). In mammals, PRR are expressed on and in epithelial cells as well as innate immune cells such as dendritic cells, natural killer cells, and macrophages. PRR's recognise non-self-structures known as microbial-associated molecular patterns (MAMPs), including oligosaccharides, peptidoglycans and lipopolysaccharides which can be found in bacterial cell walls, unmethylated CpG DNA and RNA structures. PRRs include toll-like receptors (TLR), RIG-1 like receptors (RLR), NOD-like receptors, and DNA receptors (Medzhitov and Janeway, 1997, Ozinsky et al., 2000).

When triggered by MAMPs, PRR can induce a complex range of downstream signalling cascades. A prominent example is the induction of interferon regulatory factors (IRFs) that activate type 1 interferons, such as IFN-α and IFN-β. Both of these cytokines signal through the type 1 IFN receptor and induce the expression of hundreds of interferon-stimulated genes (ISGs). The functions of ISGs include the inhibition of protein synthesis in cells limiting viral production, upregulation of soluble pro-inflammatory signals, leading to, among other things, stimulation of dendritic cells, enhancing their ability to activate CD4 and CD8 T cells, thus linking the innate and adaptive arms of the immune system (Kreijtz et al., 2011, Killip et al., 2015).

1.1.2 The adaptive immune system

The adaptive immune system is more recent in origin than the innate immune system and can only be found only in vertebrates (Rinkevich, 1999). The cells of the adaptive immune system can be broken into two lineages, B and T cell. These cells utilise somatically rearranged, antigen-specific, receptors which recognize a range of pathogen epitopes allowing for a highly specific response. These responses take time to develop and require presentation of antigen and co-stimulatory molecules generated by the innate immune response. However, the responses can help in the elimination of the pathogen and develop into a long-lasting, protective memory (Bachmann et al., 1996).

1.1.3 T cells

T cells are one of the two main lineages of the adaptive immune systems cellular components. In order to participate in an immune response, naïve T cells must recognize their cognate antigen presented in the context of major histocompatibility complex (MHC) class I or II and must receive appropriate co-stimulatory signals provided by professional antigen-presenting cells. Antigen recognition is mediated by the T cell receptors (TCR) with each TCR being specific to a constrained antigen. There are two types of TCR based upon the type of glycoprotein chain: αβ or γδ. In general, the αβ TCR dominates, though there are interspecies differences in the relative frequency of αβ and γδ T cells, with pigs and ruminants having a notably higher proportion of γδ expressing T cells (Takamatsu et al., 2006). T cells can be broadly categorised into three main subgroups, based on their function: destroying aberrant/ infected target cells (cytotoxic T cells), immunological help (Helper T cells) and modulation/ downregulation of the immune response (regulatory T cells).

1.1.4 T cell development

Precursor thymocytes develop into T cells in the thymus. During development, thymocytes express various coreceptors, proliferate, and the genes within the TCR amino-terminal region rearrange to increase TCR diversity. For αβ TCR T cells, the α chain variable (V) and junction (J) and the β chain V J and diversity (D) domains recombine. The γδ TCR rearranges in the same way as for αβ, though there is a lower number of V gene segment in both the γ and δ chains. However, much like the αβ TCR, the range combinatorial possibilities for γδ TCR is huge (Davis and Bjorkman, 1988) due to the ability of the δ gene to rearrange D domains with greater diversity compared to αβ T cells (Born et al., 2013).

The maturation process of thymocyte to T lymphocyte is tightly regulated by a system of positive and negative selection. The final rearrangement of the TCR must not bind MHC presented self-antigen strongly though must be able to bind with some affinity. If the cell does not bind to the antigen presented on MHC within the correct range, the cell will undergo apoptosis. Approximately 98% of T cells will undergo apoptosis in the thymus and not become part of the circulating T cell population. The T cells that survive this process will join the pool of naïve T cells and express a specific TCR with either a CD4 or a CD8 coreceptor (Taniuchi, 2018, Ellmeier et al., 1999).

1.1.5 CD8 T cells

Naive T cells that express the CD8 coreceptor will mainly develop into cytotoxic T cells with the capability of killing other cells. CD8 T cells express a T cell receptor (TCR) which recognise antigens presented by MHC I. MHC I is present in all nucleated cells and generally presents peptides derived from intracellular pathogens, notably viruses. Dendritic cells have the unique ability to uptake exogenous antigens and present it to CD8 cell in the lymph nodes

priming the CD8 response in a process called cross-priming (Gutiérrez-Martínez et al., 2015). Primed CD8 T cells are capable of identifying cells infected with intracellular pathogens via MHC I and initiate the killing of the infected cell (Hewitt, 2003). CD8 T cell killing is mediated through the release of the cytotoxic effector molecule perforin in concert with granzymes as well as FAS ligand-induced caspase cascade which induces apoptosis. This activation is tightly regulated to prevent inappropriate activation and requires secondary signals in addition to TCR ligation. In addition to cellular killing, once activated CD8 T cells can produce pro-inflammatory cytokines such as IFN-γ and TNF which can further activate the immune response (Harty et al., 2000, Wong and Pamer, 2003). CD8 T cells are also capable of producing IL-10, a cytokine which dampens the immune response of both innate and adaptive immune cells and prevents damage that may be induced by pro-inflammatory cytokines (Sun et al., 2009). A subset of CD8 T cells termed Tc17 are also capable of producing IL-17 which can induce a pro-inflammatory response and act upstream of neutrophil recruitment (Hamada et al., 2009)

1.1.6 CD4 T cells

CD4 T cells express the CD4 TCR coreceptor, which binds to the MHC II (Doyle and Strominger, 1987). MHC II presents exogenous antigen derived by extracellular vesicles and commonly is expressed by phagocytic innate immune cells such as dendritic cells or macrophages. CD4 expressing T cells can be further broken down into subtypes with different effector functions. The subsets of CD4 expressing T cells include T helper (T_H) 1, T_H2, T_H17, regulatory T cells and T follicular helper (T_{FH}) cells.

T_H1 are distinguished by the secretion of pro-inflammatory cytokines such as IFN-γ and TNF, which can help control bacterial and viral infections. T_H2 cells express cytokines such as IL-4,

IL-5, IL-10, IL-13 and help orchestrate the humoral response by activating plasma cells. Furthermore, T_H2 effector cytokines are considered important in the control of human parasites (Turner et al., 2003), though their response is also often associated with allergy (Maggi, 1998). T_H17 CD4 expressing cells generate IL-17 (Miossec et al., 2009). T_{FH} cells aid B cells in the production of high-affinity antibodies. Regulatory T cells express the transcription factor FOXP3 and suppress the activation of other T cells, dampening down the immune response upon resolution of infection to prevent autoimmunity (Wan and Flavell, 2009).

1.1.7 Large animal models of infectious disease

The study of cellular immune responses in the mucosa has proven difficult within humans. Capturing the immune response in action is challenging within mucosal tissues without invasive sampling methods; therefore, research in this area has leant heavily on the use of large animal models (Rajao and Vincent, 2015). Pigs, cattle and sheep are economically important livestock species that also represent relevant models for a variety of human infections, including TB in cattle (Van Rhijn et al., 2008, Waters et al., 2011), Influenza in pigs (Holzer et al., 2019a, Rajao and Vincent, 2015) and respiratory diseases, such as asthma and bacterial pneumonia in sheep (Guillamón Mde and Clau, 2010). Importantly, as a species which are naturally infected by these pathogens any advancements of immunology in these species will also have implications for veterinary medicine.

1.2 Influenza

Influenza virus infection is a significant cause of morbidity and mortality in humans, pigs and birds. It is a respiratory disease which, in humans, is estimated to cause 1 billion infections annually with approximately 3- 5 million cases of severe illness and 300-500,000 deaths per

year. There are four different subgroups of Influenza, Influenza A (IAV), Influenza B, Influenza C and Influenza D. All influenza viruses belong to the family Orthomyxoviridae and are enveloped, negative-sense, single-stranded RNA (ssRNA) viruses with segmented genomes (Samji, 2009). Within Influenza A and B virus, eight ssRNA segments encode for viral proteins. Three large RNA gene segments encode for the viral polymerases (PB1, PB2 and PA) which allow the virus to replicate within target cells. Two RNA gene segments encode the viral glycoproteins, haemagglutinin (HA), which binds to sialic acid on the surface of targets cells mediating virus entry, and neuraminidase (NA), which is involved in the release of virus from the cell membrane. One ssRNA encodes for Nuclear protein (NP), which forms the structure to which the viral RNA is bound, the same ssRNA encodes matrix 1 (M1) and Matrix 2 (M2) protein. M1 protein forms a scaffold to aid in the assembly of the virus. M2 forms a proton Ion channel and like HA and NA is bound to the lipid membrane of the virus which is derived from the infected cell; all three proteins are required for entry and exit of the virus from host cells. Similarly, non-structural 1 (NS1) protein, which is a virulence factor involved in evading host defence and nuclear export protein (NEP), which together with M1 is involved in trafficking viral RNA segments in the host cell, are also encoded by the same ssRNA. (Krammer et al., 2018). Influenza C and D viruses have 7 RNA segments and cause comparatively little disease compared to Influenza A and B, though Influenza C has been shown to cause infections, particularly in children (Matsuzaki et al., 2006). Influenza D has been shown to infect pigs and cattle but does not spread to humans (Hause et al., 2013, Hause et al., 2014, Foni et al., 2017).

Due to the segmented nature of its genome influenza is capable of reassortment, the process by which individual gene segments of different viruses may reassort when infecting the same cell. IAV, unlike the other influenza subtypes, circulates in other species as well as humans, including pigs, horses, poultry and wild birds. These different species are reservoirs for

antigenically distinct viruses which are characterised by the expression of different HA and NA serotypes. There are currently 16 HA, and 9 NA antigenically different serotypes identified among influenza viruses (not including serotypes which have only been identified in bats) (Fouchier et al., 2005). The antigenically diverse virus strains in these animal reservoirs can re-assort when infecting the same cell, thus increasing virus diversity, and potentially leading to a novel human influenza strain with pandemic potential. Pandemics occur every 10-50 years, and due to the lack of pre-existing immunity in the population are associated with higher levels of mortality (Krammer et al., 2018). Furthermore, the binding of HA to sialic acid is determined by two major linkages α(2,3) and α(2,6), which are important for species specificity of the virus. Viruses circulating in humans recognise α(2,6), whereas viruses in birds recognise α(2,3). Viruses in pigs recognise both, making pigs important mixing vessel of potentially pandemic viruses (Skehel and Wiley, 2000).

In 2009 the first pandemic of the 21st century occurred when a novel H1N1 IAV strain (H1N1pdm09) emerged from pigs (Smith et al., 2009, Mena et al., 2016). Vaccines were not available for the initial wave of infection during this pandemic, though mortality to this virus strain was low when compared to previous influenza pandemics (Donaldson et al., 2009).

1.2.1 Innate response to Influenza

Influenza gains entry to epithelial cells in the upper respiratory tract by binding to sialic acid on the surface of cellular membranes via the viral homotrimer protein HA. Upon binding, receptor-mediated endocytosis occurs, which allows entry of the virus to an endosome. The lower pH (around 5-6) of the endosome causes a conformational change in HA leading to fusion of the viral and endosomal membranes, also opening the M2 Ion channel. The M2 Ion channel acts as a proton selective ion channel acidifying the viral core leading to the release of

the viral ssRNA and internal viral proteins into the cytosol (Samji, 2009). The major PRR involved in sensing influenza infection are Toll-like receptor 3 (TLR3) and 7 (TLR7) and retinoic acid-inducible gene-I (RIG-1) (Kreijtz et al., 2011) . RIG-1 and TLR7 both sense Influenza ssRNA. RIG-1which is expressed in the cytosol of epithelial and antigen presenting cells, detects ssRNA as it is released from the viral core. RIG-1 differentiates host and virus RNA by specific recognition of 5′-triphosphates in the ssRNA (Pichlmair et al., 2006). TLR7 is expressed primarily by specialised plasmacytoid dendritic cells (pDCs), which sense viral ssRNA as it is released into acidified endosomes. TLR3 recognises double-stranded RNA (Alexopoulou et al., 2001) and can be activated in human lung epithelial cells (Le Goffic et al., 2007) as well as dendritic cells (Luber et al., 2010). Intriguingly, dsRNA is not generated during replication of influenza virus due to the presence of RNA helicase DDX39B, and therefore the exact mechanism of TLR3 sensing of Influenza remains elusive (Pulendran and Maddur, 2015). Binding of their respective ligands and activation of these 3 PRR leads to upregulation of type 1 IFN and other pro-inflammatory cytokines (Malik and Zhou, 2020).

Influenza can also be sensed indirectly via cellular stress responses. NLRP3 senses cellular stress in the form of mitochondrial dysfunction. This leads NLRP3 to recruit protease caspase 1 to the inflammasome leading to the production of the inflammatory cytokines IL-1β and IL-18 from their inactive precursors by proteolytic cleavage (Ichinohe et al., 2013) (Pang and Iwasaki, 2011). These pathways combined lead to the establishment of an “antiviral state” which inhibits viral replication.

1.2.2 Innate cellular responses to Influenza

1.2.2.1 Dendritic Cells

Dendritic cells (DC) are heterogeneous cells which play a crucial role in activating the adaptive immune response to infection. In the pig, much like within other species, they can be broken down into different subsets which are often restricted to different compartments (Summerfield and McCullough, 2009). DC can be broadly categorised into cDC and pDC. cDC are considered professional antigen presenting and can be further broken down into cDC1 which induce T helper (TH) 1 response and cDC2 which induce a T_H2 as well as T_H17 response (Maisonnasse et al., 2016). pDC are specialised to detect MAMPs and are professional IFNα producers, producing high levels in response to virus following detection by TLRs. Despite this broad classification pDCs are still capable of antigen presentation and can rapidly induce cytotoxic CD8 T cells by the presentation of exogenous ligand in 'ready-made' MHC located in endocytic organelles which do not need transporting to the cytosol (Di Pucchio et al., 2008). Indeed, there are multiple overlapping functions between the DC subsets, which have been recently characterised in pigs (Auray et al., 2016). Porcine DCs can be found enriched in the upper respiratory tract where they form a dense network both above and below the basement membrane (Bimczok et al., 2006).

1.2.2.2 Macrophage

Alveolar macrophages (AM) are a major innate cell type in the lung, where they reside just below the epithelial cell wall. Following activation macrophages are vital in the phagocytic clearance of apoptosed influenza-infected cells, limiting the spread of the virus (Hashimoto et al., 2007). The importance of this function was shown in pigs, where AM depletion leads to high levels of mortality following influenza infection (Kim et al., 2008). Macrophages in the

pig will produce IL-8, IFNβ IL-10 and TNF in response to Influenza, and this is regulated by ERK and MAP kinases following activation of RIG-1 (Gao et al., 2012). These cytokines will play a role in inducing a further immune response. However, this response may also potentially exacerbate pathology by overproduction of inflammatory cytokines (Calore et al., 2011). Therefore, AM activation is tightly regulated by a series of stimulatory or regulatory signals. TLR stimulation or response to inflammatory cytokines such as IL-1β, TNF or IFN-γ will activate AM whereas soluble regulatory signals such as IL-10 or direct cellular interactions with epithelial cells through, for example, CD200 receptor block inflammatory pathways (Hussell and Bell, 2014). In the early stages of infection, high levels of ligand stimulation are present, and down regulatory signals are minimised due to inflammatory disruption of the cell to cell inhibitors leading to AM activation. As the amount of stimulatory ligand diminishes due to viral clearance and inhibitory responses are restored with the reestablishment of damaged tissues, the AM will return to a quiescent state.

1.2.2.3 Neutrophils

Neutrophils are generally considered professional bacterial effector cells with their role in viral infections receiving comparatively less attention (Galani and Andreakos, 2015). Despite this, Neutrophils are one of the first responding cell types during influenza infection and have an important role in its pathogenesis (Galani and Andreakos, 2015). Whether their role is beneficial to the host or leads to greater collateral damage depends on a complex array of factors and likely depend on the strain of influenza as well as host specific responses (reviewed in reference (Camp and Jonsson, 2017)). Within pigs, neutrophils accumulate in the vasculature within the first 24 hours of influenza infection. Within 48 hours, these neutrophils are joined by or replaced by macrophages (Janke, 2014). Functionally little is known about the role

neutrophils play during influenza infection within pigs though neutrophils have been reported to excrete myeloperoxidase (MPO) during H1N2 infection (Kim et al., 2011) which has antiviral activity (Yamamoto et al., 1991) but also causes potential cytotoxic damage. A study in 2012 investigating pigs as a model of cystic fibrosis demonstrated that porcine neutrophils more closely resembled human than mice (Brea et al., 2012). Porcine neutrophils are capable of producing neutrophil extracellular traps (NETs) and inducing protease 3, cathepsin G and elastase (Brea et al., 2012) which have unknown antiviral activity (Galani and Andreakos, 2015) but have all been linked to pathology (Korkmaz et al., 2008).

1.2.2.4 Natural Killer (NK) cells

NK cells have been reported to have a variety of roles during the control of influenza infection through the production of cytokines (Hwang et al., 2013) and direct killing of the influenza infected cells via the direct binding of the NKp46 receptor to hemagglutinin expressed on the surface of Influenza infected cells (Mandelboim et al., 2001, Achdout et al., 2010). Within pigs, NK cells are CD3- and express CD8α+ or NKp46+ with some cells co-expressing these markers. During the first three days of Influenza infection, only NK cells expressing NKp46 are reduced in the blood, and a corresponding increase is seen in the lung particularly in infected tissue (Forberg et al., 2014). Importantly these NKp46+ NK cells were not shown to be infected by influenza or undergoing apoptosis (Forberg et al., 2014), which in other species have been reported as a mechanism of influenza escape from NK cell recognition (Mao et al., 2009, Liu et al., 2017). NK cells in pigs are also capable of antigen presentation to CD4+ T cells via MHCII and costimulatory CD80/86 with the ability to present antigens from killed cells, a feature which they share with humans but not mice (Pelsmaeker et al., 2018). This combined with the porcine NK cells not being infected by the Influenza virus, makes them

likely, very efficient cytotoxic and antigen presenting cells which help to coordinate the adaptive response.

1.2.3 Conventional T cell immunity to Influenza

It was shown by Schulman et al. in 1965 that infection with one influenza virus subtype confers some level of protection upon reinfection with another subtype of Influenza (Schulman and Kilbourne, 1965a) with this protection being referred as "partial specific heterotypic immunity" (also known as heterosubtypic immunity).

Early studies demonstrated that mice lacking CD8 T cells were more susceptible to primary influenza infection, with increased mortality and delayed viral clearance (Bender et al., 1992, Doherty et al., 1997). Similarly, many studies since in a variety of animal models, including nonhuman primates, have shown that cellular immune responses can control influenza infection in the absence of a neutralising humoral response; lowering mortality, pathology and viral shedding but not preventing infection (Yetter et al., 1980, Schulman and Kilbourne, 1965b, Straight et al., 2006, Weinfurter et al., 2011). Cytotoxic CD8 T cells cross-reactive to conserved influenza epitopes are thought to be the major contributor to this heterotypic protection (Bodewes et al., 2009, Weinfurter et al., 2011, Hayward et al., 2015, Sridhar et al., 2013, Wang et al., 2015). Early adoptive transfer experiments demonstrated that cytotoxic T cells can protect mice from influenza infection (Yap et al., 1978). More recent studies have shown that CD8 T cells which are established in initial influenza infection working in concert with alveolar macrophages and cross-reactive non-neutralising antibodies lead to increased levels of heterosubtypic protection (Laidlaw et al., 2013). CD8 and CD4 derived perforin and Fas-ligand mediated direct killing (Topham et al., 1997) and secretion of antiviral cytokines such as IFN-γ (Bot et al., 1998) are essential effector functions for CD8 cytotoxic T cells during

Influenza infection. CD4 T cells also aid in the resolution of the virus through B cell help, direct cytotoxicity, and secretion of cytokines (Doherty et al., 1997, Swain et al., 2006, Brown et al., 2012, McKinstry et al., 2012).

The first demonstration of T cells involvement in the successful resolution of influenza infection in humans was by McMichael *et al.* in 1983 (McMichael et al., 1983). More recent natural studies from the 2009 H1N1 pandemic (H1N1pdm09) and 2013 A/H7N9 outbreak demonstrated that pre-existing antigen-specific CD8 T cells lower viral shedding and reduce symptoms (Hayward et al., 2015, Sridhar et al., 2013) and leads to faster recovery from severe infection (Wang et al., 2015). Furthermore, Influenza challenge studies have shown that pre-existing CD4 T cells correlate with protection in humans (Wilkinson et al., 2012). In summary, a robust T cell response may be able to reduce the severity of disease and shedding of the virus, preventing its spread to a new host (Gilbert, 2013, Sridhar, 2016).

1.2.4 The pig as a model for Influenza

Sus scrofa, the domestic pig, is useful as a model for influenza infection for several reasons. Pigs resemble humans anatomically, have similar clinical signs when infected with Influenza and are infected by the same virus subtypes (H1N1 and H3N2). Pigs are being used increasingly in studies of influenza vaccines (Morgan et al., 2016, Holzer et al., 2018c, Lefevre et al., 2012) and studies which compared H1N1 vaccines in humans and in pigs showed very similar immunogenicity (Lefevre et al., 2012, Waddington et al., 2010, Holzer et al., 2019b) lending further weight to the use of swine as a model for both vaccine studies and more generally the study of the immune response to Influenza.

As a natural host for influenza infection with growing tools to perform immunological studies, pigs represent an ideal model for the study of the cellular immune response to Influenza virus.

Despite this, our understanding of the cellular response in the pig remains incomplete. Khatri et al. performed an early study of H1N1 Sw/OH/24366/07 virus in pigs, which like H1N1pdm09 has a history of transmission to humans, demonstrating that CD8 T cells accumulate in the lung and BAL at day six post-infection (Khatri et al., 2010). A more recent study of the frequency and activation status of leucocytes in local and systemic tissues following H1N1pdm09 infection showed increased perforin expression and proliferation of CD8 αβ cells in the respiratory tract of infected pigs (Schwaiger et al., 2019). To date, the most comprehensive analysis of T cell responses following influenza infection in pigs was performed by Talker et al. (Talker et al., 2016). This study analysed T cell dynamics in the lung, peripheral blood mononuclear cells (PBMC), Tracheobronchial lymph node TBLN and mesenteric lymph node (MLN) following intratracheal inoculation with swine H1N2 over 2, 4, 6, 9, 12, 15- and 46-days post-infection. They detected proliferating (Ki67+) CD4+ T cells at day four post-infection and demonstrated the capacity of these cells to secrete IFN-γ following re-stimulation with homologous virus at this time point. Similarly, proliferating CD8 T cells peaked in the lung at day six post-infection and were capable of IFN-γ secretion as early as day four, though with a marked increase at day six onwards. They also determined the multifunctional (IFN-γ, TNF, IL-2) response of CD4 and CD8 T cells over the time course of infection with IFN-γ and TNF single and double producing CD8 T cells more abundant (up to 30-fold) in the lung. IFN-γ/TNF/IL-2 CD8 T cells were not identified in any tissue examined. CD4 frequencies of IFN-γ and TNF double producers were detected in all tissues, though IFN-γ/TNF/IL-2 CD4 T cells were primarily identified in PBMC and TBLN.

One reason for the lack of in-depth studies of influenza-specific T cell responses in pigs has been the limited understanding of the specificity of the T cell response. The specificity of the antigen-specific T cells is dependent upon the presentation of peptide epitopes to cytotoxic T cells. The epitopes presented in any given individual is genetically determined by host major

histocompatibility complex MHC (known as Swine leukocyte antigen (SLA) in pigs). Despite centuries of agricultural inbreeding, pigs have maintained a significant level of SLA genetic diversity with 227 class 1, and 211 class ll alleles (**http://www.ebi.ac.uk/ipd/mhc/group/SLA)** identified for *Sus scrofa* in the Immuno-Polymorphism Database (IPD)-MHC database to date (Maccari et al., 2017). Studies using *in silico* prediction software have identified CD8 Influenza specific epitopes in typical swine SLA, SLA-1*0401 (Pedersen et al., 2014) and SLA-1*0702 (Baratelli et al., 2017), though these require SLA matched individuals to be of use. A way to overcome this is the use of the inbred Babraham (BM) pig which was derived from the large white commercial pig in the 1970s, showing a similar level of inbreeding to inbred mouse strains (Signer et al., 1999) and is the only inbred large animal available to biomedical research. These pigs are SLA homozygous (Schwartz et al., 2018) expressing class I SLA-1*14:02; SLA-2*11:04 and SLA-3*04:03 and class II DRB1-*05:01, DQA-*01:03 and DQB1-*08:01. The interest in the use of the BM pig as a large animal biomedical model for Influenza has increased in recent years. Recently Influenza immunodominant epitopes in BM's (Tungatt et al., 2018) have been identified. Four NP peptides from PR8 influenza virus were identified which bound SLA-1*14:02 and SLA-2*11:04. These epitopes were confirmed by peptide- SLAI tetramer staining of CD8 T cells in TBLN, PBMC and BAL. T cell reactivity to two of these epitopes ($NP_{217-225}$ and $NP_{290-298}$) was also identified in BM pigs infected with H1N1pdm09 Influenza due to conserved peptide sequences between this and the PR8 influenza strain.

1.3 Innate like T cells that bridge the innate and the adaptive immune system

The innate-like T cell family includes Gamma delta (γδ) T, natural killer T (NKT) and mucosal associated invariant T (MAIT) cells with potentially more yet to be discovered (Boudinot et al., 2016). They express invariant or public (expressed by many individuals as well as species)

semi invariant TCR, which allows them to rapidly respond to a restricted range of ligands in a manner reminiscent of a PRR. These invariant TCRs sense specific non-peptide ligands. MAIT cells and NKT cells are restricted via major histocompatibility complex (MHC) like complexes (MR1 for MAIT cells and CD1 for NKT cells) (Wencker et al., 2014). γδ T cells are not restricted through an antigen-presenting element and instead are able to bind antigen more freely in a similar manner to monoclonal antibodies (Vantourout and Hayday, 2013). Innate like T cells also express TLR and high levels of cytokine and chemokine receptors, such as IL-18R which allows them to respond to cytokines without prior TCR stimulation reminiscent of innate cells (Tomura et al., 1998). This ability to respond to cytokines independently of TCR is attributed to the expression of promyelocytic leukemia zinc finger (PLZF) in these cells, a transcription factor which is associated with an innate function (Rahimpour et al., 2015, Savage et al., 2008).

1.3.1 Natural killer T (NKT) cells

NKT cells have an overlapping phenotype of both NK and T cells. They are present in a range of mammalian species, including mice pigs and humans but not cattle (Looringh van Beeck et al., 2009a). NKT cells are restricted to CD1, which presents glycolipid ligands and can be classified broadly into type 1 and type 2. The archetypical ligand for type 1 NKT cells is α-galactosylceramide (α-GalCer) which is recognised by an invariant TCR (vα24-Jα18/Vβ11 in humans) these being referred to as invariant NKT (iNKT) cells. The invariant nature of their TCR allows for the identification of these cells via α-GalCer loaded tetramer which has been used to demonstrate their existence in pigs using cross-reactive mouse CD1d tetramers (Renukaradhya et al., 2011, Thierry et al., 2012, Schäfer et al., 2019). iNKT cells can be CD4+, CD8+ or double-negative and are involved in providing T cell help by licensing DC. Following the recognition of antigen presented on CD1d, iNKT upregulate CD40L, secrete granulocyte-

macrophage colony-stimulating factor (GM-CSF) and IFN-γ, which in turn, stimulates DC to produce IL-12 which primes CD8 T cells. This ability to indirectly activate T cells has recently gained interest as a potential potent adjuvant for influenza vaccines within pigs (Yang et al., 2018). Type 2 NKT cells can also respond to glycolipids via CD1d, but their TCR is more diverse, and they do not specifically respond to α-GalCer. NKT cells, like NK cells, can express NKp46 and cells, defined as CD3+ NKp46+, have recently been shown to increase in frequency in the lung following influenza infection (Mair et al., 2016).

1.3.2 γδ T cells

Pigs and ruminants are members of the so-called gamma delta high species with 18-47% of total circulating lymphocytes being γδ T cells in pigs (Takamatsu et al., 2006) and 10-20 % in cattle (McGill et al., 2014). This is in contrast to humans where γδ T cells consist of a smaller population of 2-10% of circulating CD3+ T lymphocytes with a notable enrichment in mucosal surfaces and skin (Zheng et al., 2013). It has been demonstrated in mice and to a lesser extent in humans that γδ T cells have a high level of functional plasticity. γδ T cells functions include direct cellular cytotoxicity, (Qin et al., 2009), cytokine release, antigen presentation (Brandes et al., 2005, Meuter et al., 2010), T regulatory functions (Kühl et al., 2009) and epithelial wound repair (Jameson et al., 2002). Unlike NKT cells and MAIT cells, γδ T cells are not restricted through a specific presentation molecule and can bind a broader range of antigens compared to their conventional counterparts (reviewed in reference (Chien et al., 2014)). However, though there is a wide range of potential TCR γδ combinations, there is an enrichment of specific combinations which bind to a constrained range of antigens (Born et al., 2013). In human peripheral blood γδ T cells can be defined based upon their usage of the Vδ1 or Vδ2 gene segments. Vδ1 γδ T cells are considered to be more like conventional T cells with respect to having a wide range of TCR diversity a large pool of naïve T cells and a smaller subset of

expanded, memory T cells (Davey et al., 2017). In contrast γδ T cells expressing the Vδ2 gene segment have a more limited TCR sequence diversity with up to 95% of this population having the Vγ9/Vδ2 pairing which respond to phosphorylated compounds (reviewed in (Pauza and Cairo, 2015)). Vδ2 γδ T cells, in addition to having a constrained TCR, are highly responsive to cytokine stimulation, a hallmark of innate like T cells (Provine et al., 2018). Thus, much like αβ- T cells, γδ- T cells have the capacity to be innate like T cells with the Vγ9/Vδ2 cells being a prominent example in humans.

1.4 MAIT cells

1.4.1 discovery of a novel innate-like T cell

The first experiment suggesting the presence of MAIT cells came in 1993 when Porcelli *et al.* identified a high level of expression of TRAV1-2 (Vα7.2) rearranged with TRAJ33 (Jα33), with limited complementary determining regions (CDR3) in human CD8- CD4- (DN) T cells (Porcelli et al., 1993). Later, Olivier Lantz and colleagues went on to quantify the level of TRAV-1 TRAJ33 expression in human blood between different T cell subsets, noting an enrichment (>200-fold) in expression in the DN population and to a lesser extent in the CD8 population compared to the CD4 positive T cells (Tilloy et al., 1999). Conservation of this invariant TCR alpha (iTCRα) was observed in mice and cattle, demonstrating that this sequence was conserved between multiple mammalian species. Olivier Lantz's group went on to show that MAIT cells could recognise MHC related protein 1 (MR1) (Miley et al., 2003) and, using MR1 knockout mice, demonstrated that MR1 is required for the development of MAIT cells in the periphery (Treiner et al., 2003). Due to the high frequency of these cells identified in the intestinal lamina propria, they named these cells mucosal associated invariant T cells.

1.4.2 MAIT cell restriction through MR1

The activating MAIT cell ligand, presented though MR1, remained elusive for some years until two seminal papers demonstrated the MAIT cells could be activated by several strains of bacteria and yeast but had no reactivity to viruses (Le Bourhis et al., 2010, Gold et al., 2010). Thus, though the activating ligand was still unknown, it was required to be a compound which was conserved between these activating microbes. The activating ligand(s) was finally identified by the groups of J. McCluskey and J. Rossjohn. When attempting to fold soluble MR1 in the presence of *S. Typhimurium* supernatant, it was noticed that the MR1 would refold in the presence of RPMI alone. RPMI contains vitamin supplements which are produced by some plants and bacteria, but not mammals. Testing the folding of MR1 in the presence of differing vitamin sources identified multiple ligands capable of refolding MR1. The initial ligand discovered was 6-formyl pterin (6-FP), a vitamin B9 derivative which binds deep within the MR1 binding groove and was unable to activate MAIT cells. Further studies revealed that derivatives of the vitamin B2 (Riboflavin), which were similar in structure, but larger than 6-FP were MAIT cell-activating ligands (Kjer-Nielsen et al., 2012). Both the activating and non-activating ligands form a covalent bond to MR1 lysine 43. Neutralisation of the lysine 43 positive charge by this bond serves as a "molecular switch" allowing for egress of MR1 from the endoplasmic reticulum to the plasma membrane (McWilliam et al., 2016). The potency of activating ligands varies widely, with the most potent activating ligand identified to date being 5-2-oxopropylideneamino-6-D-ribitylaminouracil (5-OP-RU), an unstable early intermediate of the riboflavin pathway (Corbett et al., 2014). The discovery of the MR1 ligands has allowed for the development of tetramers to identify MAIT cells (**Figure 1.1**). These tetramers defined a population which overlapped with surrogate markers Vα7.2 and CD161, which had previously used to identify MAIT cells in functional and phenotypic studies (Reantragoon et

al., 2013). MR1- tetramer identification also demonstrated that in addition to TRAJ-33 MAIT cells also express TRAJ-12 and TRAJ-20 (Reantragoon et al., 2013).

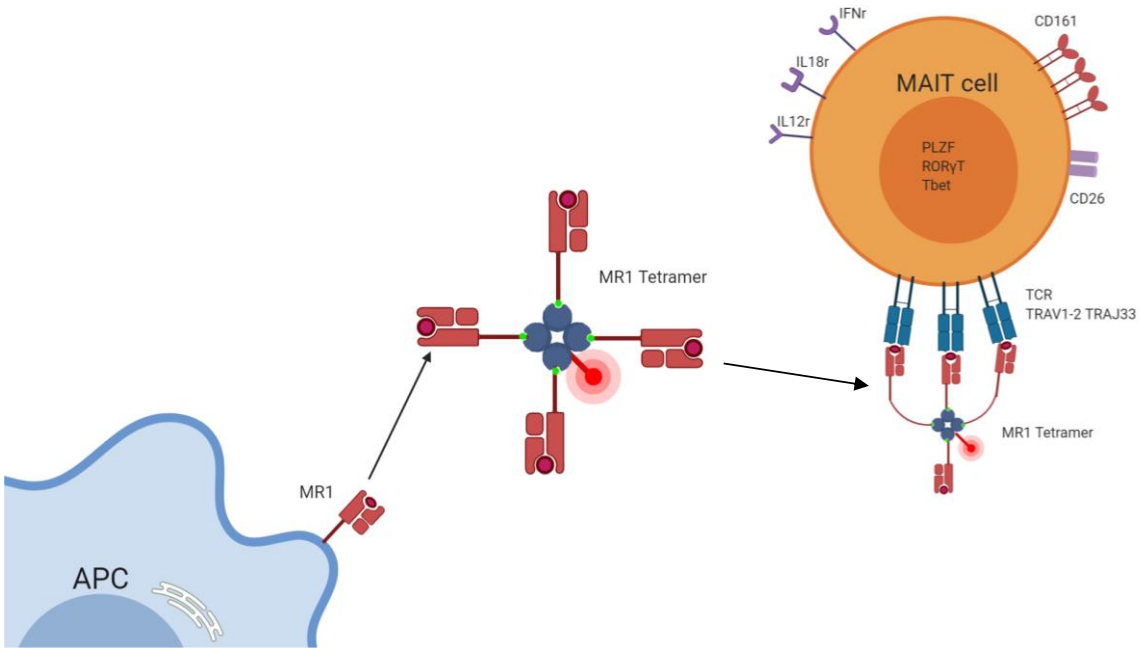

Figure 1.1 MR1 tetramer identification of MAIT cells. Created with BioRender.com.

1.4.3 MAIT cell phenotype

MAIT cells in humans emerge from the thymus in a "pre-primed" state and express an effector memory phenotype (CD45RO+ CD45RA- $CD95^{hi}$ $CD62L^{lo}$) (de Lima Moreira et al., 2020). The majority of human MAIT cells are either CD8+ or double negative DN with a rare CD4+ population (Reantragoon et al., 2013). MAIT cells in humans are a homogeneous population but possess a phenotype which enables them to be functionally versatile. In addition to their effector memory phenotype and regardless of tissue origin, they express high levels of IL-18R and the C-type lectin CD161. CD161 along and Vα7.2 can be used as surrogate markers for MAIT cell due to the high level of CD161 expression in MAIT cells (Kurioka et al., 2016) a phenotypic identification which has been largely confirmed by the use of MR1 tetramers

(Reantragoon et al., 2013). MAIT cells express high levels of PLZF which is essential for MAIT cells (and other innate-like T cells) development (Koay et al., 2016a) and responsiveness to cytokine stimulation (Rahimpour et al., 2015). Consistent with their effector phenotype MAIT cells express effector T cell transcription factors T-bet and Eomesodermin (Eomes) both transcription factors involved in the acquisition of T effector functions such as perforin upregulation and IFN-γ secretion (Araki et al., 2008, Szabo et al., 2000). MAIT cells also express RAR-related orphan receptor γt (ROR-γT), which enables the expression of IL-17 (Billerbeck et al., 2010, Walker et al., 2012).

MAIT cells have been demonstrated to be present in mice by the classical/defining phenotyping methods described above, expressing TRAV1-TRAJ33 TCR alpha and binding the ligand 5-OP-RU (Tilloy et al., 1999, Rahimpour et al., 2015). Mouse MAIT cells phenotypically overlap in many respects with human MAIT cells, including the expression of PLZF and displaying a memory phenotype ($CD44^{hi}$ $CD62L^{lo}$). However, there are differences in frequency and phenotype between the human and mouse MAIT cell populations. Mice have a much smaller MAIT cell population compared to humans, with a larger proportion expressing CD4 (Rahimpour et al., 2015). Mouse MAIT cells are also seemingly more heterogeneous than their human counterparts with at least two subsets being defined based upon the expression of the transcription factor ROR-γT and T-bet. The vast majority of mouse MAIT cells express high levels of ROR-γT and low levels of T-bet and thus secrete IL-17A. A distinct population expresses T-bet and lower levels of ROR-γT secreting IFN-γ upon stimulation (Rahimpour et al., 2015). These distinct lineages have been defined as MAIT1 ($ROR\gamma t^{-}$) and MAIT17 (RORγt+) and have differing tissue localisation (Salou et al., 2018). However, upon stimulation these populations collapse into a single population which express both transcription factors (Hinks et al., 2019).

1.4.4 MAIT cell tissue distribution

MAIT cells represent the largest antigen-specific αβ T cell population in humans. Though MAIT cells derived their name from early studies noting an enriched in the mucosa of the gut and lung (Treiner et al., 2003), it is now clear that MAIT cells are readily identifiable in the peripheral blood as well as in non-mucosal tissues. MAIT cells do, however, home preferentially to tissues, in response to engagement of chemokine receptors 6 (CCR6) and CCR9, CXC chemokine receptor (CXCR)6 (Kurioka et al., 2016). MAIT cells also express tissue residency markers, including CD103 and CD69 (Booth et al., 2015) in gut tissue and CRTAM (Slichter et al., 2016) a gene which enables tissue retention. Tetramer based identification of MAIT cells has confirmed that MAIT cells are abundant in peripheral blood with a mean of 3% total T cells (Gherardin et al., 2018). MAIT cells are enriched in the gut, though intriguingly, with differing frequencies in different compartments of the gastrointestinal tract, potentially due to the levels of microbial ligands present in differing sections of the gut. The ileum, colon and rectum each have similar MAIT cell frequencies to the blood (Serriari et al., 2014, Cosgrove et al., 2013, Leeansyah et al., 2013) whereas MAIT cells are highly enriched in the jejunum with a frequency of approximately 60% of CD4- T cells (Reantragoon et al., 2013). MAIT cells are also strikingly enriched in the liver, ranging from 5 to 55% of T cells (Dusseaux et al., 2011). MAIT cells have also been phenotypically identified in the female genital tract (Gibbs et al., 2017), lung (Loh et al., 2016), adipose tissue (Carolan et al., 2015), and TCR transcripts of the invariant TCR chain observed in prostate, ovaries and kidney (Lepore et al., 2014). There are low frequencies of MAIT cells in secondary lymph tissue consistent with their tissue homing phenotype and lack of lymph homing receptors CCR7 and CD62L (Dusseaux et al., 2011, Billerbeck et al., 2010). However, MAIT cells can be detected in secondary lymph nodes and are thought to directly recirculate between tissues and lymph,

evidenced by the fact MAIT cells are CCR7- in lymph nodes as well as blood (Voillet et al., 2018).

1.4.5 MAIT cells in bacterial infection

As may be inferred by their specificity to bacterial metabolites, MAIT cells have been implicated in bacterial infections, such as *Francisella tularensis* (Meierovics et al., 2013), *Legionella longbeachae* (Wang et al., 2018) and *Mycobacterium tuberculosis* (M.tb) (Gold et al., 2015, Vorkas et al., 2018) (**Figure 1.2**).

MAIT cells have been shown to be activated by M.tb in humans (Vorkas et al., 2018, Suliman et al., 2019), nonhuman primates (Greene et al., 2017) and mice (Chua et al., 2012). Furthermore, MAIT cells are the predominant IFN-γ producing T cell population in TB exposed individuals upon re-stimulation with Bacillus Calmette-Guérin (BCG) (Suliman et al., 2019). All these bacterial microbes produce riboflavin, so it is perhaps unsurprising that they would activate MAIT cells. However, activation of MAIT cells by BCG in humans is primarily driven by cytokine stimulation and not through TCR (Suliman et al., 2019). Furthermore, studies in macaques showed little activation of MAIT cells in the lung during M.tb infection (Kauffman et al., 2018, Bucsan et al., 2019) though increased MAIT cell numbers in the BAL did correlate with a lower burden of disease (Kauffman et al., 2018). Moreover, M.tb infected mice that had artificially upregulated MAIT cells inhibit BCG but not M.tb pulmonary infection *in vivo* (Yu et al., 2020). These data collectively suggest that M.tb. may interfere with TCR mediated activation of MAIT cells with a yet unknown mechanism.

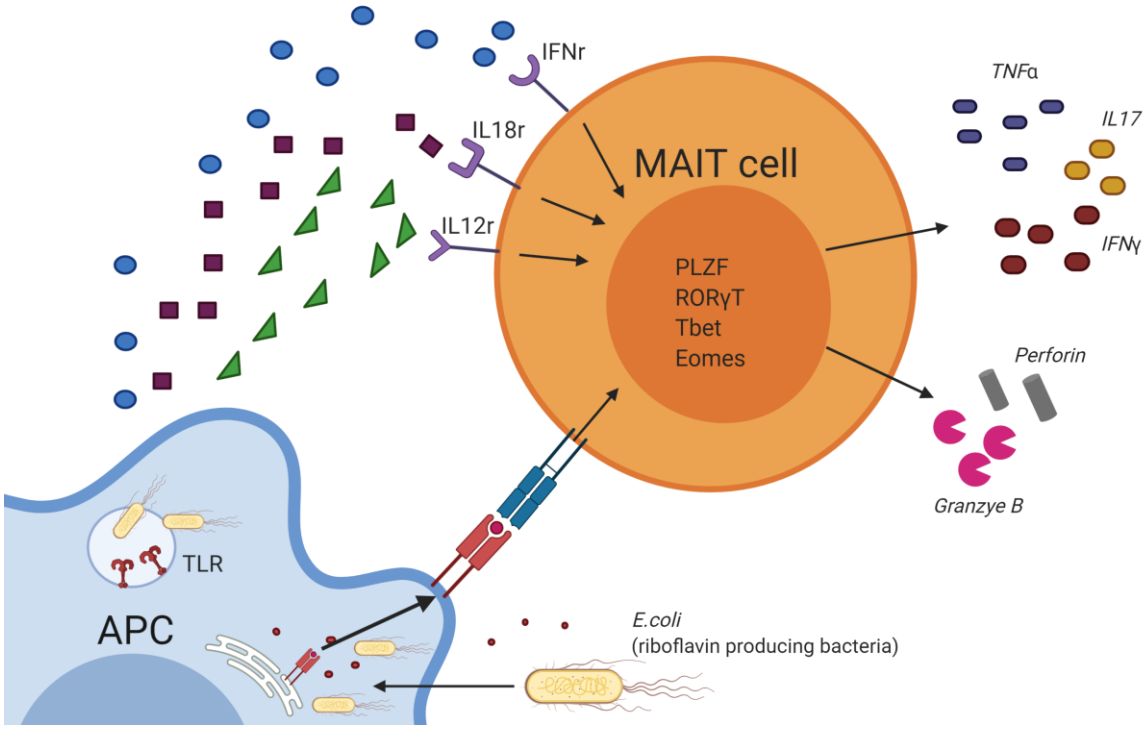

Figure 1.2 MAIT cell activation by Bacteria. Created with BioRender.com.

1.4.6 MAIT cells in viral infection

Early studies examining the role of MAIT cells with viruses, including herpes simplex virus, parainfluenza 3 virus, and an adenoviral vector or vaccinia virus, did not show any activation of MAIT cells (Gold et al., 2010, Le Bourhis et al., 2010). This lack of activation was later attributed to the fact that the transgenic murine MAIT cells and human MAIT cell clones used in these studies lacked IL-18R which was later shown to be an essential mediator of MAIT cell activation (Ussher et al., 2014). It is now evident that MAIT cells are activated in response to viral stimulation, including Influenza (van Wilgenburg et al., 2016), and contribute to Influenza immunity in humans (Loh et al., 2016), and mice (van Wilgenburg et al., 2018). This activation is not mediated by TCR stimulation, but through soluble activating signals, predominantly cytokines such as IL-18 combined with IL-12, IL-15 or interferon- α/β (van Wilgenburg et al.,

2016, Ussher et al., 2014) which are upregulated following upstream TLR ligation (**Figure 1.3**).

Many correlations have been observed with MAIT cell frequencies and viral infections, some prior to MAIT cells being formally shown to be activated by viruses. Depletion of MAIT cells has been described in chronic infections, such as human immunodeficiency virus (HIV) (Cosgrove et al., 2013, Leeansyah et al., 2013, Saeidi et al., 2016) as well as hepatitis C virus (HCV) (Spaan et al., 2016, Bolte and Rehermann, 2018, Hengst et al., 2016). Further observational data has shown that MAIT cell frequencies were inversely correlated with the severity of disease during acute influenza infections H7N9 and the pandemic H1N1 influenza (Loh et al., 2016, van Wilgenburg et al., 2016), similar to the frequencies of MAIT cells and the clinical outcome of people with HCV (Bolte and Rehermann, 2018). These correlations may be the effect of MAIT cell response to the virus itself. However, a robust MAIT cell response may also help prevent opportunistic bacterial infections such as staphylococcus aureus in acute influenza infection (Mulcahy and McLoughlin, 2016) and tuberculosis in chronic viral infection (Corbett et al., 2003).

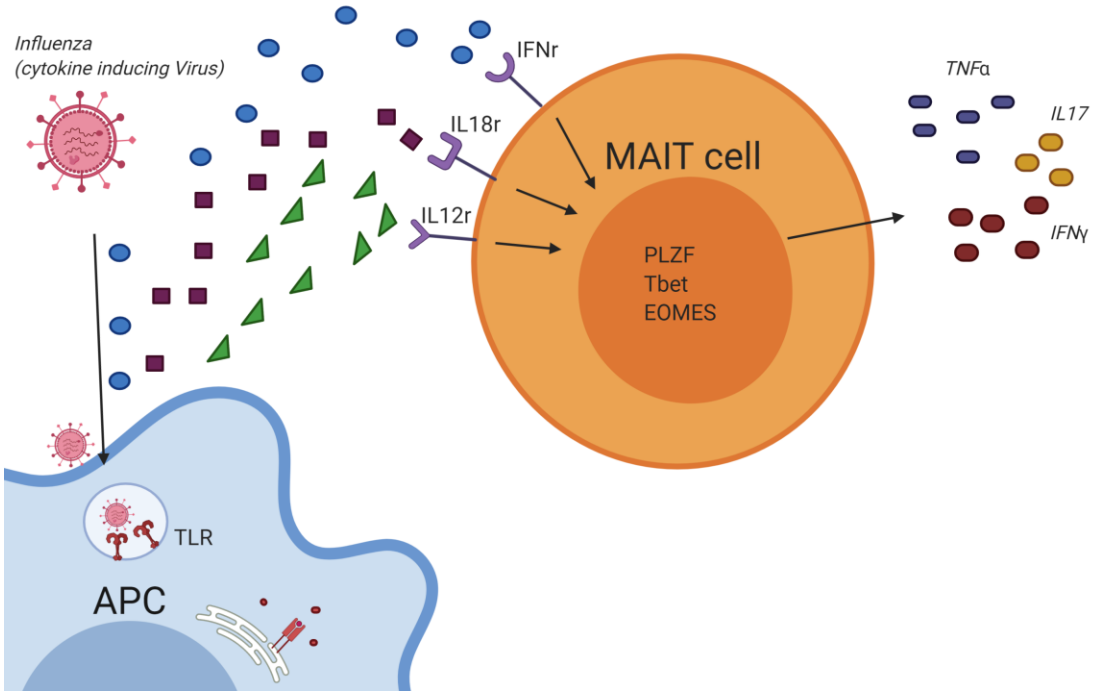

Figure 1.3 MAIT cell activation by virus. Created with BioRender.com.

1.4.7 Emerging functions of MAIT cells

Recently, three independent studies have probed the role of TCR dependent and TCR independent effector mechanisms in mice and humans using RNA sequencing methods (Leng et al., 2019, Lamichhane et al., 2019, Hinks et al., 2019). MAIT cell reactivity was studied following (1) TCR stimulation with TCR cross-linking antibodies, fixed bacteria or synthetic 5-OP-RU (Leng et al., 2019, Lamichhane et al., 2019, Hinks et al., 2019), (2) cytokine activation with differing concentrations of IL-12, IL-18 and IL-15 (Leng et al., 2019, Lamichhane et al., 2019) or (3) a combination of both (Leng et al., 2019). A key shared finding of these studies was that when triggered by TCR alone, MAIT cells exhibit a tissue repair signature, whereas stimulation by cytokine or a combination of cytokine and TCR triggered a more proinflammatory function. The tissue repair signature was derived from a recent seminal

study with a murine innate-like H2-M3-restricted CD8+ T cells which were demonstrated to strongly promote wound healing following infection with *Staphylococcus epidermidis* (Linehan et al., 2018). To experimentally support the wound healing transcriptomic signatures identified in these studies, supernatants of MAIT cells cultured with *E.coli* were shown to promote cell layer recovery of Caco2 cells in scratch assays. This effect was abrogated with MR1 blocking antibodies, thus confirming TCR mediated wound healing (Leng et al., 2019). Further, these features were identified in mice (Hinks et al., 2019), and murine MAIT cells had an overlapping transcriptional profile with human MAIT cells. Notably, upon activation murine MAIT cells express a transcriptional profile reminiscent of iNKT cells but upon resolution of the infection more closely resemble γδ T cells, highlighting the overlapping functionality of these three innate-like T cell subsets (Hinks et al., 2019). The tissue repair functions of MAIT cells have been more recently confirmed in mice by demonstrating that MR1 knock out mice had a significantly reduced wound healing ability, in the absence of γδ-T cells which could have a compensatory effect. Topical application of 5-OP-RU in wild type mice was sufficient to induce enhanced tissue repair (Constantinides et al., 2019b).

In summary, MAIT cells in their quiescent state are a homogeneous population where their effector function is finely controlled by the milieu of cytokine and ligand in their environment. MAIT cells can either promote tissue homeostasis or develop into pro-inflammatory anti-microbial T cells, depending on environmental triggers.

1.4.8 Conservation of MAIT cells between species

MR1 is highly conserved across mammalian species, first appearing around 170 Mya ago in a common ancestor of marsupial and placental mammals (Tsukamoto et al., 2013, Boudinot et al., 2016). MR1 is also the most highly conserved of all the MHC related proteins showing

>90% homology between mice and humans (Hashimoto et al., 1995). Despite this, MR1 has been lost in a select number of species, including carnivores and lagomorphs, which also lack the canonical MAIT TCR α-chain (Boudinot et al., 2016). The canonical MAIT TCR α-chain is conserved across species, with homologous TCR α-chains detected in several multiple species, including mice (Tilloy et al., 1999), cattle (Tilloy et al., 1999, Goldfinch et al., 2010), sheep (Goldfinch et al., 2010), pigs (Xiao et al., 2019a) and macaques (Greene et al., 2016). Most common laboratory mice strains have much smaller MAIT cell populations than humans, and there are differences in phenotype and tissue specificity (Koay et al., 2018). Thus mice might be considered a less relevant model for MAIT cell function in humans, though studies have described a similar developmental pathway of MAIT cells in mice and humans (Koay et al., 2018, Koay et al., 2016a). Studies in murine models have also addressed the role of MAIT cells in different infections with regards to protection (van Wilgenburg et al., 2018, Le Bourhis et al., 2010, Martin et al., 2009, Wang et al., 2018) and pathology (D'Souza et al., 2018) as well as tissue repair (Constantinides et al., 2019a).

Beyond primates and mice, the knowledge of MAIT cells in other species is limited. Pigs, cattle and sheep express the MR1 gene and the canonical MAIT cell TCRA has been identified in ruminants by qPCR (Goldfinch et al., 2010, Tilloy et al., 1999) and more recently in pigs by single-cell qPCR and TCR sequencing (Xiao et al., 2019a). Additionally, frequencies of putative MAIT cells were determined based on qPCR of the invariant MAIT cell TCR in healthy subjects of all three species (Xiao et al., 2019a, Goldfinch et al., 2010), as well as co-receptor usage and chemokine/ cytokine receptor profiles in pigs (Xiao et al., 2019a). However, no direct studies of functional MAIT cells have been performed in these species, possibly in part hindered by the lack of species-specific reagents to identify MAIT cells.

1.5 Aims of this thesis

This thesis will initially focus on the characterisation of the conventional T cell response over a time course of infection within the pig, determining the kinetics, quality and specificity of the response in multiple tissues. Further, the response between outbred pigs and the inbred Babraham pig will be compared to validate the Babraham pig line as a model of influenza infection. The conventional T cell studies will be followed by the identification of MAIT cells in multiple livestock species, including pig, cattle and sheep. Comparisons will be made between the cross-reactivity of MAIT cell tetramer reagents in these species. Finally, a more detailed characterisation of MAIT cells is carried out in cattle as a much greater MAIT cell population was identified than in other livestock species.

For clarity, this thesis will address these main aims:

- Characterise the kinetics, quality and specificity of the T cell response in the pig during H1N1pdm09 influenza infection in outbred and inbred Babraham pigs.
- Identify MAIT cells in pigs, sheep, and cattle.
- Evaluate the conservation in MR1-TCR binding between different species.
- Phenotypically characterise the MAIT cell population in cattle

Chapter 2 Material and methods

2.1 Medias and buffers

Compete media

RPMI 1640 (Sigma Aldrich) + 10% heat-inactivated fetal calf serum (FCS; Gibco) +

2mM L-Glutamine (Gibco) + 1X Penicillin-Streptomicin solution (Gibco)

MDCK media

EMEM (Sigma) + 10% heat-inactivated fetal calf serum (FCS; Gibco) +

2mM L-Glutamine (Gibco) + 1X Penicillin-Streptomicin solution (Gibco)

Freezing mix

90% heat-inactivated FCS (Gibco) + 10% dimethyl sulfoxide (DMSO; Sigma Aldrich)

MACS buffer

Phosphate buffered saline (PBS) + 2mM ethylenediaminetetraacetic acid (EDTA);

Sigma Aldrich) + 0.5% heat-inactivated FCS (Gibco)

2.2 Compounds used for cellular experiments

2.2.1 Mitogenic stimulation

All stimulation experiments were performed with positive control of either Cell Stimulation Cocktail (500X) containing (eBioscience™) containing Phorbol 12-myristate 13-acetate (PMA) and ionomycin or Concanavalin A (Con A) (SIGMA) at 4μg/ml final concentration.

2.2.2 Peptides

Overlapping peptides were designed to span the entire sequence of the NP, M1, HA and NA from H1N1pdm09 Influenza (**Appendix7.1**). Peptides were 18amino acids (aa) long overlapping by 12aa for NP and M1 and 18aa long overlapping by 14aa for HA and NA. Peptides were synthesized to >40% purity (GL Biochem Shanghai Limited) for initial peptide screens and were synthesised at >90% purity for peptide breakdown experiments.

2.2.3 MAIT cell stimulation

Ac-6-FP (Schircks Laboratories) was dissolved at 1 mM in water containing 17 mM NaOH.

5-OP-RU (as 12.3 mM stock solution in DMSO) was synthesised by collaborators at the University of Melbourne as previously described (Mak et al., 2017) and diluted in PBS to the required concentration immediately before use (DMSO content was less than 0.1% in final media).

2.3 Animal experiments

The animal experiments were approved by the ethical review processes at The Pirbright Institute, Roslin Institute and the University of Bristol and conducted according to the UK Government Animal (Scientific Procedures) Act 1986 under project licence P47CE0FF2. All three Institutes conform to the ARRIVE guidelines.

2.4 Tissue sampling and processing

Tissue sampling and processing methods were the same regardless of species.

2.4.1 PBMC

Peripheral blood was diluted 1:1 in PBS and layered over Histopaque (1.0771 g/ml) before centrifugation at 1200g for 20 minutes with the brake-off. Cells were collected at the interface washed with PBS and re-suspended in complete media.

2.4.2 Tracheobronchial lymph nodes (TBLN)

TBLN, lymph nodes were placed into a sterile petri dish, suspended in complete media before being manually disrupted and passed through a 100μm cell strainer.

2.4.3 Lung and broncho alveola lavage (BAL) cells

The lung was removed PBS was added to the lung via the trachea. Lungs were massaged, and BAL fluid poured into a sterile beaker. The BAL fluid was then transferred to 50ml Falcon tubes and centrifuged at 400g for 10 minutes to pellet the BAL cells. The remaining BAL Fluid (BALF) was frozen at -80°C. A biopsy of the lung was then taken and disassociated using the gentleMACS Octo Dissociator, in C Tubes with 7ml serum-free RPMI containing DNAse and collagenase (Sigma Aldritch). Following disassociation, the C tubes were incubated for 60 minutes at 37°C, before being dissociated a second time re-suspended in complete media and passed through a 100μm cell strainer.

2.4.4 Spleen and Ileum

After appropriate cleaning with PBS, the spleen or ileum was placed into gentleMACS Octo Dissociator (Milteny Biotec), in C Tubes (Milteny Biotec) in complete media and disassociated. Following disassociation, tissue was resuspended in complete media and passed through a 100μm cell strainer.

2.4.5 Liver

Tissue sections were placed into gentleMACS Octo Dissociator (Milteny Biotec), in C Tubes (Milteny Biotec) in complete media and disassociated. The cell suspension was resuspended in 20ml of 35% isotonic PERCOLL and diluted with complete media. The 35% PERCOLL was underlayed with 10ml 70% PERCOLL and the centrifuged at 1200g for 20 minutes. Cells were collected at the interface and resuspended in complete media before being passed through a 100μm cell strainer.

2.4.6 Milk

Milk was decanted into 50ml Falcons and centrifuged at 400g 4°C for 15 minutes. The fat layer was removed, and the cells re-suspended in PBS before centrifugation again at 400g 4°C for 15 minutes. The remaining fat layer was decanted, and cells re-suspended in PBS.

2.4.7 All tissues

Obtained single-cell suspensions were further filtered through a 100μm cell strainer, red blood cell lysed if required, washed and, if not immediately used, cryopreserved in freeze medium.

2.5 Bacterial and Virus growth

2.5.1 Bacterial growth

Tryptic soy broth (TSB) was inoculated with *Escherichia coli* strain DH5α from glycerol stocks and cultured overnight at 37 ºC at 200 RPM. The next morning a 1:100 dilution in TSB was cultured for two hours and OD at 600nm measured to estimate colony forming units (CFU)/ml (OD 600nm of 1.0 = 8 x 10^8 CFU/ml). Bacteria were washed with PBS, fixed in 1% formaldehyde for 5 min at RT, washed thrice with PBS, resuspended in TCM and stored at -20 ºC.

Mycobacterium bovis strain BCG Danish SSI 1331 (Statens Serum Institute) were cultured in glass vials in Middlebrook 7H9 broth supplemented with Tween 80, Amphotericin B (all Sigma-Aldrich), and BD Difco™ BBL™ Middlebrook ADC Enrichment at 37 ºC with agitation with a magnetic stir bar. After 25 days, the bacterial culture was vortexed vigorously, and after 1 minute, the 'supernatant' was harvested and passed several times through a 21g needle to obtain a single cell suspension. Bacteria were pelleted and resuspended in 7H9 broth supplemented with 30% glycerol, aliquoted and stored at -80 ºC. Thawed aliquots were serially

diluted 1:10 in 7H9 broth, and 100ul of these suspensions were cultured on Middlebrook 7H11 agar, supplemented with OADC (both BD), to determine CFU/ml.

2.5.2 Virus growth

Virus inoculum was diluted 1:10000 and added to 80% confluent MDCK cells (Central Service Unit, The Pirbright Institute, UK), containing serum free EMEM (SIGMA). Cells were incubated for 48-72 hours to allow for viral growth. The supernatant was harvested and centrifuged at 1000g for 5 minutes to remove cellular debris. Virus containing supernatant was aliquoted into 1.8ml cryovials and stored at -80.

2.5.3 Viral titration Plaque assay

Virus titres of MDCK grown virus or nasal swabs were determined by plaque assay on MDCK cells (Central Service Unit, The Pirbright Institute, UK). Samples were 10-fold serially diluted in Dulbecco's Modified Eagle's Medium (DMEM) and 200µl overlayered on confluent MDCK cells in 12 well tissue culture plates. After 1 hour, the plates were washed and overlayered with 2ml of culture medium containing 0.66 % Agar. Plates were incubated at 37°C for 48 to 72 hours and plaques visualized using 0.1% crystal violet. Plaques were counted at the appropriate dilution and expressed as plaque forming units (PFU) per ml of nasal swab diluent.

2.6 Flow cytometry

Cells were first washed in PBS and pelleted in a well of a 96-well U-bottom plate by centrifugation (1,800 rpm, 4minutes).

2.6.1 MR1 tetramer staining

Cryopreserved cells were thawed in complete media, and 1-3 x 10^6 cells / well were seeded into a 96 well plate. Cells were stained with either 5-OP-RU MR1 or 6-FP MR1 pre-diluted tetramer which had been previously titrated for optimum staining in PBS supplemented with

2% FCS for 40 minutes at room temperature. Cells would then be pelleted by centrifugation (1,800 rpm, 4minutes).

2.6.2 Pig SLA tetramer staining

Biotinylated NP peptide loaded SLA monomers, were freshly assembled into tetramer with streptavidin PE (Biolegend, UK) and diluted with PBS to a final concentration of 0.1 µg/µl. 1-3 million mononuclear cells were incubated with protease kinase inhibitor (Dasatinib, Axon Medchem) in PBS for 30 minutes at 37°C and 0.3 µg of tetramer was added to the cells on ice for another 30 minutes. Cells would then be pelleted by centrifugation (1,800 rpm, 4minutes).

2.6.3 Surface staining

Cell pellets were broken up and stained by a master mix containing Biotinylated/ fluorochrome-conjugated and unconjugated antibodies (**Table 2.1 List of antibodies for all experiments)** at optimised dilutions and LIVE/DEAD™ Fixable Near-IR stain (Invitrogen), an amine-reactive dye to exclude dead cells, diluted 1:500. Cells were incubated at 4°C for 20 minutes. When required fluorochrome-conjugated secondary antibodies were incubated at 4°C for 20minutes. Cells were subsequently fixed by 2% formaldehyde (Sigma Aldrich) at 4°C for 15 minutes. Cells were then washed and resuspended with PBS for flow cytometer acquisition or further intracellular staining.

2.6.4 Intracellular cytokine staining

For intracellular cytokine staining, Brefeldin A (BioLegend) was added at 1:1000 for the final 5 hours of the stimulation prior to surface staining. Cells were stained for surface markers (**Table 2.1 List of antibodies for all experiments**) and near-IR fixable Live/Dead stain (Invitrogen) prior to fixations/permeabilisation with Cytofix/Cytoperm (BD Biosciences) as per the manufacturer's instructions before intracellular staining and resuspended with

antibodies diluted in 1X Permeabilisation buffer. Following 25 minutes incubation with antibodies at 4°C, cells were washed and resuspended with PBS for flow cytometer acquisition.

2.6.5 Transcription factor stains

Transcription factor staining TFs were stained using the Foxp3/TF Staining Buffer Set (eBioscience). Cells were surface stained, washed with PBS, and resuspended in 1X Fixation/Permeabilisation buffer for 60 minutes at RT. After washing with 1X Permeabilisation buffer (eBioscience), cells were further stained in 1X Permeabilisation buffer with antibodies that detect the TFs of interest (**Table 2.1**) at optimised dilutions for 60 minutes at 4c. The cells were subsequently washed and resuspended in PBS prior to acquisition.

Table 2.1 List of antibodies for all experiments

	Purpose	Antigen	clone	Isotype	Labelling strategy	Flourochrome	Source of primary antibody
Cattle	MAIT identification / Frequency	CD3	MM1A	IgG1	Secondary antibody	AF488	In-house
		MHCII	ILA21	IgG2a	Secondary antibody	AF647	In-house
	MAIT Co receptor phenotyping	CD4	ILA12	IgG2a	Secondary antibody	APCcy7	In-house
		TCRγδ	GB21a	IgG2b	Secondary antibody	PEcy7	In-house
		CD8	ILA51	IgG1	directly conjugated	AF647	In-house
		CD3	MM1A	IgG1	directly conjugated	AF488	In-house
	MAIT memory / activation status	CD3	MM1A	IgG1	secondary antibody	AF488	In-house
		CD45RO	ILA116	IgG3	secondary antibody	PE-cy7	In-house
		CD25	CACT108a	IgG2a	secondary antibody	AF-647	In-house
		CCR-7	3D12	IgG2a	directly conjugated	eFLour780	eBioscience
	MAIT Activation assays	CD8	ILA51	IgG1	biotin-streptavidin	BV-421	In-house
		IFN-γ	CC302	IgG1	directly conjugated	AF647	Bio-Rad Laboratories
		TNF	CC327	IgG2b	directly conjugated	AF488	Bio-Rad Laboratories
	MAIT transcription factor	CD8	ILA51	IgG1	biotin-streptavidin	BV-421	In-house
		T-bet	4B10	IgG1	directly conjugated	FITC	Biolegend
		EOMES	WD1928	IgG1	directly conjugated	eFlour661	Invitrogen
		PLZF	R17-809	IgG1	directly conjugated	AF647	BD Biosciences
		ROR-γT	Q21-559	IgG2b	directly conjugated	AF647	BD Biosciences

	CD69	CD8	ILA105	IgG2a	Secondary antibody	AF647	In-house
		CD69	KTSN7A	IgG1	Secondary antibody	AF488	Kingfisher
	Perforin	CD8	ILA105	IgG2a	Secondary antibody	APC-Cy7	In-house
		Perforin	dG9	IgG2b	directly conjugated	Fitc	BD
	Sorting	CD3	MM1A	IgG1	secondary antibody	AF488	In-house
		CD8	ILA105	IgG2a	Secondary antibody	APC-Cy7	In-house
Human	MAIT identification / Frequency	CD3	BW264/56	IgG2a	directly conjugated	Vioblue	
		CD161	191B8	IgG2b	directly conjugated	APC	Miltenyi Biotec
Sheep	MAIT identification / Frequency	CD8	CC63	IgG2a	secondary antibody	PercPcy5.5	In-house
Pig	MAIT identification / Frequency	CD3	BB23-8E6-8C8	IgG2a	directly conjugated	APC	BD Biosciences
		SLAII	2E9/13	IgG2b	directly conjugated	FITC	Bio-Rad Laboratories
	Conventional T cells staining	CD4	74-12-4	IgG2b	directly conjugated	PerCP-Cy5.5	BD Biosciences
		CD8b	PPT23	IgG1	directly conjugated	FITC	Bio-Rad Laboratories
		TNF	MAb11	IgG2	directly conjugated	BV421	BioLegend
		IFN-γ	P2G10	IgG3	directly conjugated	APC	BD Biosciences
		IL-2	A150D 3F1 2H2	IgG2a	directly conjugated	PE-Cy7	ThermoFisher
	peptide stimulation ICS	CD3	BB23-8E6-8C8	IgG2a	directly conjugated	PE-Cy7	BD Biosciences
		CD4	74-12-4	IgG2b	directly conjugated	PerCP-Cy5.5	BD Biosciences
		CD8a	76-2-11	IgG2a	directly conjugated	FITC	BD Biosciences
		TNF	MAb11	IgG2	directly conjugated	BV421	BioLegend
		IFN-γ	P2G10	IgG3	directly conjugated	APC	BD Biosciences
	5-OP-RU stimulation	CD3	BB23-8E6-8C8	IgG2a	directly conjugated	PE-Cy7	BD Biosciences
		CD4	74-12-4	IgG2b	directly conjugated	PerCP-Cy5.5	BD Biosciences
		CD8a	76-2-11	IgG2a	directly conjugated	FITC	BD Biosciences
		TNF	MAb11	IgG2	directly conjugated	BV421	BioLegend
		IFN-γ	P2G10	IgG3	directly conjugated	PE	BD Biosciences
		TCR1 delta	PGBL22A	IgG1	Secondary antibody	APC	Kingfisher
	SLA matched tetramer staining	CD3	BB23-8E6-8C8	IgG2a	directly conjugated	PE-Cy7	BD Biosciences
		CD4	74-12-4	IgG2b	directly conjugated	PerCP-Cy5.5	BD Biosciences
		CD8b	PPT23	IgG1	directly conjugated	FITC	Bio-Rad Laboratories

2.6.6 Data acquisition and analysis

Data were acquired on a MACSQuant Analyser (Miltenyi Biotec) or BD Fortessa and analysed using FlowJo software (Tree Star, Inc.). The expression of markers was determined according to the appropriate isotype control or fluorescence minus one (FMO) or unstimulated sample.

Unless otherwise stated, all flow cytometry experiments were first gated for live single-cell lymphocytes using forward scatter (FSC)/ side scatter (SSC) and LIVE/DEAD Fixable die negative gating (**Figure 2.1**). All subsequent gating is described in individual figure legends.

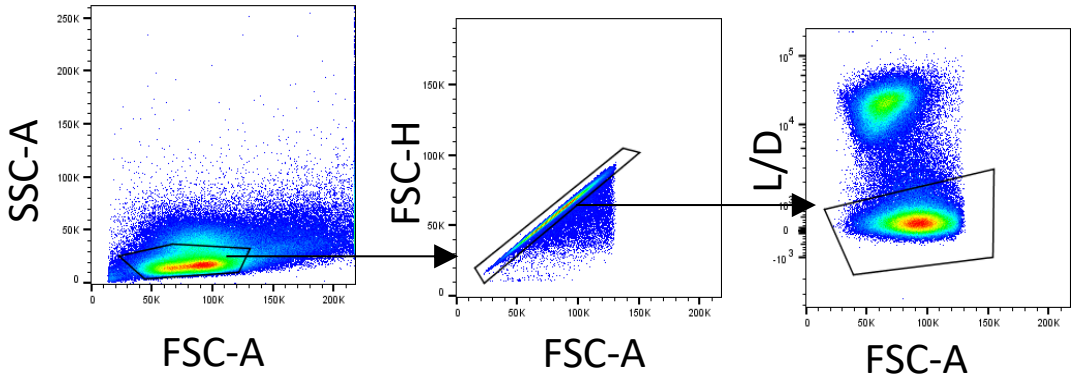

Figure 2.1 Live lymphocyte gating strategy All flow cytometry experiments were first gated for live single cell lymphocytes using forward scatter (FSC) and side scatter (SSC) and gating LIVE/DEAD Fixable die negative cells .

2.7 ELISpot

Frequencies of IFN-γ secreting cells were determined by ELISpot IFN-γ assay. MultiScreen-HA ELISPOT plates (Merck Millipore) were coated with primary anti-IFN-γ Pig clone P2G10 (BD Pharmingen 0.5µg/ml), human clone 1-D1K (Mabtech-34 5µg/ml) cattle and sheep clone cc330 (Serotec, 2µg/ml) and incubated at 4°C overnight. Plates were washed and blocked with complete media for 2 hours. Plates were seeded with 2.5 x 10^5 human, cattle, pig or sheep PBMC and stimulated with either 1µM 5-OP-RU, 1µM AC-6-FP, 4µg/ml ConA (Sigma-Aldrich) or media control. Plates were incubated overnight at 37°C before washing with PBS containing 0.05% Tween 20 and addition of secondary biotinylated IFN-γ detection Abs (Pig

clone P2C11 (BD Pharmingen 0.5μg/ml), human clone 7-B6-1 (Mabtech 0.25μg/ml) cattle and sheep clone cc302 (Serotec 2μg/ml)). Plates were incubated for 2 hours at room RT, washed a further five times, and streptavidin–alkaline phosphatase (Invitrogen) was added for 1 hour. Spots were visualised using alkaline phosphatase substrate kit (Bio-Rad), and the reaction stopped using water. Immunospots were enumerated using the AID ELISPOT reader (AID Autoimmun Diagnostika). Results expressed as the total number of IFN-γ producing cells per 10^6 input PBMC following subtraction of the average number of IFN-γ positive cells in medium control wells.

2.8 Cell sorting and depletion

MACS isolation and depletion were performed on cryogenically stored or freshly isolated cells. For cattle CD8 cell isolation, cattle cells were incubated with biotinylated mAb ILA51 (anti-CD8, produced in-house) in MACS buffer on ice for 15 minutes with resuspending every 5 minutes. Following washing, cells were stained with magnetic anti-biotin beads (Miltenyi Biotec), and labelled cells were isolated using MS columns (Miltenyi Biotec) according to the manufacturer's instruction. For depletion cells were incubated with PE- labelled CD8β (Clone PPT23 Bio-Rad) or CD4 or CD4 antibodies (clone 74-12-4 BD) in MACS buffer on ice for 15 minutes with resuspending every 5 minutes. Following washing, cells were stained with magnetic anti-PE (Miltenyi Biotec), and labelled cells were depleted using LD columns (Miltenyi Biotec) according to the manufacturer's instruction.

2.9 Statistical analysis

All statistical analyses were performed using Prism software version 8 (GraphPad). Data presented in the text and figures are means with the standard error of the mean (SEM) or standard deviation (SD). * $p<0.05$, ** $p<0.01$, *** $p<0.001$, **** $p<0.0001$, by the indicated statistical test in each figure legend.

Chapter 3 Kinetics, magnitude and specificity of conventional T cell responses during H1N1pfm09 infection in outbred and inbred pigs.

3.1 Aims and rationale

Though the previously discussed studies have tried to address the conventional T cell response to influenza infection in pigs, no detailed analysis of the cellular immune responses to H1N1pdm09 virus has been performed. This strain crosses the species barrier from humans to pigs and vice versa. H1N1pdm09 circulating in swine herds maintains antigenic similarity to human seasonal strains, providing an opportunity to study a virus with continuing zoonotic (and reverse zoonotic) potential. Further, no detailed study of the T cell immune response in BAL has been performed; a location which we have shown to contain tissue resident memory cells that are essential for heterosubtypic protection (Holzer et al., 2018a).

As the Babraham pig is SLA homozygous between individuals, they make an ideal model for the study of the specificity of the immune response to influenza in a large animal model. To this end, our group has previously identified immunodominant CD8 epitopes in the BM pig (Tungatt et al., 2018). However, these epitopes were defined in pigs immunised with the candidate single cycle influenza vaccine, signal minus flu (S-FLU), which derives its internal proteins from the PR8 influenza strain (Tungatt et al., 2018). Indeed, of the four immunodominant epitopes identified only two ($NP_{217-225}$ and $NP_{290-298}$) cross-reacted with H1N1pdm09 infected animals with only $NP_{290-298}$ being wholly conserved between the PR8 and H1N1pdm Influenza. Furthermore, only one CD4 epitope has been identified in the BM

pig again using the PR8 influenza strain internal proteins (Baratelli et al., 2020). Therefore, further identification of novel H1N1pdm09 influenza epitopes will be a useful step in determining the fine specificity of the cellular response in the BM pig.

This chapter is focused on the characterisation of influenza specific T cell responses in inbred Babraham (BM) and outbred (OB) pigs during H1N1pdm09 influenza infection to address the following specific aims.

1. Quantify the magnitude of the CD8 and CD4 response in different tissues during influenza infection in OB and BM pigs.
2. Determine the quality of CD8 and CD4 T cell responses in terms of IFN-γ, TNF and IL-2 production over time in OB and BM pigs
3. Compare the response between OB and BM pigs to validate the Babraham pig as a model for influenza infection.
4. Determine the specificity of the immune response to influenza proteins (NP, M1, HA, NA) in the Babraham pig
5. Determine novel H1N1pdm09 CD8 epitopes recognised by the Babraham pig
6. Determine Novel H1N1pdm09 CD4 epitopes recognised by the Babraham pig

3.2 Chapter specific methods

3.3 influenza H1N1pdm09 challenge

Thirty two outbred old Landrace x Hampshire cross (from a commercial high health status herd) and 56 inbred Babraham pigs (bred at Animal Plant Health Agency, APHA Weybridge, UK) were screened for the absence of IAV infection by matrix gene real time RT-PCR and for antibody-free status by HAI using four swine influenza virus - H1N1pdm09, H1N2, H3N2 and avian-like H1N1. The average age of the outbred pigs seven days before the challenge was 8.7

weeks and of the Babrahams 8.3 weeks. Pigs were challenged intra-nasally with 1×10^7 PFU of MDCK grown swine A(H1N1) pdm09 isolate, A/swine/England/1353/2009, derived from the 2009 pandemic virus, swine clade 1A.3. (H1N1pdm09) in a total of 4 ml (2 ml per nostril) using a mucosal atomisation device MAD300 (MAD, Wolfe-Tory Medical).

3.3.1 In vitro influenza stimulation

Cryopreserved mononuclear cells from BAL, lung, TBLN blood and spleen were thawed and stimulated for 18 h for ICS or 36 h for ELISPOT at 37˚C with live MDCK cell–grown strain A/Sw/ Eng/1353/09 (MOI of 1). For ICS Golgi Plug (BD Biosciences) was added according to the manufacturer's instructions for a final 5 h before intracellular cytokine staining. Following stimulation, cells were stained as described in chapter 2.6

3.3.2 In vitro Peptide stimulation

Cryopreserved mononuclear cells from BAL, lung, TBLN blood and spleen were thawed and stimulated for 6 h for ICS or 36 h for ELISPOT at 37˚C with synthesised peptides (Shanghai Biochem) re-suspended in DMSO (final DMSO concentration always <0.5%). For ICS Golgi Plug (BD Biosciences) was added according to the manufacturer's instructions for a final 5 h before intracellular cytokine staining. Following stimulation, cells were stained as described in chapter 2.6.

3.4 Influenza time course: experimental design, viral load and cellular dynamics.

Five experiments were performed to characterise local and systemic cellular immune responses. In each experiment, ten 8-week-old pigs were infected intranasally with H1N1pdm09 virus and monitored for clinical signs. One pig was culled on each of days 1 to 7, 9, 11 and 13 post-infection. Four uninfected controls were sampled in parallel two on the day of infection and two at day eight post-infection. Two experiments with outbred Landrace x

Hampshire cross (OB) pigs (referred to as OB1 and OB2) and two with inbred Babraham (BM) pigs (referred to as BM1 and BM2) were performed**.** The final fifth experiment was carried out with 18 BM (experiment BM3) in which three pigs were culled on each of days 6, 7, 13,14, 20 and 21 post-infection (**Figure 3.1).** Viral load was determined in daily nasal swabs **(Figure 3.2).**

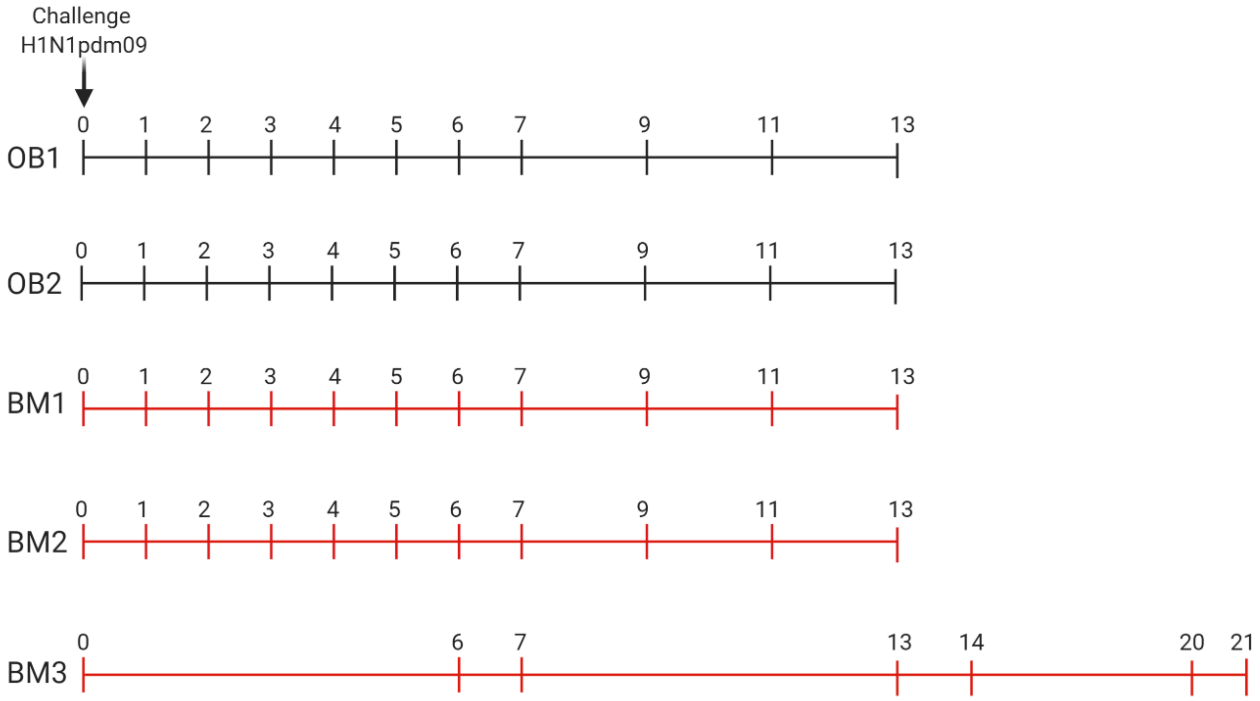

Figure 3.1 Influenza time course experimental design Pigs were infected with H1N1pdm09 and culled on the days indicated. Two experiments with outbred (OB1 and OB2, black line) and two with inbred Babraham pigs (BM1 and BM2, red line) were performed. Two in-contact animals were included in each experiment one culled at day 11 and one at day 13 post infection. An extended time course of 21 days was performed with 18 inbred Babraham pigs (BM3, red line) with animals culled on the indicated days.

Viral load for each experiment was determined by plaque assay of nasal swabs collected at each time point until the cull day of each animal other than days 8, 10 and 12 or until DPI 10 in the case of the BM3 animals. No detectable virus was present in the nasal swabs of any animal at day 0 (data not shown). Following intranasal delivery of H1N1pdm09 viral titre in nasal swabs peaked on day one post-infection (DPI), and was maintained until day 4, declining sharply after 4 DPI with no detectable virus after 7 DPI. In some animals, but most notably in BM1 and BM3, two peaks of virus shedding were detected at 1 and 4 DPI.

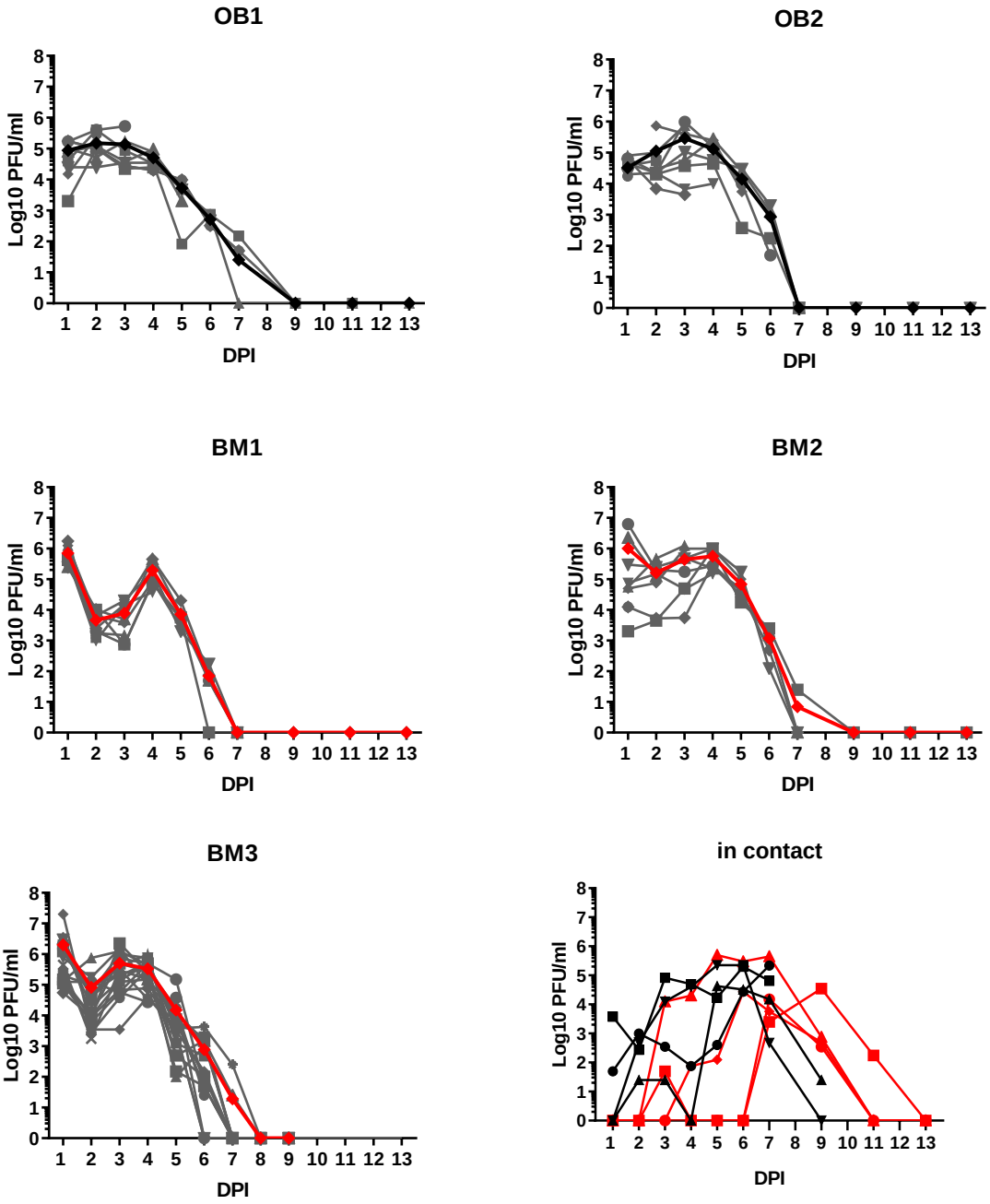

Figure 3.2. Influenza time course viral load. All pigs were swabbed each day following infection until their day of cull. Viral titre was determined by plaque assay and expressed as PFU/ ml. Line graphs depict the viral titre of each animal at each DPI, with thick black (OB1 and OB2) or red (BM1 BM2 and BM3) lines showing mean viral titre of all animals at each time point.

The proportion of CD8β, CD4 cells over the time course in broncho-alveolar lavage (BAL), lung, tracheobronchial lymph node (TBLN), PBMC and spleen were determined by flow cytometry analysis in the outbred (OB1 and OB2) and Babraham (BM1 and BM2) animals (

Figure 3.3). The CD8 population over the time course remained at a steady state until DPI 7, at which point an increase in percentage population is observed in the Babraham pigs. A corresponding increase was not seen in the OB animals, though inter animal variability was also higher in the OB animals compared to the BM. The CD4 population remained at a steady state over the time course of infection with no clear increase at any time point following infection. Interestingly, the BM animals had a significantly lower proportion of CD8β T cells than OB, apparent in all tissues in naïve unexposed animals - 6.6% in BM vs 24.2% in OB in BAL, 4.2% vs 16.2% in lung, 3.2% vs 9.4% in PBMC, 7.6% vs 11.5% in TBLN and 3.5% vs 9.5% in spleen (**Figure 3.4**). The CD4 population was comparable between the outbred and Babraham animals with no significant differences.

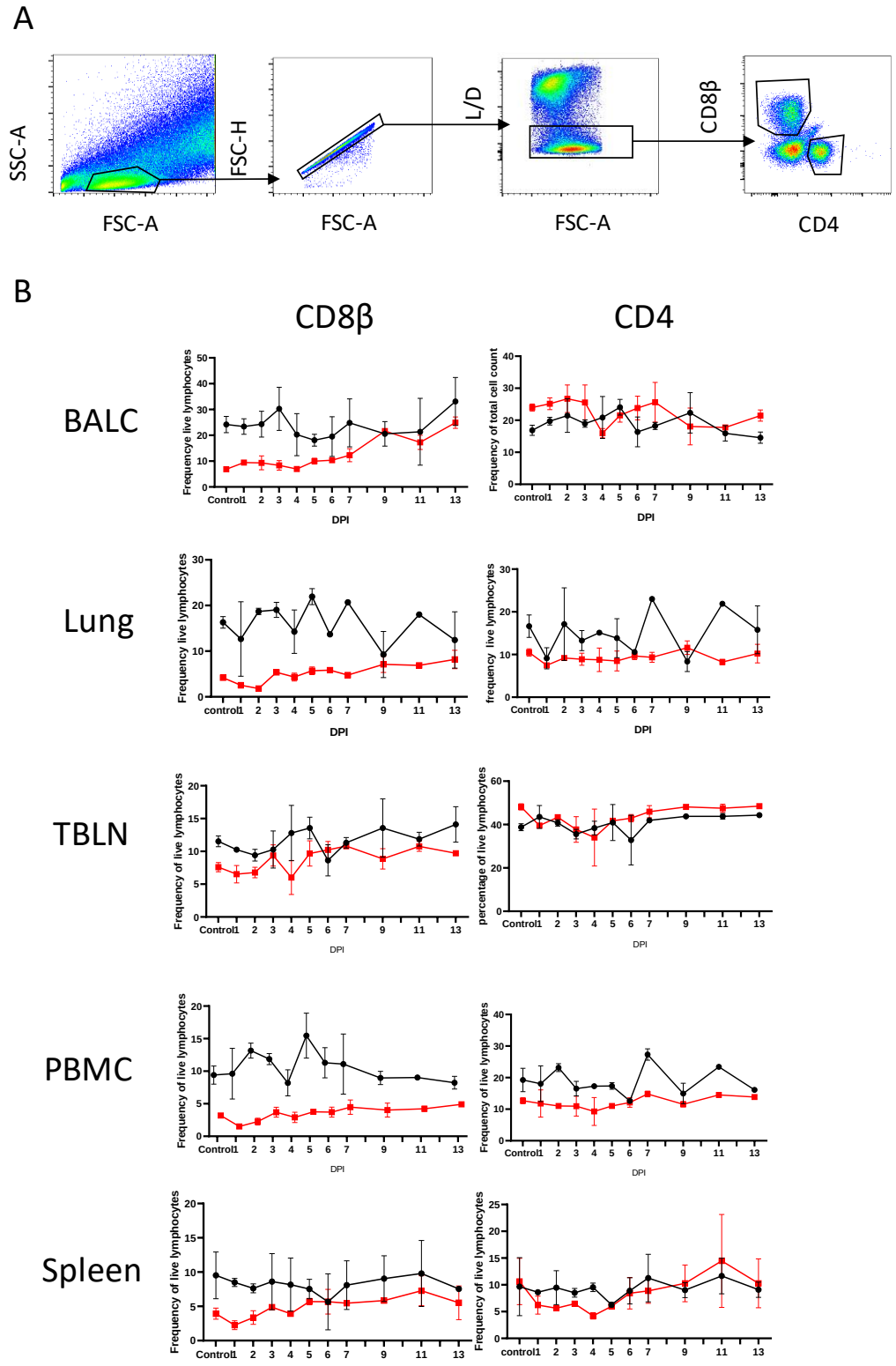

Figure 3.3. CD8β and CD4 T cell populations as a percentage of total lymphocytes. **(A)** Gating strategy for CD4 and CD8 T cell identification. **(B)** Line graphs depicting the mean CD8β and CD4 populations identified in BAL, lung, TBLN, PBMC and spleen over time in the OB1 and OB2 (black line) and BM1 and BM2 (red line) animals at each time point following influenza infection.

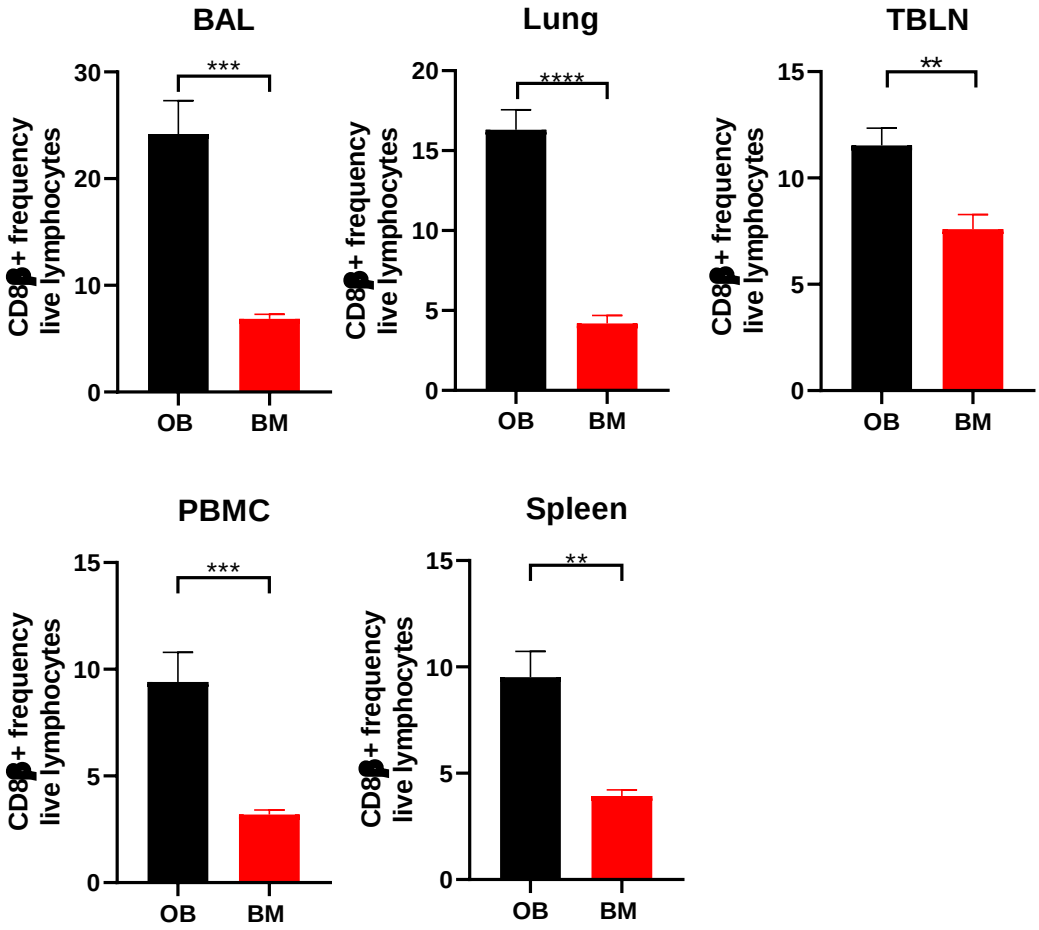

Figure 3.4. Comparison of CD8β population in outbred (OB1 and OB2) and inbred (BM1 and BM2) control animals. The live CD8β populations in naïve control OB and BM animals were identified by gating lymphocytes followed by FSC-A and FSC-H to exclude doublets. Near-Infrared Fixable LIVE/DEAD negative cells were selected before CD8β+ identification. Bar graphs depict mean CD8β+ population in OB (black) and BM (red) animals. Mean with SEM are depicted with two-way ANOVA comparing the mean of the OB and BM CD8β population. Asterisks denote * $p \leq 0.05$, ** ≤ 0.005, *** ≤ 0.0001.

To determine the kinetic of the conventional T cell immune response following infection, IFN-γ secreting cells from H1N1pmd09 infected pigs were enumerated by ELISpot following ex vivo stimulation with H1N1pdm09 (**Figure 3.5**). IFN-γ spot forming cells (SFC) were detectable from 6 DPI and maintained in all tissues until 21 DPI. While at the early stage of infection the strongest responses were in the TBLN (474 SFC at day 7 DPI) from 14 to 21 DPI the highest IFN-γ secretion was detected in the lung with SFC continuing to expand in this tissue (average 368 SFC at DPI 14 and 972 SFC at DPI 21). The response in the BAL appeared lower than lung, but the proportion of lymphocytes, and therefore T cells, is much lower in the BAL as a percentage of the total cellular population due to the large alveolar macrophage population in this compartment (data not shown). The response in the PBMC was lowest across all the tissues peaking at 13 DPI (296 SFC at 13 DPI). Analysis of spleen by ELISpot was irreproducible with very high background and therefore, was not included. Despite the differences observed in the frequency of CD8 between BM and OB, no difference was observed between breeds in the ELISPOT response.

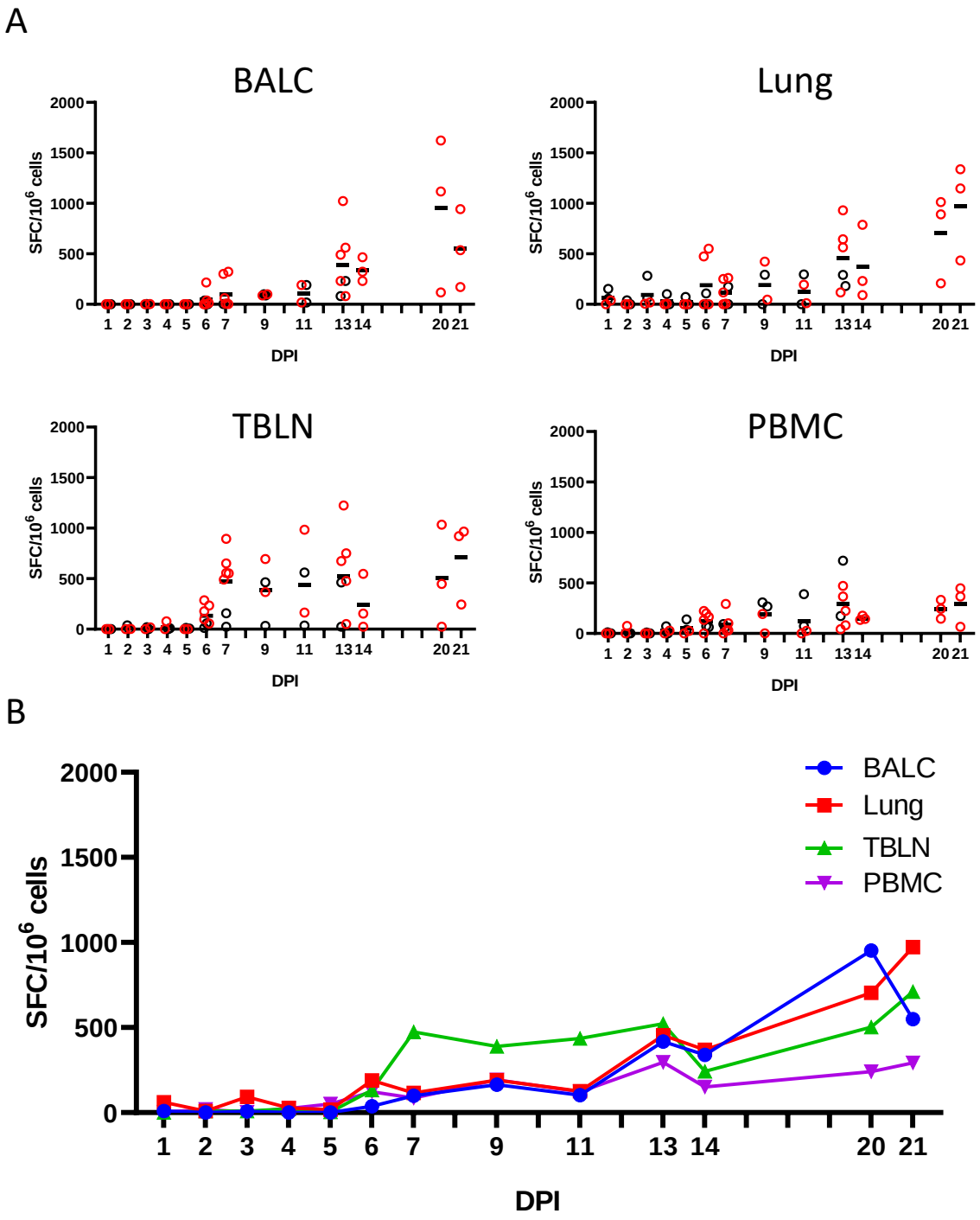

Figure 3.5 IFN-γ cellular response during influenza infection. **(A)** IFN-γ secreting spot forming cells (SFC) in BAL, lung, TBLN and PBMC in outbred (black circles) and inbred (red circles) pigs were enumerated after stimulation with H1N1pdm09 or medium control. **(B)** The mean SFC for each population is shown. DPI 1 to 7, 9, 11 and 13 each show results from 2 outbred and 2 inbred pigs. DPI 6, 7, 13, 14, 20 and 21 also include results from 3 additional inbred pigs.

3.5 CD8 T cell responses in different tissues during influenza infection in outbred and inbred Babraham pigs.

ELISpot can be useful in identifying IFN-γ secreting cells and can give a general overview of the level of IFN-γ response. However, it does not give any phenotypic information about the responding cellular subset. Therefore, to further dissect the T cell response antigen-specific CD8β T cells were enumerated using previously characterised peptide-loaded SLA tetramers, which specifically identify CD8 β+ T cells in Babraham pigs that are reactive to$NP_{290-298}$ (DFEREGYSL)(Tungatt et al., 2018). Tetramer binding T cells were measured in BM1, BM2 and BM3 (**Figure 3.6**). Detectable $NP_{290-298}$ responses were seen in BAL and lung at 6 DPI, peaking at 9 DPI in BAL with 4% of total CD8β T cells with this response contracting but still present at DPI 21 (1.5% CD8β T cells). The response of the $NP_{290-298}$ reactive T cells in the lung was lower than in the BAL and did not reach its peak until 20 DPI (2% of CD8β+ T cells). In TBLN one animal responded at 5 DPI, but the peak was at 9 – 11 DPI, and tetramer positive cell were still present at 21 DPI. Compared to the local tissues, the responses in PBMC and spleen were low and transient, less than 0.3% of PBMC and 0.4% of spleen CD8β T cells were detected by the $NP_{290-298}$ tetramer at any time point, and negligible response was detectable by 20-21 DPI.

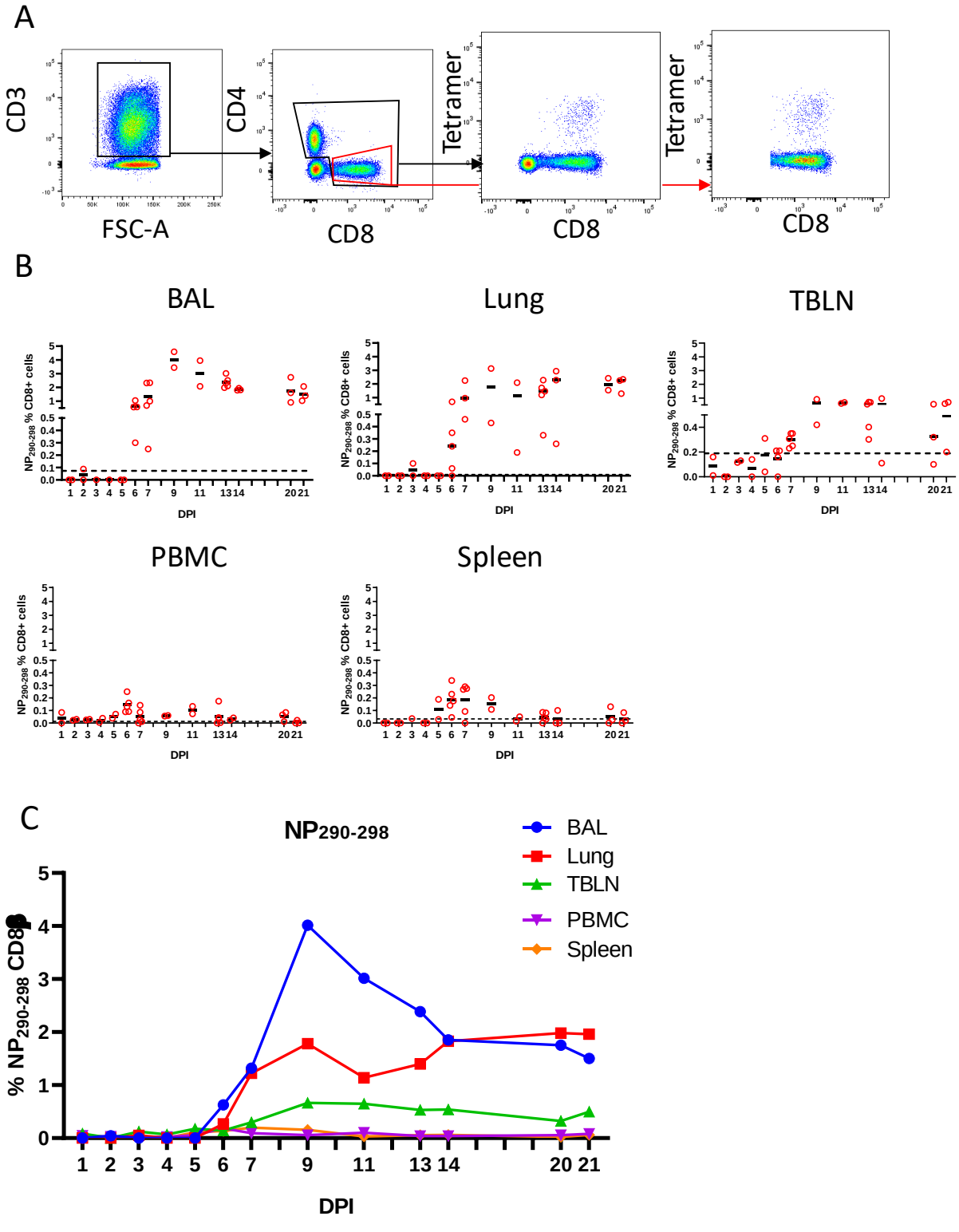

Figure 3.6 CD8 NP290-298 specific tetramer response over a time course of influenza infection **(A)** Representative flow cytometry plots and gating strategy for tetramer identification, cells were previously gated for life single cells. **(B-C)** Proportions of $NP_{290-298}$ CD8 T cells in tissues. SLA matched tetramers containing irrelevant peptide was subtracted at each time point. Dotted lines indicate proportions of tetramer positive cells in uninfected animals. 2 inbred pigs are shown for days 1 to 5 and 9 to 11. DPI 6, 7, 13, 14, 20 and 21 show data from 3 additional inbred pigs.

To analyse the functional response of the CD8β T cells cytokine production of IFN-γ, TNF and IL-2 were assessed following stimulation with homologous H1N1pdm09 influenza (**Figure *3.7***). The kinetic of the cytokine response was similar when compared to ELISpot and tetramer binding. There was minimal response up to 5 - 6 DPI, followed by a marked increase in cytokine producing T cells particularly in the BAL (peak of 7.9% IFN-γ and 7.6% TNF at 9 DPI) and lung (peak of 1.3% IFN-γ and 0.6% TNF at 9 DPI). CD8 produced minimal IL-2 in all tissues other than BAL, where a peak of 1.3% was detected at 11 DPI. TBLN, PBMC and spleen had a much lower proportion of cytokine producing CD8 cells with maximum 0.21 IFN-γ and 0.15 TNF in PBMC at 9 DPI. The cytokine response was maintained in all tissues up until day 21, other than PBMC, where a greater than 6-fold decrease in IFN-γ response was observed between DPI 9 and 21.

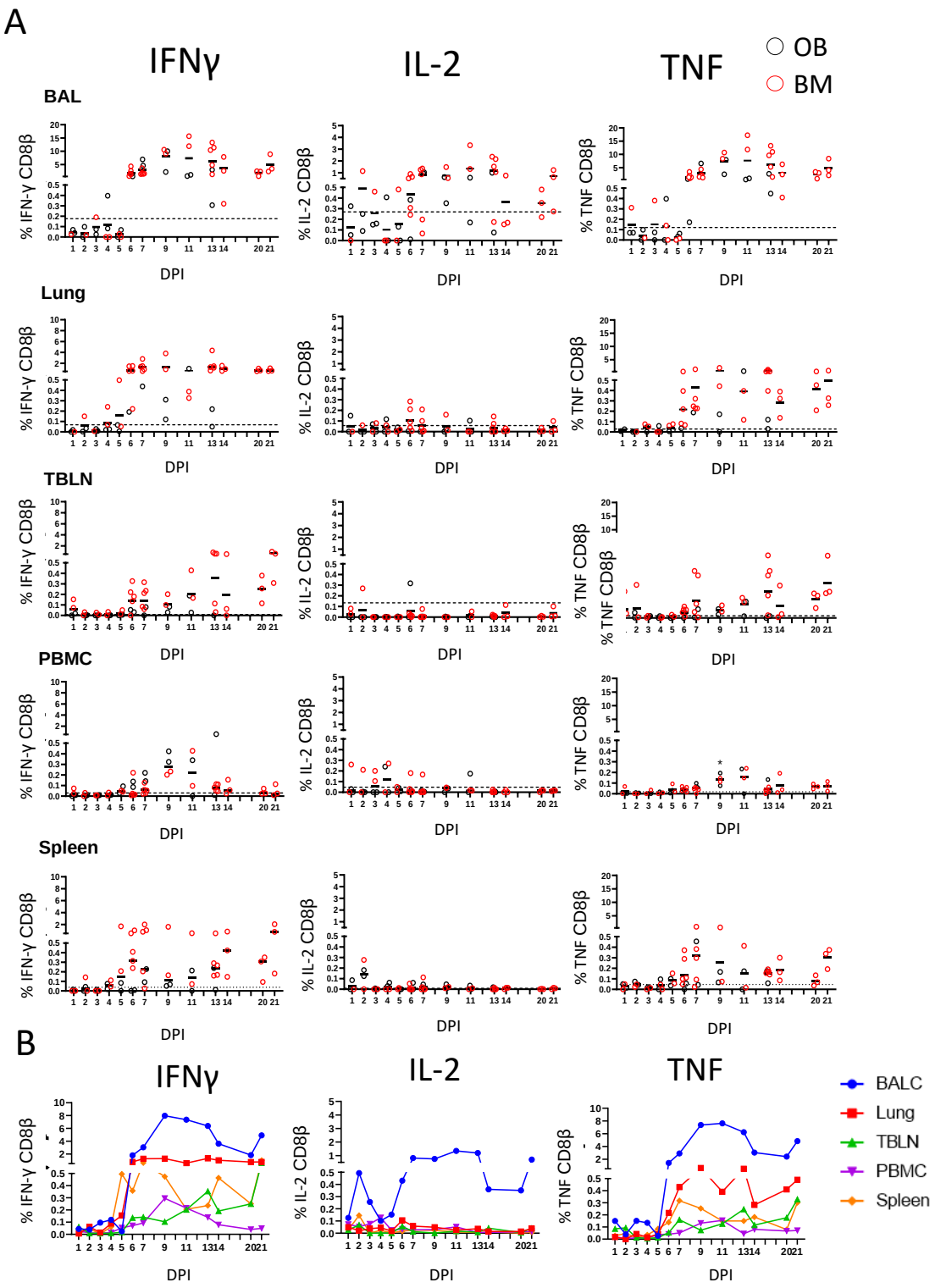

Figure 3.7 CD8β T cell cytokine response. . **(A)** Cytokine response of CD8β T cells in outbred (black circles) and inbred (red circles) pigs at each time point following influenza infection. BAL, lung, TBLN or PBMC cells were stimulated with H1N1pdm09 and cytokine secretion measured using intra-cytoplasmic staining. The mean of the 22 uninfected control animals is represented by a dotted line. DPI 1 to 7, 9, 11 and 13 each show results from 2 outbred and 2 inbred pigs. DPI 6, 7, 13, 14, 20 and 21 also include results from 3 additional inbred pigs. (B) The mean percentages for IFN-γ, TNF and IL-2 in each tissue for both OB and BM together are shown over the time course.

The polyfunctionality of the CD8 response was also determined (**Figure 3.8**). Responses were dominated by IFN-γ single producing cells with IFN-γ/TNF double producing cells also present in all tissues, but at a higher proportion in BAL. A triple secreting IFN-γ/TNF/IL-2 population was observed in the BAL, and these produced higher levels of IFN-γ per T cell as measured by MFI. (**Figure 3.9**). The functionality of the cytokine response was comparable between BM and OB animals, with no apparent differences in the quality of response between breeds. In all tissues, the higher proportion of double and triple secreting T cells coincides with time points where a greater magnitude of cytokine response is detected.

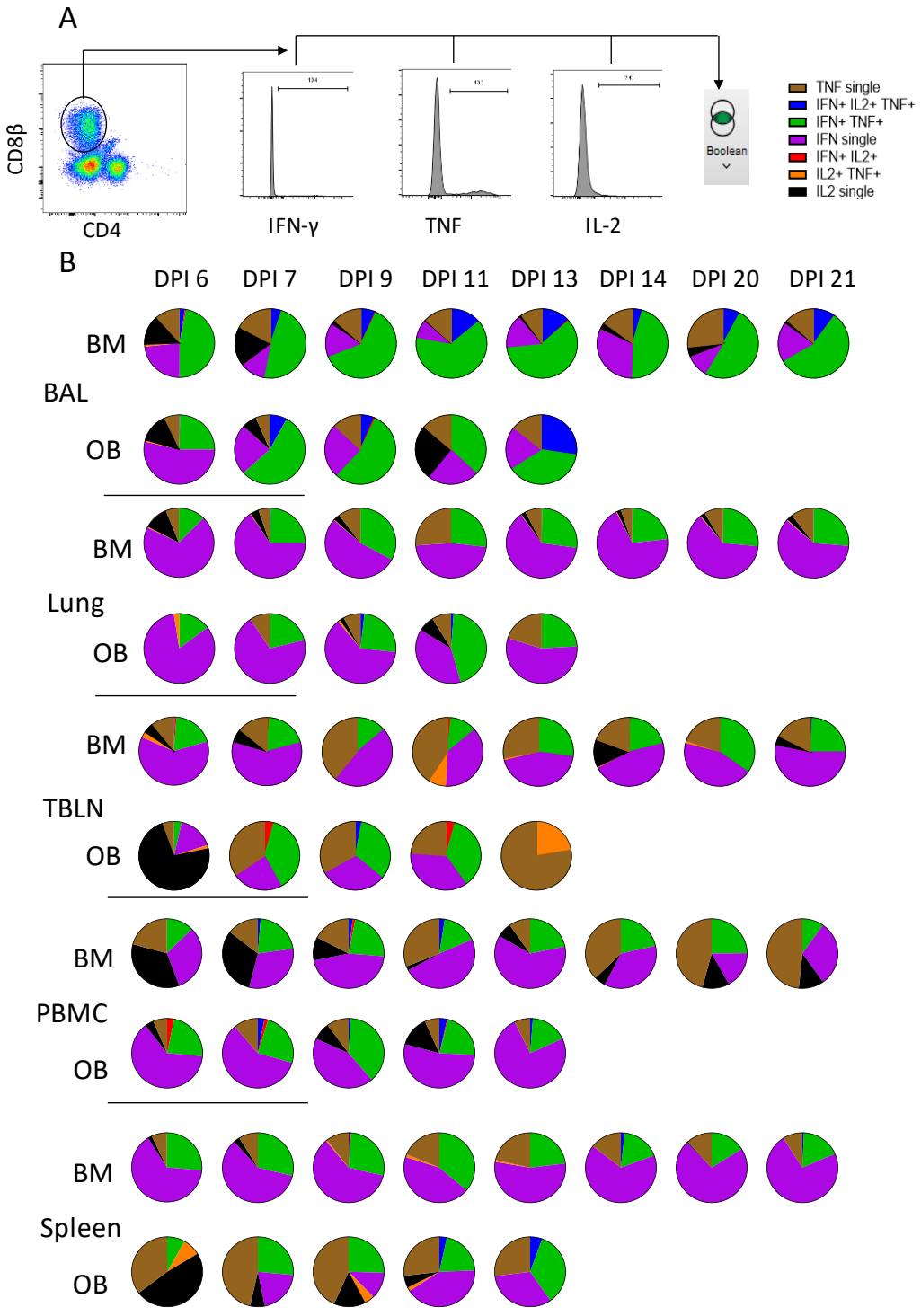

Figure 3.8 CD8 T cell cytokine response **(A)** Representative image of Boolean gating of cytokine positive CD8β T cells to determine cytokine responses in multiple tissues. **(B)** Pie charts depict the mean proportion of each group of single, double and triple IFN-γ, IL-2 and TNF cytokine secreting CD8β T cells as a percentage of the total cytokine production in BAL, lung, TBLN, PBMC and spleen. OB and BM animals are presented for comparison. Cytokine response from DPI 6, 7, 9, 13 and 21 are shown. All cytokine populations were media control deducted.

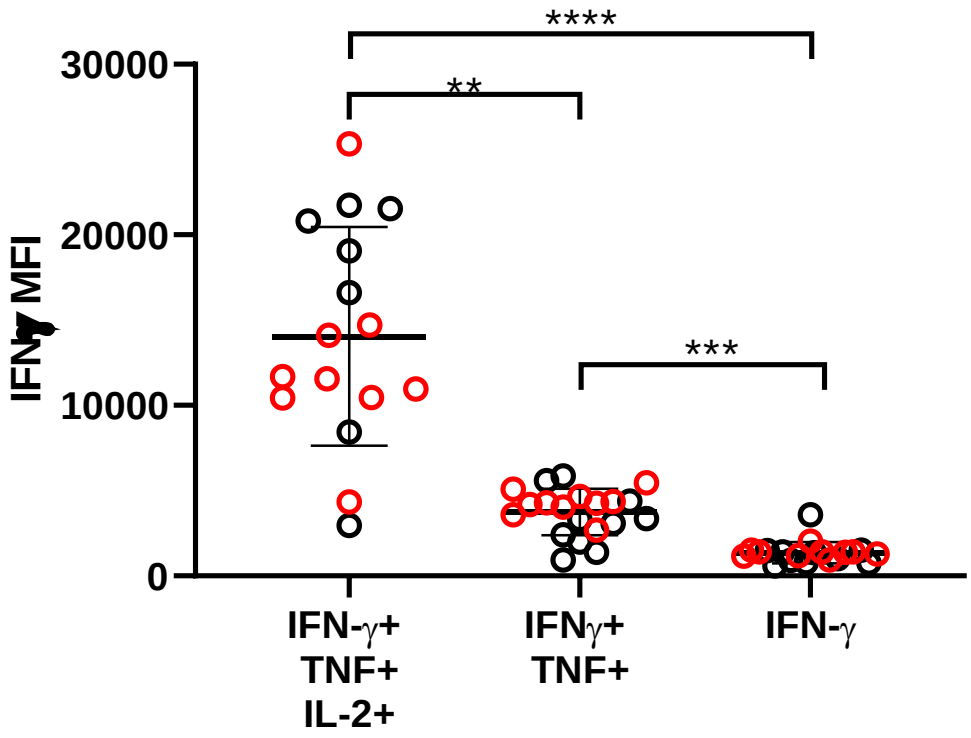

Figure 3.9. Comparison of IFN-γ MFI in single, double and triple secreting CD8βT cell. MFI of IFN-γ secretion was determined in cells that had previously been characterised as IFN-γ single, IFN-γ/TNF double or IFN-γ/TNF/ IL-2 triple secreting T cells. MFI of IFN-γ is plotted for BM (red circles) and OB (black circles) animal. Statistical analysis was performed using the Kruskal-Wallis test followed by Dunn's multiple comparisons post hoc test comparing the mean MFI of each group **p≤0.01 and ***p ≤ 0.001.

In summary, following H1N1pdm09 infection, the CD8 T cell response develops from day 5 onwards peaking at day 9 in the lower respiratory tract (BAL). The magnitude of response was much greater at the site of infection with the peak IFN-γ 27 times greater in the BAL than the PBMC. CD8 T cells in the BAL also display a greater level of multifunctionality (TNF, IL-2 and IFN-γ triple secreting) than other tissues and these polyfunctional T cells secrete greater levels of IFN-γ per cell than single and double secreting T cells.

3.6 CD4 response in different tissues during influenza infection in outbred and inbred Babraham pigs.

The magnitude (**Figure 3.10**) and quality, in terms of the type of cytokine secretion (**Figure 3.11**), of the CD4 response was also characterised. The CD4 response developed earlier than the CD8 response, with low but detectable IFN-γ response (0.073%) in the lung and IFN-γ/ TNF (0.06% and 0.2% respectively) co-producers in the BAL at day four. This response expanded 5-7 days post-infection, at which point cytokine responses were detectable in all tissues. The CD4 T cell cytokine response was lower compared to the CD8, with a peak of 1.6% IFN-γ and 2.1 % TNF in the BAL at day 9 DPI. The CD4 response was also less focused to the local tissues than CD8 with comparable response detected between tissues, though the greatest response was detected in the BAL, where itwas 5-fold larger than PBMC at 9 DPI. The CD4 response was less well maintained than the CD8 over the time course of the study with >9 fold decrease in IFN-γ secretion between the peak of the response in BAL at 9 DPI and the final time point at 21 DPI. This trend was observed in all tissues though was less pronounced in the spleen, which better maintained the CD4 response until the end of the study (<2-fold decrease between peak DPI 13 and DPI 21).

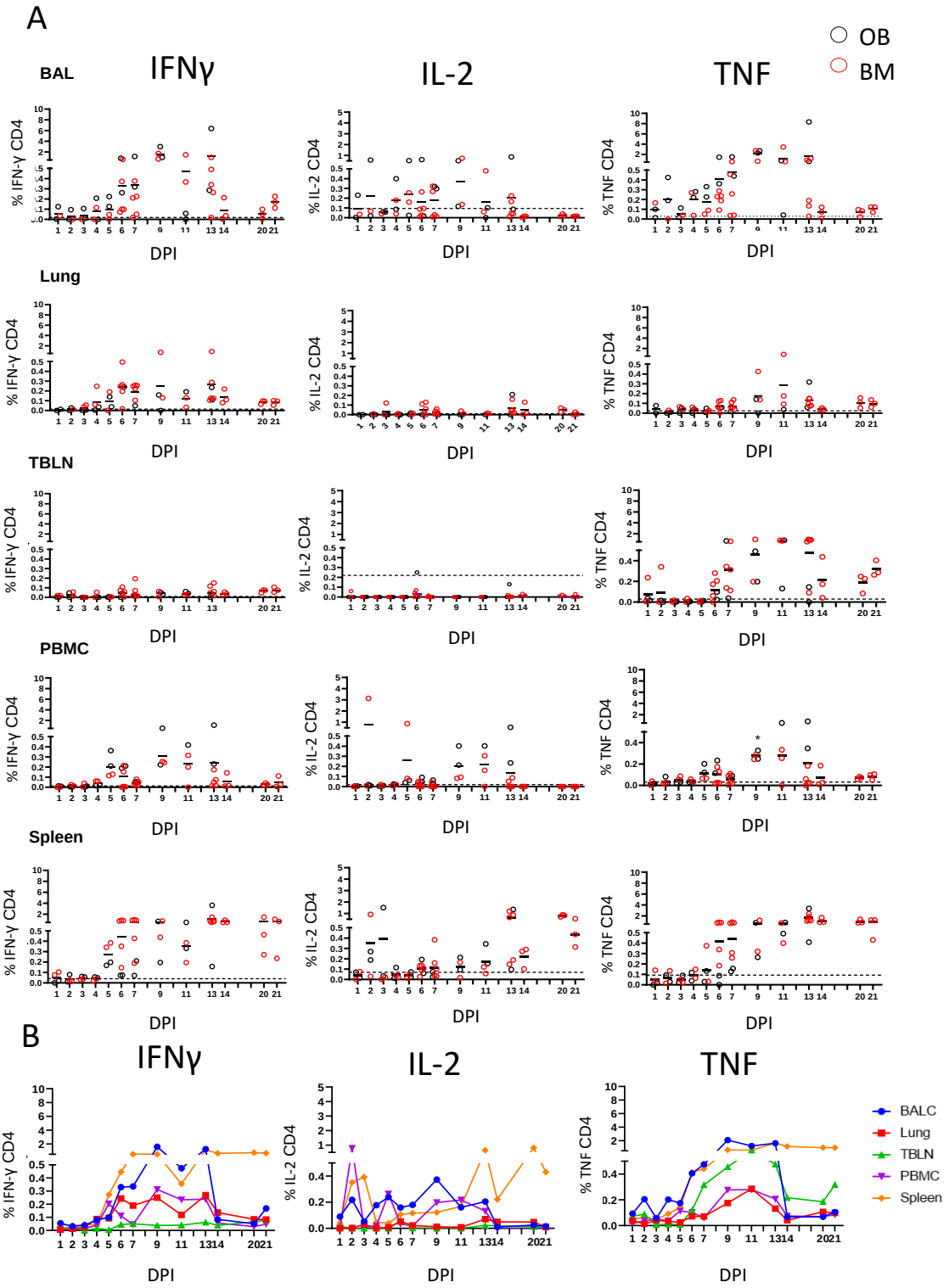

Figure 3.10 CD4 cytokine response. **(A)** Cytokine response of CD4 T cells in outbred (black circles) and inbred (red circles) pigs at each time point following influenza infection. BAL, lung, TBLN or PBMC cells were stimulated with H1N1pdm09 and cytokine secretion measured using intra-cytoplasmic staining. The mean of the 22 uninfected control animals is represented by a dotted line. DPI 1 to 7, 9, 11 and 13 each show results from 2 outbred and 2 inbred pigs. DPI 6, 7, 13, 14, 20 and 21 also include results from 3 additional inbred pigs. **(B)** The mean percentages for IFN-γ, TNF and IL-2 in each tissue for OB and BM together are shown over the time course.

Qualitative differences in cytokine production were detected in the CD4 populations in different tissues (**Figure 3.11**). Single, double and triple cytokine secreting CD4 cells could be detected in all tissues over the time course of infection. However, the response in the lung was dominant in IFN-γ secretion, and the TBLN was focused on TNF production, suggesting compartmentalisation of CD4 function, reminiscent of the CD8 response. The cytokine profile of CD4 cells was comparable between the OB and BM animals.

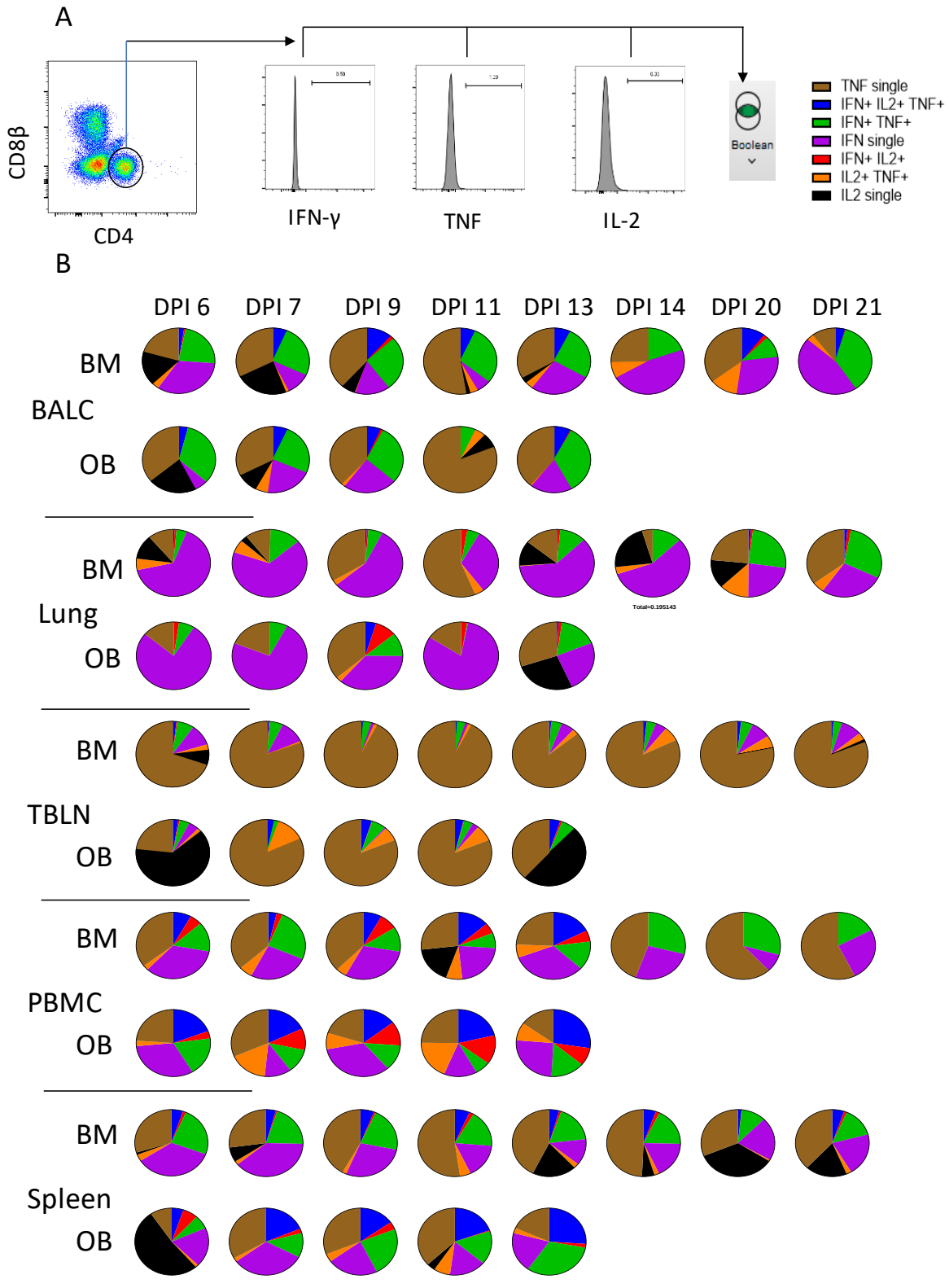

Figure 3.11 CD4 T cells cytokine responses **(A)** representative image of Boolean gating of cytokine positive CD4 T cells to determine cytokine responses in multiple tissues. **(B)** Pie charts depict the mean proportion of each group of single, double and triple IFN-γ, IL-2 and TNF cytokine secreting CD4 T cells as a percentage of the total cytokine production in BAL, lung, TBLN, PBMC and spleen. OB and BM animals are shown for comparison. Cytokine response from DPI. 6, 7, 9, 13 and 21 are shown. All cytokine populations were media control deducted

3.7 T cell responses in the BAL of in-contact pigs.

For time course experiments 1-4 two in-contact pigs were housed with experimentally infected pigs (**Figure 3.1**). As expected, not all in-contact pigs were infected on the first day of the experiment. Most in-contact animals became infected within the first 3 days of co-housing. Interestingly, however, one animal remained uninfected until day 6. The pattern of the duration of infection was similar between animals experimentally infected with a MAD device compared to in-contact infected animals (**Figure 3.12**). The kinetics of the T cell response was determined from the first day of detectable virus in nasal swabs. Viral loads were comparable between pigs infected with a MAD device and in contact infection. The frequency (**Figure 3.12B**) and quality, in terms of types of cytokine secreted (**Figure 3.12C**), of the in contact animals CD4 and CD8 responses was comparable to that observed in the experimentally infected animals. These data suggest that experimental intranasal infection using a MAD device induces comparable cellular responses in the BAL to naturally in-contact infected animals.

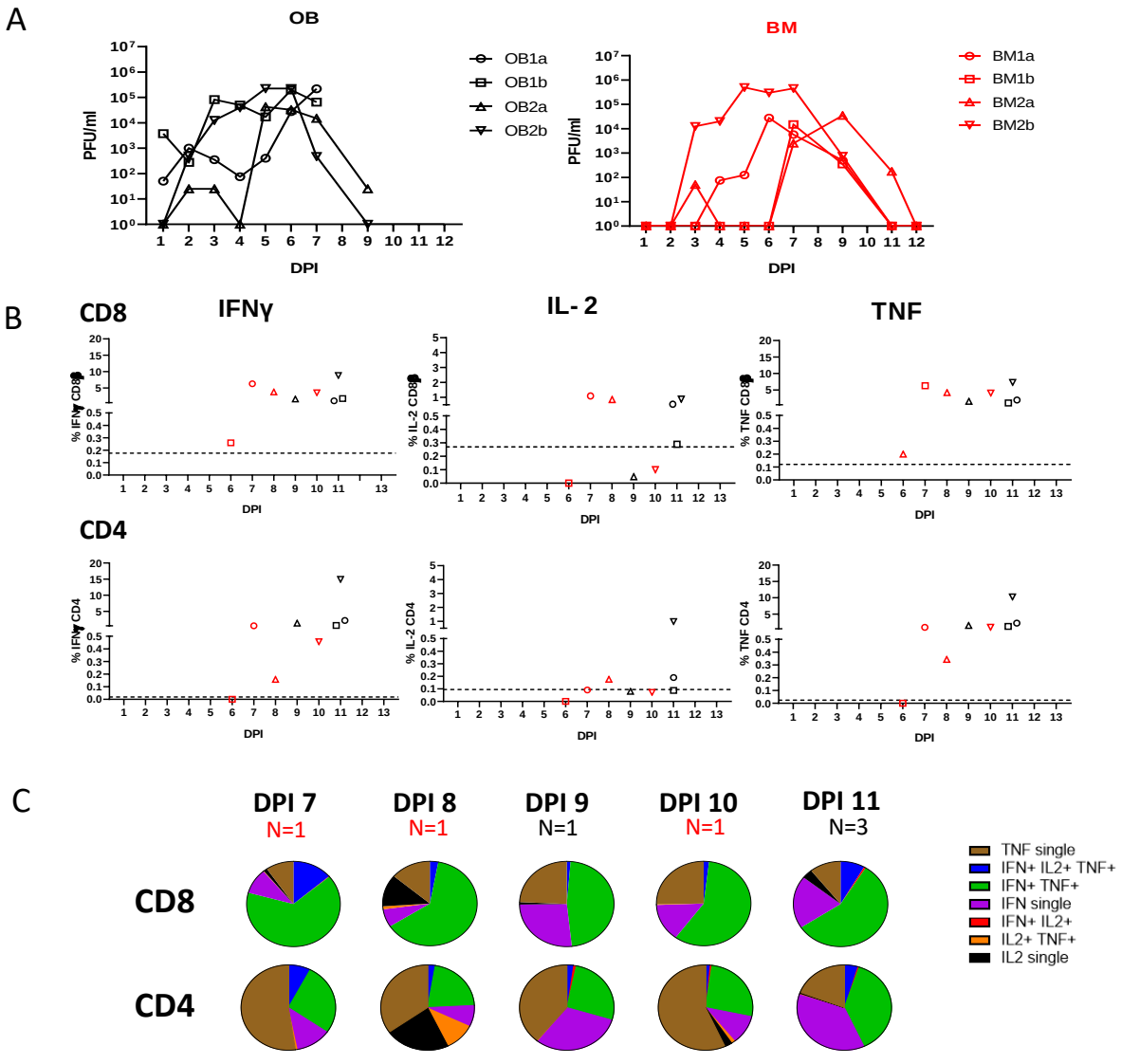

Figure 3.12 CD8β and CD4 cytokine response in BAL of in-contact animals. *(A)* Virus load in in-contact animals was determined by plaque assay of daily nasal swabs at the indicated time points for outbred (black) and inbred Babraham (red) pigs. (B) BAL CD4 and CD8 cytokine responses were determined by intracytoplasmic staining and shown as the days post infection counting from the first day the animal shed virus. (C) Pie charts show the proportion of single, double and triple cytokine secreting CD8 T cells for IFN-γ, TNF and IL-2.

3.8 The specificity of influenza response in the inbred Babraham pig

Both CD8 and CD4 T cells recognise and are activated by linearised peptides presented by MHC class I and class II, respectively. Upon activation, CD8 and CD4 cells secrete a variety of cytokines which include IFN-γ. These linearised peptides can be synthesised and systematically tested to determine the peptide specificity of responding cells. Thus, the antigen-specific epitope of responding T cells can be identified.

Initially, the entire NP, M1, HA and NA protein sequence was broken down into pools of 10 or 11 peptides of 18aa length overlapping by 12 aa for NP and M1 and 14aa for HA and NA (**Appendix 7.1**). This made a total of 8 pools for NP (81 peptides total) and four pools for M1 (40 peptides total) and 13 pools for both HA (138 peptides total) and NA (114 peptides total). BAL, lung, TBLN, PBMC and spleen samples from BM3 at 21 DPI were stimulated with peptide pools and response enumerated by IFN-γ ELISpot (**Figure 3.13- Figure 3.17**). As was seen with whole virus stimulation (**Figure 3.5**), the response to NP, M1, HA and NA varied between tissues with the greatest NP peptide response seen in the lung (mean NP response 4387 SFC/10^6 cells) followed by BAL (mean NP response 1320 SFC/10^6 cells) and TBLN (mean NP response 1383 SFC/10^6 cells). The response in PBMC was lower than in tissues (mean NP response 441 SFC/10^6 cells). The hierarchy of response differed between tissues. The greatest peptide response was to NP in all tissues other than PBMC, where there was a greater response to NA. The M1 peptides stimulated the second-highest level of IFN-γ in lung while in TBLN HA had the second-highest response followed by M1 and NP (**Figure 3.13**). The specificity of response for different NP, M1, HA and NA peptide pools was similar between tissues though not identical. The NP response was highest in pool 4 in all tissues followed by pool 3 and pool 5 and pool 7 (**Figure 3.14**). In M1 pool 3 induced the highest level of IFN-γ in TBLN and PBMC, whereas pool 4 showed a greater response in lung and BAL

(**Figure 3.15**). Low levels of IFN-γ were detected to HA though pool 2 showed a higher level of response, particularly in TBLN (**Figure 3.16**). For NA peptides the greatest response was detected in pool 1, particularly in the BAL and lung with pools 5 and 7 also stimulating IFN-γ production above the levels of the other pools (**Figure 3.17**). The differing hierarchy of the response between tissues could be explained by differences in the responding cell type and the type of response seen in terms of cytokine secreted (**Figure 3.8 and Figure 3.11**). Another possible explanation is that the hierarchy of different epitope responses is tissue-dependent; for example, TRM maintaining a differing hierarchy of response to circulating T cells (Martini et al., 2020). As TBLN peptide responses were of a reasonable magnitude with the least background (**Figure 3.16),** this tissue was chosen to perform a further break-down of the peptide pools**.**

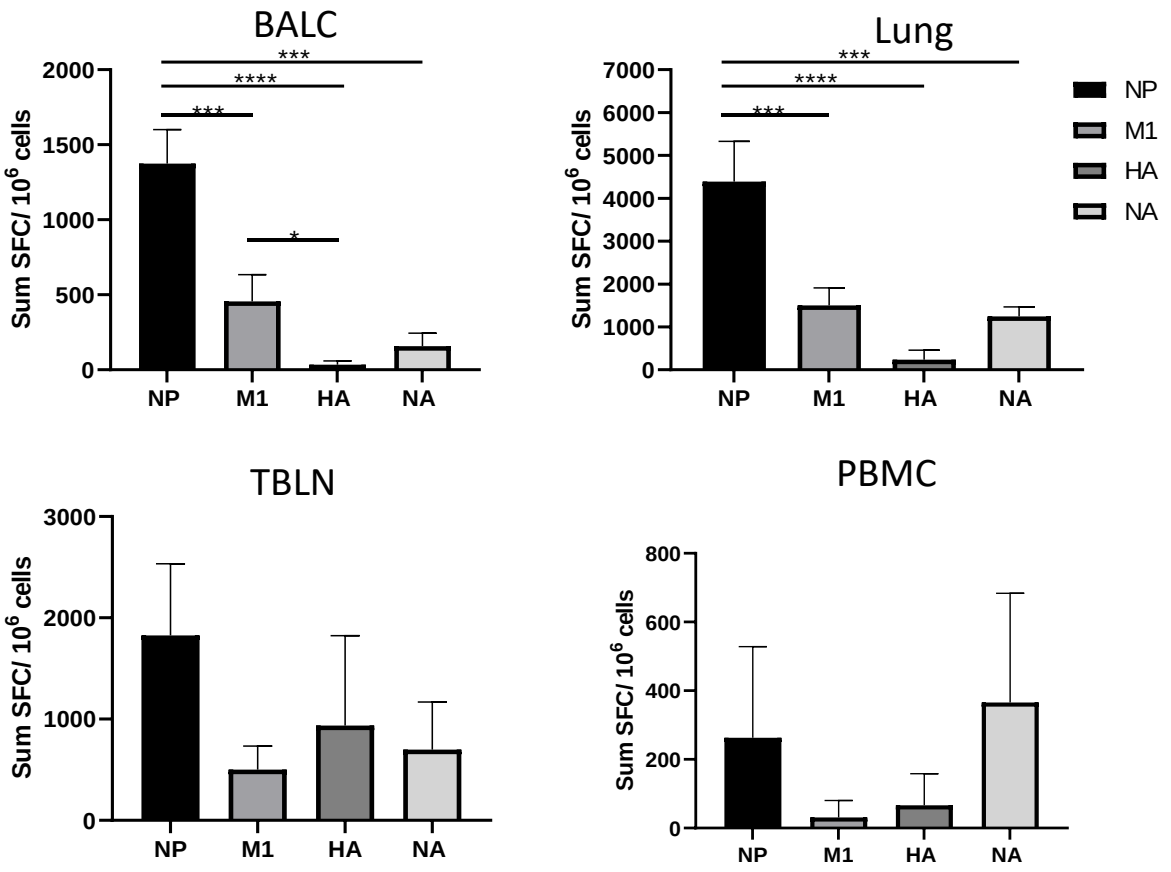

Figure 3.13 Sum of the peptide pool response to H1N1pdm09 influenza proteins in BAL lung TBLN and PBMC. IFN-γ secreting cells were enumerated in BAL, lung, TBLN and PBMC following stimulation with peptide pools containing the entire H1N1pdm09 influenza NP, M1, HA and NA sequences. SFC were enumerated, and SFC/10^6 response calculated for each peptide pool after deducting the medium only response. Bar charts depict the mean sum of the pool response for 3 animals from DPI21 (n=3 mean ±SD). Data were analysed using one-way ANOVA followed by Tukey's multiple comparisons post-hoc test with single pooled variance comparing the mean of the pooled ELISpot response in each tissue.

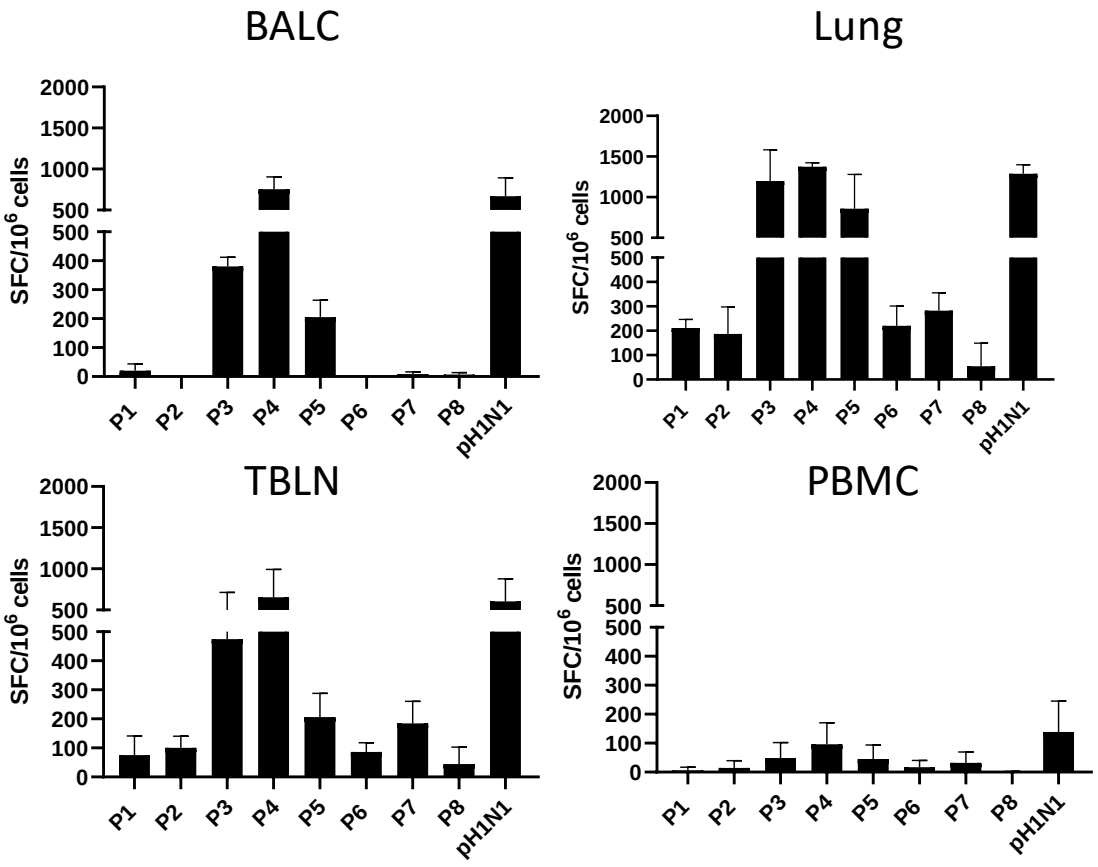

Figure 3.14 *Peptide screen of Nuclear protein (NP) in tissues of H1N1pdm09 infected pigs.* IFN-γ secreting cells were enumerated in BAL, lung, TBLN and PBMC following stimulation with peptide pools containing the entire H1N1pdm09 influenza NP sequences broken down into 8 pools over 10-11 peptides of 18aa length. H1N1pdm09 influenza virus stimulation was used as a control. SFC were enumerated, and SFC/10^6 response calculated for each peptide pool after deducting the medium only response. Mean response SEM from DPI21 (n=3)

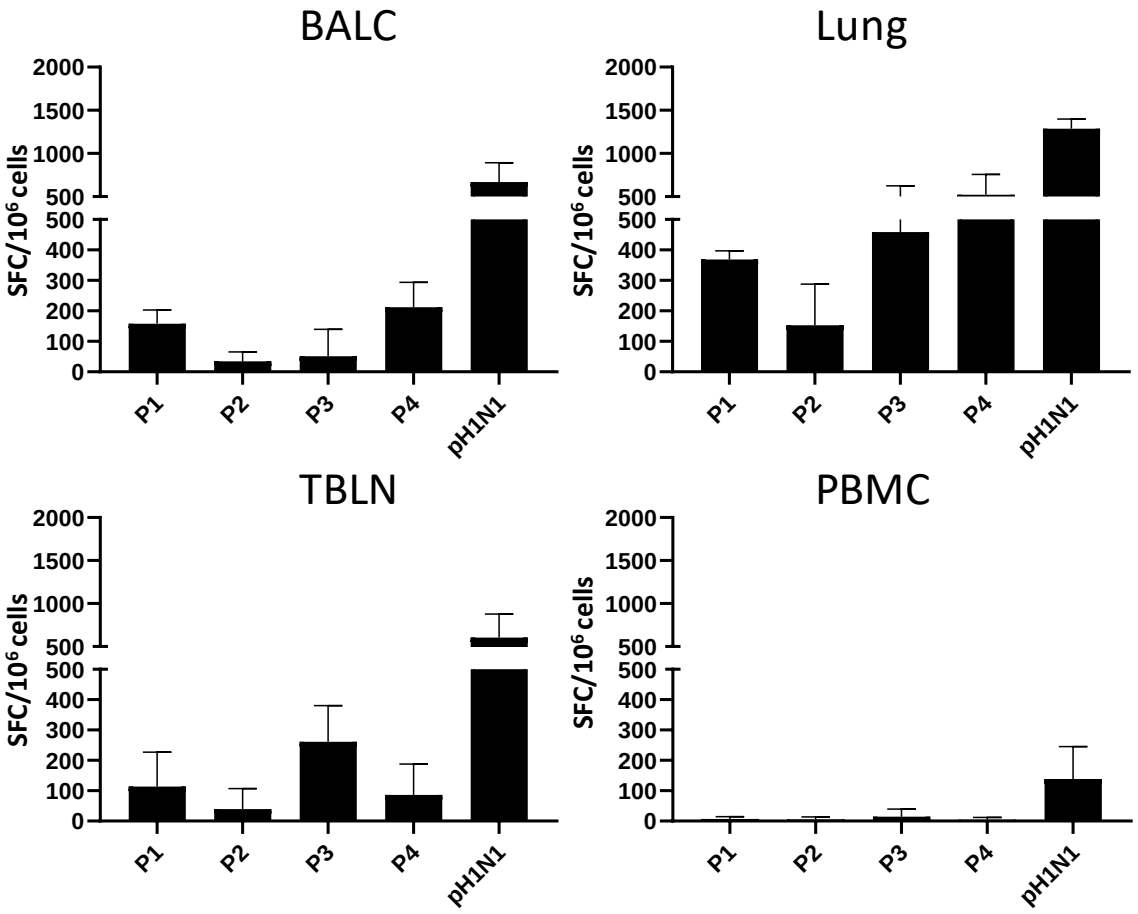

Figure 3.15 *Peptide screen for Matrix 1 protein (M1) in tissues of H1N1pdm09 infected pigs.* IFN-γ secreting cells were enumerated in BAL, lung, TBLN and PBMC following stimulation with peptide pools containing the entire H1N1pdm09 influenza M1 sequences broken down into 8 pools over 10-11 peptides of 18aa length. H1N1pdm09 influenza virus stimulation (pH1N1) was used as a control. SFC were enumerated, and SFC/10^6 response calculated for each peptide pool after deducting the medium only response. Mean response SEM from DPI21 (n=3)

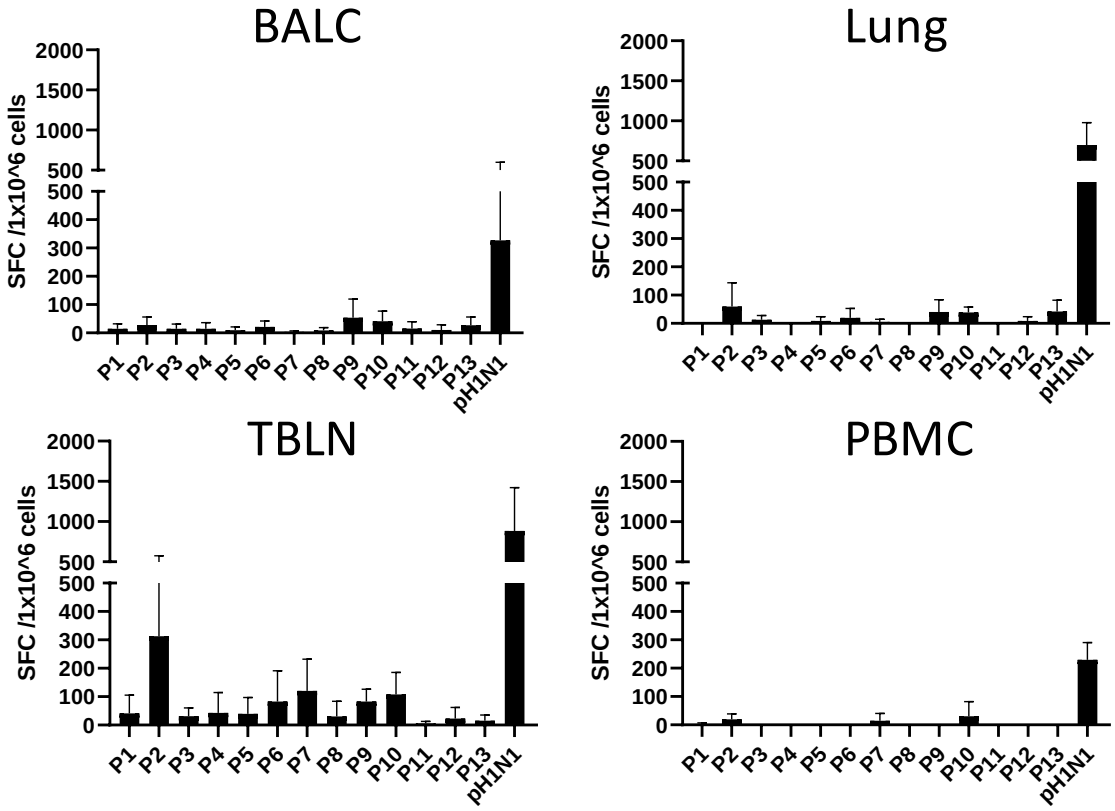

Figure 3.16 *Peptide screen of Haemagglutinin (HA) in tissues of H1N1pdm09 infected pigs.* IFN-γ secreting cells were enumerated in BAL, lung, TBLN and PBMC following stimulation with peptide pools containing the entire H1N1pdm09 influenza NA sequences broken down into 13 pools of 8-14 peptides of 18aa length. H1N1pdm09 influenza virus stimulation (pH1N1) was used as a control. SFC were enumerated, and SFC/10^6 response calculated for each peptide pool after deducting the medium only response. Mean response SEM from DPI21 (n=3)

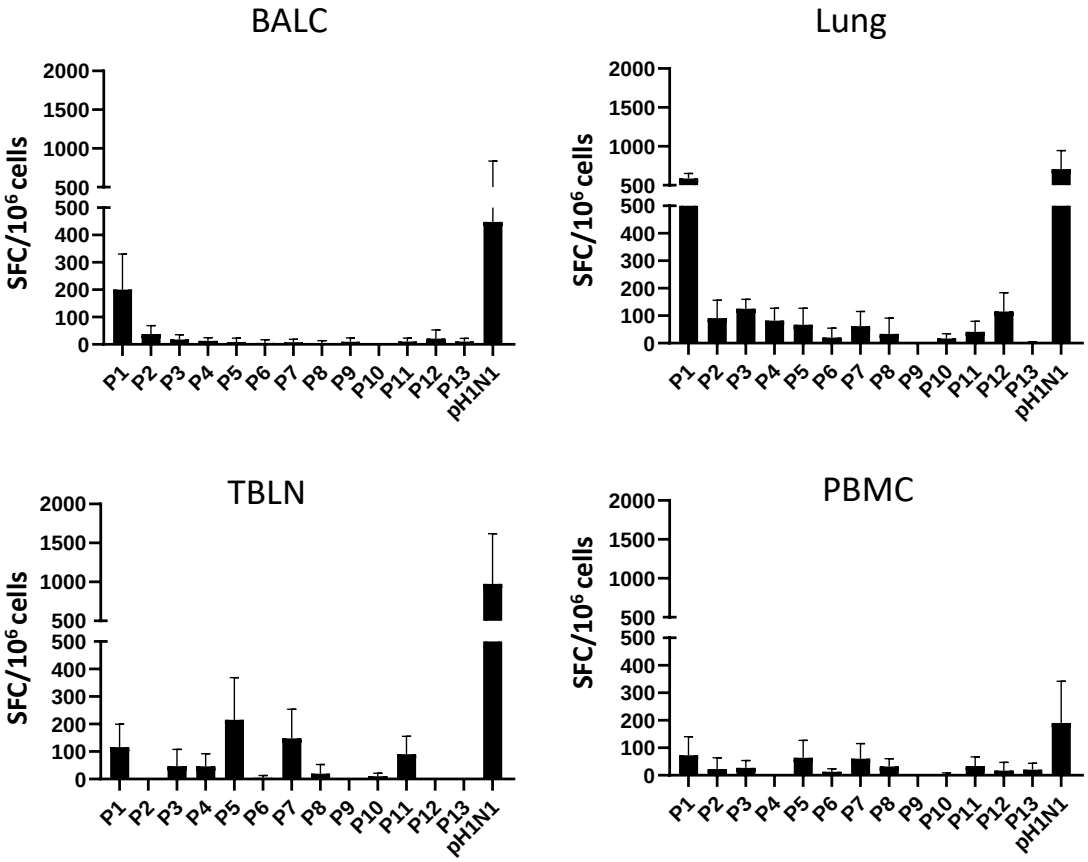

Figure 3.17 *Peptide screen of neuraminidase (NA) in tissues of H1N1pdm09 infected pigs.* IFN-γ secreting cells were enumerated in BAL, lung, TBLN and PBMC following stimulation with peptide pools containing the entire H1N1pdm09 influenza NA sequences broken down into 13 pools of 8-14 peptides of 18aa length. H1N1pdm09 influenza virus stimulation (pH1N1) was used as a control. SFC were enumerated, and SFC/10^6 response calculated for each peptide pool after deducting the medium only response. Mean response SEM from DPI21 (n=3)

3.9 Peptide pool break-down to minimum responding peptides

When comparing the specificity of response in TBLN to different peptide pools (**Figure 3.16**), NP pools 3, 4 and 7 had the highest response and were chosen for further break-down to single peptides. Though pools 5 also had a high response, it was not chosen for further break-down as this pool contains the previously identified immunodominant epitope DFEREGYSL (Tungatt et al., 2018). Pool 4 contains the previously identified cross-reactive epitope IAYERMCNI (VAYERMCNI in H1N1pdm09 strain), this pool was chosen to break-down to confirm the epitope and corroborate this method of epitope identification. M1 peptide pool 3, HA pool 2 and NA pool 1, 5 and 7 were chosen for further break-down. When separating pools to individual peptides (**Figure 3.18**) each peptide overlaps its neighbouring peptide by 12aa for NP and M1 and 14aa for HA and NA. Therefore, the stimulating response from one peptide should overlap with shared peptide sequences from a neighbouring peptide. Thus, responses from two adjoining peptides were considered a confirmation of response. For NP peptides, pool 3 peptide 30, pool four peptide 31 (overlapping with pool 3 peptide 30), 36 and 37 and pool seven peptide 67 and 68 were the dominant stimulating peptides. For M1 pool three, peptides 28 and 29 were selected. For HA peptides 12, 15 and 19 were selected. For NA peptides 6, 37, 38, 53 and 54 were selected (**Figure 3.18).**

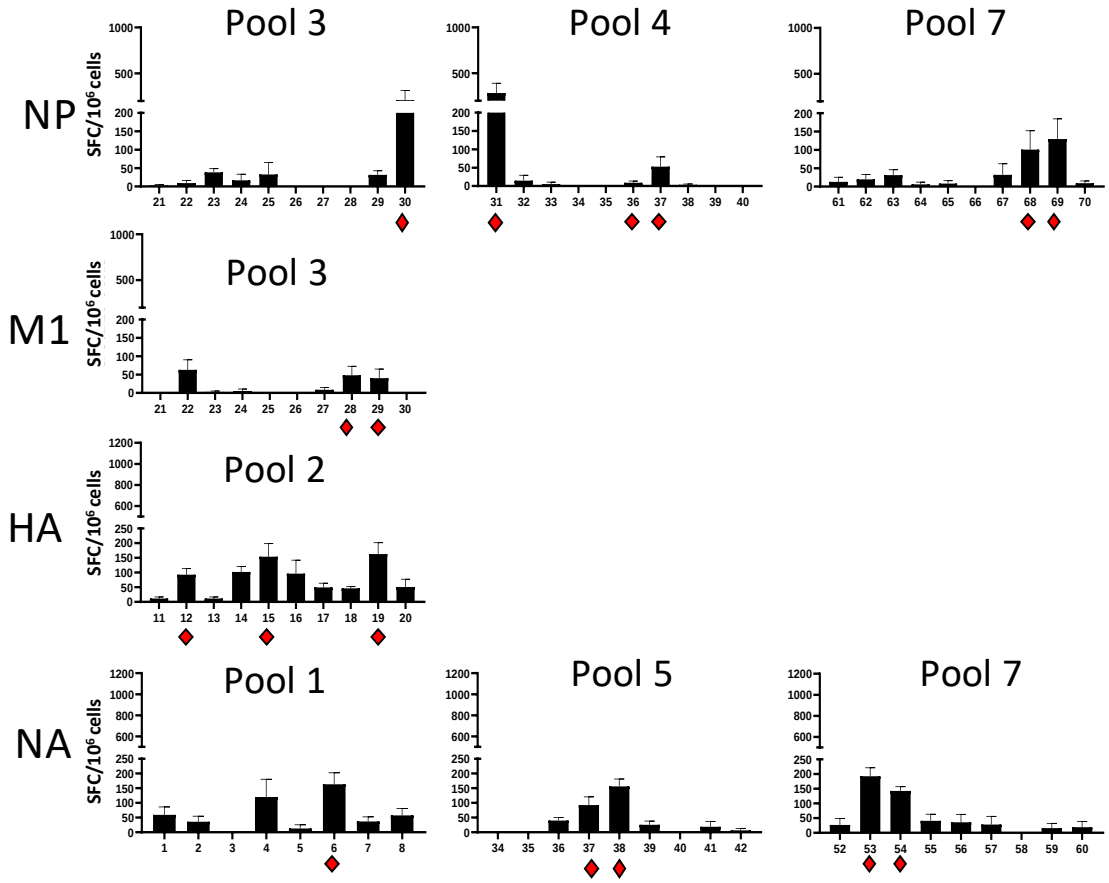

Figure 3.18 Peptide pool break-down. Enumeration of IFN-γ secreting cells from TBLN following stimulation with individual peptides from previously identified immunodominant pools from NP, M1, HA and NA. Response was calculated for each peptide after deducting the medium control response. Mean response and SEM from DPI 13 animals (n=3) are depicted. Red diamonds indicate dominant peptide responses which were chosen for further analysis.

3.10 Determining which cell type responds to single peptides

Depletion ELISpot was performed to determine whether the identified peptides induced either a CD4 or a CD8 response. CD8 or CD4 T cell populations from TBLN were depleted ex vivo prior to stimulation with peptides **(Figure 3.19).** NP peptides 31, 37, 68 and NA 6 induced a CD8 response, as the SFC/10^6 increased upon depletion of CD4. HA 12, NA 38 and NA 53 stimulated a CD4 response as CD4 depletion abrogated the response, but CD8 depletion had no effect. Peptides HA 15 and 19, M1 28 were inconclusive as neither CD4 nor CD8 depletion affected the response and it is, therefore, possible that these peptides contain both CD8 and CD4 epitopes.

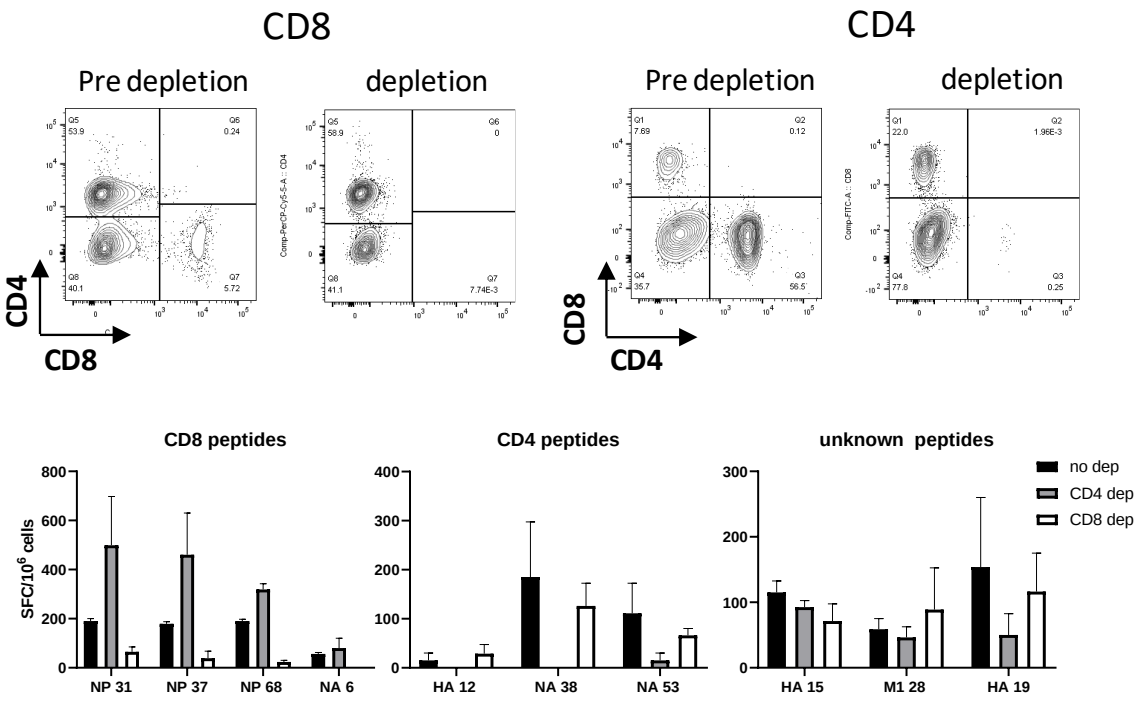

Figure 3.19 CD4 and CD8 depletion. CD8 and CD4 cells were depleted from TBLN of H1N1pdm09 infected animals' *ex vivo*, prior to stimulation with stimulating peptides. IFN-γ response was calculated for each peptide in un-depleted (no dep), CD4 depleted (CD4 dep) and CD8 depleted (CD8 dep) sample after deducting the medium control response. Mean response and SEM from one DPI 13 and one DPI 20 animal (n=2) is shown.

3.11 Peptide break-down to minimum epitope

Three peptides which had been shown to contain CD8 epitopes (**Figure 3.19**) were further broken down to minimum epitopes by analysing the overlapping regions of adjoining peptides and synthesising new peptides with aa trimmed from either end down to 9aa. NP 36/37, which was expected to contain the previously identified minimum epitope VAYERMCNI (VAY) in H1N1pdm09 (IAYERMCNI in PR8 influenza) was chosen to corroborate this method of epitope identification. The other peptides chosen were the novel CD8 stimulating peptides NP 30/31 and NP 68/69. For the peptide NP36/37, the minimum responding peptide was VAYERMCNI as expected. For NP 30/31 and NP 68/69, the minimum peptide identified was AAVKGVGTI (AAV) and TFSVQRNLPF (TFS) respectively (**Figure 3.20**).

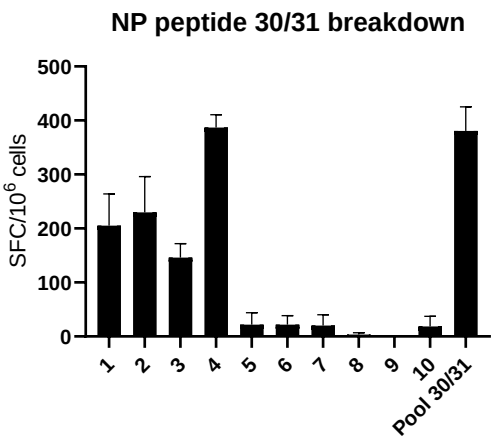

Peptide name	Sequence	length
P3/4 30/31. 1	AAVKGVGTIAME	12
P3/4 30/31. 2	AAVKGVGTIAM	11
P3/4 30/31. 3	AAVKGVGTIA	10
P3/4 30/31. 4	AAVKGVGTI	9
P3/4 30/31. 5	AVKGVGTIAME	11
P3/4 30/31. 6	VKGVGTIAME	10
P3/4 30/31. 7	KGVGTIAME	9
P3/4 30/31. 8	AVKGVGTIAM	10
P3/4 30/31. 9	AVKGVGTIA	9
P3/4 30/31. 10	VKGVGTIAM	9

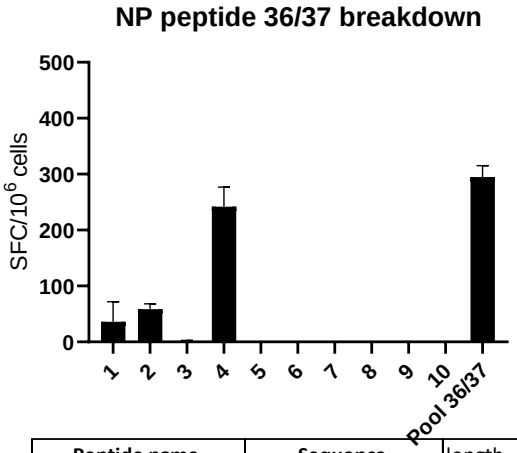

Peptide name	Sequence	length
P4 36/37. 1	VAYERMCNILKG	12
P4 36/37. 2	VAYERMCNILK	11
P4 36/37. 3	VAYERMCNIL	10
P4 36/37. 4	VAYERMCNI	9
P4 36/37. 5	AYERMCNILKG	11
P4 36/37. 6	YERMCNILKG	10
P4 36/37. 7	ERMCNILKG	9
P4 36/37. 8	AYERMCNILK	10
P4 36/37. 9	YERMCNILK	9
P4 36/37. 10	AYERMCNIL	9

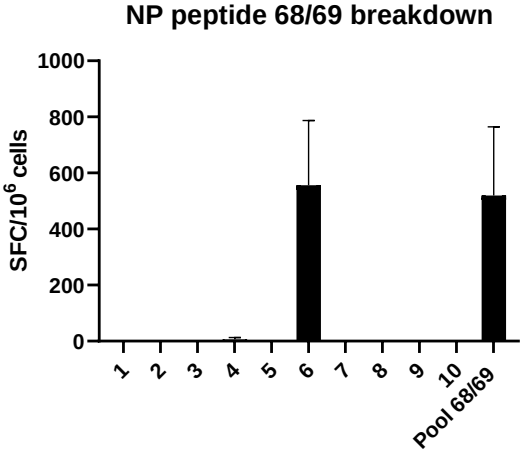

Peptide name	Sequence	length
P7 68/69. 1	QPTFSVQRNLPF	12
P7 68/69. 2	QPTFSVQRNLP	11
P7 68/69. 3	QPTFSVQRNL	10
P7 68/69. 4	QPTFSVQRN	9
P7 68/69. 5	PTFSVQRNLPF	11
P7 68/69. 6	TFSVQRNLPF	10
P7 68/69. 7	FSVQRNLPF	9
P7 68/69. 8	PTFSVQRNLP	10
P7 68/69. 9	TFSVQRNLP	9
P7 68/69. 10	PTFSVQRNL	9

Figure 3.20 Peptide break-down to the minimum epitope. The 12aa overlapping region between peptides previously identified as CD8 responding were sequentially truncated to a minimum of 9aa. Peptides were screened by IFN-γ ELISpot to identify minimum length peptide sequence, to induce an IFN-γ response. DPI 13 animals (n=2) were used for with mean and SEM depicted for each peptide. The minimum peptide is highlighted in yellow.

3.12 Further peptide break-down using influenza re-infected animals

Though the responses from the time course samples were adequate to identify CD8 epitopes by IFN-γ ELISpot, it was clear that the CD4 response was much lower, likely due to the CD4 cytokine response TBLN being dominated by TNF combined with the response waning in these experimentally infected animals at the time points used (**Figure 3.10**). As the identification of CD4 epitopes was a major goal of this study, peptide break-down experiments were repeated in animals which had been experimentally challenged with H1N1pdm09. The NP and HA pools had similar responses to the previous break-down performed in individually infected animals, so no further break-down was performed in the sequentially infected animals (data not shown). The M1 response was further dissected with pool 1 and pool 3 for M1, showing the greatest response (**Figure 3.21**). Overall, there was a greater response to M1 from animals which were initially infected with H1N1pdm09 followed by H3N2, than animals that were infected with H3N2 first followed by H1N1pdm09. When breaking down M1, pools 1 and 3, peptides 2, 3, 7, 22, 24 and 29 were identified as individual peptides (**Figure 3.21B**) capable of stimulating an IFN-γ response. Interestingly, the greater response of animals infected with H1N1pdm09 followed by H3N2 was not observed in the NA peptides. Further, there was a higher response to pool 5 in the H3N2 infected H1N1 re-infected animals, suggesting a differing focusing of response to different H1N1 proteins depending on influenza challenge strain. When breaking down the NA response, pool 5 and pool 7 showed the greatest response (**Figure 3.22A**). H3N2 infected animals re-infected with H1N1 showed the greatest response to pool 5. Therefore, these animals were used to break-down the pool. In NA pool 5, peptides 36, 37, 38 and 39 were individual peptides which could induce and IFN-γ response (**Figure 3.22B**). In pool 7 peptides 22, 24 and 27 were individual peptides capable of stimulating an IFN-γ response (**Figure 3.22B).**

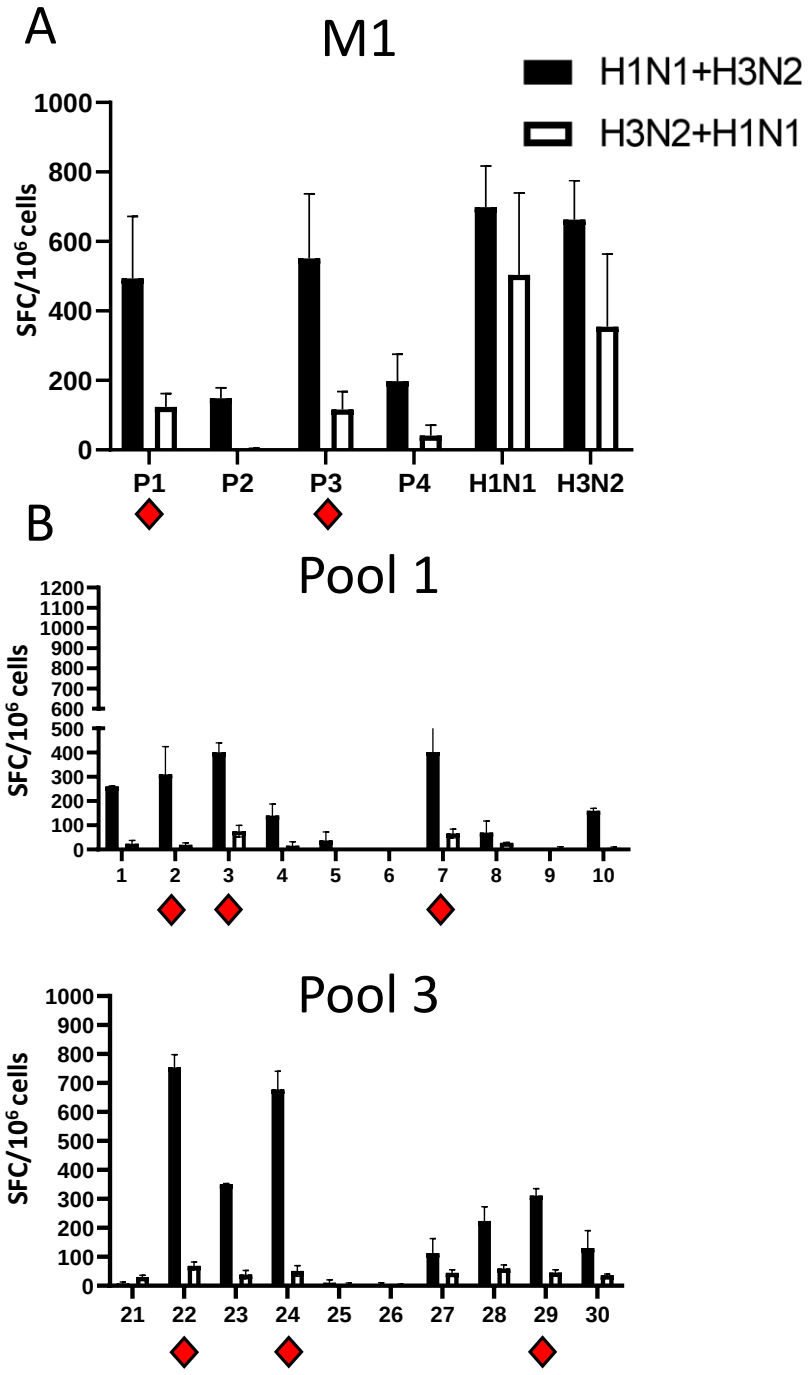

*Figure 3.21 M1 Peptide pool break-down in TBLN using re-infected animals.*A) IFN-γ secreting TBLN cells were enumerated, following stimulation with 4 peptide pools of 8-11 peptides overlapping by 14aa covering the length of the M1 protein B) peptide pool break-down to individual peptides from previously identified immunodominant pools from M1 as identified in A. Response was calculated for each peptide after deducting the media control response. Mean response and SEM experimentally re-infected animals at DPI 4 (n=3) are depicted. Red diamonds indicate peptide pools or individual peptides chosen for further analysis.

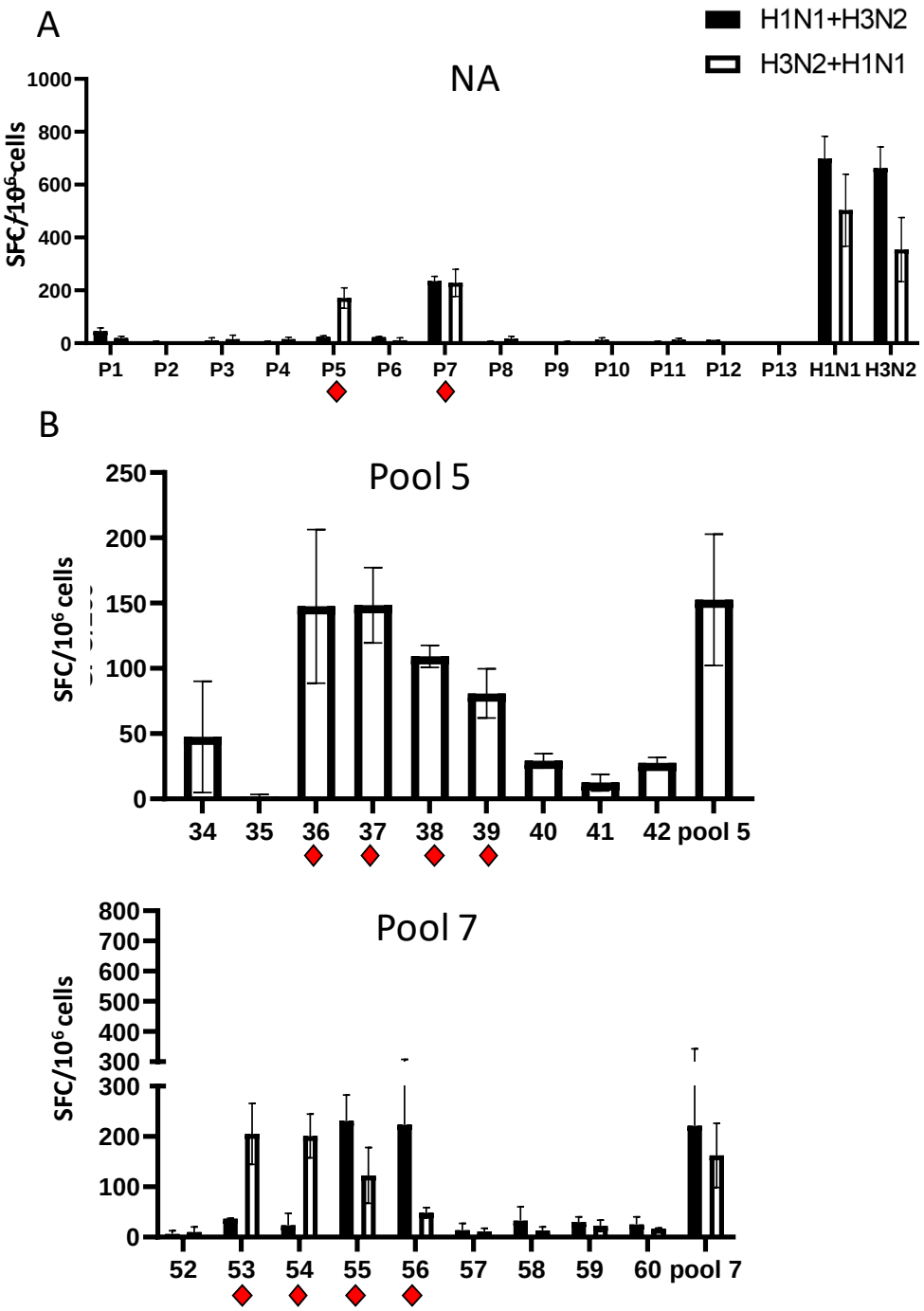

Figure 3.22 NA Peptide pool break-down in TBLN using sequentially infected animals. A) IFN-γ secreting TBLN cells were enumerated, following stimulation with 13 peptide pools containing 8-11 peptides overlapping by 14aa covering the length of the NA protein of H1N1pdm09 influenza B) peptide pool break-down to individual peptide, from immunodominant pools of NA as identified in A. Response was calculated for each peptide after deducting the medium response. Mean response and SEM from experimentally re-infected animals at DPI 4 (n=3) are depicted. Red diamonds indicate peptide pools or individual peptides chosen for further analysis.

3.13 ICS to determine which cell type responds to minimal epitopes

To confirm the depletion experiments shown in Figure 3.19, ICS was performed on single-cell suspensions from TBLN stimulated with selected peptides previously identified in both the single and sequentially challenged animals. Cells were stimulated with peptides, gated for CD8, CD4 or CD4/CD8 double positive cells and IFN-γ/ TNF secretion quantified (**Figure 3.23**), As expected, the previously identified NP minimum peptides stimulated CD8 T cells to produce both TNF and IFN-γ (**Figure 3.24**). In contrast, M1 peptides 3, 7, 22 and 29 induced a robust CD4 response with negligible CD8 response detected and peptide 28 stimulated both CD4 and CD8 T cells **(Figure 3.24**), in agreement with the depletion assay (**Figure 3.19**). This suggests that peptide 28 contains a CD8 epitope which peptide 29 does not share, while they may share a stimulating CD4 epitope. The NA peptides 36 and 38 induced CD4 and CD8 responses, whereas peptide 55 stimulated only CD4 cells. NA 38 was previously shown to activate CD4 positive T cells by depletion assay solely (**Figure 3.19**) and responses detected by ICS were very low. Further experiments need to be performed to determine whether peptide 38 is a CD4 or CD8 stimulating peptide. HA peptides 12, 15 and 19 all showed a response in both the CD4 and CD8 T cells, similarly to the depletion assay. HA 12 did not activate CD8 cells in the depletion assay. These HA peptides overlap quite significantly, and they may contain shared CD8 and CD4 epitopes which stimulate both CD4 and CD8 positive T cells.

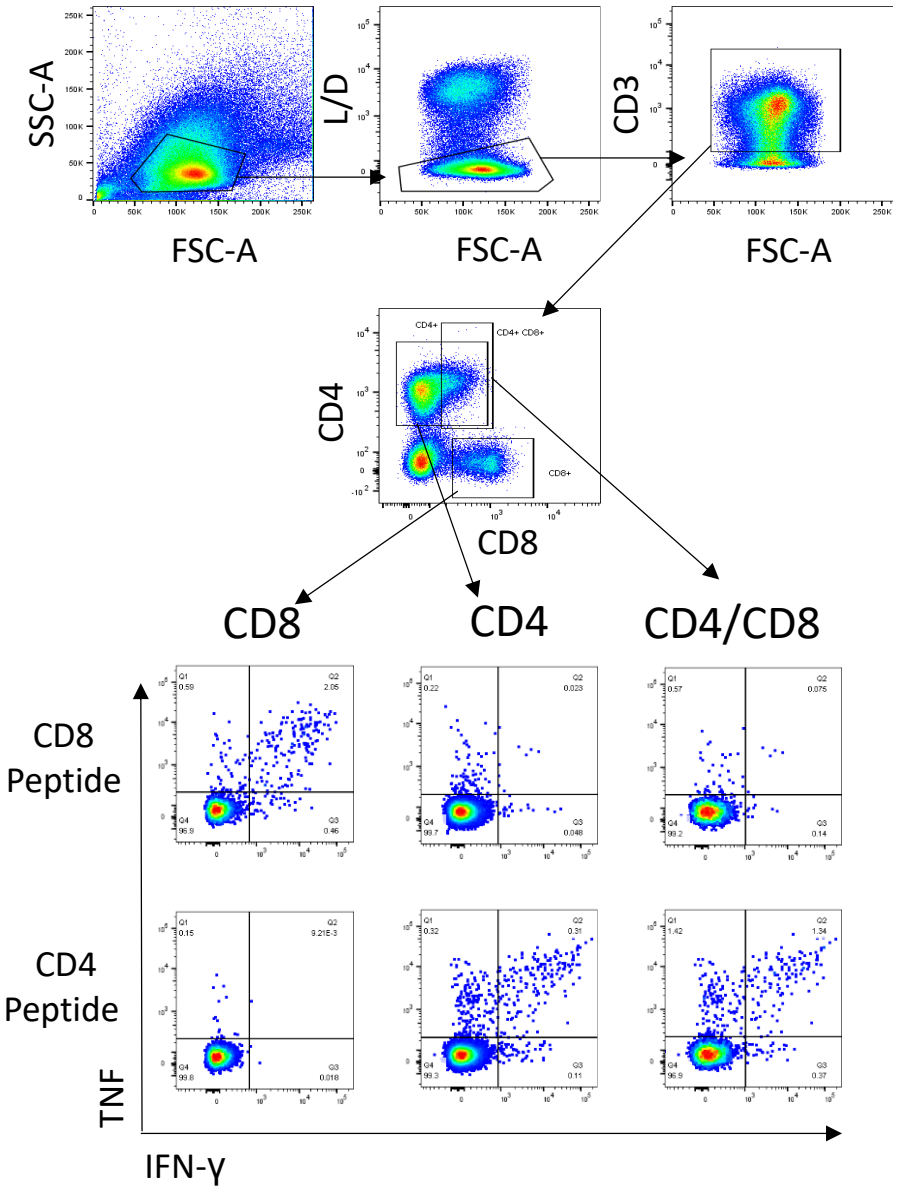

Figure 3.23 ICS to determine responding cell type to single peptides from pdmH1N1 internal peptides.

Gating strategy for determining CD8 CD4 and CD4/ CD8 double-positive T cells and representative flow cytometry plots depicting TNF and IFN-γ secretion in CD8, CD4 and CD8/CD4 double-positive T cells following stimulation with single peptides indicated from M1 protein.

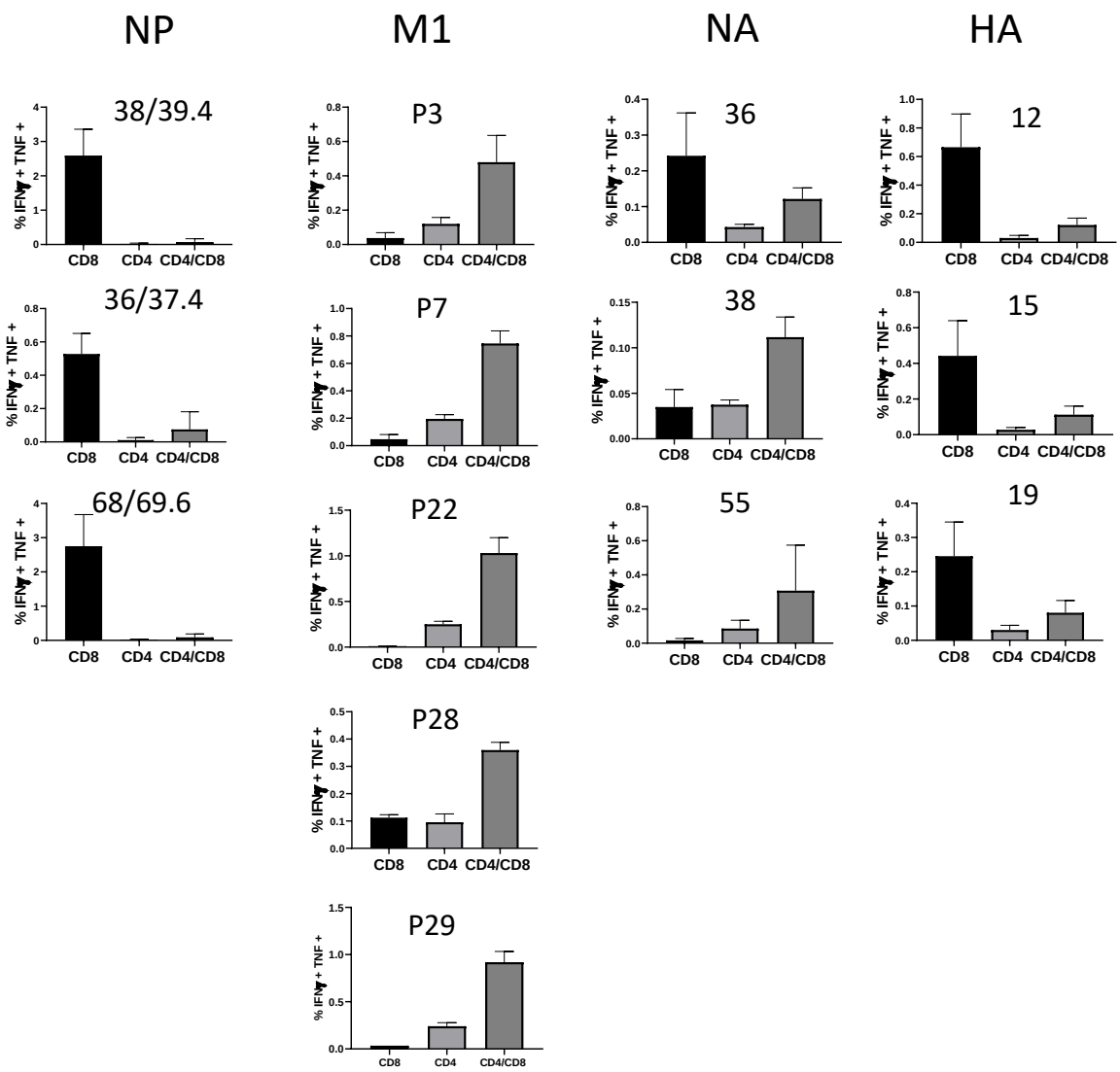

Figure 3.24 Cytokine response to minimum peptides in CD8, CD4 or CD8/CD4 double positive T cells protein. Minimum peptides were used to stimulate TBLN single cell suspensions from influenza challenged Babraham pigs. Bar charts depicting mean IFN-γ TNF double-positive T cells within CD8, CD4 and CD4/CD8 double-positive T lymphocytes as indicated (mean +/- SEM N=3). Medium control is deducted from each stimulus.

3.14 Discussion

In this chapter, I have described the conventional T cell response in inbred Babraham and outbred pigs following intranasal infection with H1N1pdm09 influenza virus. Significant CD8 cytokine response developed between 5-7 DPI, a time point which coincided with the first detectable $NP_{290-298}$ T cells, though a low level of cytokine response was detectable from 4 DPI in the lung of some animals. The CD8 response in TBLN, PBMC spleen, and lung were mainly IFN-γ and IFN-γ/TNF co-producers with minimal IL-2 secretion. These findings are broadly in agreement with Talker and colleagues (Talker et al., 2016). However, in the BAL, the response is dominated by IFN-γ/TNF co-producers, and a clear IFN-γ/TNF/IL-2 triple secreting population is present. The polyfunctionality of T cells has previously been described as a measure of the quality of response (Seder et al., 2008). Indeed, the level of IFN-γ secretion per cell (determined by MFI) in the BAL is much higher on average in the triple IFN-γ/TNF/IL-2 (Mean MFI 13058) and double IFN-γ/TNF (Mean MFI 3744) cytokine secreting cells compared to the single IFN-γ secreting cells (Mean MFI 1357) (***Figure 3.9***). Similarly, previous studies have shown that the cytotoxic potential of multiple cytokine-producing T cells is higher than single producing CD8 T cells (Lichterfeld et al., 2004). This higher proportion of double and triple secreting cytotoxic T cells in the BAL demonstrates these multifunctional T cells are preferentially recruited to the site of infection.

Cytokine secretion differed in the CD4 population found in different tissues. The CD4 population in the lung mainly consisted of IFN-γ single producing cells, particularly at early time points. IFN-γ has antiviral properties and is also required for antibody class switching (Baumgarth and Kelso, 1996), which may be critical functions for these newly recruited CD4 cells. Conversely, TNF secreting CD4 cells were enriched in the TBLN. Tissue compartmentalisation of CD4 functions following infection has been described in mice, with the majority of influenza specific CD4 cells in the lung expressing a Th1 phenotype and

secreting IFN-γ (Brown et al., 2012). Interestingly, the CD4 cells in the BAL showed a higher degree of polyfunctionality, with single, double and triple producing cells present. This poses the question of whether specialised CD4 cells are compartmentalised due to the migration of CD4 subsets to specific tissues, as has been proposed in mice (Strutt et al., 2013) or whether the tissue environment alter cytokine production.

The cellular responses to H1N1pdm09 stimulation observed in the OB and BM animals were highly comparable. The only difference identified between the two breeds was a significantly lower frequency of CD8 T cells in the BM pigs at the outset of the study. This may be due to a genetic difference, though may also be a result of different housing conditions as the BM pigs are housed in specific pathogen free conditions, whereas the outbred pigs were obtained from a commercial breeder. The responses, in terms of tissue localisation, cytokine profile, and magnitude overlap between the outbred and inbred animals. The responses observed here also agree with previously reported studies with outbred animals (Talker et al., 2016). Overall, the data presented here suggest that the immune response in the BM pig following influenza infection is comparable to that of outbred animals.

The specificity of the CD4, and CD8 T cell response in the Babraham pig to influenza antigens NP, M1, HA, and NA derived from H1N1pdm09 influenza virus was also characterised. Three novel CD8 antigenic peptides were identified: two in NP and one in NA. Five CD4 antigenic peptides were identified, four in M1, and one in NA. Five peptides with unknown CD4 or CD8 response were also identified, three in HA, two in NA and one in M1. Furthermore, two dominant NP CD8 peptides NP30/31 and NP68/69 were broken down to their minimum epitopes of AAVKGVGTI and TFSVQRNLPF, respectively (**Figure 3.20**). The peptides identified in this study are summarised in **Table 3.1**. This data demonstrates that this method can be utilised to identify antigen-specific T cells in the Babraham pig. Further work will characterise the peptides identified here as well as evaluating the response to other proteins.

This work will generate a library of H1N1pdm09 specific antigens recognised by the BM pig allowing for the dissection of the fine specificity of the T cell response following infection or immunisation.

Table 3.1 Immunodominant influenza peptides identified in the Babraham pig.

Protein	peptide number	sequence	peptide length	responding cell type
NP	N/A	AAVKGVGTI	9aa	CD8
	N/A	VAYERMCNI	9aa	CD8
	N/A	TFSVQRNLPF	10aa	CD8
M1	3	SIIPSGPLKAEIAQRLES	18aa	CD4
	7	TDLEALMEWLKTRPILSP	18aa	CD4
	22	CMGLIYNRMGTVTTEAAF	18aa	CD4
	28	RQMATTTNPLIRHENRMV	18aa	CD4/CD8
	29	TNPLIRHENRMVLASTTA	18aa	CD4
HA	12	HSVNLLEDKHNGKLCKLR	18aa	CD4/CD8
	15	KLCKLRGVAPLHLGKCNI	18aa	CD4/CD8
	19	NIAGWILGNPECESLSTA	18aa	CD4/CD8
NA	6	NLILQIGNIISIWISHSI	18aa	CD8
	36	NDKHSNGTIKDRSPYRTL	18aa	CD4/CD8
	38	IKDRSPYRTLMSCPIGEV	18aa	CD4/ CD8
	55	KSWRNNILRTQESECACV	18aa	CD4

3.15 Summary

For both CD4 and CD8 T cells, a significant expansion in the response was detectable 5-7 DPI in the outbred and inbred animals, which is just prior to viral clearance. Though some CD8 and CD4 responses could be detected as early as day four, these were of low frequency. The antibody response in this time course appeared at day six onwards (data not presented here). Whether the induction of the adaptive response played a major role in the resolution of the primary infection in these animals is unclear. Studies in mice have shown that the adaptive response is required for complete clearance of virus following initial infection. The pdmH1N1 strain used in these studies generates a relatively mild infection. In these animals, the innate response likely contained the infection (Malik and Zhou, 2020), with the adaptive response

developing to enable final viral clearance. The adaptive response is likely to be more critical in a more severe respiratory infection or upon reinfection.

This poses the obvious question of what the mechanisms for the control of the virus are during the early time points of infection. Innate mechanisms such as the induction of the inflammasome and the antiviral state play an important role in the early control of the virus. Additionally, innate and innate like cellular subsets such as NK, NKT, TCRγδ, and MAIT cells are also likely to play important roles in the antiviral response. The remainder of this thesis is devoted to the study of the latter cellular subset, MAIT cells.

Chapter 4 Identification of MAIT cells in different species

4.1 Aims and rationale.

Beyond primates and mice, the knowledge of MAIT cells in other species is limited. Cattle, sheep and pigs are economically important livestock species that also represent relevant models for a variety of human infections, including TB in cattle (Van Rhijn et al., 2008) respiratory disease in sheep (Guillamón Mde and Clau, 2010) and influenza in pigs (Holzer et al., 2019a). These species express the *MR1* gene, and the canonical MAIT cell TCRA has been identified in ruminants by qPCR (Goldfinch et al., 2010, Tilloy et al., 1999). At the outset of this study, there was no information on MAIT cells in pigs, though recent studies have shown that pigs express MR1 (Xiao et al., 2019b) and express the canonical MAIT TCRA sequence (Identified by qPCR and TCR sequencing) (Xiao et al., 2019a). Additionally, frequencies of MAIT cells and co-receptor usage were determined based on qPCR in healthy individuals of all three species (Xiao et al., 2019a, Goldfinch et al., 2010), as well as chemokine and cytokine receptor profiles in pigs (Xiao et al., 2019a). However, no direct studies of functional MAIT cells have been performed, possibly in part hindered by the lack of species-specific reagents to identify MAIT cells.

In humans and mice, as well as more recently in macaques, fluorescently labelled MR1 tetramers loaded with the MAIT cell-activating ligand 5-OP-RU represent the gold standard in identifying MAIT cells in the blood and cellular suspensions in tissues (Reantragoon et al., 2013, Corbett et al., 2014, Rahimpour et al., 2015, Chen et al., 2017, Gherardin et al., 2018, Juno et al., 2019, Greene et al., 2017). Tetramers loaded with the MR1 ligand 6-formylpterin (6-FP) (Kjer-Nielsen et al., 2012, Eckle et al., 2014) or its acetylated analogue, Acetyl-6-FP (Ac-6-FP) (Eckle et al., 2014), typically do not bind to MAIT cells and are often used as negative controls of MR1-5-OP-RU tetramer staining in humans (Souter et al., 2019).

The availability of newly developed MR1 tetramers offers the opportunity to formally assess the level of xeno-reactivity of tetramer reagents between species and to study the level of conservation of the MAIT-MR1 axis between species, which has only previously been assessed based upon the MR1 and TCRα chain sequence similarities and xeno-reactivity with selected MAIT cell clones (Huang et al., 2009, Lopez-Sagaseta et al., 2013).

In this chapter, newly developed species-matched pig and bovine MR1-tetramers and previously characterised species-mismatched MR1 tetramers are utilised to identify MAIT cells in the major livestock species pigs, cattle and sheep. The level of cross-reactivity of MR1 tetramers is also compared between humans, cattle, pigs and sheep. These findings are supported by *in vitro* ligand stimulation and qPCR analysis of the MAIT TCR genes and will address these main goals

- Analyse the conservation of the α1- and α2-domains of MR1 between species
- Phenotypically identify MAIT cells in pigs, cattle, and sheep with species-specific and species mismatched MR1 tetramer.
- Compare levels of MR1 tetramer cross-reactivity in distantly related mammalian species.
- Confirm the tetramer specific identification of MAIT cells in these with *in vitro* stimulation with 5-OP-RU and qPCR techniques.

4.2 Chapter specific methods

4.2.1 Generation of Sus scrofa and Bos taurus MR1 tetramers

S. scrofa and B. taurus genes encoding β_2-microglobulin (β2m) (*S. scrofa* GenBank ID: AB436775.1, *B. taurus* GenBank ID: BC118352.1) and the soluble portion of MR1 (*S. scrofa* GenBank ID: MH796644.1, *B. taurus* GenBank ID: FJ028657.1) codon optimized for

Escherichia coli expression were purchased (Life Technologies Australia). The gene encoding the soluble portion of *S. scrofa* MR1 was modified to include a mutation to facilitate correct disulphide bond formation, C262S; G262 of *B. taurus* was not mutated. A C-terminal cysteine for biotinylation using Maleimide-PEG2 biotin (Thermo Fisher Scientific), C272, was introduced in the genes encoding the soluble portions of both *S. scrofa* and *B. taurus* MR1.

Genes encoding *S. scrofa* MR1 and β2m, as well as *B. taurus* MR1 and β2m were expressed separately in BL21 *E. coli*, and inclusion body protein was prepared and solubilized in 8 M urea, 20 mM Tris-HCl (pH 8), 0.5 mM Na-EDTA, and 1 mM DTT. MR1 (56 mg per 400 ml folding buffer) and β2m (28 mg per 400 ml folding buffer) were folded in the presence of 6-formylpterin (6-FP; 2 ml per 400 ml folding buffer of a 5 mM solution of powder from Schircks Laboratories, dissolved in water, supplemented with 17 mM NaOH) or 5-amino-6-D-ribitylaminouracil [5-A-RU; 105 µl per 400 ml folding buffer of a 100 mM solution in DMSO generated in house (Mak et al., 2017)] and methylglyoxal (637 µl per 400 ml folding buffer of a 40% solution from Sigma-Aldrich), respectively by limiting dilution in a buffer adjusted to pH 8–8.5, containing 5 M urea, 100 mM Tris, 2 mM Na-EDTA, 400 mM l-arginine–HCl, 0.5 mM oxidized glutathione, 5 mM reduced glutathione, PMSF, and pepstatin A and dialyzed in 10 mM Tris before fast protein liquid chromatography purification by sequential DEAE anion exchange, gel filtration, and Mono-Q anion exchange chromatography. Purified protein was then reduced with 25 mM DTT for 15 min before buffer exchange into PBS using a PD-10 column (GE Healthcare). The cysteine-tagged MR1–5-OP-RU and MR1–6-FP monomers were biotinylated with Maleimide-PEG2 biotin (Thermo Fisher Scientific) with a 30:1 M ratio of biotin reagent to protein at 4°C for 16 h in the dark and subjected to Mono-Q anion exchange chromatography to eliminate free biotin and isolate biotinylated MR1–5-OP-RU and MR1–6-FP monomers. Biotinylated MR1–5-OP-RU and MR1–6-FP monomers were stored at −80°C. For tetramerization, aliquots were thawed out and tetramerized with streptavidin conjugated to

PE (BD Biosciences) or Brilliant Violet 421 (BV421; Invitrogen) at a 8:1 M ratio of MR1 to streptavidin–fluorochrome to a final concentration of 143 ng/μl.

4.2.2 qPCR

qPCR of MAIT TCR. Total RNA was extracted from lysed cells using RNeasy Mini Kit (Qaigen) as per manufacturer's instructions. cDNA was created via reverse transcription using SuperScript™ III Reverse Transcriptase (Thermo Fisher Scientific) as per manufacturer's instructions. Real time PCR was performed using a universal probe library (Roche) and primers designed specifically TRAV1, TRAV1-TRAJ33 as well as GAPDH for normalisation and CD3 for comparison. CT scores were normalised to GAPDH before TRAV1 and TRAV1-TRAJ33 RNA amplification was compared to total CD3 RNA amplification.

primer sequences were as follows:

TRAV1:

- FWD-TTACAATGTTCTGGATGGTTGG,
- Rev-GCAACAGAGTGACTAAGGTATGAAGA
- Probe-GAGGAGAG,

TRAV1/TRAJ33:

- FWD-GCACATGAAAGACTCTGCCTT
- Rev-TGGCTTTATAATTAGCTTGGTTCC,
- probe-CTGGGGCT,

CD3:

- FWD-GCTCCCTGGGCAAATCTT
- Rev- GGTATGAGTTCCCCACAAGG
- Roche universal Probe #80

GAPDH:

- FWD- ACAGACACGCGTGTGTTCC
- REV- ACCTTCACCATCGTGTCTTA
- Roche universal Probe #28.

4.3 Comparison of MR1 α1- and α2-domains between species.

Protein sequence alignments of the MR1 α1- and α2-domains (**Figure 4.1A**) were performed to determine sequence similarity between species for which we had MR1-tetramers available or where MAIT cells were being identified. Overall there was a high level of sequence conservation between species with up to 45aa differences between any of the species out of the total 179aa sequence with 21 of these differences having strongly similar biochemical properties (**Figure 4.1A**). This is in line with previous studies showing MR1 to be highly conserved between species, in particular in the α1-/α2-domains, a feature which is not seen in any of the other MHC-I like, classical, or non-classical MHC molecule (Boudinot et al., 2016, Tsukamoto et al., 2013, Yamaguchi et al., 1997, Huang et al., 2009). When comparing the phylogenetic relationship of the MR1 α1/α2 sequences (**Figure 4.1B**), the MR1 of *Homo sapiens* (human) sequence aligned most closely with the non-human primate *Macaca nemestrina* (pigtail macaque) sequence. The *mus musculus* (mouse) sequence was also more closely aligned to human and pigtail macaque. The *Bos Taurus* (cattle) and *Ovis aries* (sheep) α1/α2 sequences aligned most closely together. These phylogenetic relationships mirror the phylogenetic relationship of their respective species (**Figure 4.1C**). Interestingly, the *Sus scrofa* (pig) MR1 sequence aligns most closely with mouse, human, and pigtail macaque, despite being more closely related to sheep and cattle based upon species phylogenetic taxonomy (**Figure 4.1B/C**).

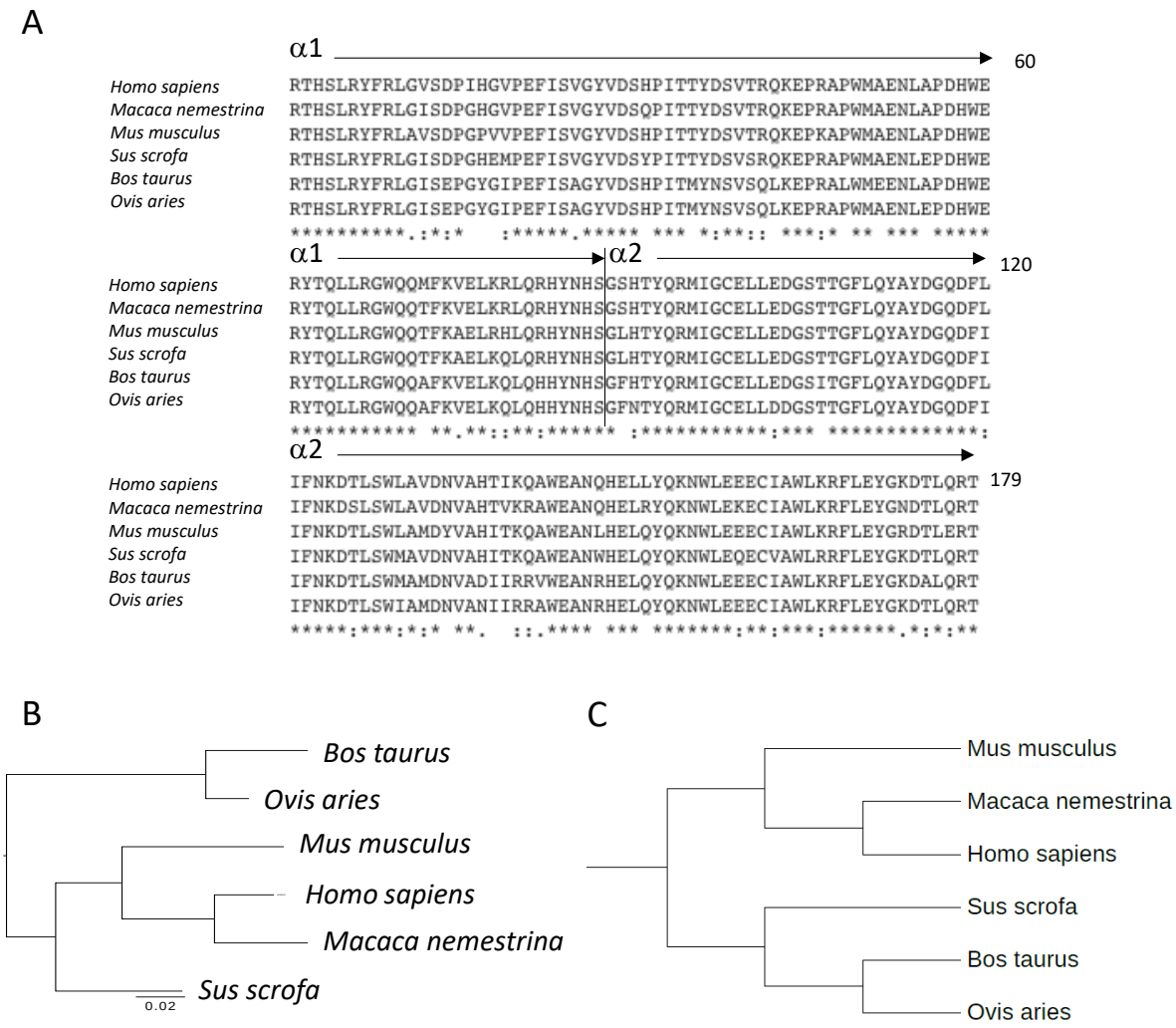

Figure 4.1 Protein sequence alignments and phylogenetic tree of different species MR1 **(A)** Protein sequence alignment of the α1 and α2 domains (indicated) of MR1 from *Homo sapiens* (GenBank ID: AJ249778.1), *Macaca nemestrina* (NCBI Reference Sequence: XM_011746239.*1*), *Mus musculus* (GenBank ID: AF035672.1), *Sus scrofa* (GenBank ID: MH796644.1), *Bos taurus* (GenBank ID: FJ028657.1) and *Ovis aries* (GenBank ID: FJ423039.1) using the EMBL-EBI Clustal Omega multiple sequence alignment program (ref: *DOI: 10.1093/nar/gkz268*). Asterisk indicates a position which has a single, fully conserved residue, colon indicates conservation between aa of strongly similar properties, period indicates conservation between aa of weakly similar properties. **(B)** Phylogenetic tree inferred from the protein sequence alignment of the α1 and α2 domains of MR1 as per A using IQ-Tree 2 by maximum likelihood (ref https://doi.org/10.1093/molbev/msaa015) and FigTree (ref: Andrew Rambaut, Computer program distributed by the author, website: http://tree.bio.ed.ac.uk/software/figtree/) for visualisation, indicating the branch length and scale. **(C)** Phylogenetic tree based on the NCBI taxonomy of Mus Musculus, Macaca nemestrina, *Homo sapiens*, *Sus Scrofa*, *Bos Torus*, and *Ovis ares* using phylot v2 tree generator (ref: Letunic and Bork (2019) Nucleic Acids Res DOI: 10.1093/nar/gkz23)

Though MR1 is highly conserved between species (**Figure 4.1**) (Boudinot et al., 2016, Tsukamoto et al., 2013, Yamaguchi et al., 1997, Huang et al., 2009), only single amino acid changes are needed to affect binding. For example, residue 151 on the MR1 α2 helix (Leu in human, Glu in sheep and cattle, and Arg in macaque) has previously been shown to be essential for ligand-independent activation of mouse MAIT cell hybridoma C62 (Huang et al., 2009) and when mutated to Ala in humans has been shown to enhance MR1 autoreactivity (Reantragoon et al., 2012). To determine the difference in MR1/ TCR contact residues between species, previously described TCR contact residues of MR1 presenting 5-OP-RU (Corbett et al., 2014, Eckle et al., 2014) (**Figure 4.2**) were identified and compared between species to determine if any of the amino acid differences observed between species were likely to affect cross-reactive binding. A total of 15aa residues have been shown to be contacted by MAIT TCRs (***Figure 4.2***), with only two of these, Tyr 62 (α1 helix) and Tyr 152 (α2 helix) being contacted in all crystal structures. Amino acid differences between all species were generally located far from the antigen-binding cleft and were in locations where no MR1/TCR contact has been shown in any of the previously published human crystal structures (Corbett et al., 2014, Eckle et al., 2014) (**Figure 4.3**). Arg 41 was the exception, which is replaced with Glu in sheep and cattle, though Arg and Glu are similar in terms of their biochemical properties. Taken together, these data suggest that there is a high likelihood of cross-reactivity of MR1 between species. There may however be species-specific differences in MR1 binding between MAIT cell clones from different species.

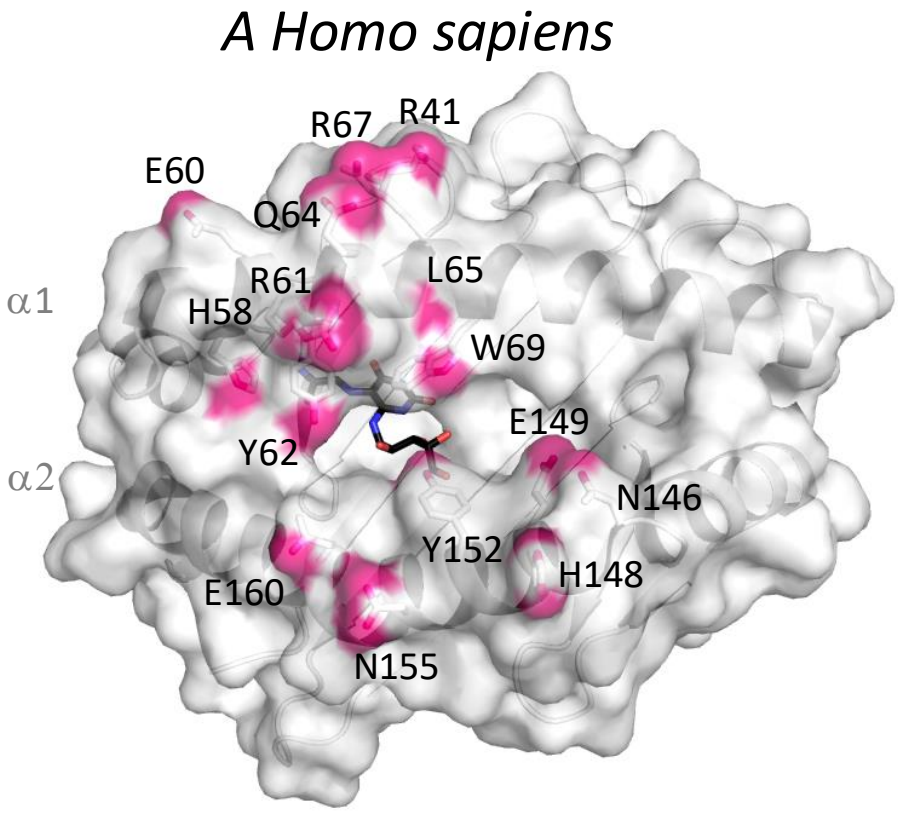

Figure 4.2: MR1 and TCR contacts from all published 5-OP-RU-MR1-TCR crystal structures. Cartoon and surface display (light grey) of the MR1 Ag-binding cleft and stick display of 5-OP-RU (black) based on the protein data bank (PDB) deposited crystal structure featuring the human A-F7 MAIT TCR (Tilloy et al., 1999) in complex with human MR1-5-OP-RU (PDB ID: 4NQC, (Corbett et al., 2014). MR1 atoms contacted in hydrogen bonds (there are no residues contacted in salt bridges), based on analysis using PDBsum (ref: PMID: 9433130) in any of the available crystal structures of human MAIT TCRs in complex with human MR1-5-OP-RU (PDB ID: 4NQC (Corbett et al., 2014); PDB IDs: 4PJ7, 4PJ8, 4PJ9, 4PJA, 4PJB, 4PJC, 4PJD (Eckle et al., 2014)), are highlighted in magenta, residue side-chains displayed in stick format and residues labelled. All contacts include atoms of side-chains except for L65, where the main chain is contacted. The only MR1 residues contacted in all analysed structures are Tyr62 and Tyr152. This figure was generated by Sidonia Eckle using the software The PyMOL Molecular Graphics System, Version 2.3.5 Schrödinger, LLC, and is presented here with permission.

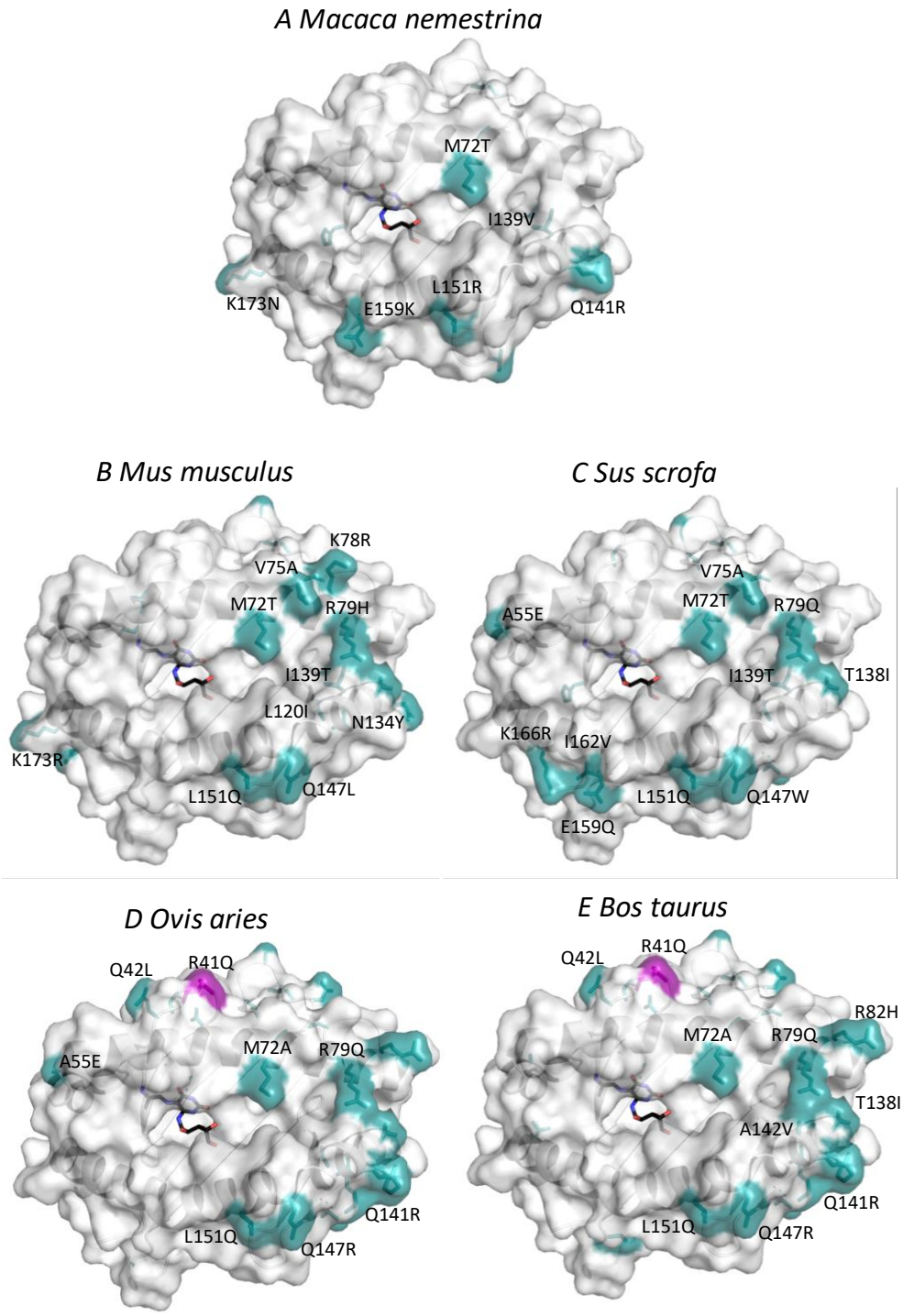

Figure 4.3: Comparisons of α1 and α2 domains of selected species MR1 with MR1 TCR contact residues from all published 5-OP-RU-MR1 TCR structures. Side-chains of residues that differ between human MR1 and MR1 of other species (as indicated) are highlighted in teal and residue side-chains displayed in stick format. Differing residues at the TCR-MR1 interface are labelled as follows: human amino acid residue-residue number – other species amino acid residue. Except for R41 in *Ovis aries* and *Bos taurus* (D, E; highlighted in purple), all the human MR1 residues contacted by human TCRs in hydrogen bonds are conserved between human and other MR1 species (A-E). R41 is a TCR contact residue in 2 crystal structures (PDB IDs: 4PJB, 4PJD ref (Eckle et al., 2014)). This figure was generated by Sidonia Eckle using the software The PyMOL Molecular Graphics System, Version 2.3.5 Schrödinger, LLC, and is presented here with permission.

4.4 Generation of pig and cattle MR1 tetramers

Biotinylated pig and bovine MR1 monomers had molecular weights as expected for βbiotinylated MR1 and β2m when analysed by gel electrophoresis (**Figure 4.4**). The purity of the MR1 monomers was comparable to the human MR1 monomers.

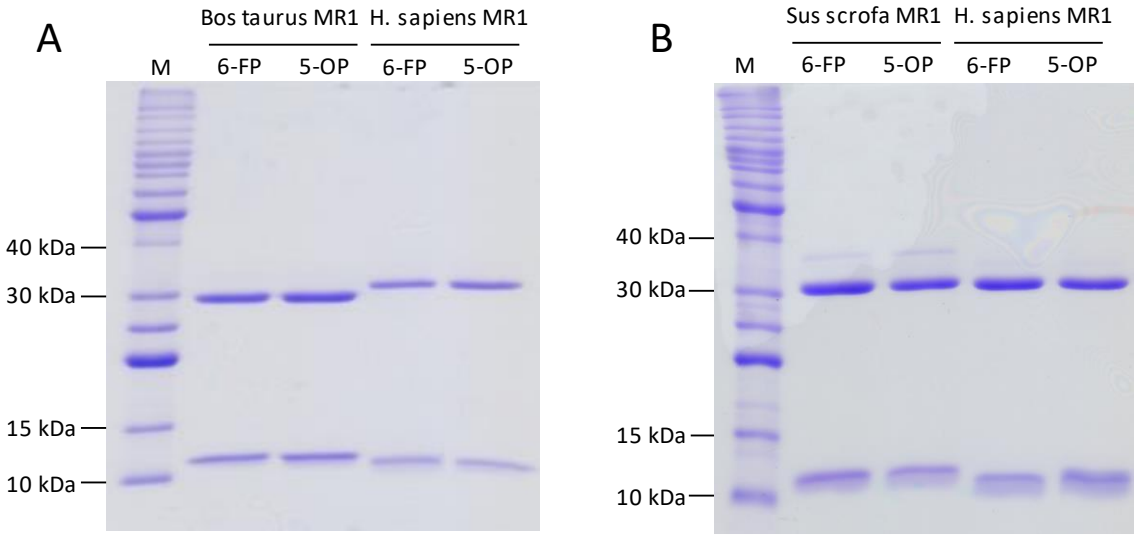

Figure 4.4 Molecular weights of bovine, and pig MR1 5-OP-RU and MR1 Ac-6-FP monomers A, B) 15 % SDS-PAGE under non-reducing conditions of 1.5 µg purified biotinylated bovine, pig and human MR1 in complex with β2m and loaded with 5-OP-RU (5-OP) or 6-FP in comparison to a protein ladder (M) with protein weightsindicated as relevant. Accounting for loss of 4 H atoms and 2 H atoms due to formation of two disulphide bonds in MR1 and one disulphide bond in β2m, the molecular weights of biotinylated MR1 and β2m are: human: MR1: 32,258 Da, β2m: 11,860 Da; bovine MR1: 32,403 Da, β2m: 11,764 Da; pig MR1: 32,526 Da, β2m: 11,542 Da. This data was generated at the Peter Doherty institute by Sidonia Eckle and is presented with permission.

It has previously been shown that the human MR1 specific, conformation-dependent Ab clone 26.5, cross-reacts in flow cytometric staining with mouse, rat, bovine (Huang et al., 2009, Huang et al., 2005) and pig (Xiao et al., 2019b) MR1, as well as in ELISA with human, mouse, and pigtail macaque MR1 (Kjer-Nielsen et al., 2012, Juno et al., 2019). Similarly, the conformation-dependent Ab clone 8F2.F9 (McWilliam et al., 2016), specific for mouse MR1,

had been shown to cross-react with rat, bovine, and human MR1 in flow cytometry (Chua et al., 2011), and with human, mouse and pigtail macaque MR1 in ELISA (Juno et al., 2019). Therefore, 26.5 and 8F2.F9 antibodies were utilised to assess the fold of the newly generated biotinylated pig and bovine MR1 monomers, which differ from the human MR1 α1 and α2 domains in 20 and 28 aa, respectively (**Figure 4.1**). Both 26.5 and 8F2.F9 Abs (**Figure 4.5**), but not isotype controls (**Figure 4.6**), bound bovine MR1–5-OP-RU and MR1–6-FP in a dose-dependent manner though with higher ELISA with EC_{50} values when compared to binding to human monomer. Intriguingly, 26.5 but not 8F2.F9 bound to pig 6-FP loaded MR1, whereas both 26.5 and 8F2.F9 bound pig 5-OP-RU loaded MR1. This data indicates that there are species specific differences in antibody binding of MR1, dependent on MR1 confirmation which is ligand dependent. The binding to human monomers was similar to those observed for human MR1 monomers previously reported (Juno et al., 2019).

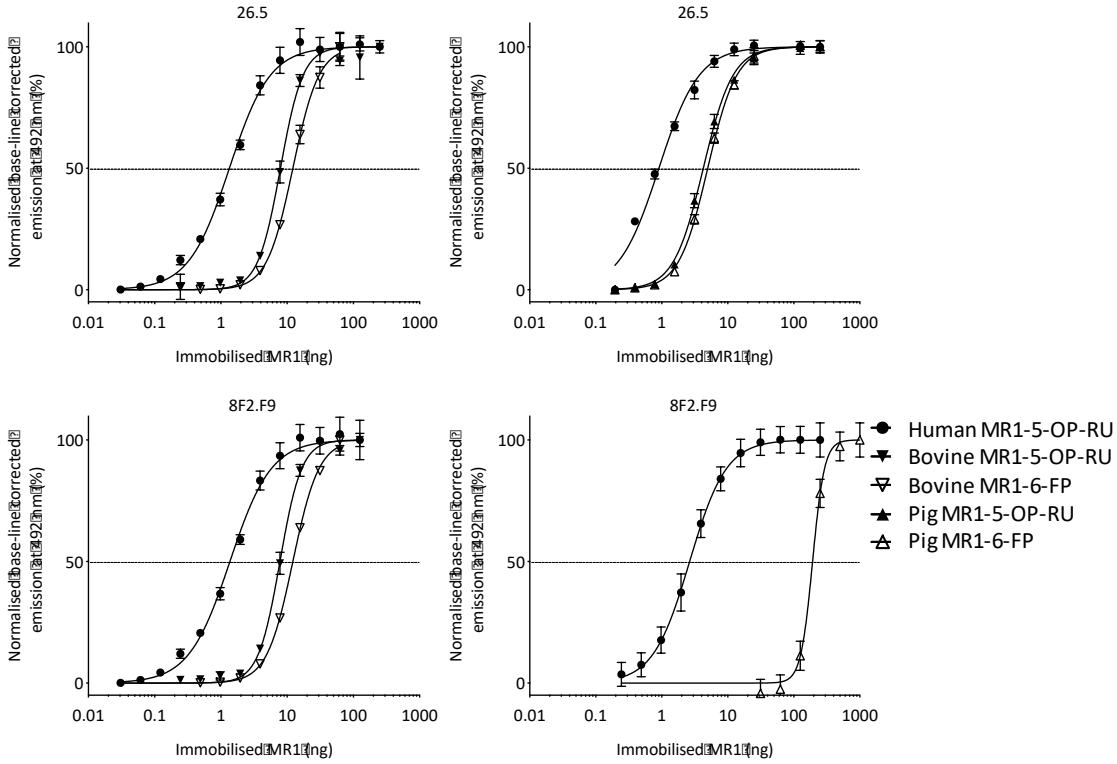

EC50 of antibody binding to MR1 complexes

Protein	26.5 EC50 Mean ± SD (ng MR1)	8F2.F9 EC50 Mean ± SD (ng MR1)
Human MR1-5-OP-RU	0.85 ± 0.02	2.66 ± 0.31
Pig MR1-5-OP-RU	4.25 ± 0.12	No binding
Pig MR1-6-FP	4.98 ± 0.13	193 ± 4
Human MR1-5-OP-RU	1.33 ± 0.06	1.37 ± 0.04
Bovine MR1-5-OP-RU	7.65 ± 0.07	7.82 ± 0.18
Bovine MR1-6-FP	12.3 ± 1.5	12.3 ± 1.4

Figure 4.5 Assessment of the protein folding of biotinylated 5-OP-RU and 6-FP loaded Bovine and pig MR1 molecules 5-OP-RU and 6-FP loaded bovine and pig MR1 monomers in comparison to biotinylated human MR1-5-OP-RU (assessed previously alongside other species' MR1 molecules, (Juno et al., 2019)) in ELISA with 26.5 and 8F2.F9 antibodies showing normalised, base-line corrected dose-response curves (n=3 mean ±SD). EC50 values, as summarised in a table, were determined based on non-linear curve fits shown in the charts. This data was generated at the Peter Doherty institute by Sidonia Eckle and is presented with permission.

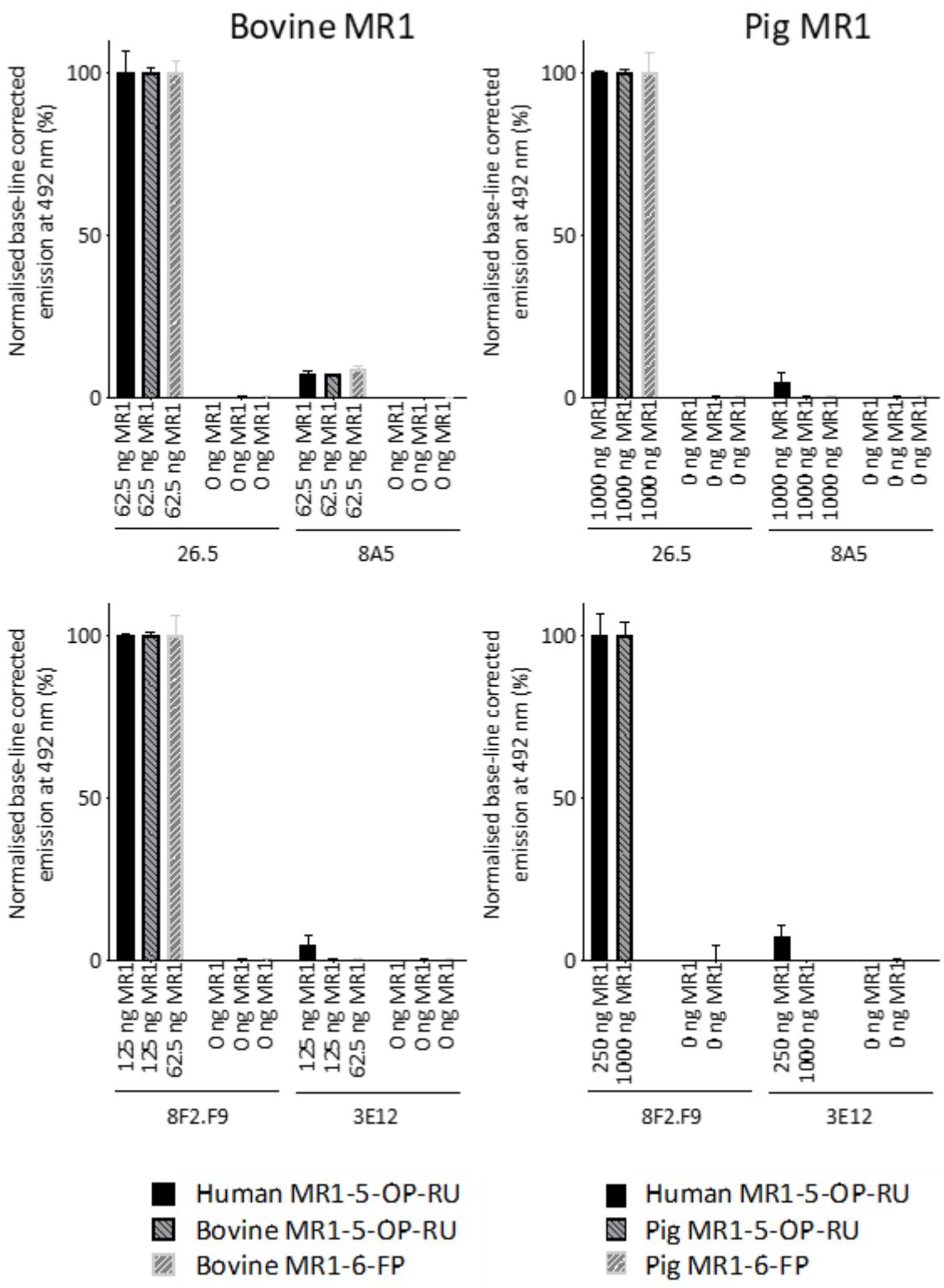

Figure 4.6 Comparison of antibodies 26.5 and 8F2.F9 to isotype control. Isotype controls of the assessment of the protein folding of biotinylated 5-OP-RU and 6-FP loaded bovine and pig MR1 molecules in comparison to biotinylated human MR1-5-OP-RU in ELISA with 26.5 and 8F2.F9 antibodies. This data was generated at the Peter Doherty institute by Sidonia Eckle and is presented with permission.

In summary, biotinylated pig and bovine MR1 monomers were generated that, from a biochemical perspective, appeared suitable for studying MAIT cells in their respective species by flow cytometry, in their tetrameric fluorochrome-tagged version.

4.5 Species-specific and mismatched xeno-reactive tetramers identify MAIT cells in multiple species

Consistent with the high level of conservation of both MR1 (Boudinot et al., 2016, Tsukamoto et al., 2013, Yamaguchi et al., 1997, Huang et al., 2009) (**Figure 4.1**) and the MAIT TCR α-chain conservation (Boudinot et al., 2016, Goldfinch et al., 2010, Tilloy et al., 1999, Tsukamoto et al., 2013, Xiao et al., 2019a), xeno-reactivity between MAIT cells and MR1 has been observed to be microbial-independent (Huang et al., 2009, Lopez-Sagaseta et al., 2013, López-Sagaseta et al., 2013) as well as microbial-dependent (Greene et al., 2017, Koay et al., 2019, Gherardin et al., 2018). Depending on species as well as MAIT cell clone used, cross-species reactivity has previously been observed to be greater (López-Sagaseta et al., 2013, Lopez-Sagaseta et al., 2013) or diminished (Vinton et al., 2016) in terms of affinity of cells captured and staining intensity, or not to occur (Huang et al., 2009, Greene et al., 2017). Here all available MR1 tetramers, including human (Corbett et al., 2014, Reantragoon et al., 2013), mouse (Reantragoon et al., 2013, Rahimpour et al., 2015, Chen et al., 2017), pigtail macaque (Juno et al., 2019) and the newly developed pig and cattle MR1 tetramers were utilised to stain human (**Figure 4.7**), pig (**Figure 4.8**), cattle (**Figure 4.9**) and sheep (**Figure 4.10**) PBMC.

When analysing human PBMC (**Figure 4.7**), a clear MAIT cell population is identified with the human-specific 5-OP-RU MR1-tetramers with a mean tetramer-positive population of 2.7% of the CD3+ population, which is in agreement with the previously described mean of

3.1% (Gherardin et al., 2018). All other 5-OP-RU MR1-tetramers identified a similar sized population regardless of species origin, with a mean fraction of 2.34%, 2.41% 2.23%, 2.34% of the CD3+ population for pig, cattle, mouse, and macaque MR1 tetramers respectively. Differences were observed in the geometric mean fluorescent intensity (GMFI) of the tetramers+ population with a GMFI of 5260, 2695, 6041, 5471, and 10529 for human, pig, cattle, mouse, and macaque 5-OP-RU MR1 tetramer+ populations respectively. As expected, hardly any cells were identified with the human 6-FP tetramer (0.01%) and the same was true for the macaque (0.02%) and pig (0.008%) tetramers, though slightly more cells were stained by the cattle (0.38%) and the mouse (0.22%) reagents.

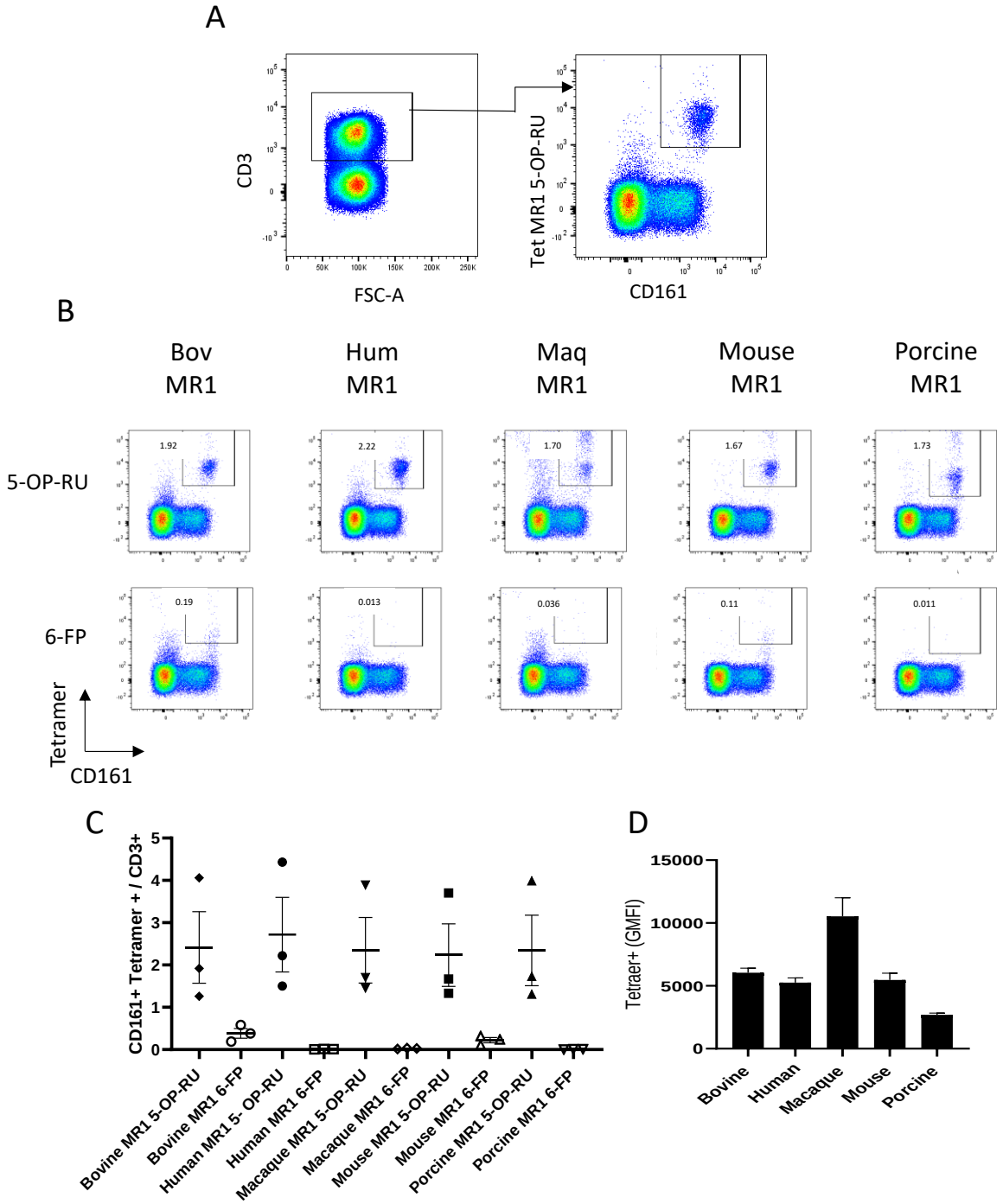

Figure 4.7 Species-specific and xenogenic tetramer stain of human PBMC. A) Gating strategy for MAIT cell identification. B) Representative images of cattle, human, macaque, mouse, and pig MR1-tetramer binding in human CD3+ PBMC. MR1 tetramer binding is plotted against CD161 expression. C) Percentage of cattle, human, macaque, mouse, and pig MR1-5-OP-RU or MR1 6-FP tetramer-positive cells as a percentage of total CD3+ human lymphocytes. D) geometric mean fluorescent intensity (GMFI) of tetramer+ populations as determined in B. Experiments were performed twice with similar results each time.

Unexpectedly, the pig MR1-5-OP-RU tetramer and all other species tetramers identified a very low frequency of cells in pig PBMC (**Figure 4.8**). The mean tetramer-positive population was 0.01% of the CD3+ population with pig specific MR1 tetramer and 0.02, 0.03, 0.01, and 0.01 for human, cattle mouse, and macaque tetramers, respectively. These frequencies are lower than previous estimates of pig MAIT cell numbers estimated to be around 0.2% of all TCRα constant region expressing T cells based on qPCR technique (Xiao et al., 2019a). Similar and in some cases, higher proportions of 6-FP tetramer staining were observed with 0.02% of the CD3+ population using pig specific 6-FP tetramer and 0.06, 0.08, 0.01, and 0.005 for human, cattle, mouse, and macaque MR1 tetramers.

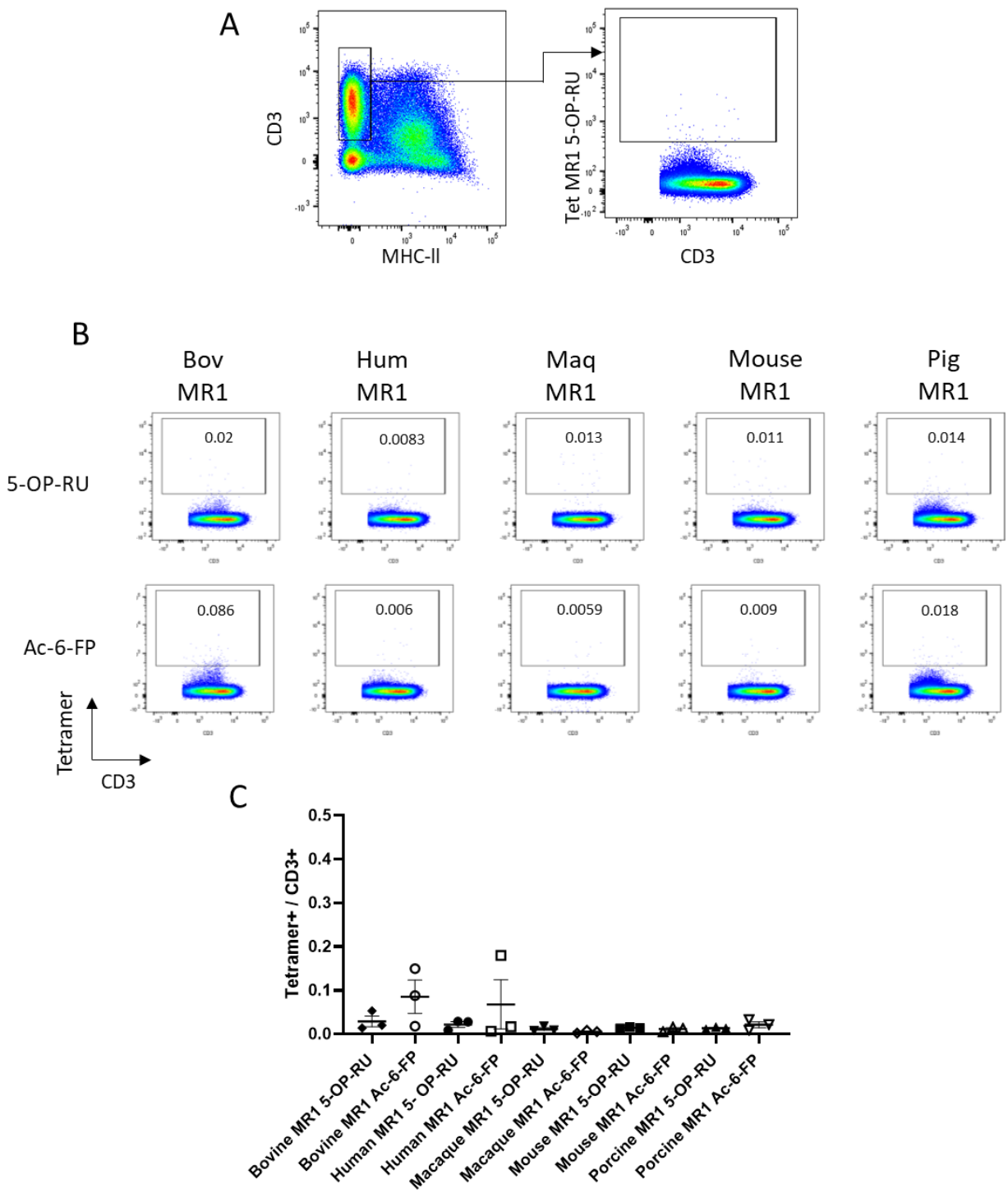

Figure 4.8 Species-matched and xenogenic tetramer staining of pig PBMC. A) Gating strategy for MAIT cell identification. B) Representative images of cattle, human, macaque, mouse, and pig MR1-tetramer expression in pig CD3+ MHCII- PBMC. MR1 tetramer expression is plotted against CD3 expression. C) Percentage of cattle, human, macaque, mouse, and pig MR1-5-OP-RU or MR1 6-FP tetramer-positive cells as a percentage of total CD3+ pig lymphocytes.

Using the newly developed Bovine 5-OP-RU MR1-tetramer, a clear MAIT cell population could be detected in cattle PBMC (**Figure 4.9**) with a mean frequency of 0.32% of the total CD3+ population. The mean frequencies obtained using the species xenogenic reagents were 0.36%, 0.32%, 0.21%, and 0.19% of the cattle CD3+ PBMC for human, pig mouse, and macaque tetramers, respectively. These frequencies are comparable to estimates of cattle MAIT cell numbers using qPCR-based methods where ~0.2% of all TCRα constant region expressing T cells was reported (Goldfinch et al., 2010). Low frequencies of 6-FP tetramer staining were observed with the Bovine tetramer (0.1 %), though this was a comparatively higher frequency when compared to the human, pig, mouse, and macaque MR1 tetramers (0.02, 0.01, 0.03, and 0.01 respectively). The GMFI of the 5-OP-RU-MR1 tetramer+ population also varied between different tetramers of with a GMFI of 2861, 2065, 1215, 2086, and 3022 for cattle, human, pig, mouse, and macaque 5-OP-RU tetramer+ populations.

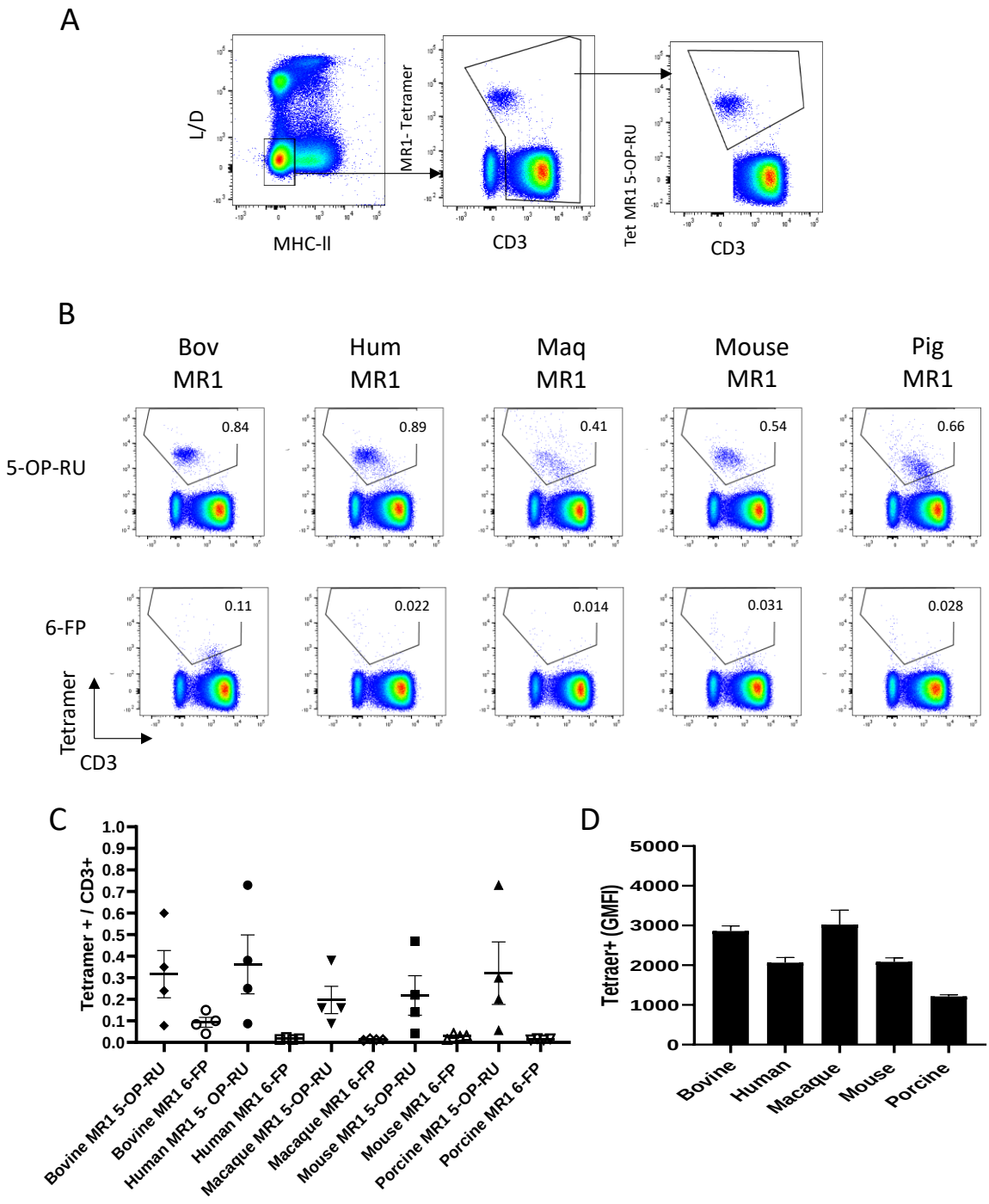

Figure 4.9 Species-matched and xenogenic tetramer stain with cattle PBMC Cattle. A) Gating strategy for MAIT cell identification. B) Representative images of cattle, human, macaque, mouse, and pig MR1-tetramer binding in cattle MHC2- CD3+ PBMC. MR1 tetramer expression is plotted against CD3 expression. C) Percentage of cattle, human, macaque, mouse, and pig MR1-5-OP-RU or MR1 6-FP tetramer-positive cells as a percentage of total CD3+ cattle lymphocytes. D) Geometric mean fluorescent intensity (GMFI) of tetramer+ populations as determined in B-C. Experiments were performed twice with similar results each time

Each of the 5-OP-RU MR1-tetramers identified a comparable MAIT cell population in sheep PBMC (**Figure 4.10**) though no sheep matched reagent was available. The mean frequencies obtained using the species xenogenic reagents were 1.3%, 1.1%, 1.3%, 1.2% and 1.3% of the CD8+ population for human, pig, cattle mouse and macaque MR1 tetramers respectively. Frequencies were obtained within the CD8 population as there is currently no CD3 reagent available for sheep. The lack of a CD3 reagent makes comparisons with previous estimates of sheep MAIT cell numbers difficult, though the population identified here is likely higher than the <0.1% of all TCRα constant regions previously reported using qPCR-based methods (Goldfinch et al., 2010). There were low frequencies of 6-FP tetramer staining with all species tetramers, with mean of 0.24%, 0.19%, 0.2%, 0.18%, and 0.25% binding of human, pig, cattle, mouse, and macaque MR1 tetramers to the sheep CD8+ population. The GMFI of the tetramer+ population also varied between tetramers with GMFI of 2986, 1969, 3113, 2784, and 5805 for cattle, human, pig, mouse, and macaque 5-OP-RU tetramer+ populations, respectively.

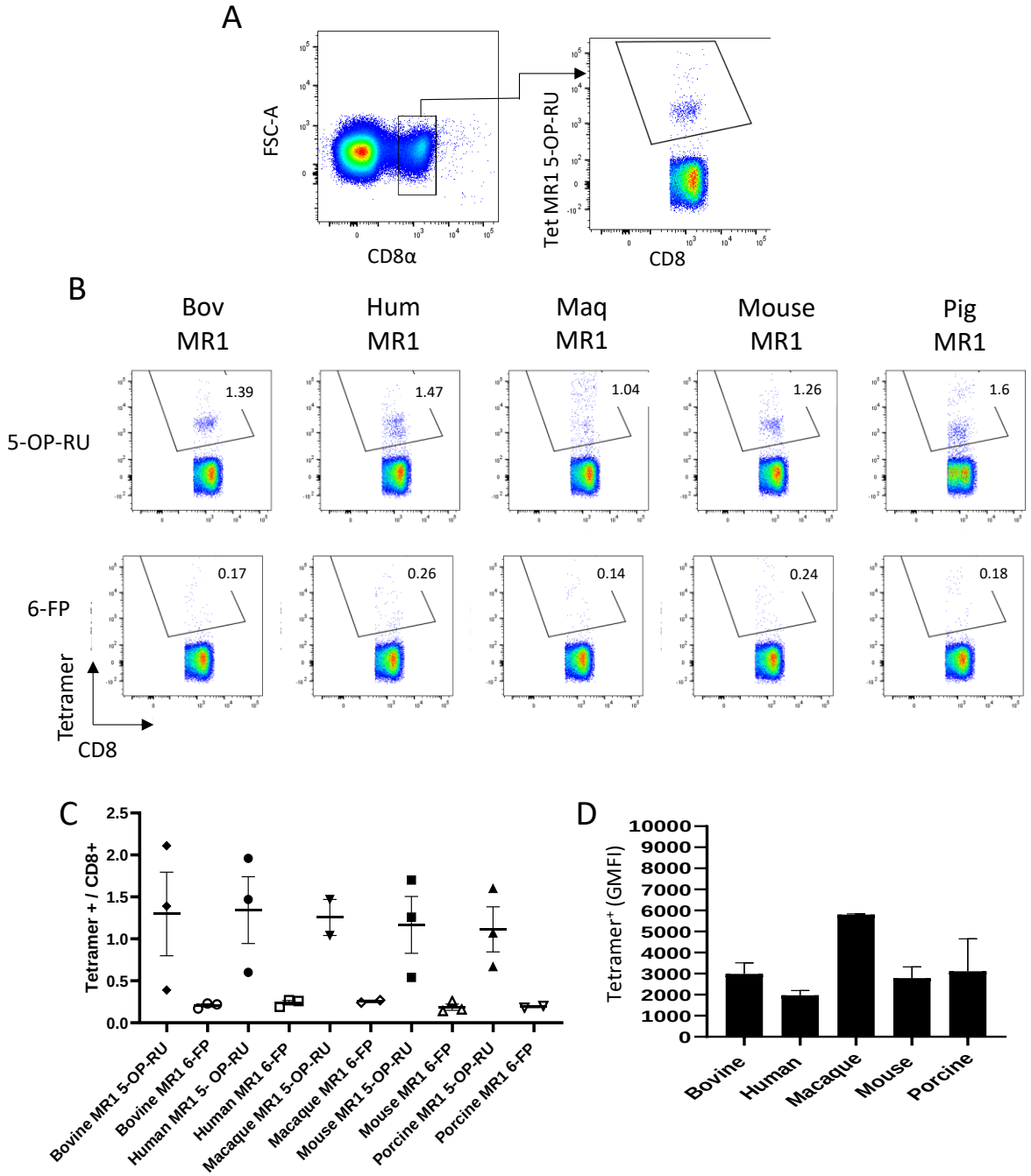

Figure 4.10 Species-matched and xenogenic tetramer stain of sheep PBMC. A) Gating strategy for MAIT cell identification. B) Representative images of cattle, human, macaque, mouse, and pig MR1-tetramer expression in sheep CD8+ PBMC. MR1 tetramer expression is plotted against CD8 expression. C) Percentage of cattle, human, macaque, mouse, and pig MR1-5-OP-RU or MR1 6-FP tetramer-positive cells as a percentage of total CD8+ sheep lymphocytes. D) Geometric mean fluorescent intensity (GMFI) of tetramer+ populations as determined in B-C. Experiments were performed twice with similar results each time

Co-staining of human and pig MR1 tetramers, as well as human and bovine MR1 tetramers, was performed on cattle PBMC to confirm these reagents were staining the same populations in this species (**Figure 4.11**). Both pig and human MR1 tetramers stained similar populations with the majority (78%) binding both tetramers. 20% of MR1-5-OP-RU tetramer+ cells were stained by the human reagent alone, while only 2 % were stained by the pig reagent (**Figure 4.11A**). A similar pattern was observed when co-staining with the human and cattle MR1 tetramers on cattle PBMC (**Figure 4.11B**), where 59% of the tetramer positive cells were co-stained by both 5-OP-RU reagents, 35% stained by the human reagent alone and 6% were stained by the bovine MR1 tetramer alone. While these differences in staining are likely explained by non-specific binding of the reagent, there remains the possibility that tetramers from differing species origin identify slightly different cellular populations.

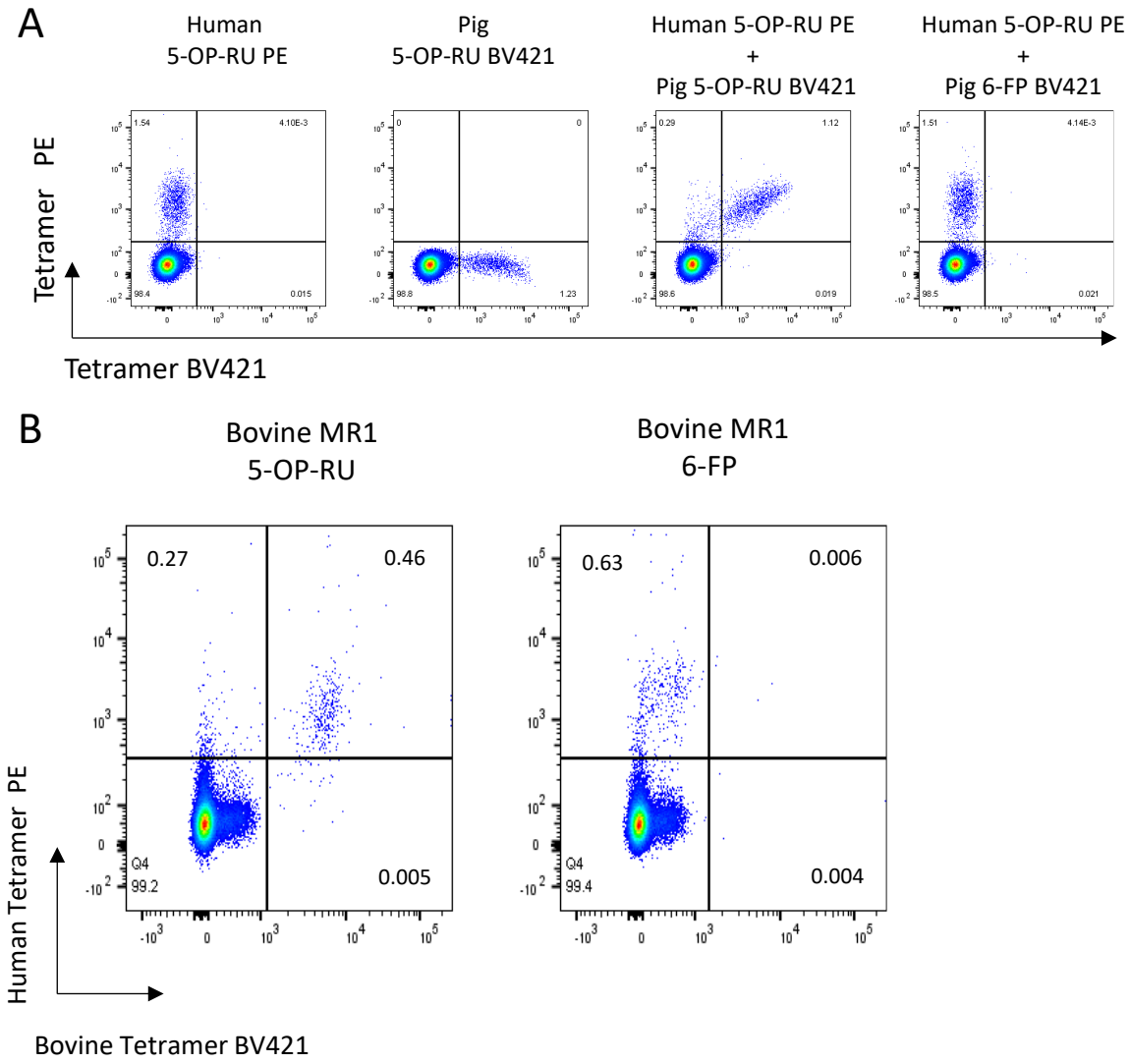

Figure 4.11 Tetramer co-staining on cattle PBMC A) Representative flow cytometry plots for individual and co-staining of cattle PBMC with human and pig MR1 tetramer. Human and pig MR1-5-OP-RU or pig MR1-6-FP tetramers (as indicated) were sequentially added to cattle PBMC. B) Representative flow cytometry plots for co-staining of cattle PBMC with human and bovine MR1 tetramer. Human and bovine MR1-5-OP-RU or bovine MR1-6-FP tetramers were sequentially added to cattle PBMC.

4.6 In vitro stimulation with MAIT cell ligands

In addition to tetramer identification, 5-OP-RU ELISpot was performed in parallel to determine the frequencies of 5-OP-RU reactive T cells in humans, cattle, sheep, and pig PBMC (**Figure 4.12**). As MAIT cells are the only known cellular subset to respond to 5-OP-RU and secrete IFN-γ upon activation (Kurioka et al., 2016), this assay was chosen to confirm the tetramer identification (**Figure 4.12A/B**). Of the 5-OP-RU reactive species, humans had the largest number of IFN-γ responding cells with a mean of 749 SFC/10^6 cells, followed by cattle, which had a mean of 422 SFC/10^6 cells. Sheep had the smallest 5-OP-RU reactive population with a mean IFN-γ response of 243 SFC/10^6 cells (**Figure 4.12B**). The mean number of pig IFN-γ responding cells was 17 SFC/10^6 cells, whereas the response from media alone was 20 SFC/10^6 cells; therefore if any 5-OP-RU reactive T cells are present in the pig, their frequency is below the sensitivity of this assay. Furthermore, the frequencies of tetramer+ cells were compared to the SFC count of each individual animal tested to more closely compare the trends of the two assays (**Figure 4.12B**). The trends for the total numbers of IFN-γ secreting cells were generally in line with the proportion of MR1 tetramer+ cells. The larger MAIT cell 5-OP-RU Tetramer positive populations having correspondingly more 5-OP-RU stimulated T cells.

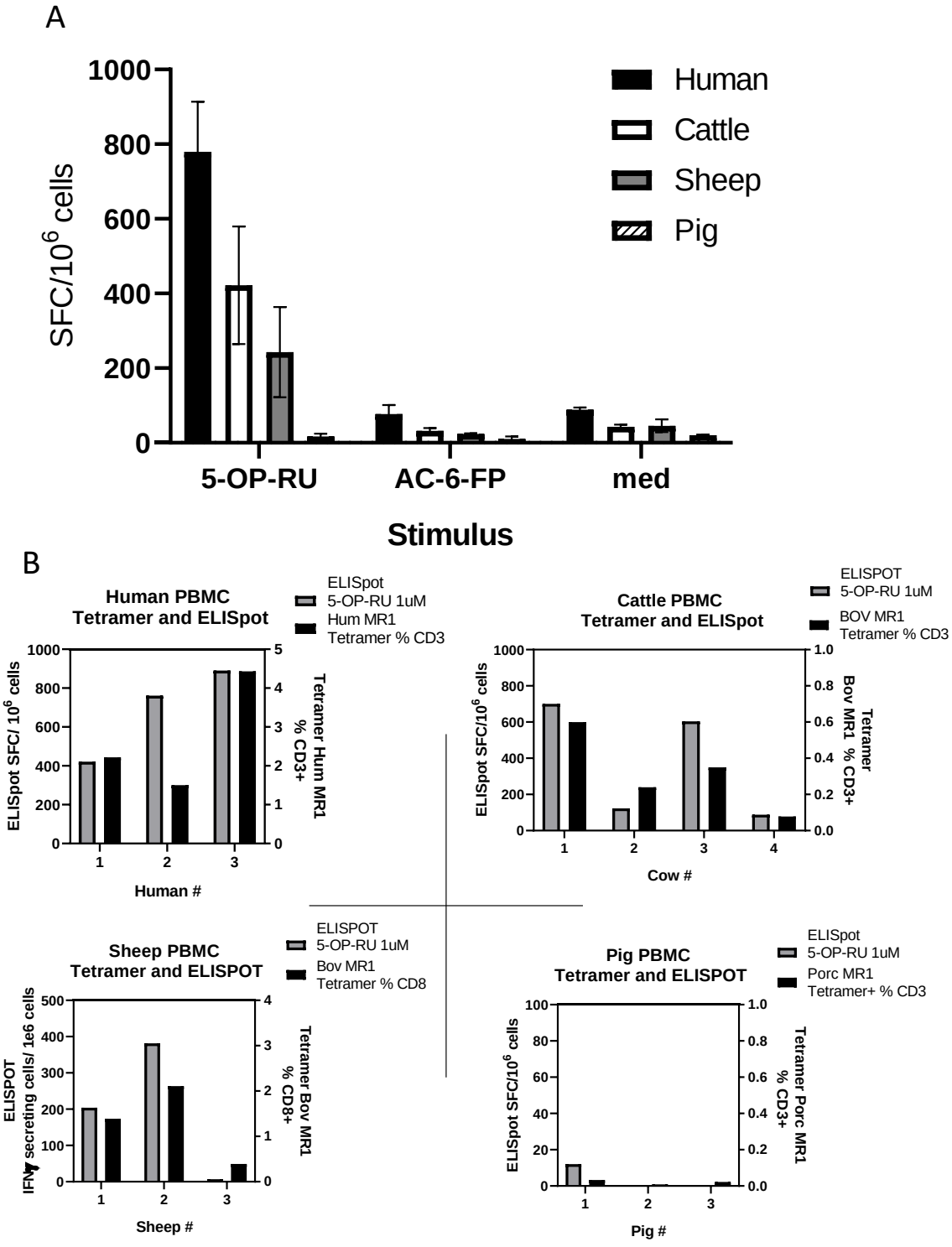

Figure 4.12 ELISpot enumeration of 5-OP-RU reactive T cells in human cattle sheep and pig PBMC.

(A) IFN-γ ELISpot SCF/10^6 cells for human (n=3), cattle (n=4) sheep (n=3) and pig (n=3) PBMC stimulated with 5-OP-RU, Ac-6-FP or medium control. Mean SCF/10^6 cells with SEM are shown for each animal. (B) comparisons of tetramer identification and 5-OP-RU stimulation in human, cattle, sheep and pig PBMC. For each animal, ELISpot response (grey) is shown on the left Y-axes tetramer response (black) is shown on the right Y axes.

4.7 Further assessment of the MAIT cell population in pigs

The lack of a detectable MAIT cell population using species-matched MR1 tetramer or 5-OP-RU stimulation in pigs was unexpected. At the outset of this project, it was known that pigs had the MR1 gene and therefore, would be likely to have MAIT cells. Additionally, it was recently published that pigs express MR1 protein (Xiao et al., 2019b) and have T cells expressing the canonical MAIT cell TCR rearrangement TRAV1-TRAJ33 are present (Xiao et al., 2019a). Though the previous enumerations of pig MAIT cells by qPCR techniques suggested they are in a low abundance (Xiao et al., 2019a), the numbers reported should be detectable by flow cytometry-based methods. Therefore, further assays were performed to determine if a MAIT cell population could be identified in the pig.

In the species xeno-reactive staining (**Figure 4.8**) it appeared that there was a very low tetramer staining with the pig tetramer on pig PBMC regardless of ligand, which was outside the assigned tetramer+ gate. Subsequent staining using the same pig specific reagent showed some level of staining but was not well separated and potentially nonspecific (data not shown). Firstly, in order to lower potential levels of background staining with the MR1 tetramer reagent, the MR1 monomers were tetramerised with streptavidin conjugated to either PE or BV-421 fluorochromes. The tetramer staining was then performed sequentially (PE tetramer followed by BV421) to identify pig MAIT cells with only the double-positive tetramer population being defined as 5-OP-RU tetramer+ MAIT cells (**Figure 4.13**). The same was performed with 6-FP tetramer to compare to the 5-OP-RU tetramer. As it had previously been established that the pig MR1 tetramer reagent cross-reacted onto cattle MAIT cells, cattle PBMC were used as a positive control. In pig PBMC (**Figure 4.13**), the mean frequency of pig MR1 5-OP-RU tetramer double-positive T cells was 0.03% of the CD3+ TCRγδ- population; this compares to 0.008 with the 6-FP tetramer. In cattle PBMC, the frequency of 5-OP-RU tetramer double-positive MAIT cells was 0.53% of CD3+ T cells. Further, the same staining was performed in

single-cell suspensions from TBLN, spleen, BAL, Lung, and Liver (**Figure 4.13**). In pig BAL, liver, and spleen, a higher frequency population, in comparison to PBMC, was identified with the 5-OP-RU tetramers. A mean frequency of 0.31% in BAL, 0.15% in liver, and 0.17% in the spleen of CD3+ TCRδγ- T cell population, which compared to 0.089, 0.005, and 0.081 respectively using the 6-FP tetramer. There was a higher frequency of staining with the 6-FP tetramer compared to the 5-OP-RU tetramer in the lung, with 0.086% of CD3+ TCRγδ- T cells for 6-FP compared to 0.047% with the 5-OP-RU tetramer.

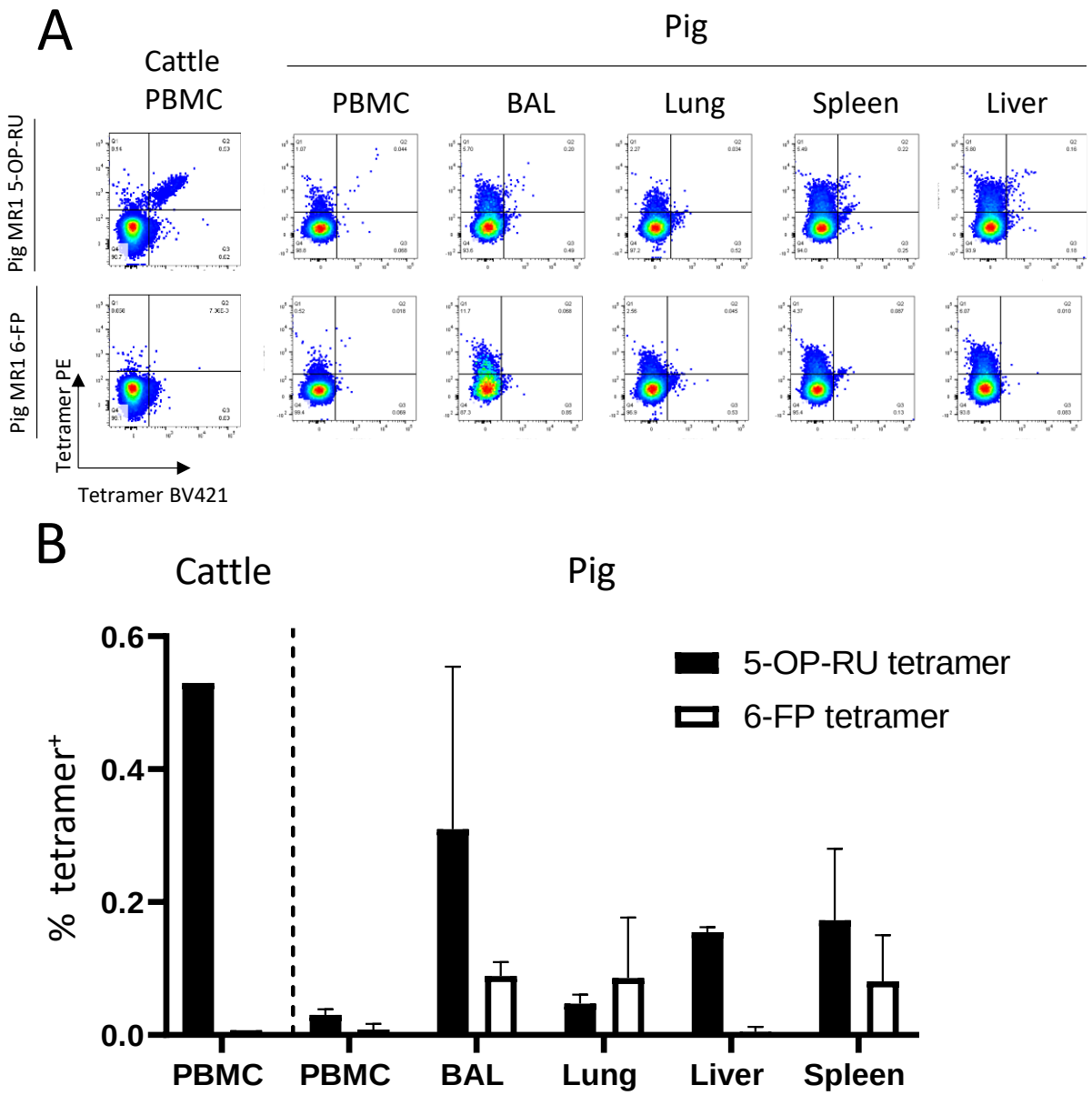

Figure 4.13 Pig MR1 tetramer identification of pig MAIT cells. Pig (n=6) and cattle (n=1) PBMC, BAL (n=3), lung (n=3), liver (n=2) and spleen (n=3) were sequentially stained with PE and BV-421 labelled pig MR1tetramer. A) representative images of cattle and pig PBMC, BAL, lung, liver, spleen co-stained with 5-OP-RU MR1 PE and BV-421 and 6-FP MR1 PE and BV-421 control. For pig CD3+ TCRγδ- T cells are presented. For cattle, CD3+ cells are presented. B) Bar graphs depicting the percentage of cattle and pig MR1 PE and MR1 BV-421 tetramer double-positive T cells within total CD3+ T cells in cattle or CD3+ TCRγδ- T cells in pig pig PBMC.

In parallel to the double-positive tetramer stain pig PBMC cells from TBLN, spleen, BAL, lung, and liver were stimulated with 1μM 5-OP-RU and reactive T cells were quantified by ICS for IFN-γ and TNF secretion (**Figure 4.14**). This was simultaneously performed in cattle PBMC as a control. In cattle CD8+ PBMC, a frequency of 4.8% CD8+ T cells were double positive for IFN-γ and TNF following stimulation with 5-OP-RU. In contrast, in pig CD3+ TCRγδ- T cells, the frequency of IFN-γ TNF double-positive T cells was 0.033%, which compares to a mean 0.023% in the unstimulated PBMC. Similarly, there was little detectable 5-OP-RU induced IFN-γ TNF double producing T cells in tissues with a frequency of 0.081% in BAL, 0.076% in lung, 0.035% in liver, and 0.029% in the spleen. This compares to an unstimulated IFN-γ TNF double positive cells of 0.147% in BAL, 0.044% in lung, 0.105% in liver and 0.036% in spleen.

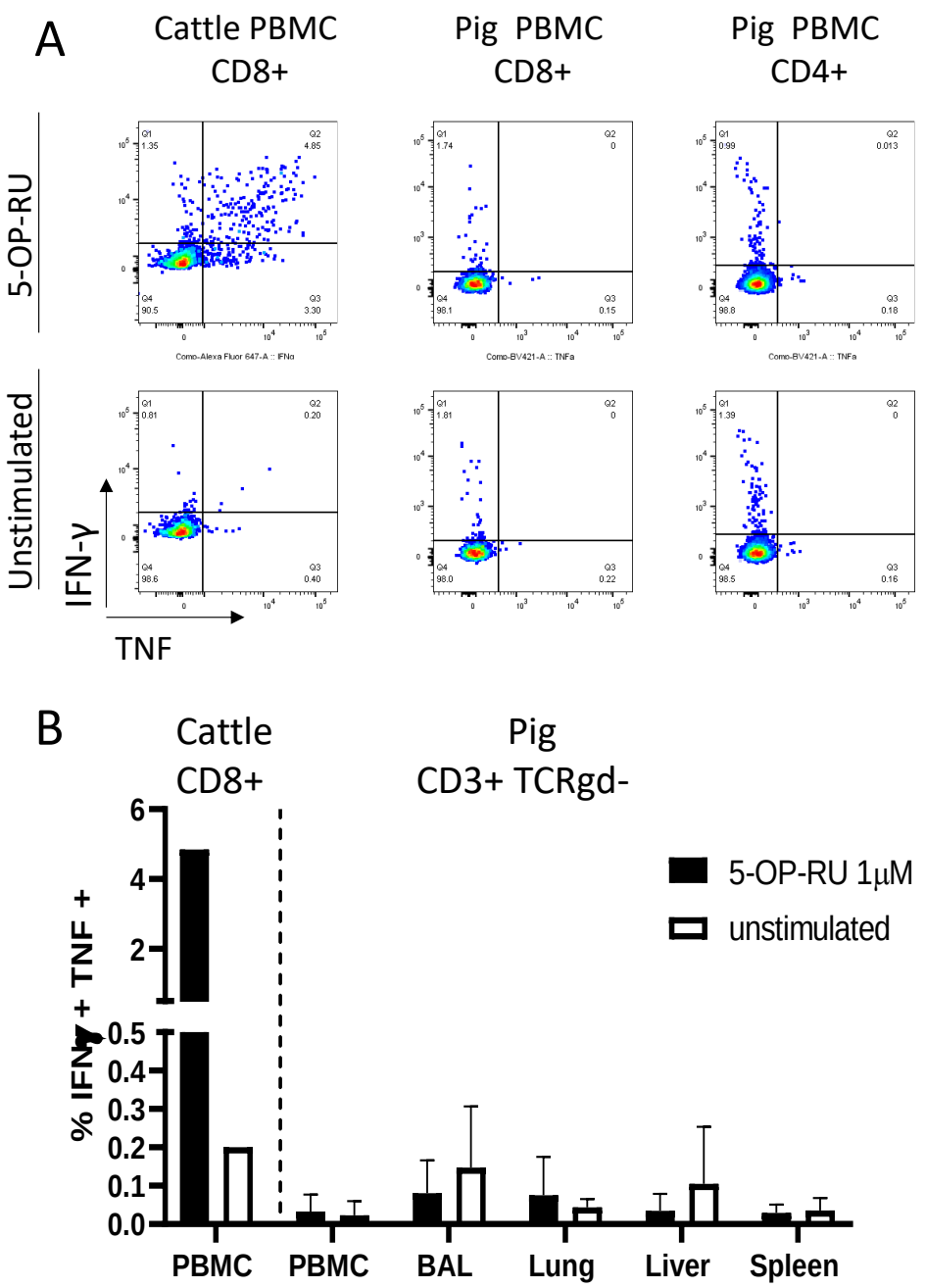

Figure 4.14. Quantification of 5-OP-RU reactive T cells in multiple tissues. A) Representative images of IFN-γ and TNF secretion in cattle CD8+ T cells and pig CD8+ or CD4+ T cells in PBMC following stimulation with 5-OP-RU, or medium control. Previous gating for lymphocytes by FSC and SSC followed by FSC area and height to exclude doublets was performed. Dead cells were excluded with a live/ dead discrimination dye. Cattle PBMC were subsequently gated for CD8α+ T cells. Pig PBMC were gated for CD3+ TCRγδ- T cells and further divided into CD8 or CD4 expressing T cells. Flow cytometric plots depict IFN-γ and TNF secretion in each subset. B) Frequency of IFN-γ and TNF double producing T cells in pig CD3+ TCRγδ- T cells and as a control cattle CD8+ T cells. Bar chart depicts the mean frequency of IFN-γ+ TNF+ cells +/- SEM.

Finally, quantification of the MAIT cell TCR transcript as a relative RNA expression in comparison to CD3 in pig PBMC, TBLN, spleen, BAL, lung, and liver was performed to estimate MAIT cell numbers (**Figure 4.15**). Primers were designed to amplify the TRAV1 and the TRAV1-TRAJ33 transcript (**Figure 4.15A**) and compared to the amplification of CD3. All qPCR reactions were normalised to primers designed to amplify GAPDH. In PBMC, the TRαV1 qPCR had and average relative RNA amplification of 2.2% compared to CD3. However, when amplifying the canonical MAIT TRAV1-TRAJ33 TCR rearrangement, a much lower comparative RNA amplification is observed with a mean of 0.003% of the CD3 amplification. This lower level of amplification compared to CD3 was replicated in tissues with 0.014% in spleen, 0.006% in lung, 0.04% in TBLN, 0.015% in BAL, and 0.009% in liver. These data suggest that there is a low level of TRαV1-TRαJ33 TCR usage within the pig.

A

TRAV1 **Fwd**, **Rev**, **Probe**
TRAV1 TRAJ33 **Fwd**, **Rev**, **Probe**

>pig_TRAV1 – from USDA genome
ATGTGGGGATTTTTCCTTCTTTATGTTTCCCTGACAGTGAGAGGGCAACACTGTGGGAGGAGGCATT
GAGCAGCCCAGTGAGTTGACGGCCATGGAAGGAGCCTCTGTCCAGGTCAACTGCACCTACCAGACAT
TTGGGTTCAACGGGCAGTATTGGTACCAGCACCATGATGGTGGCATACCCTTGTTTCTCAT**TTACAA**
TGTTCTGGATGGTTGGGA**GAGGAGAG**GTCATTTT**TCTTCATACCTTAGTCACTCTGTTGC**ATACAGT
TACCTCCTTGTGAAGGAGCT**GCACATGAAAGACTCTGCCTT**GTACCTCTGTGCTGTGAGAGA

>pig_TRAJ33 – from USDA genome
TGGATAGCAGCTATCAGTTGAT**CTGGGGCT**CT**GGAACCAAGCTAATTATAAAGCCA**G

B

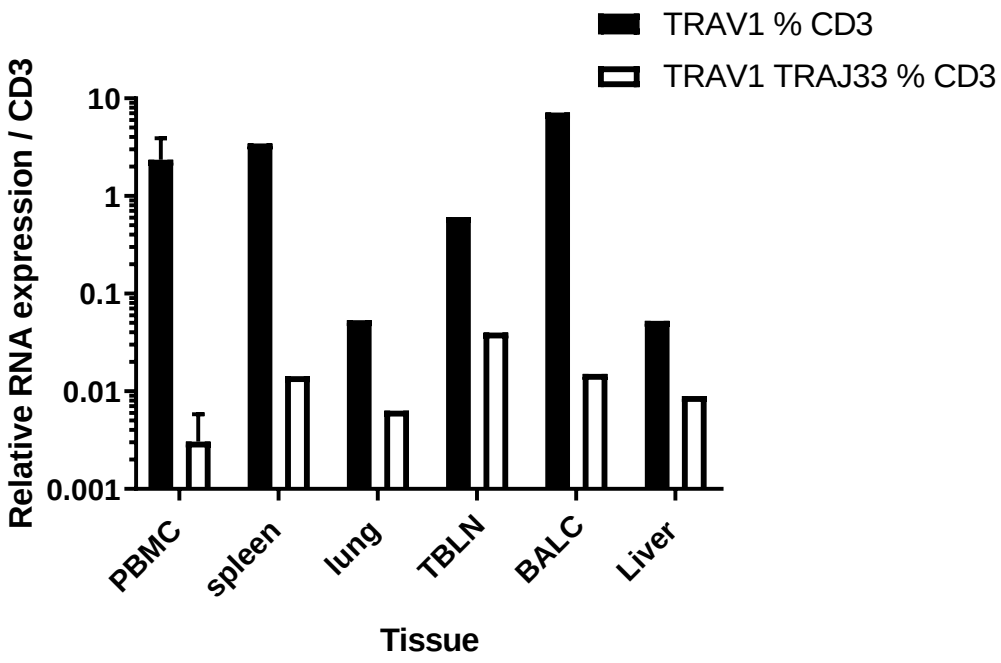

Figure 4.15 qPCR detection of TRAV1-TRAJ33 MAIT TCR sequence. A) primer locations of TRAV1 (not underlined) and TRAV-1 TRAJ33 (underlined) sequence amplification primers. FWD primer (Blue), probe (red), and reverse primer (green) are shown B) relative abundance TRAV1 and TRAV1-TRAJ33 RNA amplification in comparison to CD3 amplification in pig PBMC (N=3), spleen (N=1), lung (N=1), TBLN (N=1), BAL (N=1) and liver (N=1) . 4 reactions were performed for each sample in duplicate with amplification of both TRAV1 and TRAV1-TRAJ33 RNA normalised to GAPDH and then compared to CD3 amplification.

4.8 Discussion

Previous studies have primarily looked at MR1 reactivity across species at the clonal level. In line with the high level of conservation of the MAIT TCR-MR1 axis (Boudinot et al., 2016, Tsukamoto et al., 2013, Yamaguchi et al., 1997, Huang et al., 2009, Tilloy et al., 1999, Goldfinch et al., 2010) xeno-reactivity between MAIT cells and MR1 has been observed between mouse MAIT cells and bovine and rat MR1 (Huang et al., 2009) and between human MAIT cells and rat, mouse and bovine MR1 (Huang et al., 2009, López-Sagaseta et al., 2013, Lopez-Sagaseta et al., 2013). However, the degree of cross-reactivity between human MR1 and MAIT cells from non-human primates appeared to vary (Greene et al., 2017, Vinton et al., 2016); whilst macaque MR1 was able to bind to human MAIT cells (Greene et al., 2017).

The data presented in this chapter represents the most comprehensive study of MR1 tetramer xeno-reactivity between species to date. A high level of xeno-reactivity between differing species MAIT cells and MR1 of distantly related species was observed. This tetramer cross-reactivity was primarily ligand dependent as 5-OP-RU tetramers of each species origin cross-reacted onto each species which had MAIT cells identified by their species-specific reagent, whereas 6-FP MR1 tetramers detected comparatively low frequencies of T cells. Similar frequencies of MAIT cells were identified regardless of tetramer species origin though small differences in total frequency and more considerable differences in GMFI were observed between tetramers. When performing co-staining with human pig and cattle MR1 tetramers on cattle PBMC (**Figure 4.11**), the tetramers of different species origin co-stained most of the same cells. However, small populations were observed which only stained with one species tetramer. Therefore, I conclude that though using xeno-reactive tetramers can be a good proxy for the identification of MAIT cells in different species using the species-matched reagent is preferable to be sure that no rare populations are missed, or no antigen-independent xeno reactivity confounds results.

The frequency of MAIT cells varied between species and individuals. Humans had the largest population with an average 2.7% of CD3+ T cells (human MR1 tetramer figure 2B) akin to the previously described mean of 3.1 % (Gherardin et al., 2018), followed by cattle and sheep with an average of 0.3% CD3+ T cell and 1.1% CD8+ T cells respectively (cattle MR1 tetramer).

4.9 Summary

At the outset of this project, the focus of MAIT cell identification was in pigs, intending to identify MAIT cells in the pig and study them in the context of influenza studies (as described in Chapter 3). However, no discernible population of T cells was detected in pigs with MR1-5-OP-RU tetramers, even when using the pig specific MR1 tetramer reagent. The pig MR1 tetramer did, however, identify populations of T cells in all other species that were similar in size and level of tetramer fluorescence as those detected by other species MR1-5-OP-RU tetramers (**Figures 4.7-10**). Further, the majority of the cattle PBMCs that stained with human MR1- 5-OP-RU tetramer, co-stained with pig MR1-5-OP-RU tetramer (**Figure 4.11**), suggesting that the pig MR1 tetramer was functional. Further assessment of the pig MAIT cell population by tetramer identification in multiple tissues (**Figure 4.13**), ligand stimulation (**Figure 4.12** and **Figure 4.14**), and qPCR (**Figure 4.15**) all showed that the pig MAIT cell population is at the limits of detection with no assay detecting a greater than 0.1% of the T cell population in PBMC. Though greater frequencies were identified in tissues (**Figure 4.14B**), the staining profiles of these cells were poorly separated and the cells identified likely an over-estimate (**Figure 4.14A**). I therefore conclude that MAIT cells in pigs characterised as T cells which are phenotypically identified by binding to 5-OP-RU MR1 tetramers or cytokine responsiveness to 5-OP-RU ligand are either not present or present at levels which are at the edge of flow-cytometric detection. These findings partially agree with the previous finding by Xiao *et al.*, though they estimate a small MAIT cell population of ~0.2% of T cells (in PBMC), the data presented here suggest that the population may be smaller than their estimates.

The very low numbers of pig MAIT cells identified in this study preclude performing a detailed analysis of the MAIT cell population in the time course samples described in chapter 3. However, the larger MAIT cell population in ruminants, particularly cattle, identified in this study created an opportunity to study MAIT cells in more detail in this species. Chapter 5 will concentrate on further analysis of the MAIT cell population identified in cattle.

Chapter 5 Phenotype and response to bacterial infections of cattle MAIT cells

5.1 Aims and rationale

The results presented in chapter 4 demonstrate that cattle have the largest MAIT cell population identified outside of primates. Previous studies of MAIT cells in cattle have relied on genomic methods to estimate cattle MAIT cells frequencies and phenotype (Tilloy et al., 1999, Goldfinch et al., 2010) which limited their ability to characterise these cells in detail. Having established an MR1-tetramer-based staining strategy, I next focussed efforts on characterising cattle MAIT cells in more depth. MAIT cells were identified by xeno-reactivity of human and pig MR1 tetramers prior to the generation of the bovine MR1 tetramer. Therefore, the subsequent characterisation of cattle MAIT cells was performed using the human MR1 tetramer. Detailed studies of cattle MAIT cell identification with species matched and mismatched MR1 tetramers (presented in Chapter 4), demonstrated that these reagents identified similarly sized populations with similar staining profiles. Furthermore, most cattle T cells identified with human MR1-5-OP-RU tetramer co-stained with bovine MR1-5-OP-RU tetramer, suggesting that human MR1 tetramers can act as a good proxy for identifying cattle MAIT cells.

MAIT cells are unconventional T cells with functional properties and a specific phenotype which distinguish them from conventional T lymphocytes. In humans, these properties include an effector memory phenotype prior to antigen exposure (Dusseaux et al., 2011), enrichment in mucosal tissues (Kurioka et al., 2016) and expression of specific transcription factors such

as PLZF (Koay et al., 2016b). Further phenotyping of the MAIT cell population was performed to determine whether MAIT cells in cattle share these characteristics.

The aims of this chapter are to characterise the cattle MAIT cell population in detail, including ex vivo phenotyping functional assays *in vitro* and ex vivo during infection. The main aims of this chapter are as follows:

- Enumerate and phenotype cattle MAIT cells. Determine their frequency, co-receptor usage, activation status, and effector phenotype. Phenotypically compare MAIT cells in different tissues.
- Perform TCR sequencing in the MAIT cell population to determine TCR usage of the MR1 tetramer + MAIT cell population.
- Determine the reactivity of MAIT cells to known MAIT cell ligands as well as cytokine stimulation and activation with disease-relevant bacteria
- Study the MAIT cell population in the context of common bacterial infections in cattle. Namely tuberculosis and mastitis.

5.2 Chapter specific methods

5.2.1 TCR sequencing

CD8+humMR1-5-OP-RU- and CD8+humMR1-5-OP-RU+ T cell populations for TCR sequencing sequential MACS isolation and cell sorting were performed as described in Cell sorting and depletion (Chapter 2.8) a. Isolated cells were stained with human MR1-5-OP-RU tetramer, followed by staining with mAbs MM1a (anti-CD3) and ILA105 (anti-CD8) and secondary antibodies and Fixable Yellow Dead Cell Stain (Thermofisher Scientific). Purity of ungated sorted CD8+ human MR1-5-OP-RU+ cells was between 91-99% 9 (**Figure 5.1**) These cells were sorted using a FACSAria III (BD). CD8+ human MR1-5-OP-RU- and CD8+ human

MR1-5-OP-RU+ T cell populations were sorted directly into lysis buffer for RNA isolation (RNeasy Plus Micro kit, Qiagen). RNA was isolated from 20,000 cells using the RNeasy Plus Micro kit according to manufacturers' instruction, with the addition of 4ng/ul carrier RNA. cDNA was generated using the SuperScript IV kit (ThermoFisher Scientific) with a SMART oligo containing unique molecular identifiers (AAG CAG UGG TAU CAA CGC AGA GTUNNNNUNNNNUNNNNUCTTggggg (where N represents a mixture of A, T, G and C and lower case 'g' represents RNA bases) and the uracil-containing primers subsequently removed by treatment with UDG (NEB, Hitchin, UK). TRA and TRB primers sequences were amplified using a pair of 5' 'step-out' primers specific for the SMART oligo (Long 5' primer - CTA ATA CGA CTC ACT ATA GGG CAA GCA GTG GTA TCA ACG CAG AGT, and short 5' primer - CTA ATA CGA CTC ACT ATA GGG CAA GCA G) in combination with TRAC- (TGG GGT TGG GGT CCT TGA CTT) and TRBC- (GAC SYG GCT CAG ATC ATC) specific 3'primers. PCR amplification was conducted using Phusion HF reagents (NEB) and employed the following cycling conditions: manual hot start, 30s at 98°C, 35 cycles of (98°C for 10s, 65°C for 30s, 72°C for 30s) and a final extension period of 5 min at 72 °C. PCR products of the anticipated size were excised following agarose gel electrophoresis, purified using AMpure beads (Beckman Coulter, Indiana, US) and sent to Edinburgh Genomics for sequencing on the Illumina MiSeq v3. Platform. Analysis of the TCR repertoire was conducted using the MiXCR package (Bolotin et al., 2015) using an external database of bovine TRAV, TRBV, TRAJ and TRBJ genes derived from a combination of published (Connelley et al., 2014, Connelley et al., 2009) and unpublished data. A list of the top 50 frequency sequences obtained from the tetramer positive population is shown in **Appendix 7.2**.

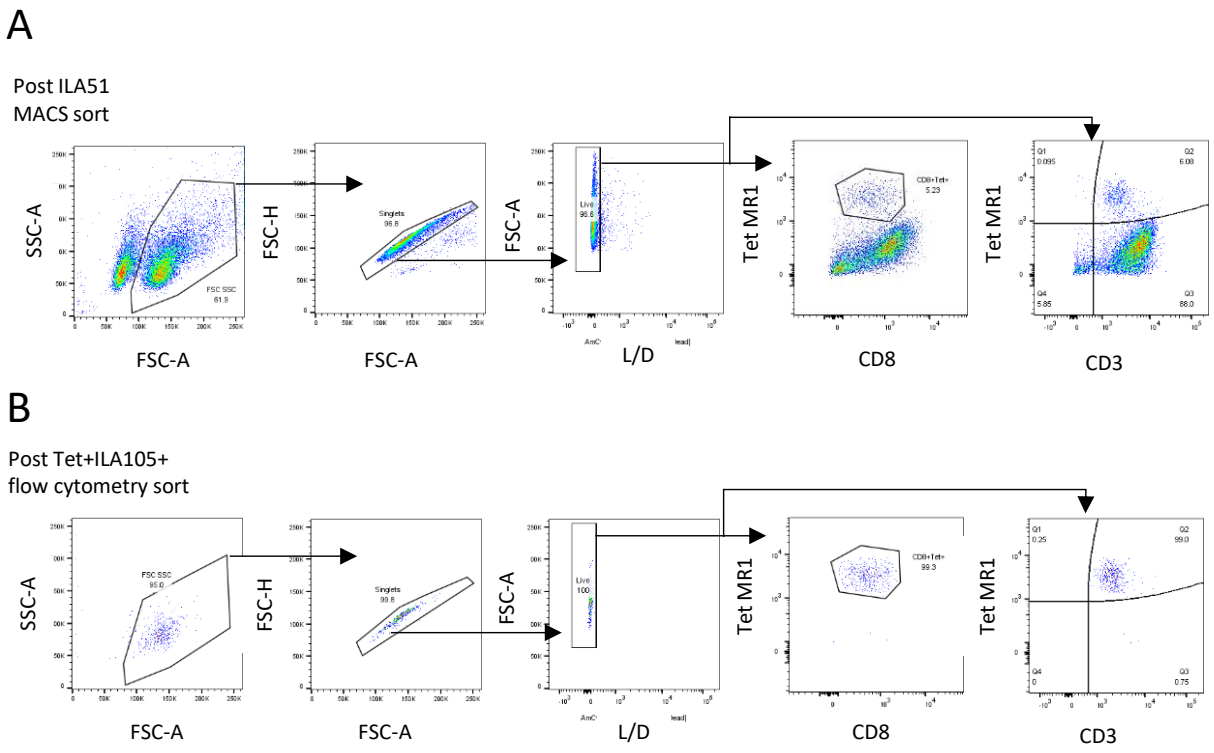

Figure 5.1 MAIT cell sorting **(A)** Representative of 5-OP-RU-MR1 tetramer staining following ILA51 (CD8) MACS sorting **(B)** Representative of 5-OP-RU-MR1 tetramer staining following ILA51 (CD8) sorting and subsequent ILA105 (CD8) and 5-OP-RU-MR1 tetramer flow cytometry sorting.

5.3 5-OP-RU MR1 tetramer-positive T cells are an expanded population in cattle peripheral blood.

Testing a cohort of cattle (n=17) of varying age (3 to 56 months) (**Figure 5.2**) confirmed that MAIT cells are an expanded population, representing a mean frequency 0.6% and median frequency of 0.5% of T cells. The frequency of MAIT cells varied considerably between individuals with a range of 0.18-1.72% and an interquartile range (IQR) of 0.33-0.66% of total T cells. This is analogous to studies in humans where frequencies of MAIT cells vary widely between individuals with a mean of 3.1% of total T cells, varying from 0.1-9.2% with a median of 2.6% and an IQR of 1.3-4.5% (Gherardin et al., 2018). No association between age and MAIT cell numbers was identified (**Figure 5.2**). Cattle give birth to their first calf around 24 months of age; therefore, the majority of the animals tested could be considered juvenile or young adults.

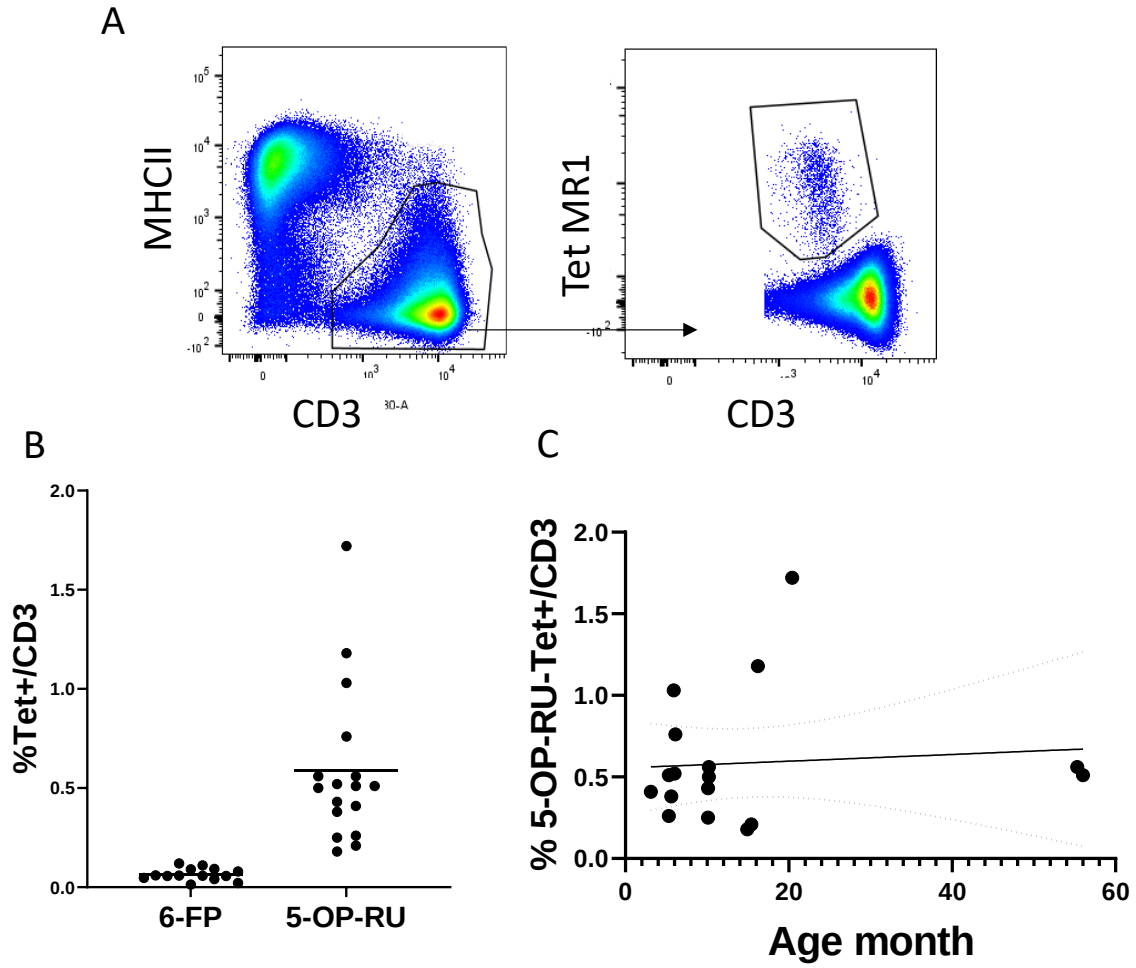

Figure 5.2: Fraction of Human MR1-5-OP-RU + MAIT cells in cattle PBMC. A) Gating strategy for enumeration of MR1-5-OP-RU and MR1-6-FP tetramer+ cells. B) Proportion of human MR1-5-OP-RU (mean 0.59, range 0.18-1.72, n=17) and 6-FP (mean 0.06, range 0.01-0.12, n=14) tetramer+ populations within MHC-II- CD3+ lymphocytes in cattle PBMC of various ages. C) XY plot and linear regression model of MR1-5-OP-RU MAIT cells vs animal age.

5.4 Cattle 5-OP-RU tetramer + MAIT cells express the canonical TRAV1-TRAJ33 MAIT TCR and transcription factors associated with MAIT cells

The canonical MAIT TCRα chain (TRAV1-TAJ33) has previously been identified in cattle by sequencing of a limited number of unsorted T cells with no pre-identification of MAIT cells (Tilloy et al., 1999, Goldfinch et al., 2010). Here deep TCR profiling of bovine CD8+ MR1-5-OP-RU tetramer+ MAIT cells was performed and compared to MR1-5-OP-RU tetramer- CD8+ T cells. The sorted tetramer+ MAIT cell populations were highly enriched for the canonical TRA variable gene segment 1 (TRAV1) (73.3%) and the corresponding TRA joining gene segment 33 (TRAJ33) (72%) which were not enriched in the CD8α+ non-MAIT cell population (**Figure 5.3 and Figure 5.4A**). The TCRβ chain of bovine MAIT cells was more diverse than the TCRα chain, though an enrichment of TRBV4, TRBV7 and TRBV20 was seen in the MAIT cell population compared to the non-MAIT CD8α+ population (**Figure 5.4A**), accounting for 35% 13% and 23% of total TRBV sequences in MAIT cells respectively. This mirrors findings in humans where the critical residues for MR1 recognition are found in the TCRα chain (Reantragoon et al., 2012, Patel et al., 2013) and the TCRβ chains are more highly variable, though specific TRBV, particularly TRBV6, dominate (Reantragoon et al., 2013, Eckle et al., 2014, Gherardin et al., 2018, Gold et al., 2014, Lepore et al., 2014, Held et al., 2015). The CDR3α of CD8α+ MAIT TCRs were primarily 12aa long (**Figure 5.4B**) similar to the canonical human MAIT cell TCR, accounting for 76 % of all MAIT cells, whereas CDR3α loops of non-MAIT TCRs varied much more in length and most (73 %) were longer. The CDR3β loops of CD8α+ MAIT TCRs were more varied in length than the CDR3α and displayed a similar length distribution as compared to those of non-MAIT CD8α+ TCRs. In humans the MAIT TCRα rearrangements TRAV1-2-TRAJ33/20/12 account for the majority (~95%) of MAIT TCR clonotypes in the blood (Reantragoon et al., 2013, Gherardin et al.,

2018, Gold et al., 2010, Gold et al., 2014, Lepore et al., 2014, Held et al., 2015). When analysing the MR1-5-OP-RU tetramer+ MAIT cell population at the clonal level (**Figure 5.4C**), 62-76% of the tetramer + population expressed the canonical TRAV1-TRAJ33 TCR rearrangement, similar to what Greene et al. previously described in macaque blood where 70 % of MAIT TCRs were TRAV1-2+(Greene et al., 2016). TRAV1-TRAJ33+ cattle MAIT TCRs featured two highly similar CDR3 sequences, the predominant sequence of which was CVVMDGNYQWIW with a secondary sequence observed in all animals with a single aa substitution of methionine to isoleucine at position 91 (**Figure 5.4C**). The same position in addition to the neighbouring residue also varies in human TRAV1-2-TRAJ33+ MAIT cell TCRs (CAXXDSNYQLIW) (Tilloy et al., 1999, Gold et al., 2010, Gherardin et al., 2018, Held et al., 2015). These sequences agree with previously predicted putative cattle MAIT TCR CDR3α sequences (Goldfinch et al., 2010, Tilloy et al., 1999). Both of the cattle CDR3 sequences are conserved in Tyr95, which is critical for MR1 and antigen-binding in humans (Reantragoon et al., 2012). This data demonstrates that the human MR1 5-OP-RU tetramer-positive population express the canonical MAIT TCR rearrangement.

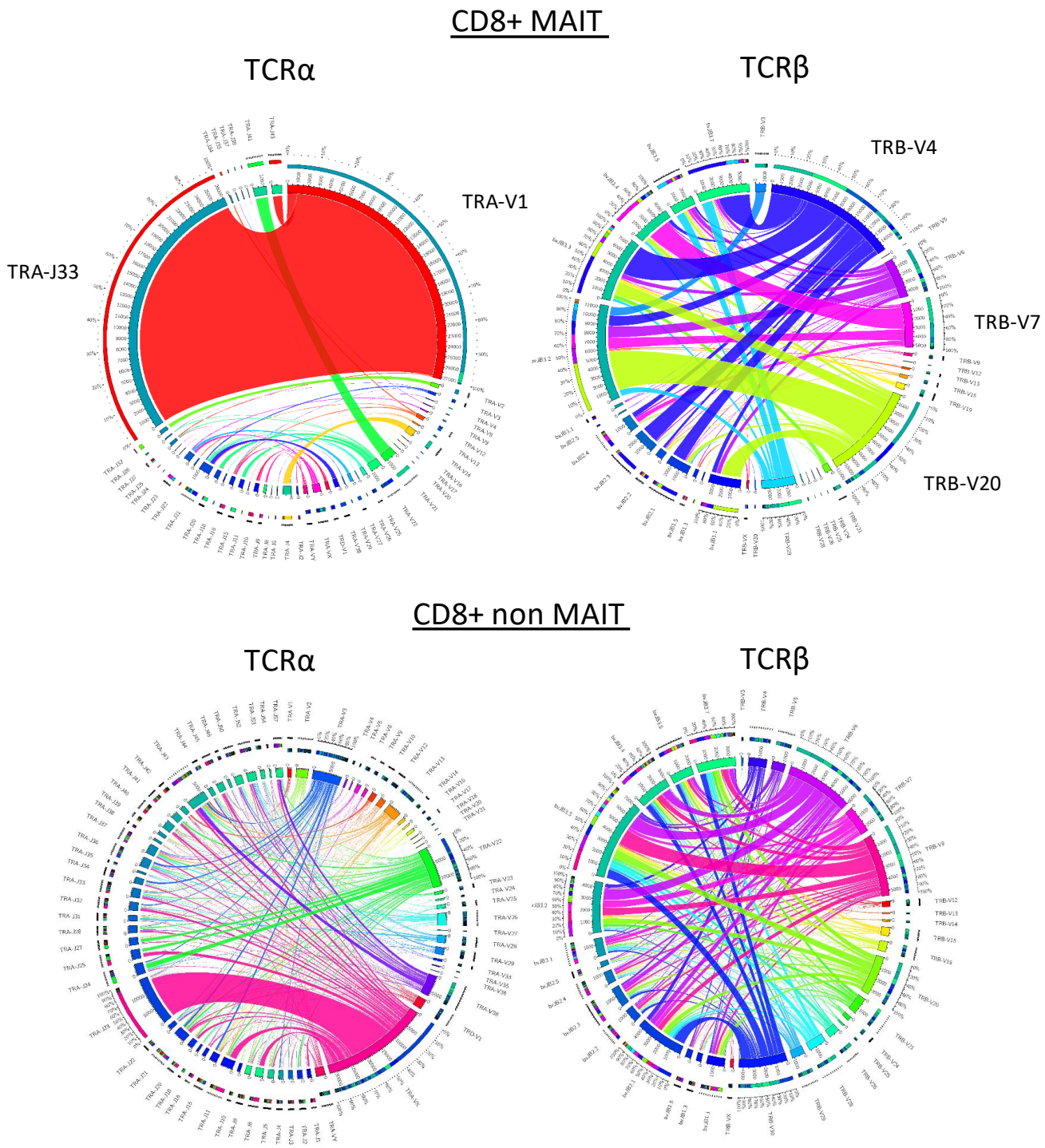

Figure 5.3. TCRα combinatorial diversity in 5-OP-RU tetramer+ MAIT cells and CD8+ non MAIT cells. Circus plots depicting TRAV-J combinatorial diversity within MAIT and non-MAIT T cells. The inner-circle shows the number of sequence reads per V and J gene and TRAV/J combinations are indicated by proportional bands linking the genes using the colour of the V gene. Expanded labelling indicates genes which are enriched in sequence frequency in MAIT cells. The outer ring shows the frequency of pairing for each TCR gene segment to the reciprocal gene segment coloured according to the paired gene. Representative plots from a single individual.

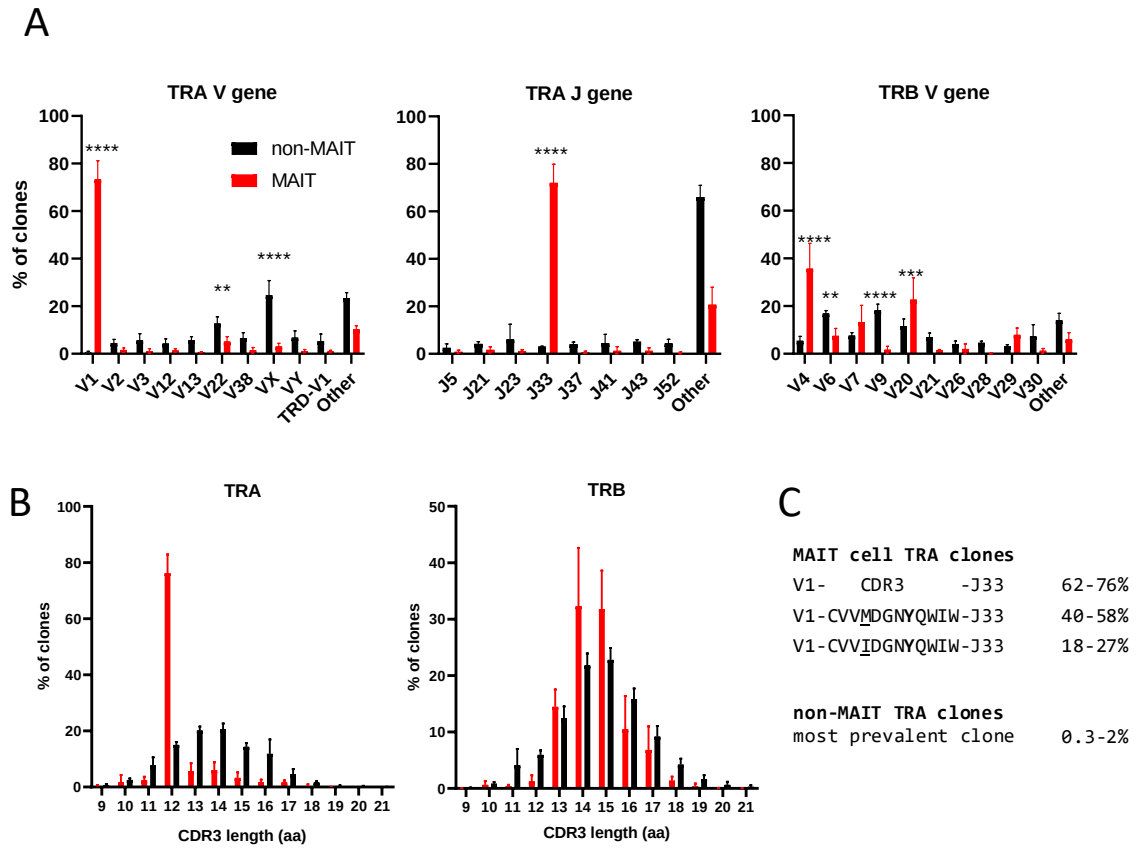

Figure 5.4 Conserved TCR alpha chain and limited beta chain diversity in bovine MAIT cells. (A) Bar graphs showing TCR alpha (TRA) V and J and TCR beta (TRB) V gene usage in MAIT (CD8+ human MR1-5-OP-RU tetramer+) and non-MAIT (CD8+ human MR1-5-OP-RU tetramer-) T cells. Bars represent the percentage of total TRA or TRB sequences obtained from high throughput TCR sequencing of populations sorted from PBMC (mean ±SD, n=4, number of sequences in **Appendix 7.2**). Data were analyzed using two-way ANOVA with repeated measures within animal, followed by Sidak's multiple comparisons post-hoc test comparing gene usage between MAIT and non-MAIT T cells. (B) Distribution of TRA and TRB CDR3 amino acid (aa) length. (C) Alignment of the TCR alpha CDR3 region of the dominant MAIT cell clones. This data was generated by Tim Connelly, Siddharth Jayaraman and Christina Vrettou at the Roslin Institute and is presented with permission.

MAIT cells have differing levels of transcription factor expression to that of conventional T lymphocytes expressing PLZF as well as higher levels of EOMES and RORγT when compared to conventional CD8+ T cells, while both populations express similar levels of T-bet. To confirm if this is also true in cattle, the expression of transcription factors was determined in CD8α+ MAIT cells compared to CD8α+ non MAIT cells. CD8α+ MAIT cells were chosen to compare to CD8α+ non MAIT cells as this gives a uniform population (cytotoxic T cells) to compare to MAIT cells. Unfortunately, cattle specific antibodies against the transcription factors PLZF, EOMES, ROR-γT and T-bet are not available. However, transcription factors are highly conserved between species and monoclonal antibodies have previously been shown to cross-react between species. Antibodies specific to human PLZF (clone R17-809) and EOMES (clone WD192A) cross-reacted with bovine cells and expression was significantly higher in CD8α+ MAIT cells compared to CD8α+ non MAIT T cells (**Figure 5.5**). Antibodies specific for RORγT (Clone Q21-599) and T-bet (clone 4B10) were also tested with no differences were observed between the CD8α+ MAIT and the CD8α+ non MAIT population. However, RORγT and T-bet showed a low-level expression above isotype control, suggesting that these antibodies may not cross-react with cattle. Positive staining was obtained in human PBMC with all antibodies (**Figure 5.5**) confirming that the staining was technically correct. Hence, while further studies need to be carried out to determine the expression of RORγT and T-bet in cattle MAITs, the data obtained here show that they express PLZF and EOMES in the same manner as their human counterparts.

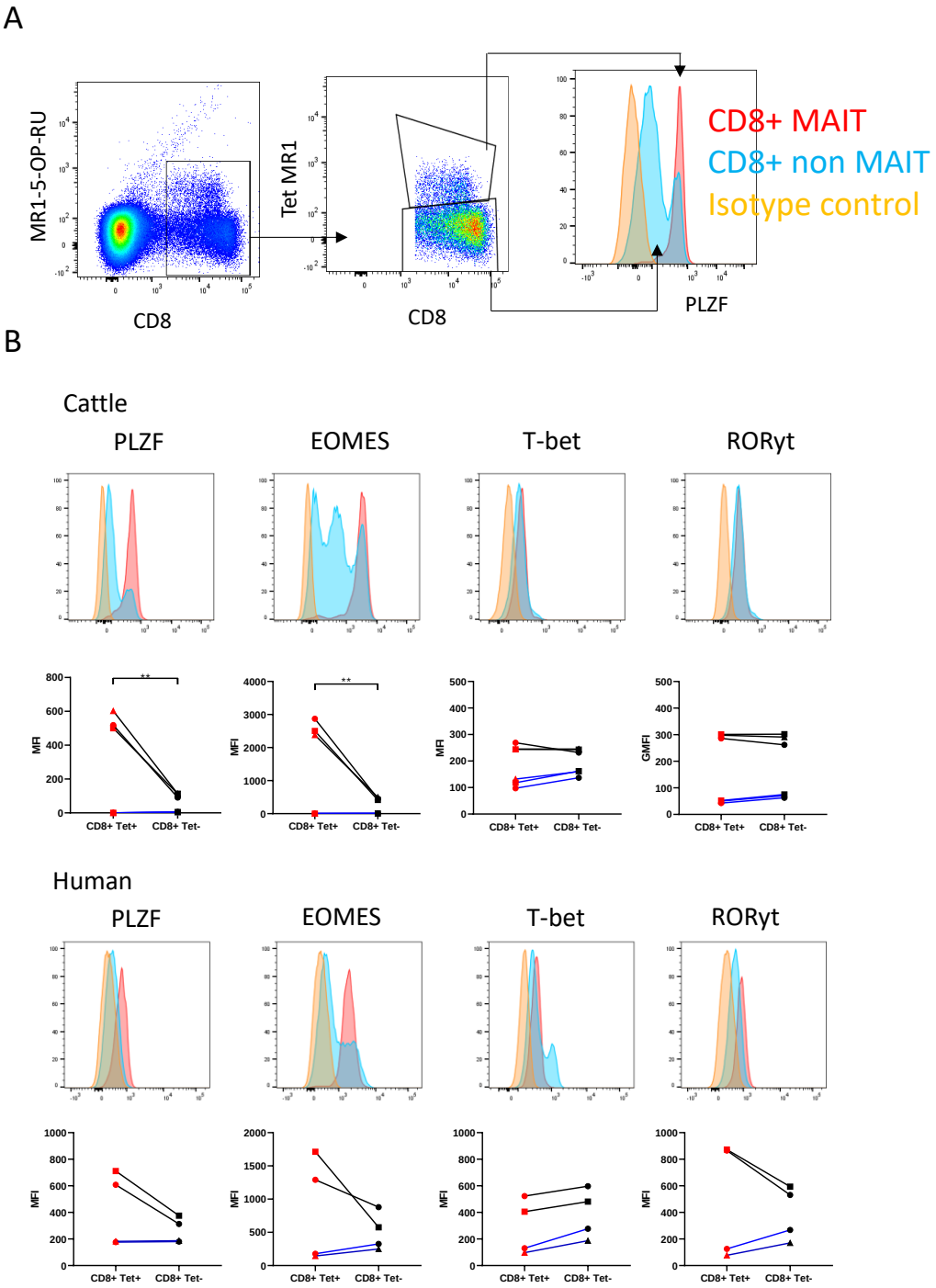

Figure 5.5: Expression of the transcription factors in cattle and human peripheral blood CD8α+ MAIT cells. A) Representative gating of transcription factor stains of cattle CD8+ MAIT cells. B) MR1-5-OP-RU tetramer+ MAIT cells (CD8+Tetramer+) and non-MAIT CD8α+ T cells (CD8+ tetramer-) from cattle and human PBMC; representative flow cytometry histograms showing antibody expression in CD8+ MAIT cells (red) CD8+ non MAIT (blue) and isotype control in CD8+ total T cells (orange). Quantification of median fluorescence intensities (MFI) (n=3) are displayed for CD8+ MAIT cells (red) and CD8+ non-MAIT cells (black) with black line connecting MFI of populations within animal. MFI of isotype control in CD8+ MAIT cells (red) and CD8+ non MAIT cells (black) are shown, connected by a blue line. Paired T-test within animal.

Combined the data presented in this section demonstrates that the human 5-OP-RU-MR1 tetramer identifies an expanded population in cattle which express the canonical MAIT cell TCR rearrangement and high levels of transcription factors PLZF and EOMES which are associated with MAIT cell functions. Therefore, the human 5-OP-RU-MR1+ tetramer population can be defined as true MAIT cells.

5.5 The phenotype of cattle MAIT cells and comparisons of MAIT cells between tissues

In order to characterise MAIT cells, tissues were collected from 7 cattle (aged 10, 10, 10, 10, 20, 55 and 56 months) and MAIT cells enumerated and phenotypically characterised in these samples. The number of samples used for each experiment is depicted in **Table 5.1**.

Table 5.1 tissues collected for multi tissues MAIT cell characterisation and numbers of animals for each phenotyping panel.

Corresponding Figure	PBMC	Lung	Spleen	Liver	Ileum	BAL	LN mesenteric	LN pre-scapular
Figure 5.6: Frequency of MAIT cells in cattle tissues.	7	7	7	7	4	7	4	7
Figure 5.7: MAIT cell co-receptor usage and TCRγδ expression in MR1-5-OP-RU tetramer+ T cells.	7	7	7	6	4	6	4	7
Figure 5.8**:** Phenotype of MAIT cells in tissues.	7	5	7	5	4	6	4	7
Figure 5.9 MAIT cells IL-2Rα (CD25) receptor expression in multiple tissues.	7	5	7	5	4	6	4	7

In cattle PBMC, approximately 0.6% of CD3+ lymphocytes (**Figure 5.2**) are MAIT cells. The 7 animals which had tissues collected for MAIT cell analysis had a similar percentage of MAIT cells in peripheral blood with a mean of 0.6% (median 0.5%, IQR 04.3-0.56%) of CD3+ T cells or 4.6 % (median 2.9% IQR 2.3-5.9%) of CD8α+ T cells (**Figure 5.6B**). MAIT cells in humans are enriched in mucosal tissues and liver (Kurioka et al., 2016). This is also true in cattle, with MAIT cells comprising a greater frequency of CD3+ T cells in lung (mean 1.7%, median 1.8%, IQR 0.8-2.5%), spleen (mean 1%, median 0.9%, IQR 0.8-1.2%), liver (mean 2.7%, median 1.3%, IQR 0.9-3.7%) and BAL (mean 1.8%, median 1.5%, IQR 0.5-3%) compared to PBMC.

MAIT cell frequencies in the ileum (mean 0.6% median 0.3% IQR 0.3-1% of CD3+ T cells) were comparable to those in PBMC. Of note, an enrichment of MAIT cells was seen in the mesenteric lymph node (mean 3.5%, median 3.4%, IQR 2.5-4.5% of CD3+ T cells), but not in the pre-scapular lymph node (mean 0.6%, median 0.5%, IQR 0.4-0.8%) (**Figure 5.6B**). This was not seen in a recent study of the pigtail macaque (Juno et al., 2019) and may be specific to cattle, speculatively due to the presence of large microbial populations in the rumen and large intestines. In all tissues, the Ac-6-FP tetramer+ population was much smaller than the 5-OP-RU tetramer+ MAIT cell population (**Figure 5.6B**). However, differences in Ac-6-FP tetramer binding were observed in different tissues. For example, the average frequency of Ac-6-FP tetramer+ cells identified in the spleen was >4 fold greater than the population identified in PBMC. Ac-6-FP reactive T cells that are restricted through MR1 have been identified previously (Gherardin et al., 2016) and this data suggests that there may be an enrichment of these cells in certain tissues.

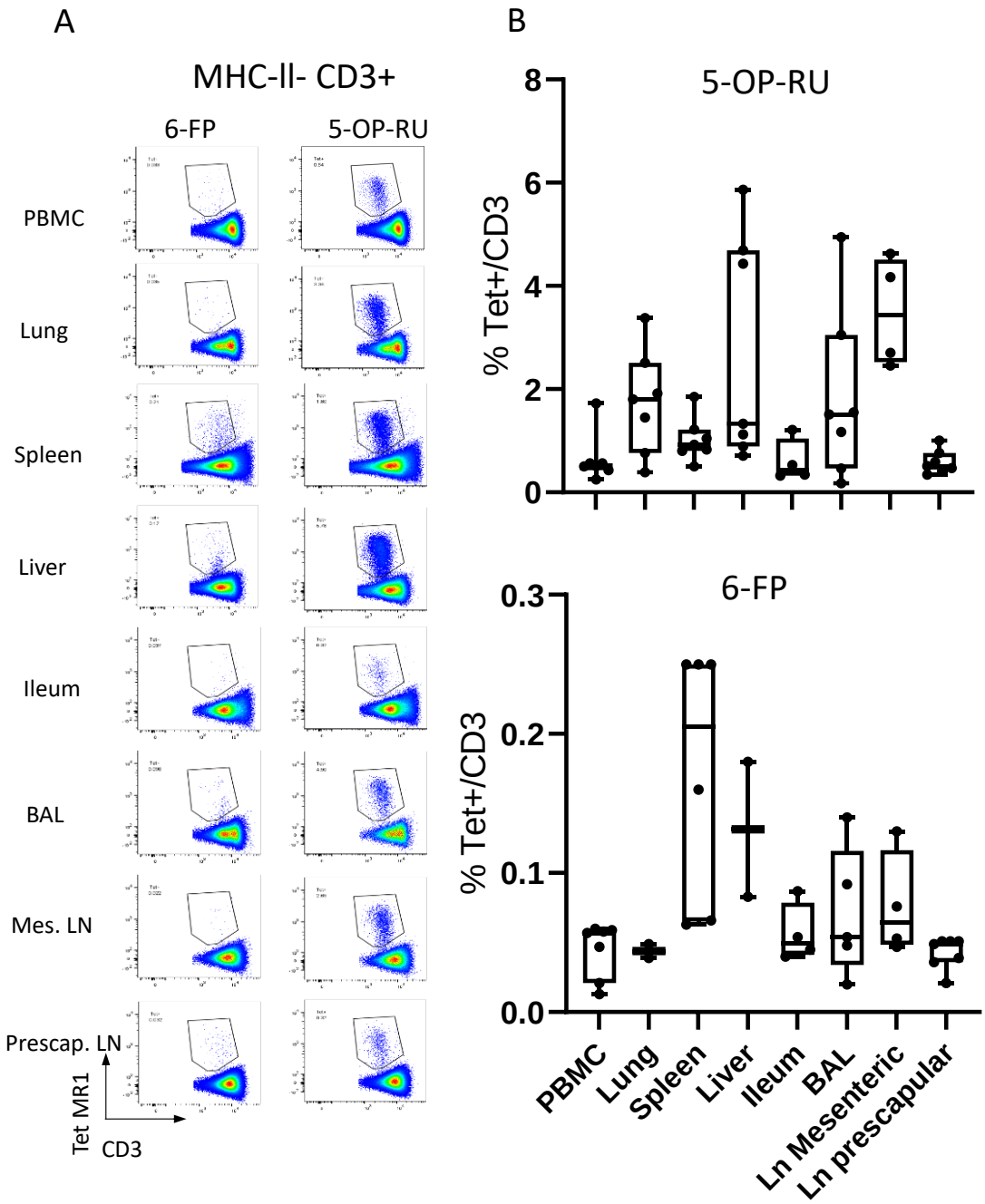

Figure 5.6: Frequency of MAIT cells in cattle tissues. **(A)** Frequencies of CD3+ 5-OP-RU tetramer+ MAIT cells and Ac-6-FP tetramer+ cells in different tissue from cattle. **(B)** Box and whiskers plots depict frequency of MR1-5-OP-RU and MR1-6-FP tetramer+ populations in differing tissues.

When determining co-receptor expression (**Figure 5.7**), cattle peripheral blood MAIT cells are predominantly CD8α+ (mean 73.9%, IQR 64-87%), with lower proportions of double-negative (mean 19.7%, IQR 12.7-27.5%) and a small fraction of MAIT cells expressing CD4 (mean 2.7% IQR 0.9-3.4%). Interestingly, some of the tetramer-positive cells were TCR γδ+ (8.33% IQR 2.3-13.3% of total 5-OP-RU tetramer+ population in PBMC) (**Figure 5.7**). This equates to a mean frequency of 0.08% of total γδ+ T cells in cattle. Cattle are a member of the γδ T cell high species with ~10-20% of circulating lymphocytes being TCRγδ positive in adult animals (McGill et al., 2014). This observation mirrors a recent report of human γδ T cells binding to MR1 (Le Nours et al., 2019). Differences in MAIT cell co-receptor usage between blood and tissues were observed. MAIT cells residing in peripheral blood had the largest CD8 population (mean 76.4% IQR 60.6-79.4% CD8+) with no significant difference in CD8 expression of MAIT cells in lung (mean 74% IQR 69.3-64.6% CD8+), spleen (68% IQR 53.1-86.3% CD8+), and liver (mean 68%, IQR 42.7-85.8% CD8+)(**Figure 5.7C**). Significant differences in CD8 expression compared to PBMC were identified in the pre-scapular (mean 54% IQR 51.8-65.6% CD8+) and mesenteric (mean 52% IQR 37.9-65.3% CD8+) lymph nodes as well as BAL (mean 58% IQR 43.9-71.3% CD8+). IIleum had the lowest frequency of CD8 expression (mean 37% IQR 29.1-45.1% CD8+). A corresponding increase was seen in the double negative T cells with a strong negative correlation between the fraction of CD8+ and CD8-CD4-TCRγδ- MAIT cells (R^2=0.90) (**Figure 5.7D**). The frequencies as a proportion of CD8+ T cells was greater than that of CD3 with a mean of 8.2% in lung (median 8.5% IQR 8.5 -14.7%), 2.6% in spleen (median 2.6 IQR 2.1-2.8%), 6.6% in Liver (median 5.6% IQR 3.5-9.2%), 1.6% in IIleum (Median 1% IQR 0.8-3.1%) , 6.8% in BAL (median 5.5% IQR 2.9-9.8%), 9.7% in mesenteric lymph node (median 10.4% IQR 7-11.8%) and 1.9% in the pre-scapular lymph node (median 1.9% IQR 1-2.4%) (Figure 5.7**E**).

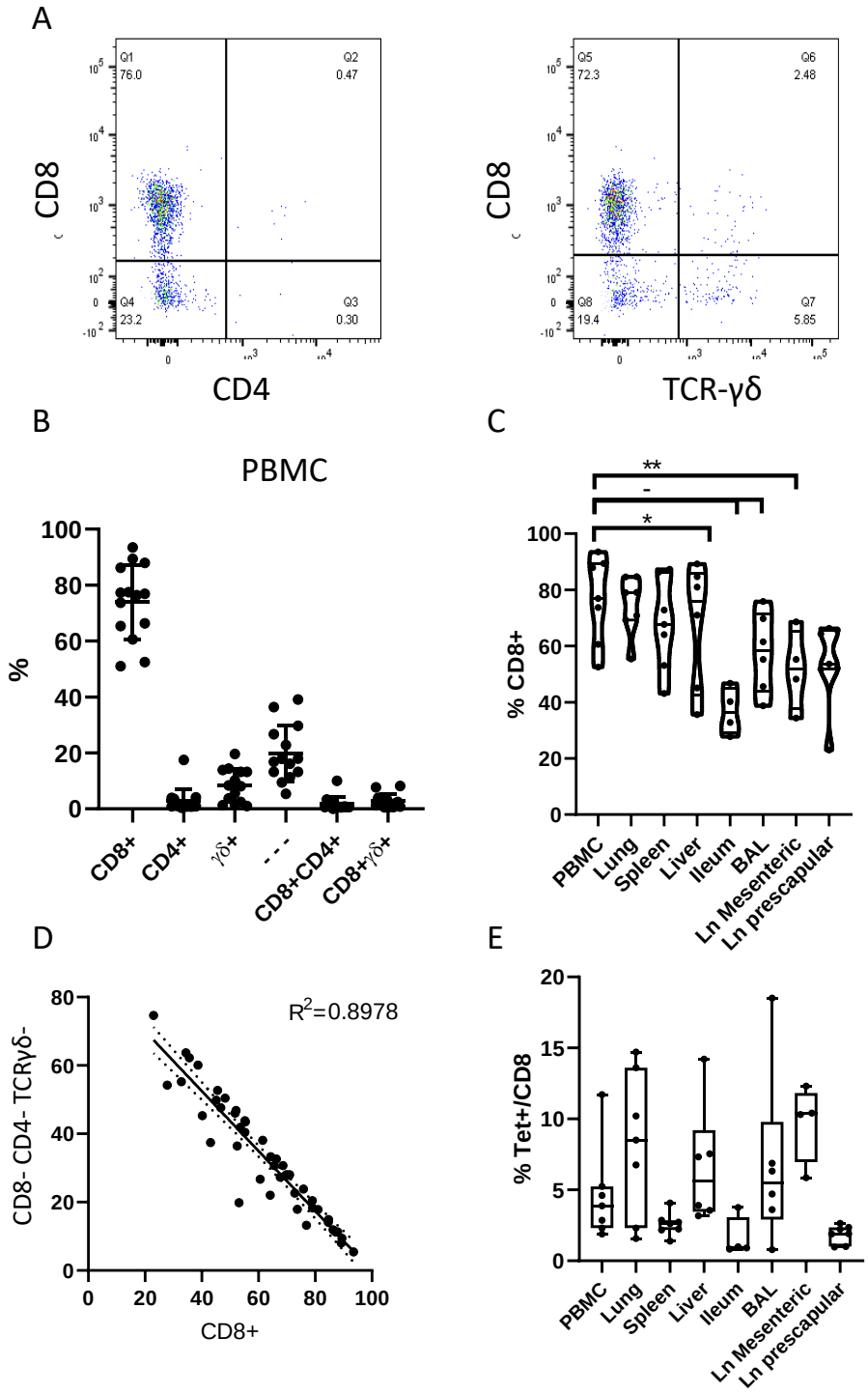

Figure 5.7: MAIT cell co-receptor usage and TCRγδ expression in MR1-5-OP-RU tetramer+ T cells.
A) Representative flow cytometry plots of TCR co-receptor and TCRγδ expression in CD3+ MAIT cells in cattle PBMC. Live lymphocytes were previously gated for CD3+ MR1-5-OP-RU tetramer+ MAIT cell identification. B) Frequencies of co-receptor and γδTCR expression of MAIT cells in PBMC (n=14, mean ±SD). C) Violin plot showing the frequency of CD8+ MAIT cells (CD3+Tetramer+) in multiple tissues. Mixed-effects model with matching across tissue, followed by Dunnet's multiple comparisons post-hoc test comparing differences between PBMC and other tissues. D) XY plot and linear regression model of CD8+ vs CD8- CD4- TCRγδ- T cells in all tissues from figure C. E) Box and whiskers plots depicting the Frequency of CD8+ T cells which are 5-OP-RU tetramer+ in multiple tissues.

The majority of MAIT cells in peripheral blood had a T effector memory phenotype ($CD45RO^+$ $CCR7^-$) (mean 95% IQR 88.9-96.8%) (**Figure 5.8B**) which parallels their human counterparts (Dusseaux et al., 2011). As expected, the proportion of effector memory non-MAIT T cells varied greatly across tissues, whereas MAIT cells predominantly had an effector memory phenotype irrespective of origin (mean 96.5%, 91.1%, 96.4%, 95%, 94.9%, 97.4%, 94.3% T effector phenotype in lung, spleen, liver, ileum, BAL, mesenteric lymph node, and pre-scapular lymph node respectively) (**Figure 5.8C**).

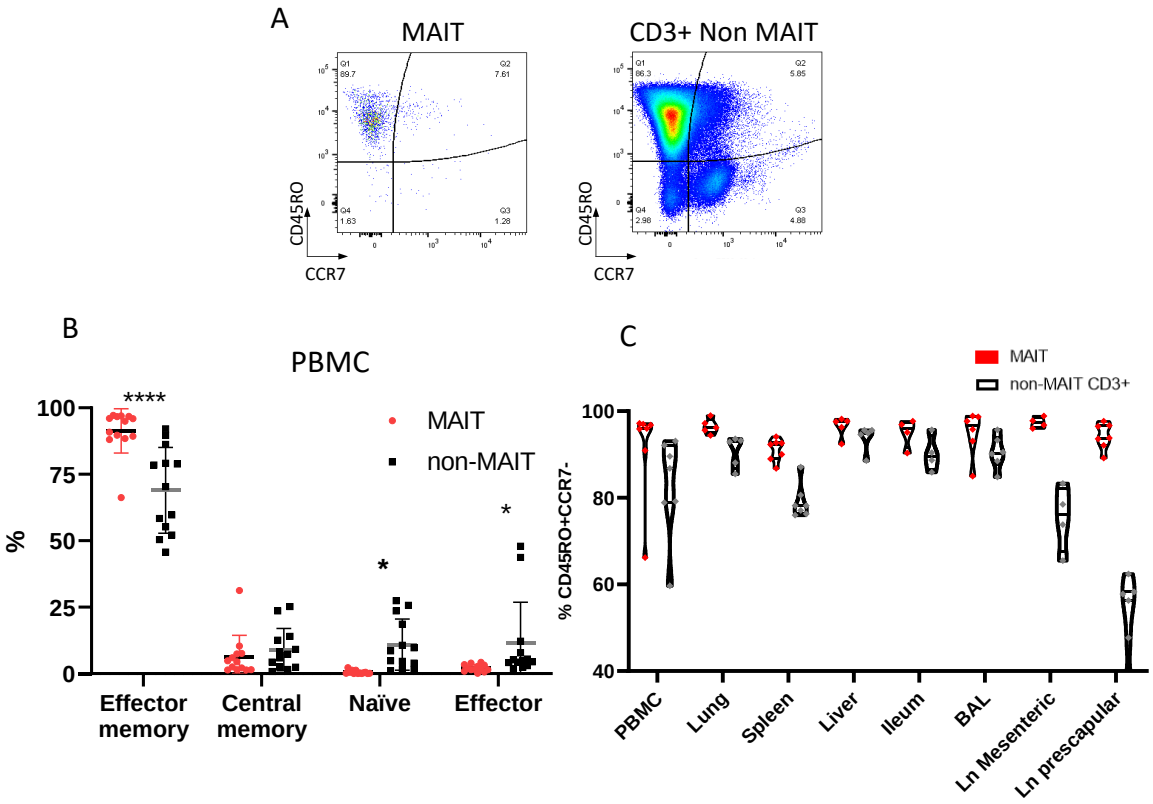

Figure 5.8: Phenotype of MAIT cells in tissues. A) Representative flow cytometry plots of CD45RO and CCR7 expression in CD3+ MAIT cells and non MAIT cells in PBMC. Previous gating to identify live lymphocytes by forward and side scatter followed by live dead discrimination die prior to CD3+ tetramer+ MAIT cell identification. B) Memory phenotyping of peripheral blood MAIT and non-MAIT T cells based on CD45RO and CCR7 expression. Effector memory (CD45RO+CCR7-), central memory (CD45RO+CCR7+), naïve (CD45RO-CCR7+) and effector (CD45RO-CCR7-). Data were analyzed using two-way ANOVA with T cell population as repeated measures, followed by Sidak's multiple comparisons post-hoc test comparing memory phenotype between populations. Representative flow cytometry plots and summarized data (mean ± SD, n=13) are shown. C) Violin plot showing the frequency of effector memory (CD45RO+CCR7-) MAIT (CD3+ MR1-5-OP-RU tetramer+) and non-MAIT T cells (CD3+ MR1-5-OP-RU tetramer-). Mixed-effects model with matching across tissue and cell population, followed by Sidak's multiple comparisons post-hoc test comparing differences between MAIT and non-MAIT cells within tissues.

Differences in IL-2Rα chain (CD25) expression were also noted between MAIT cells identified in different tissues (**Figure 5.9**). A greater frequency of CD25 high MAIT cells in some tissues, including BAL (mean 61%), Ileum (mean 51%) and liver (mean 45%) as well as in the pre-scapular (mean 69%) and mesenteric (mean 81.2%) lymph nodes compared to MAIT cells residing in peripheral blood (mean 25%). The tissues with increased CD25 expression are in contact, or drain, locations with a large microbiome, which may explain why they induce high levels of CD25. MAIT cells residing in lymph node enter from tissues via the lymphatics and not blood, which potentially explains the comparatively high CD25 expression of MAIT cells in the lymph node compared to PBMC (Voillet et al., 2018).

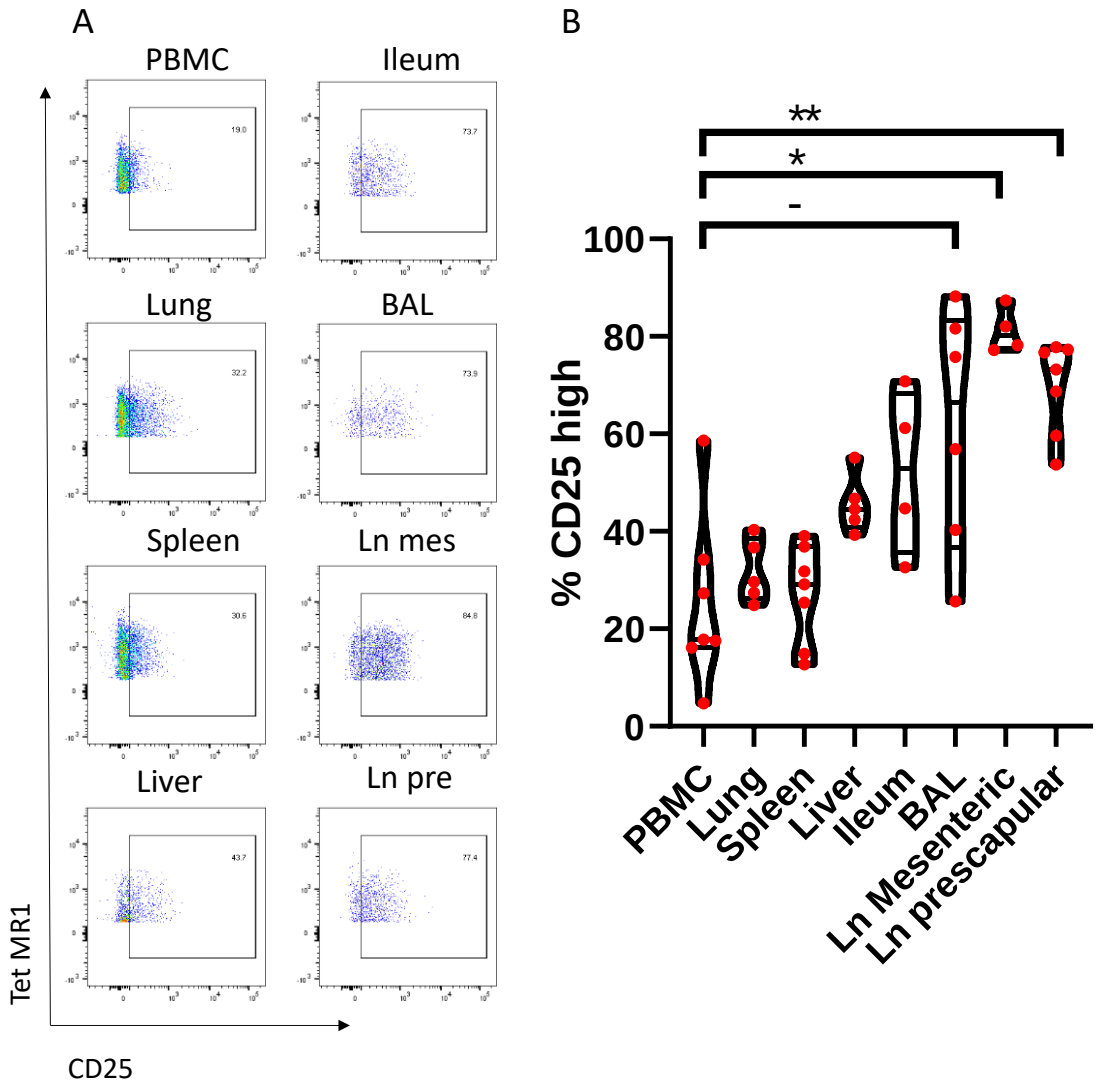

Figure 5.9 MAIT cells IL-2Rα (CD25) receptor expression in multiple tissues. A) Representative images of CD25 expression in CD3+ MAIT cells and CD3+ non MAIT cells. Previous gating was performed to identify live lymphocytes by forward and side scatter followed by live dead discrimination die prior to CD3+ and 5-OP-RU MR1 tetramer identification B**)** Violin plot showing the frequency of CD25 high MAIT cells (MR1- 5-OP-RU tetramer+). Mixed-effects model with matching across tissues, followed by Dunnet's multiple comparisons post-hoc test comparing differences between PBMC and other tissues.

In summary, as in humans, MAIT cells in cattle are enriched in tissues, particularly liver, BAL, and lung where their frequency is as greater (>4 fold) than PBMC. Cattle MAIT cells are primarily CD8+ or CD4/ CD8 double negative cells and express higher levels of CD8 in the peripheral blood. The vast majority of cattle MAIT cells have T effector memory phenotype regardless of tissue localisation, and CD25 (IL-2 receptor) was more highly expressed in MAIT cells which were identified in mucosal tissues or recirculated to the lymph node.

5.6 Activation of MAIT cells in cattle

5.6.1 5-OP-RU and cytokine stimulation of cattle MAIT cells

In humans and mice, MAIT cells can be activated through TCR recognition of bacterial riboflavin synthesis derived metabolites such as 5-OP-RU presented by MR1 (Corbett et al., 2014). The MR1 ligand Ac-6-FP does not activate human and mouse MAIT cells and can inhibit MAIT cell activation by 5-OP-RU (Eckle et al., 2014, Keller et al., 2017) To determine if this is also the case in cattle, activation and blocking experiments were performed using synthetic 5-OP-RU and Ac-6-FP. Cattle MAIT cells were stimulated by 5-OP-RU stimulation, leading to robust upregulation of IFN-γ and TNF expression at concentrations as low as 50pM (**Figure 5.10B**). The frequency of tetramer+ MAIT cells decreased as the concentration of the 5-OP-RU stimulus increased (**Figure 5.11A-B**) and over time (**Figure 5.11C**), correlating with a reciprocal increase in tetramer- IFN-γ+ cells. This indicated that the MAIT cells are downregulating TCR upon binding ligand, as has been previously shown (José et al., 2000). Low frequencies of cytokine-producing non-MAIT CD8a+ T cells (**Figure 5.10**) are therefore inferred to be MAIT cells that were not captured by MR1 tetramers due to downregulation of TCR.

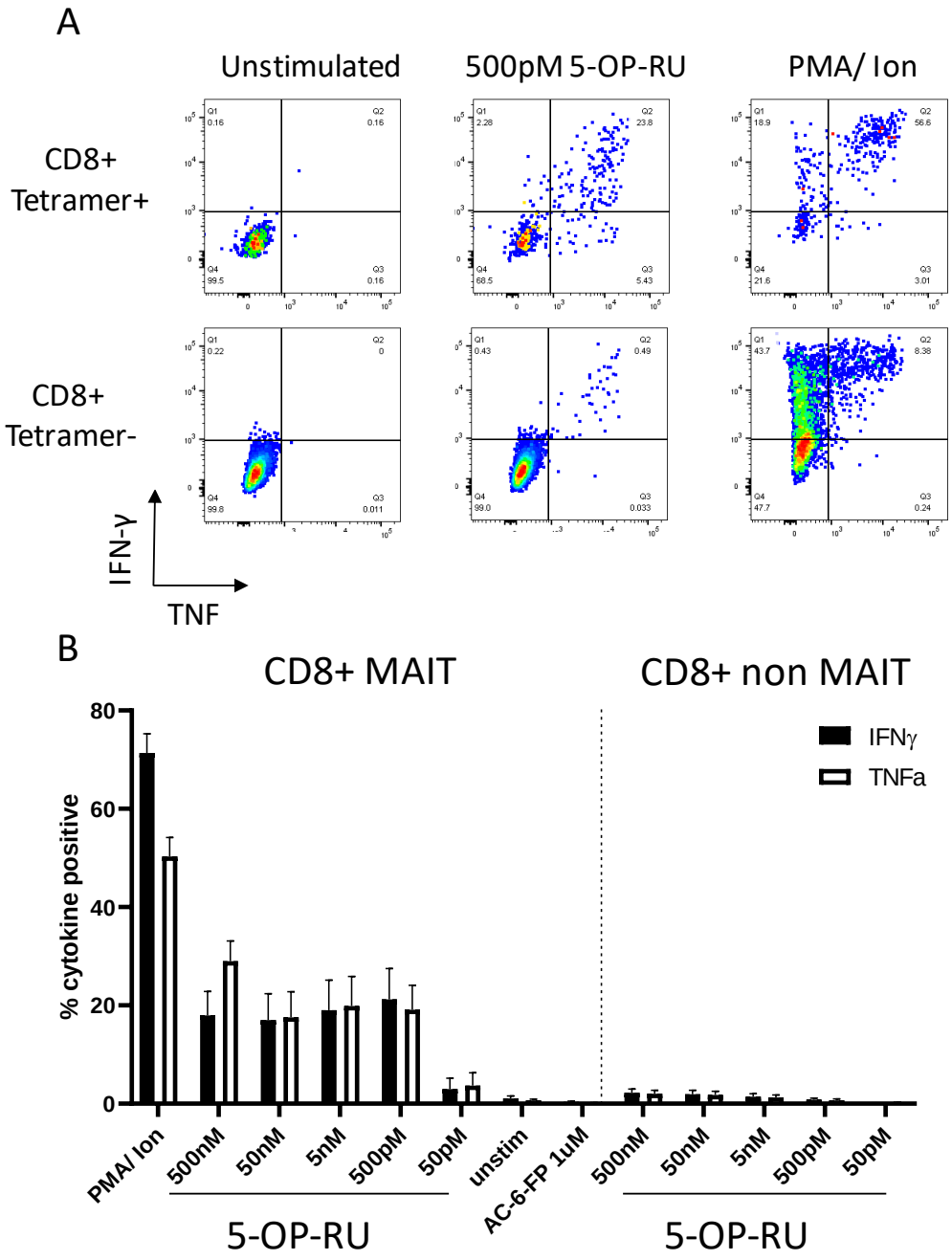

Figure 5.10 MAIT cell activation by 5-OP-RU. A) Representative flow cytometry plot of CD8α+ MAIT cells and for comparison CD8+ non MAIT cells with 5-OP-RU for 7h at a concentration of 500pM. PMA/ Ionomycin (PMA/Ion) stimulated, and medium controls are also shown. B) Cattle PBMC were stimulated for 7 hours with 5-OP-RU titrated over a range of 500nM to 50pM Ac-6-FP at a concentration of 1µM was also tested Unstimulated cells, and PMA/ Ionomycin (PMA/Ion) stimulated and unstimulated controls are also shown. The proportions of cytokine+ live CD8α+Tetramer + MAIT cells and, for comparison, of CD8α+ Tetramer - non MAIT cells are depicted (data combined from two experiments, mean ±SEM, n=6 for each concentration other than 50pM where n=3).

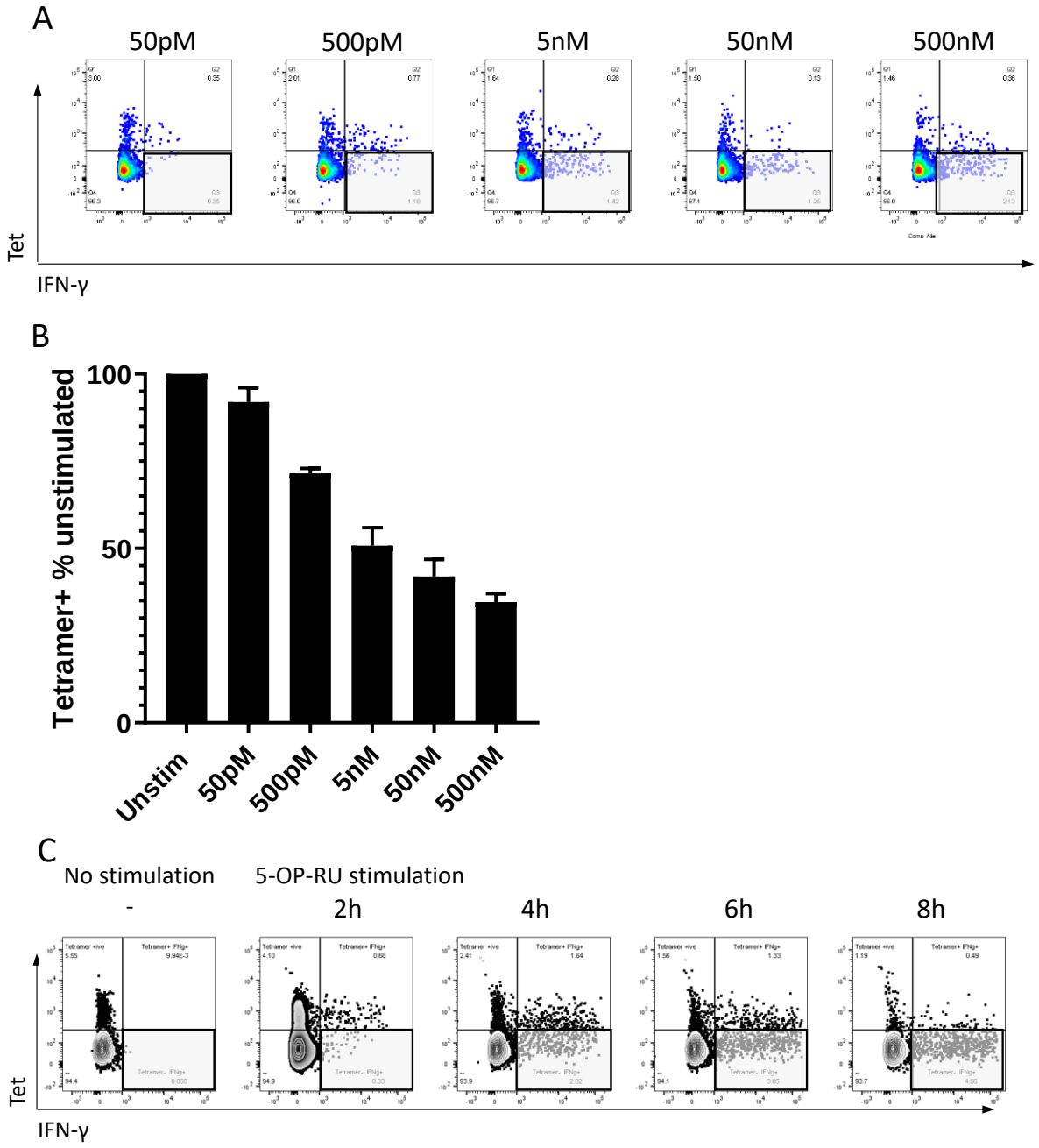

Figure 5.11 TCR downregulation upon activation of MAIT cells. A) Bovine PBMC were stimulated with various concentrations of 5-OP-RU (50pM- 500nM) 5-OP-RU for 7 hours Lymphocytes were gated for FSC&SSC, singlets, live and CD8 expression. Flow cytometry plots show MR1-5-OP-RU tetramer vs IFN-γ staining. Grey boxes indicate IFN-γ + T cells which are not detected by tetramer. B) The fraction of Tetramer+ MAIT cells following stimulation with 5-OP-RU relative to the fraction of tetramer+ MAIT cells in unstimulated PBMC from the same animal (mean ±SEM, n=6). C) Bovine PBMC were stimulated with 1µM 5-OP-RU and 50ng/ml IL12 and IL-18 over a time course of 2 to 8 hours. Previous gating as in A. Flow cytometry plots shows MR1-5-OP-RU tetramer vs IFN-γ staining. Grey boxes indicate IFN-γ + T cells which are not detected by tetramer

Ac-6-FP did not stimulate bovine MAIT cells (**Figure 5.10**), and it has been shown to inhibit the activation of MAIT cells by 5-OP-RU. Differing concentrations of Ac-6-FP were added to PBMC 30 minutes prior to stimulation with 5-OP-RU to determine whether Ac-6-FP can competitively inhibit activation of cattle MAIT cells. As the tetramer- IFN-γ+ 5-OP-RU simulated T cells were previously inferred to be MAIT cells which had downregulated their TCR this population was included in the analysis. Ac-6-FP competitively inhibited 5-OP-RU activation in a dose-dependent manner in both MR1 tetramer+/ IFN-γ+ and the total CD8+ T cell population (**Figure 5.12**). The MR1 specific antibody 26.5 did not block 5-OP-RU specific MAIT cell stimulation in *ex vivo* assays (data not shown).

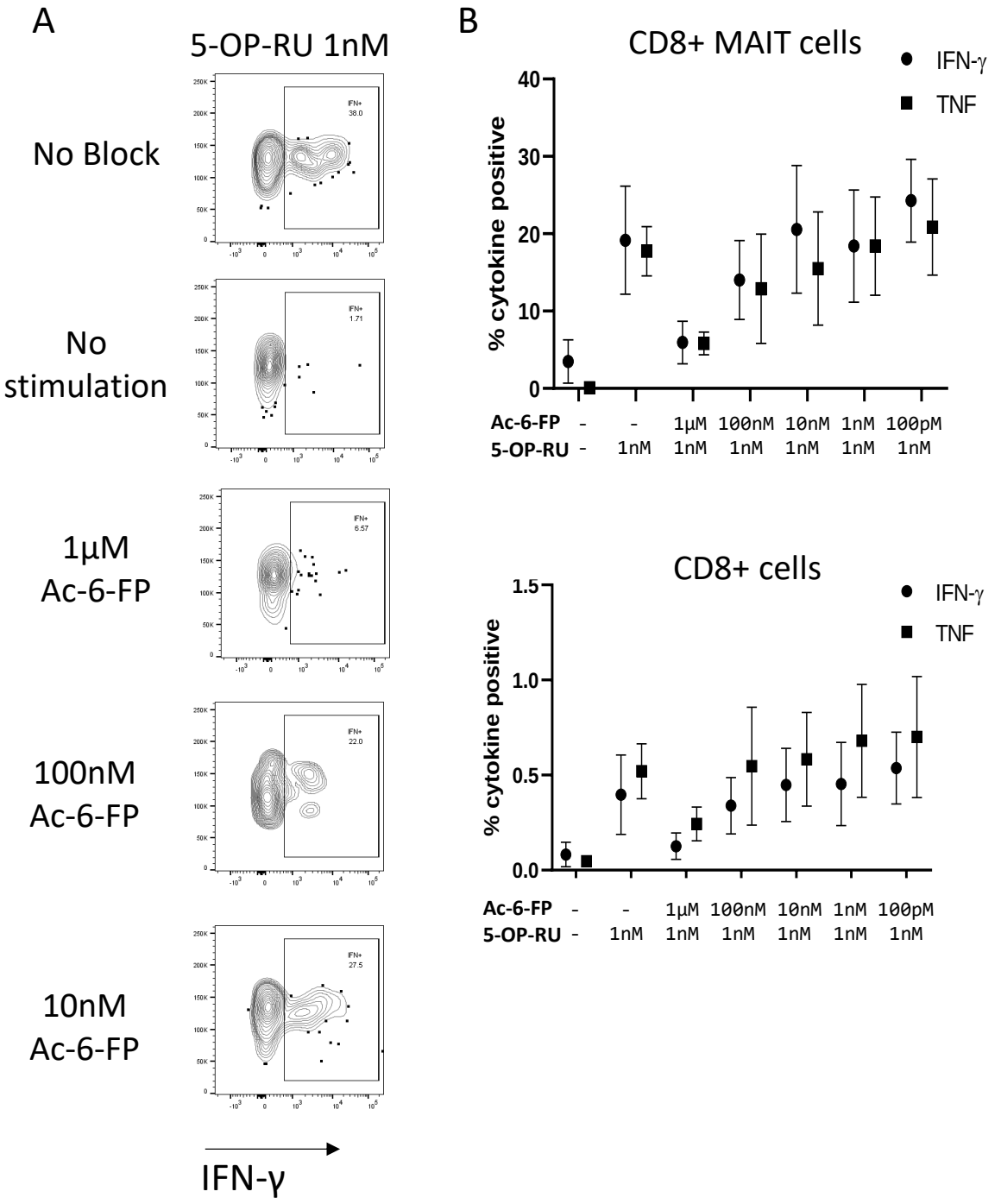

*Figure 5.12 Competitive inhibition of 5-OP-RU MAIT cell activation by Ac-6-FP.*A) Representative plot of cattle PBMC incubated with Ac-6-FP for 30 minutes prior to the addition of 1 nM 5-OP-RU for 7 hours. Lymphocytes were gated for FSC&SSC, singlets, live and CD8 expression followed by tetramer + / IFN-γ+ gating. The fraction of IFN-γ and TNF positive cells within MAIT cells (CD8+ Tetramer+ or IFN-γ+) and the total CD8+ population was determined following incubation (mean ±SEM, n=3).

MAIT cells express high levels of cytokine receptors on their surface and are sensitive to indirect activation through cytokines such as IL-12 and IL-18 (Ussher et al., 2014, Loh et al., 2016). Non-TCR mediated activation of bovine MAIT cells was determined by stimulation with human IL-12 and IL-18 cytokines (**Figure 5.13**). Effective dose of these cytokines was determined by previous titrations with human MAIT cells. When stimulated with IL-18, cattle MAIT cells produced IFN-γ (mean 31% IFN-γ+) and low levels of TNF (mean 2% TNF+). There was no significant response to IL-12 alone by MAIT or non-MAIT T cells. The addition of IL-12 did, however, significantly increase the frequency of MAIT cells producing IFN-γ (mean 56% IFN-γ+) compared to IL-18 alone. PMA and Ionomycin stimulation-induced high levels of TNF expression in a large fraction of MAIT cells, demonstrating that the majority of bovine MAIT cells are capable of TNF production. IL-18 and IL-12 induced activation was significantly higher for MAIT cells than for non-MAIT CD8+ T cells. No downregulation of TCR was seen when stimulating with IL-12 and IL-18 (data not shown).

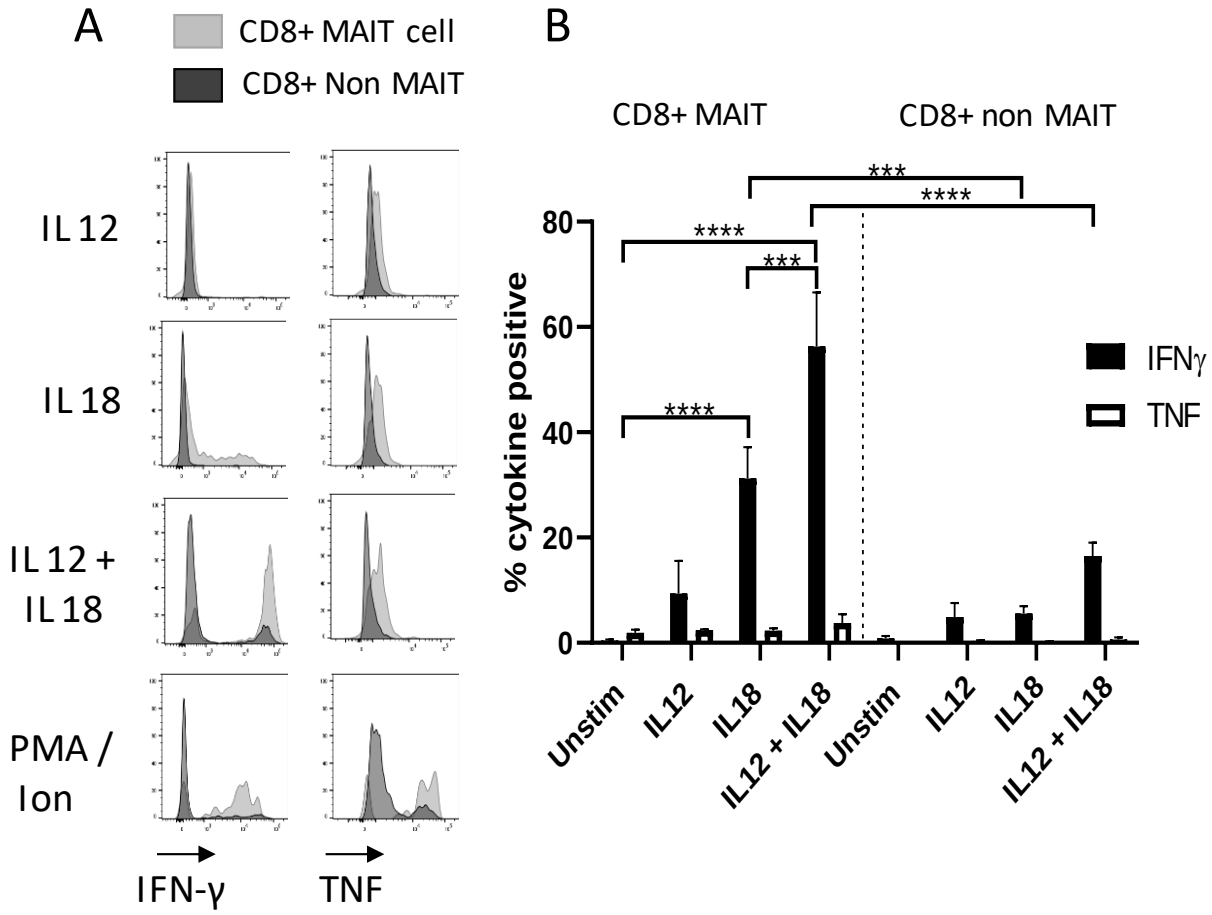

Figure 5.13 cytokine stimulation of cattle MAIT cells A) Cattle PBMC were stimulated for 18 hours with IL-12, IL-18 or a combination of both (all at 50ng/ml). Representative flow cytometry histogram plots show IFN-γ and TNF expression within CD8+ MAIT cells overlaid with CD8+ non MAIT cells. B) Bar graphs showing the fraction of cytokine positive CD8+ MAIT and non-MAIT cells (mean ±SEM, n=4). Data were analysed using two-way ANOVA with repeated measures within animal, followed by Sidak's multiple comparisons post-hoc test comparing IFN-γ and TNF expression of stimulated CD8α+ MAIT to unstimulated MAIT cells and to CD8α+ non MAIT cells.

5.6.2 Activation of cattle MAIT cells by bacteria

To determine whether cattle MAIT cells respond to riboflavin biosynthesis competent bacteria, PBMC were stimulated with *Escherichia coli* (*E. coli*), and the attenuated *Mycobacterium Bovis* strain Bacillus Calmette–Guérin (BCG). Initially, *E. coli* and BCG were titrated onto cattle PBMC over-night and for 7 hours to determine the optimal conditions for stimulation (**Figure 5.14**). *E. coli* was titrated over a range of 0.001-100 bacteria per cell (BpC) whereas BCG was titrated over a range of 0.01-1 BpC as BCG stocks had a lower concentration of bacteria available. When stimulating with *E.coli* for 7 hours the frequency of cytokine-producing MAIT cells rose with the rising concentration of co-incubated bacteria until 100BpC at which point the response decreased. When stimulating over-night, lower concentration of incubated bacteria induced a higher response with no response seen in in the 100BpC. These responses are likely due to MAIT cell death when stimulated overnight with high concentrations of bacteria. When stimulating with BCG for 7 hours, little response was observed at any dose, likely due to the low dose of bacteria used. When stimulating overnight, higher levels of response were seen though with little difference between bacterial concentrations. Of note, for both *E.coli* and BCG when stimulating overnight, a lower level of TNF producing cells are observed compared to IFN-γ, suggesting that duration of activation may drive different cytokine responses from MAIT cells. 7-hour stimulation with 30 *E.coli* BpC was chosen for further stimulation experiments. Overnight stimulation was chosen for BCG with a concentration of 3BpC.

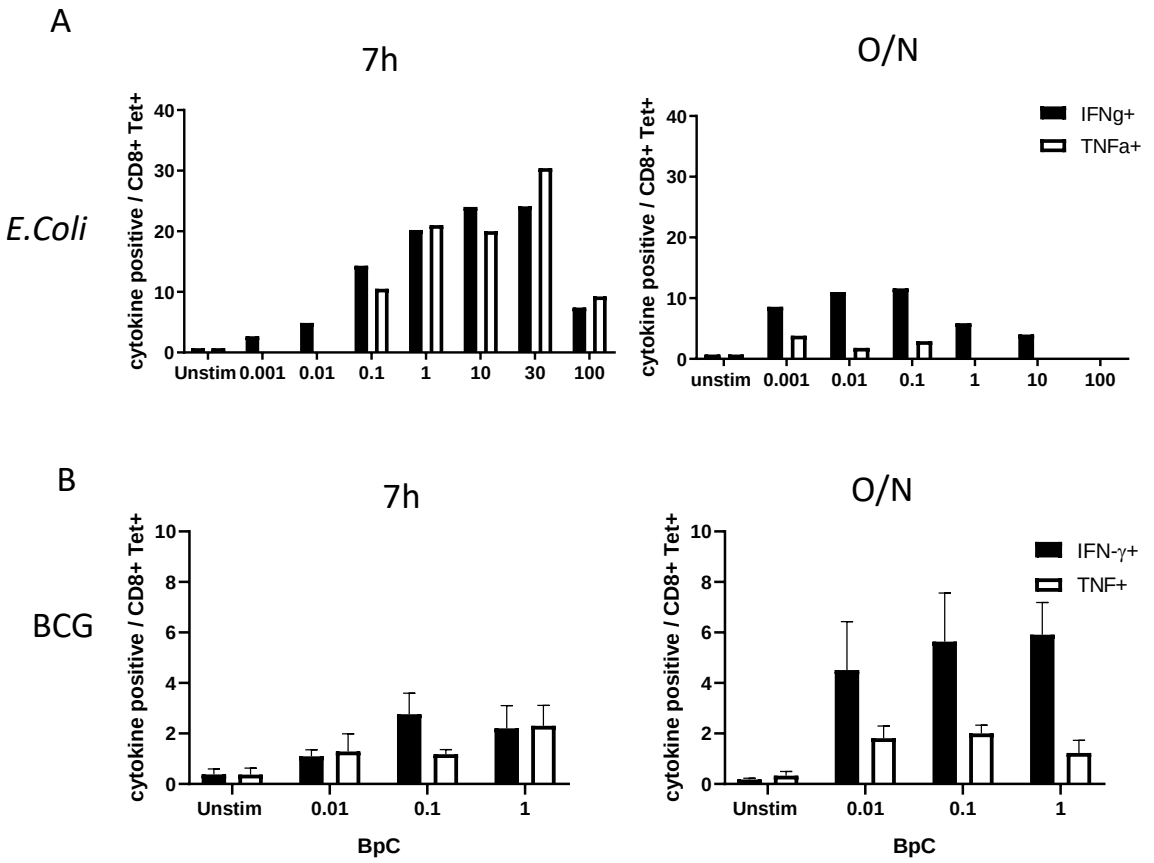

Figure 5.14 MAIT cell stimulation by bacteria (A) Cattle PBMC were incubated in the presence of E. coli for 7 hours (7h) or overnight (O/N) titrated over a range of 0.001-100 bacteria per cell (BpC) (n=1). Graphs depict the percentage of IFN-γ and TNF producing cells for each stimulation condition. Unstimulated cells (unstim) are shown as a control. (B) Cattle PBMC were incubated in the presence of M. bovis BCG for 7 hours or overnight titrated over a range of 0.01-1 bacteria per cell (BpC). Graphs depict the percentage of IFN-γ or TNF producing cells for each stimulation condition. Unstimulated cells (unstim) are shown as a control (mean ±SEM, n=4). For both (A) and (B). Lymphocytes were gated for FSC&SSC, singlets, live and CD8 expression followed by tetramer + prior to determining the percentage cytokine positive.

Further stimulation with 30 BpC *E. coli* for 7 hours led to robust IFN-γ and TNF upregulation by MAIT cells. Tetramer negative CD8α+ T cells showed limited activation (**Figure 5.15**), and this likely includes activated MAIT cells that had downregulated their TCRs. When stimulated with 3 BpC BCG overnight, MAIT cells displayed robust IFN-γ production whilst TNF expression was limited (**Figure 5.16**) similar to stimulation with *E.coli* overnight (**Figure 5.14**) (Suliman et al., 2019). The dominant IFN-γ response may be the result of low MR1 ligand concentration coupled with a longer duration of stimulation driving MAIT cells towards IFN-γ secretion. Alternatively, this is in agreement with human MAIT cell responses to BCG stimulation, which was mediated primarily by IL-12/IL-18 rather than TCR-antigen-MR1 stimulation and showed IFN-γ but not TNF production comparable with the cytokine profile observed upon IL-12/IL-18-stimulation

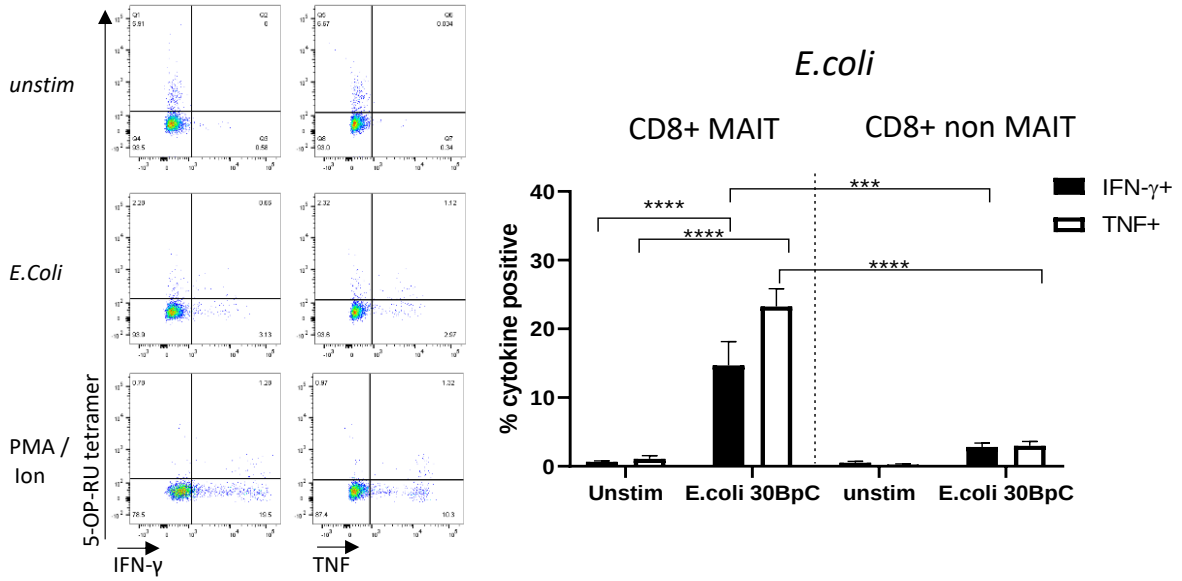

Figure 5.15 E. coli stimulation of cattle MAIT cells. Cattle PBMC were stimulated for 7 hours with 30 *E. coli* bacteria per cell (BpC). Unstimulated or phorbol myristate acetate (PMA)/Ionomycin (Ion) stimulated PBMC were used as control. Graphs depict IFN-γ and TNF producing live CD8+ MAIT and non-MAIT cells (mean ±SEM, n=4). CD8+ MR1-5-OP-RU tetramer + live lymphocytes were gated prior to determining the percentage cytokine positive cells. Representative flow cytometry histograms of IFN-γ and TNF expression for different stimuli are shown. Data was analysed using two-way ANOVA with repeated measures within animal, followed by Sidak's multiple comparisons post-hoc test comparing IFN-γ and TNF expression stimulated CD8α+ MAIT to unstimulated MAIT cells and to CD8α+ non MAIT cells.

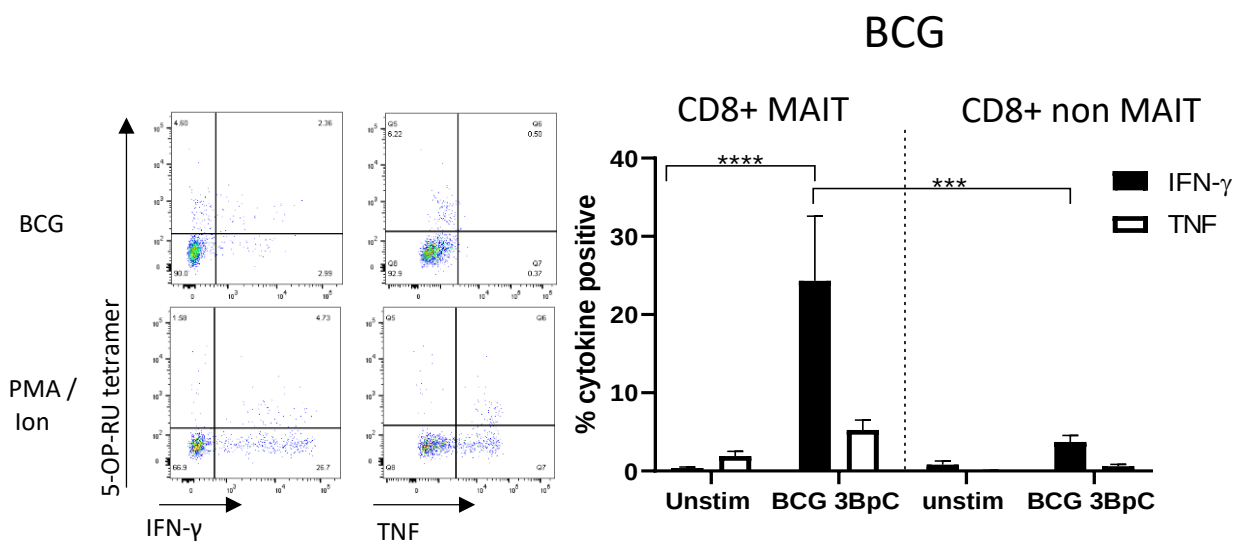

Figure 5.16 Stimulation of cattle MAIT cells with M. Bovis BCG. Cattle PBMC were stimulated for 18 hours with 3 BpC *M. Bovis* BCG. Unstimulated or phorbol myristate acetate (PMA)/Ionomycin (Ion) stimulated PBMC were used as control. Graphs depict IFN-γ and TNF producing live CD8+ MAIT and non-MAIT cells (mean ±SEM, n=4). Representative flow cytometry histograms of IFN-γ and TNF expression for different stimuli are shown. Lymphocytes were gated for FSC&SSC, singlets, live and CD8 expression followed by tetramer + prior to determining the percentage cytokine positive. Data were analysed using two-way ANOVA with repeated measures within animal, followed by Sidak's multiple comparisons post-hoc test comparing IFN-γ and TNF expression stimulated CD8α+ MAIT to unstimulated MAIT cells and to CD8α+ non MAIT cells.

Taken together, these data suggest that bovine MAIT cells can be activated through MR1- TCR interactions as well as through MR1 independent cytokine stimuli and are capable of responding to major animal and zoonotic pathogens *in vitro*.

5.7 *In vivo* response of MAIT cells to pathogens in cattle

Next, cattle MAIT cells were characterised in cattle *in vivo* during infection as well as in a vaccination challenge model. Mastitis is an inflammation of the mammary gland, most often due to bacterial infections. It is the most frequent disease in dairy cattle, presenting a major impact on animal welfare and is associated with economic losses (Petersson-Wolfe et al., 2018). *E. coli* which stimulated bovine MAIT cells *in vitro* (**Figure 5.17**), is a major mastitis-causing pathogen in cattle (Keane, 2019). Milk contains many different blood-derived immune cells (Harp et al., 2004, Paape et al., 2003), and MR1-tetramer staining of cells in milk from healthy cattle revealed a distinct MAIT cell population consistently present in bovine milk (mean 0.8% of CD3+, IQR 0.6-1.1%, range 0.4-1.4%, n=6) (**Figure 5.17)**. Somatic cell count (SCC) is a measure of the number of cells in milk and is used to detect the increased migration of immune cells to milk during mastitis where animals with an elevated SCC (>200,000 cells/ml) are considered to have mastitis (van den Borne et al., 2010). Cattle with an elevated SCC had on average a greater than 5-fold increase in MAIT cells as a percentage of CD3+ T cells, indicating increased migration of MAIT cells relative to other T cells from blood to milk during mastitis (**Figure 5.17**), and suggesting a possible direct or bystander role of MAIT cells in this inflammatory condition.

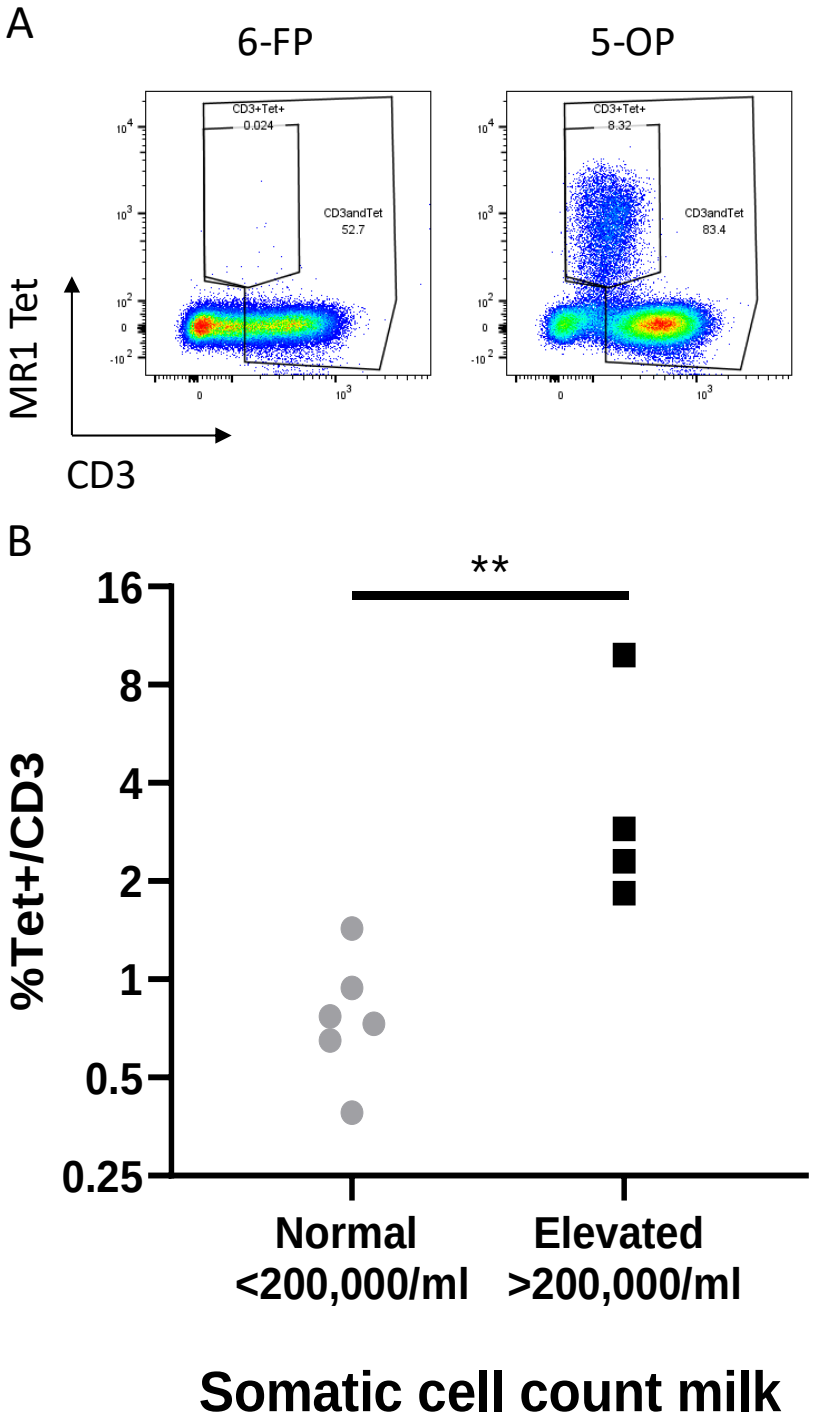

Figure 5.17 increased frequency of MAIT cells in milk in mastitis. A) Representative flow cytometry plots of MAIT cell staining in milk. Milk cells were gated on FSC&SSC, singlets and live cells. The percentage of MAIT cells (human MR1-5-OP-RU tetramer+) within the total T cell population (CD3+) in milk, grouped according to normal versus elevated milk somatic cell count (SCC). SCC is a measurement of the number of nucleated cells per millilitre milk and predominantly consists of white blood cells. SCC above 200.000 cells/ml is commonly used as a threshold for mastitis, inflammation of the mammary gland. Groups were compared using a Mann–Whitney U test. This data was generated by Lindert Benedictus at the Roslin Institute and is presented with permission

Bovine MAIT cells are activated following *M. Bovis* BCG stimulation *in vitro*. In macaques, MAIT cells activation was detectable *in vivo* in peripheral blood following both BCG vaccination and *M. tuberculosis* challenge (Greene et al., 2016). We assessed CD8+ MAIT cell responses to *Mycobacterium Bovis* infection longitudinally in cattle vaccinated with BCG following endobronchial challenge with the virulent *M. Bovis* strain AF2122/97. Perforin and granzyme production has previously been established as a means to license MAIT cells to kill *in vitro* (Kurioka et al., 2016) and can be used as activation markers. In cattle, no changes in the frequency of perforin expressing MAIT cells were found *ex vivo* in PBMC following BCG vaccination (**Figure 5.18**). However, two weeks following endobronchial challenge with *M. Bovis*, a significant, transient, increase was detected in the fraction of perforin expressing CD8+ MAIT cells in animals that showed tuberculosis associated lesions in the lungs and lymph nodes, signs of pathology consistent with severe infection (Figure 5.19**A**). In contrast, in animals without lesions, the fraction of perforin expressing CD8+ MAIT cells was unchanged. The fractions of perforin expressing MAIT cells in animals with lesions were also significantly increased compared to before challenge, while there was no change in the frequencies of perforin expressing tetramer negative (non-MAIT) CD8+ T cells (Figure 5.19**B**). No significant changes in CD69 expression, or in CD8+ MAIT cell frequencies were detected in peripheral blood (Figure 5.19**C-D**) in agreement with BCG vaccination in humans (Suliman et al., 2019)

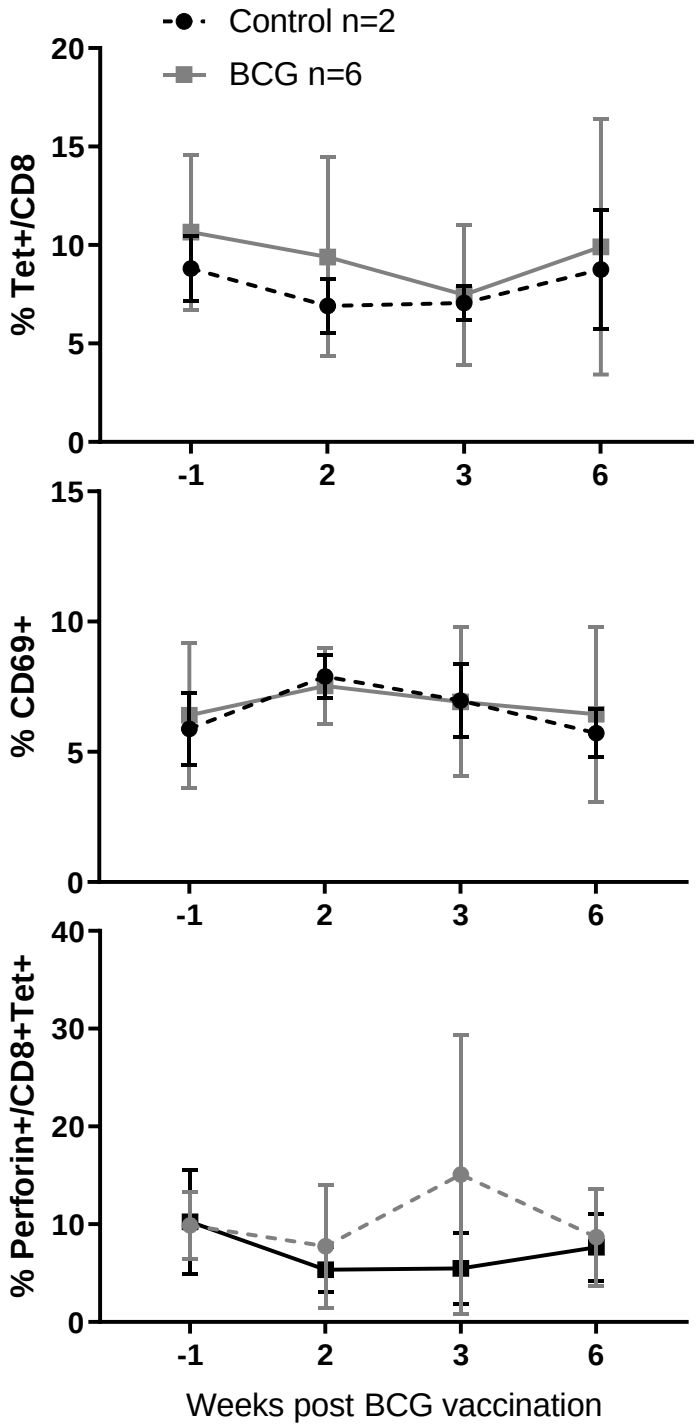

Figure 5.18 Characterisation of MAIT cells in cattle PBMC following BCG vaccination Six calves were vaccinated with $4.6x10^6$ CFU BCG Danish SSI 1331 subcutaneously. The percentage of total CD8+ MAIT as well as the percentage of CD69+ or perforin+ CD8+ MAIT cells (CD8+ MR1 tetramer+) in PBMC was measured longitudinally in blood. Data were analyzed using two-way ANOVA with time as repeated measures, followed by Sidak's multiple comparisons post-hoc test comparing differences between groups at each time point. Mean ± SD is indicated. This data was generated by Lindert Benedictus at the Roslin institute and is presented with permission

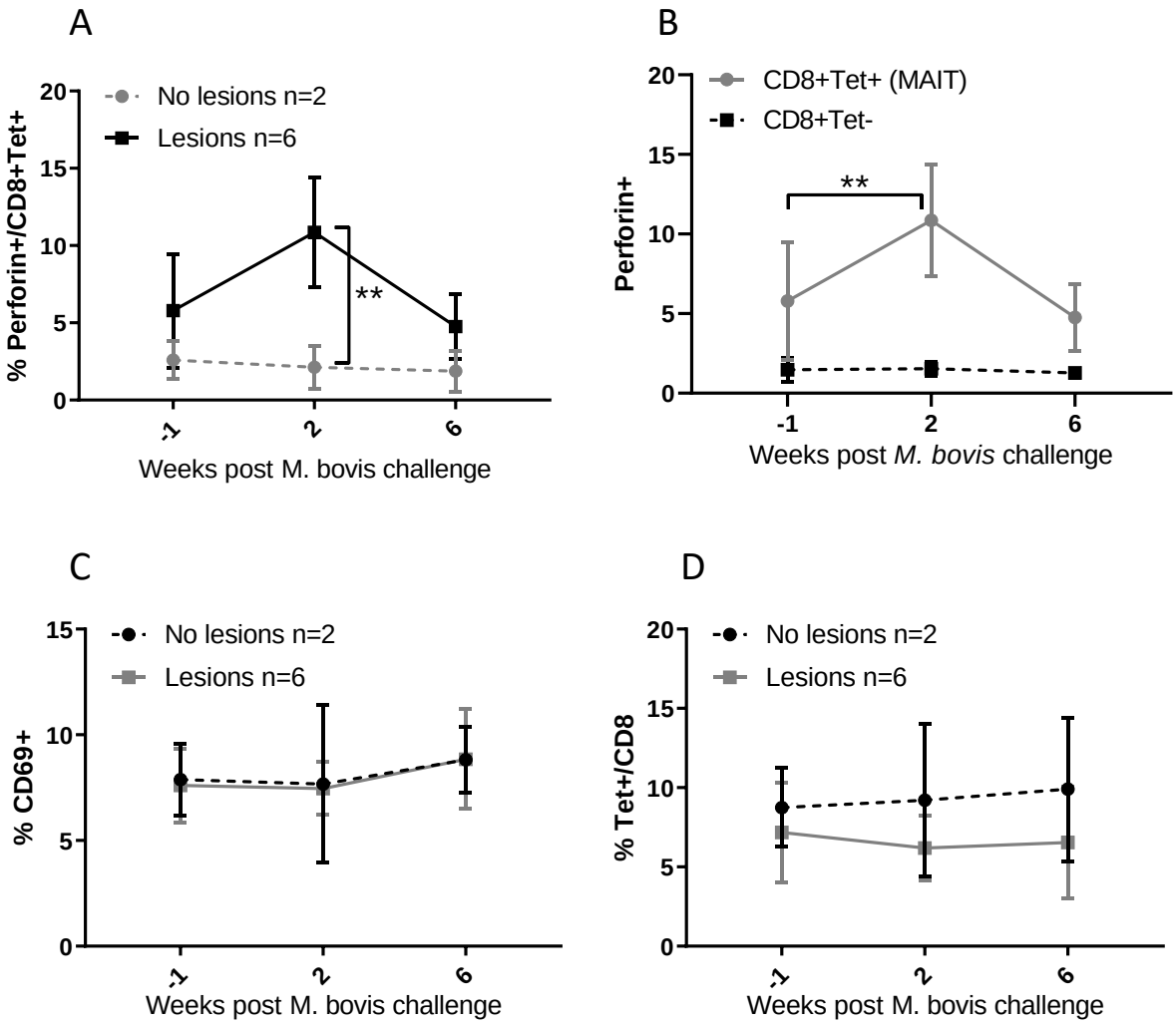

Figure 5.19 Characterization of MAIT cells in cattle PBMC following M. bovis challenge MAIT cell activation was measured longitudinally following *Mycobacterium bovis* challenge. Calves (n=8) were challenged endobronchially with 10^4 CFU *M. bovis* AF2122/97. Animals were grouped based on the presence of tuberculosis associated lesions in lungs and lymph nodes 11 weeks post-challenge at post-mortem examination. A) the percentage of perforin+ MAIT cells was compared between the group which contained lesions at post-mortem (n=6) to the group which contained no lesions (n=2). B) Comparison of perforin expression over time by MAIT cells (CD8+ tetramer+) and CD8 T cells (CD8+ tetramer-) within the animals which contained lesions at postmortem examination (n=6). C) Percentage of MAIT cells (CD8+ tetramer+) with high CD69 expression. D) MAIT cell frequencies within CD8 positive cells in peripheral blood over time. Data were analyzed using two-way ANOVA with time as repeated measures, followed by Sidak's multiple comparisons post-hoc test comparing changes in perforin expression over time within MAIT cells and CD8 T cells for B and comparing differences between groups at each time point for C-F. Mean ± SD is indicated in all graphs. This data was generated by Lindert Benedictus at the Roslin Institute and is presented with permission

5.8 Discussion

The canonical MAIT cell TCR α-chain was first identified in cattle alongside humans and mice over 20 years ago (Tilloy et al., 1999), but no phenotyping or characterisation has been carried out of cattle MAIT cells. The use of cross-reactive human MR1 tetramers has allowed the characterisation of the phenotype and function of cattle MAIT cells *in vitro* and *in vivo*. Overall, this data demonstrates that cattle MAIT cells are phenotypically and functionally similar humans, including expression of an orthologous conserved T cell receptor α-chain (**Figure 5.4**), expression of key transcription factors (**Figure 5.5**), an effector memory phenotype (**Figure 5.8**), enrichment in mucosal tissues (**Figure 5.6**) and swift responses to synthetic 5-OP-RU, cytokine stimulation and riboflavin biosynthesis competent bacteria (**Figure 5.10, Figure 5.15, Figure 5.16**). Though no direct activation has been shown of cattle MAIT cells by virus stimulation, MAIT cells were sensitive to IL-12 and IL-18 (**Figure 5.13**) Cytokine simulation which has previously been shown to be the mechanism of MAIT cell activation by viruses (van Wilgenburg et al., 2016, Wilgenburg et al., 2018) suggests that MAIT cells in cattle may be involved in anti-viral immunity. These similarities indicate that MAIT cells in cattle are also likely to respond to pathogens in a similar way to their counterparts identified in other species and may make cattle a useful model for the study of MAIT cells in certain disease contexts.

MAIT cells are the predominant IFN-γ producing T cell population in TB exposed individuals upon restimulation with BCG (Suliman et al., 2019). Recently, 5-OP-RU vaccination of MAIT cells in mice was not shown to be protective from subsequent TB infection and contributed to a delayed CD4 response to the infection. However, treatment with 5-OP-RU during chronic TB infection led to an increase in MAIT cell frequencies and a lowering of bacterial burden, which was dependent on IL-17 expression (Sakai et al., 2020). Whether MAIT cells are friend or foe during TB infection remains to be determined. The increased proportion of perforin+

MAIT cells in cows with TB lesions and responsiveness of MAIT cells to BCG shown in this thesis suggests that MAIT cells also play a role in bovine TB. Vaccination with the attenuated *M. Bovis* BCG strain causes local infection, and it is therefore not surprising that MAIT cell activation was not detectable in peripheral blood. In contrast, severe infection with virulent *M. bovis,* resulting in lesions in multiple organs leads to more widespread MAIT cell activation that can be detected in peripheral blood. No changes in CD69 expression, or in CD8+ MAIT cell frequencies were detected in peripheral blood in agreement with BCG vaccination in humans (Suliman et al., 2019) and *M. tuberculosis* challenge in macaques (Greene et al., 2016). Overall, these data indicate that severe *M. bovis* infections in cattle led to the activation of MAIT cells *in vivo*. MAIT cells have been shown to be activated by *Mycobacterium tuberculosis* in humans (Vorkas et al., 2018, Suliman et al., 2019), non-human primates (Greene et al., 2017) and mice (Chua et al., 2012). As a natural host of TB and with the possibility for repeated (tissue) sampling and cannulation of lymph nodes, cattle are an appropriate large animal model with a unique potential to study MAIT cells longitudinally in tissues *in vivo*.

The identification of MAIT cells in milk and their increased frequency in mastitis also poses some interesting questions. Mastitis in cattle is predominantly bacterial in origin and is characterised by a massive migration of neutrophils to the mammary gland (Rainard and Riollet, 2003). Bacteria induced cytokine responses by MAIT cells in the context of mastitis could be a driving force in the neutrophil influx and inflammation associated with intramammary bacterial infections (Hinks and Zhang, 2020). Further studies tracking MAIT cells longitudinally in milk and tissues during intramammary infections, will shed light on the role of MAIT cells in mastitis, such as the temporal relation to the neutrophil influx. Maternal immune cells in milk play a role in the development of the neonatal immune system (Wang et al., 2012, Reber et al., 2005) and milk derived CD8+ T cells preferentially home to the payers

patches of the small intestine (Cabinian et al., 2016). MAIT cells are donor-unrestricted, i.e. conserved between individuals given the monomorphic nature of their restriction element MR1 (Van Rhijn and Moody, 2015). Speculatively, MAIT cells present in milk and possibly also in colostrum may be transferred to the neonate. The neonatal conditions of the digestive tract allow for the survival of maternal lymphocytes, where they could play a role in passive immunity and the development of long term immunity (Laouar, 2020).

Chapter 6 General discussion and future recommendations

6.1 Key findings of this thesis

6.1.1 Chapter 3. Kinetics, magnitude and specificity of conventional T cell responses during H1N1pfm09 infection in outbred and inbred pigs.

The data presented in chapter 3 adds to the expanding literature of T cell response of pigs to IAV virus. A detailed analysis of the kinetics and magnitude of the T cell response was performed as well as antibody responses (antibody data not presented in this thesis). Differences in terms of magnitude and function of the CD4 and CD8 cellular responses were observed between tissues. For example, there was a 27 times higher proportion of CD8 antigen-specific cells in the BAL compared to the blood. This mirrors findings in humans were antigen-specific CD8 responses in BAL of patients infected with H1N1pdm09 were much higher than in the blood (Zhao et al., 2012). The CD4 response varied less between tissues, perhaps reflecting their role providing help to other cellular subsets which would require them to be less focussed at the site of infection. There were also differences in the functionality of the T cell response between tissues. For example, in the CD8 population, triple cytokine (IFN-γ, TNF, IL-2) secreting cells were only identified in the BAL, and these cells expressed greater levels of IFN-γ (as measured by MFI) than the single or double cytokine-producing cells.

These differences would not be identified if not for the ability to sample local sites of immunity which is possible using animal models. They demonstrate that peripheral blood is not a good representation of the immune response at the site of infection. These differences in local and systemic T cells have implications for T cell vaccine studies, where it will be essential to study the induction of the local immune response. The possibility to induce long lasting cross reactive T cells as a potential universal vaccine continues to be of great interest (Coughlan et al., 2018,

Koutsakos et al., 2019, Holzer et al., 2018b). With the advantage of comparative size and anatomy to humans and the ability to study the T cell response in the mucosa, the pig will be an asset to the study of these vaccine approaches.

The Babraham pig line shows great promise as a biomedical model as their level of inbreeding reduces variation between animals, increasing reproducibility, thereby potentially reducing the number of animals required for an experimental group. There is also potential to perform cellular depletions as well as adoptive transfer experiments in these animals which would allow for the study of these cellular responses in a more defined context. However, no previous attempt has been made to compare the immune responses of the Babraham pig with outbred pigs to IAV virus infection until now. Overall, the responses of the Babraham pig to H1N1pdm09 infection were comparable to the outbred animals, with no statistically significant differences observed. This data helps validate the Babraham pig as a model of pig immune responses to pandemic influenza. Furthermore, the fact that the Babraham pig is SLA homozygous allows for the fine specificity of the T cell response to be studied in these animals. In this thesis, a previously described CD8 epitope identified in the Babraham pig allowed for the tracking of IAV specific T cells during the time course of infection. Further characterisation of the antigen-specific T cells during the time course of influenza infection is currently being carried out by our group, determining the induction of effector T cells and the development of resident memory following infection with IAV. Other epitopes that have been identified in this study will be a useful tool for these future studies enabling the characterisation of the specificity of response in multiple tissues.

A summary of the immune responses characterised in **chapter 3** is presented in **Figure 6.1**. The T cell and antibody response develops from day four onwards with a large expansion from days 5-6, which coincides with viral clearance. It is likely that these adaptive immune responses contributed to viral clearance as has been previously shown in other species (Bender

et al., 1992, Doherty et al., 1997, Mozdzanowska et al., 1997, Gerhard et al., 1997). However, the viral load was contained in the period before the adaptive response is detectable, indicating the importance of innate immune mechanisms in influenza infection. The absence of MAIT cells during phenotypic assessments in the pig meant that no further investigation of these cells in the context of influenza infection was feasible. However, there are still samples available from this study, and the early time points could be utilised to interrogate the innate responses to influenza infection which controlled the virus prior to the induction of the adaptive immune response.

Something which has long held back the use of non-mouse models of infection is the scarcity of species-specific reagents, particularly monoclonal antibodies for flow cytometric analysis. RNA sequencing technologies are becoming more commonly used in pigs (Li et al., 2016, do Nascimento et al., 2018, Schroyen and Tuggle, 2015). The combination of the Babraham pig with RNA sequencing could be a powerful tool to determine the T cell response at different time points in tetramer sorted T cells, tracking the cellular proliferative and functional responses in multiple tissues, and correlating the sequencing data with protection. RNA sequencing may also guide efforts to develop a wider range of monoclonal antibodies for immunological studies in pigs by demonstrating the expression of specific proteins at the RNA level. An RNA sequencing approach would also likely be a useful tool for these studies to overcome the lack of reagents to characterise innate and innate like subsets in the pig in detail. A study of the transcriptome of lymphocyte populations at different time points of infection would generate a wealth of data and aid in the development of new hypotheses on the role of innate and innate like subsets in the early stages of influenza infection. Experiments such as these would perhaps be aided by the use of the Babraham model, as these animals will have less inherent variation which can be confounding in these experiments (Schroyen and Tuggle, 2015).

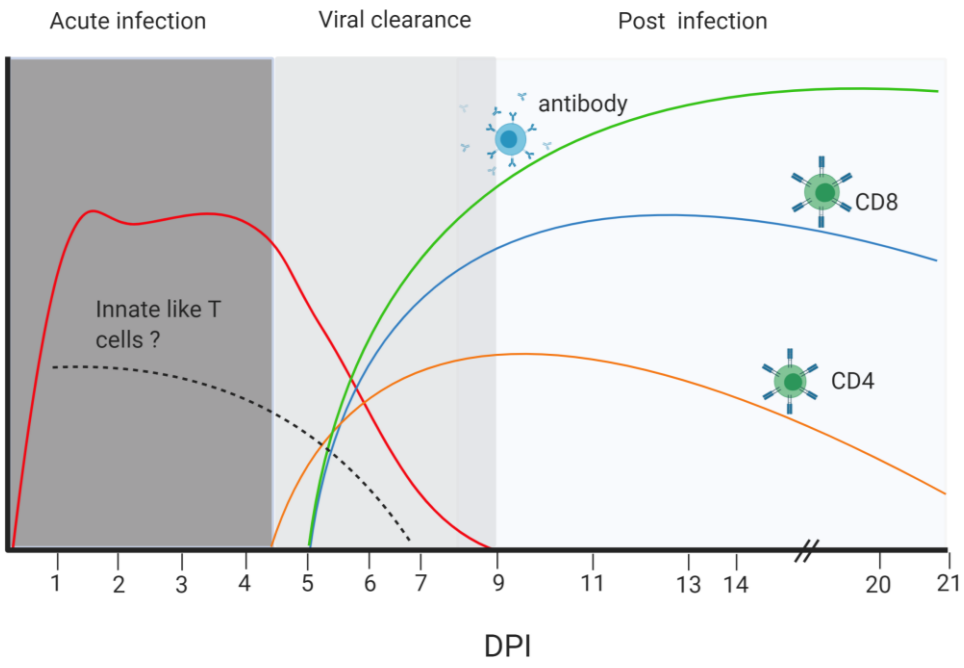

Figure 6.1 Dynamics of viral load, T cell and Ab responses. Stylised presentation of kinetics and magnitude of viral load and immune responses. The different colour lines represent the antibody and cellular responses as indicated, and the red line the virus load. The figure was created with BioRender.com.

Future work:

- Dissect the responses to different CD4 and CD8 epitopes between tissues. Raises the question of the utility of peptide-based vaccines, which could be tested in pigs
- Perform RNAseq on antigen specific CD4 and CD8 populations from different tissues at different time points, with the aim of illuminating why the responses are different in different tissues. Identify a protective signature of responses by correlation with morbidity and mortality
- Perform cell transfer experiments in Babraham pigs to establish the role of different cell subsets (for example transfer of BAL CD8 cells)
- Perform RNAseq in sorted innate and innate-like T cell subsets, such as NK, NKT and γδ T cells in local tissues in the early time course of influenza infection, to determine response at a transcriptomic level

6.1.2 Chapter 4 and 5. Identification of MAIT cells in multiple species and characterisation of MAIT cells in cattle.

The level of MR1 cross-reactivity shown in this study between species which have been evolutionarily separated by millions of years is remarkable and suggests an essential role of this antigen-presenting pathway in microbial defence. Contradicting the importance of MAIT cells is the loss of MR1 and MAIT cells in some species (Boudinot et al., 2016) and the low frequency MAIT cell population in laboratory mouse strains (Tilloy et al., 1999, Rahimpour et al., 2015), suggesting a redundancy to their role. This study adds to these findings by identifying MAIT cells in cattle and sheep, while MAIT cells in pigs were at the limit of phenotypic detection. The species-specific differences in MAIT cell frequencies are also seen in other innate-like T cells with some of these differences summarised in **Table 6.1** with the findings of this study highlighted in red.

Table 6.1 Comparisons of innate like T cell frequencies between species.

	Human	Mouse	Cattle	Pig	Sheep
MAIT cells	~3.1% PBMC **(1)**	~0.1% PBMC higher frequency in tissues **(2)**	~0.6% CD3 in PBMC	Very low frequency/ not present	~1.3% CD8
iNKT cells	~0.1% of TCRβ+ PBMC **(3)**	5-10% in thymus **(3)**	Not present (CD1d is present but does not present aGalCer) **(4) (5)**	1% at 2 weeks of age decreasing to 0.1% by 16 weeks in PBMC **(6)**	Not present **(4)**
TCRγδ cells	~4% in PBMC **(7) (8)**	1-4% in thymus and secondary lymphoid organs **(8)**	~20% in adult cattle PBMC **(8) (9)**	~40% CD3+ lymphocytes in PBMC **(10)**	~30% of PBMC in lambs **(8) (9)**

References: **(1)** (Gherardin et al., 2018) **(2)** (Rahimpour et al., 2015) **(3)** (Garner et al., 2018) **(4)** (Looringh van Beeck et al., 2009b) **(5)** (Nguyen et al., 2013) **(6)** (Schäfer et al., 2019) **(7)** (Provine et al., 2018) **(8)** (Chien et al., 2014) **(9)** (Hein and Mackay, 1991) **(10)** (Takamatsu et al., 2006)

The important role of MAIT cells, a prominent population in humans and cattle, may be supplanted by other cell types which share overlapping functions. It has previously been suggested by Koay *et al*. (Koay et al., 2018, Koay et al., 2016a) that iNKT cells may compete for the same immunological niche with MAIT cells, evidenced by the finding that iNKT cell depletion in mice leads to increased MAIT cell numbers (Koay et al., 2016a). In line with this hypothesis, iNKT cells are identifiable in pigs (Schäfer et al., 2019) while they could not be functionally identified in ruminants (Looringh van Beeck et al., 2009b, Wang et al., 2012, Nguyen et al., 2013) and iNKT cells are a much smaller population in humans than mice (Garner et al., 2018). Further, MAIT cells have overlapping functions with iNKT cells (Garner et al., 2018) and the Vδ2 subset of human γδ T cells (Provine et al., 2018). A recent study also found a human individual with a rare point mutation in MR1, leading to the loss of MAIT cells also had a high proportion of Vγ9Vδ2 γδ T cells (Howson et al., 2020). Therefore, it is possible that no individual innate-like T cell subset is vital for overall immune function; but instead, the indispensable immune function is dominated by different innate-like T cell subsets within each species.

If and how iNKT, γδ T and MAIT cells compete for an immunological niche remains to be determined. There may also be as yet undiscovered innate-like T cells which also have overlapping functions with MAIT cells as previously proposed by Boudinot *et al* (Boudinot et al., 2016). There is high diversity in unconventional T cell populations between animals, though their central function(s) may be conserved. Advances in sequencing technology may be a useful tool for further studying these innate-like T cell populations. If a specific transcriptomics signature could be identified, which is shared between T lymphocytes from different species, a more fundamental understanding of the underlying functions of innate-like T cells could be determined. Human MAIT cells could be used as the archetypal innate-like T cell for this study.

The inability to identify MAIT cells in the pig disagrees with previously published qPCR based findings that MAIT cells are a small population but one that should be identifiable by flow cytometric methods (Xiao et al., 2019a). Variation in pig breeds may contribute to differences in reported findings. It may also be that subtle differences in the pig MAIT cell TCR may prevent binding to or activation by 5-OP-RU. Further studies in a wider range of pig breeds as well as exploring whether different antigens can activate pig MAIT cells would be needed to answer these questions. The generation of pig MAIT cell clones based upon putative TCR sequences as well as cells expressing pig MR1 as antigen-presenting cells would be useful for these studies. Pig MAIT cell clones could be utilised to study their reactivity to differing MAIT cell ligands, whereas cells expressing pig MR1 could determine if pig MR1 can stimulate MAIT cell populations from other species. TCR sequencing of pig T cells may also generate useful information on the relative frequency of the canonical MAIT cell TCR sequence in this species.

The identification and characterisation of MAIT cells in cattle enable this species to be included as a potential model for the study of MAIT cells. The phenotyping of cattle MAIT cells identified variation in co-receptor usage and CD25 expression, dependent on tissue localisation. Further studies comparing the MAIT cell populations identified in different tissues, including RNA sequencing experiments, will aid in determining the role of these T cells in differing tissues.

Cattle are a model for TB (Waters et al., 2011, Van Rhijn et al., 2008) which remains an important disease in cattle (Harris et al., 2018) and a major public health concern in humans (Furin et al., 2019). Recently, intravenous but not intradermal administration of BCG was shown to transiently (up to 8 weeks) increase MAIT cell frequencies in the BAL of non-human primates but did not affect MAIT cells in peripheral blood (Darrah et al., 2020). Their data also showed a limited response by MAIT cells in the periphery to subcutaneous BCG vaccination

and demonstrates that route of vaccine administration and tissue localisation are important factors to consider when studying the MAIT cell response to vaccination. Studies in cattle, a natural host for TB, would aid in defining the role of MAIT cells in this disease. MAIT cells are also activated during viral infections in humans (van Wilgenburg et al., 2016) and mice (Wilgenburg et al., 2018). Though the studies presented here did not formally show that cattle MAIT cells respond to viruses, they were responsive to the cytokines IL-12 and IL-18, which is the mechanism by which they are activated by viruses in other species (Loh et al., 2016, van Wilgenburg et al., 2016). Viral diseases such as foot and mouth disease virus, in cattle, can have a devastating economic impact (Poonsuk et al., 2018) and cattle are a relevant model for human viral infections such as respiratory syncytial virus (Blodörn et al., 2015). It would therefore be of interest to study cattle MAIT cells in the context of these viral infections. Vaccinating cattle with MAIT cell ligands such as 5-OP-RU prior to exposure with bacteria or virus or during chronic infection would justify future investigation as a target of therapeutic intervention.

Future recommendations:

- RNA sequencing of lymphocyte populations in a range of species to identify innate-like T cell signatures
- Further studies to identify MAIT cells in pigs including studies with different ligands, generating MAIT cell clones, generating MR1 expressing cell lines and screening further pig breeds for MAIT cell populations
- Further characterise the MAIT cell population identified in cattle including in-depth sequencing and phenotyping of the population in different tissues
- In vivo studies of MAIT cells in TB and viral infections such as FMDV
- Studies in cattle to determine whether techniques to manipulate the MAIT cell population such as 5-OP-RU vaccination are possible in large animals

6.2 Summary of thesis

This thesis adds to the rapidly developing understanding of T cell immunity in livestock species. The data presented in chapter 3 advances our understanding of the T cell response over a time course of infection in the pig model, validating the Babraham pig as an appropriate inbred animal model. Ongoing studies of influenza infection and immunisation in both inbred and outbred pigs will develop our understanding of T cell correlates of protection to influenza virus in a large animal, which will aid future vaccine design and testing. The differing frequencies of MAIT cells in livestock species identified in this study add to the growing literature demonstrating innate-like T cells to be highly diverse between species. This highlights the importance of understanding these differences when inferring immune responses from one species to another. Selecting the correct model when studying these cell types in detail will be essential. For example, pigs may not be a useful model for the study of MAIT cells, but they may be more appropriate as a model of NKT cells, as they express a comparable range of CD1 genes (Van Rhijn et al., 2015) and express similar frequencies of iNKT cells (Schäfer et al., 2019) to humans. Further, the differing frequencies of innate-like T cells suggest that these cells may compete for a similar immunological niche. RNA sequencing and deep phenotyping of these immune cells may further reveal a shared function which is vital for host immunity.

Finally, the phenotypic identification of MAIT cells in cattle enables studies of TB infection, where cattle offer a unique opportunity to study this infection in the local tissues of a large animal which is also a natural host for the disease.

The data presented here contribute to the understanding of conventional and innate-like T cells of livestock species that represent relevant models for human diseases. These findings will be of interest to both veterinary and human medicine.

References

ACHDOUT, H., MENINGHER, T., HIRSH, S., GLASNER, A., BAR-ON, Y., GUR, C., PORGADOR, A., MENDELSON, M., MANDELBOIM, M. & MANDELBOIM, O. 2010. Killing of Avian and Swine Influenza Virus by Natural Killer Cells. *Journal of Virology,* 84**,** 3993.

ALEXOPOULOU, L., HOLT, A. C., MEDZHITOV, R. & FLAVELL, R. A. 2001. Recognition of double-stranded RNA and activation of NF-kappaB by Toll-like receptor 3. *Nature,* 413**,** 732-8.

ARAKI, Y., FANN, M., WERSTO, R. & WENG, N.-P. 2008. Histone acetylation facilitates rapid and robust memory CD8 T cell response through differential expression of effector molecules (eomesodermin and its targets: perforin and granzyme B). *Journal of immunology (Baltimore, Md. : 1950),* 180**,** 8102-8108.

AURAY, G., KELLER, I., PYTHON, S., GERBER, M., BRUGGMANN, R., RUGGLI, N. & SUMMERFIELD, A. 2016. Characterization and Transcriptomic Analysis of Porcine Blood Conventional and Plasmacytoid Dendritic Cells Reveals Striking Species-Specific Differences. *J Immunol,* 197**,** 4791-4806.

BACHMANN, M. F., ODERMATT, B., HENGARTNER, H. & ZINKERNAGEL, R. M. 1996. Induction of long-lived germinal centers associated with persisting antigen after viral infection. *The Journal of experimental medicine,* 183**,** 2259-2269.

BARATELLI, M., MORGAN, S., HEMMINK, J. D., REID, E., CARR, B. V., LEFEVRE, E., MONTANER-TARBES, S., CHARLESTON, B., FRAILE, L., TCHILIAN, E. & MONTOYA, M. 2020. Identification of a Newly Conserved SLA-II Epitope in a Structural Protein of Swine Influenza Virus. *Frontiers in Immunology,* 11.

BARATELLI, M., PEDERSEN, L. E., TREBBIEN, R., LARSEN, L. E., JUNGERSEN, G., BLANCO, E., NIELSEN, J. & MONTOYA, M. 2017. Identification of cross-reacting T-cell epitopes in structural and non-structural proteins of swine and pandemic H1N1 influenza A virus strains in pigs. *J Gen Virol,* 98**,** 895-899.

BAUMGARTH, N. & KELSO, A. 1996. In vivo blockade of gamma interferon affects the influenza virus-induced humoral and the local cellular immune response in lung tissue. *Journal of virology,* 70**,** 4411-4418.

BENDER, B. S., CROGHAN, T., ZHANG, L. & SMALL, P. A., JR. 1992. Transgenic mice lacking class I major histocompatibility complex-restricted T cells have delayed viral clearance and increased mortality after influenza virus challenge. *The Journal of experimental medicine,* 175**,** 1143-1145.

BILLERBECK, E., KANG, Y.-H., WALKER, L., LOCKSTONE, H., GRAFMUELLER, S., FLEMING, V., FLINT, J., WILLBERG, C. B., BENGSCH, B., SEIGEL, B., RAMAMURTHY, N., ZITZMANN, N., BARNES, E. J., THEVANAYAGAM, J., BHAGWANANI, A., LESLIE, A., OO, Y. H., KOLLNBERGER, S., BOWNESS, P., DROGNITZ, O., ADAMS, D. H., BLUM, H. E., THIMME, R. & KLENERMAN, P. 2010. Analysis of CD161 expression on human CD8+ T cells defines a distinct functional subset with tissue-homing properties. *Proceedings of the National Academy of Sciences of the United States of America,* 107**,** 3006-3011.

BIMCZOK, D., POST, A., TSCHERNIG, T. & ROTHKOTTER, H. J. 2006. Phenotype and distribution of dendritic cells in the porcine small intestinal and tracheal mucosa and their spatial relationship to epithelial cells. *Cell Tissue Res,* 325**,** 461-8.

BLODÖRN, K., HÄGGLUND, S., GAVIER-WIDEN, D., ELÉOUËT, J.-F., RIFFAULT, S., PRINGLE, J., TAYLOR, G. & VALARCHER, J. F. 2015. A bovine respiratory syncytial virus model with high clinical expression in calves with specific passive immunity. *BMC Veterinary Research,* 11**,** 76.

BODEWES, R., KREIJTZ, J. H. C. M., BAAS, C., GEELHOED-MIERAS, M. M., DE MUTSERT, G., VAN AMERONGEN, G., VAN DEN BRAND, J. M. A., FOUCHIER, R. A. M., OSTERHAUS, A. D. M. E. & RIMMELZWAAN, G. F. 2009. Vaccination against human influenza A/H3N2 virus prevents the induction of heterosubtypic immunity against lethal infection with avian influenza A/H5N1 virus. *PloS one,* 4**,** e5538-e5538.

BOLOTIN, D. A., POSLAVSKY, S., MITROPHANOV, I., SHUGAY, M., MAMEDOV, I. Z., PUTINTSEVA, E. V. & CHUDAKOV, D. M. 2015. MiXCR: software for comprehensive adaptive immunity profiling. *Nat Methods,* 12**,** 380-1.

BOLTE, F. J. & REHERMANN, B. 2018. Mucosal-Associated Invariant T Cells in Chronic Inflammatory Liver Disease. *Seminars in liver disease,* 38**,** 60-65.

BOOTH, J. S., SALERNO-GONCALVES, R., BLANCHARD, T. G., PATIL, S. A., KADER, H. A., SAFTA, A. M., MORNINGSTAR, L. M., CZINN, S. J., GREENWALD, B. D. & SZTEIN, M. B. 2015. Mucosal-Associated Invariant T Cells in the Human Gastric Mucosa and Blood: Role in Helicobacter pylori Infection. *Frontiers in immunology,* 6**,** 466-466.

BORN, W. K., KEMAL AYDINTUG, M. & O'BRIEN, R. L. 2013. Diversity of gammadelta T-cell antigens. *Cell Mol Immunol,* 10**,** 13-20.

BOT, A., BOT, S. & BONA, C. A. 1998. Protective role of gamma interferon during the recall response to influenza virus. *Journal of virology,* 72**,** 6637-6645.

BOUDINOT, P., MONDOT, S., JOUNEAU, L., TEYTON, L., LEFRANC, M. P. & LANTZ, O. 2016. Restricting nonclassical MHC genes coevolve with TRAV genes used by innate-like T cells in mammals. *Proc Natl Acad Sci U S A,* 113**,** E2983-92.

BRANDES, M., WILLIMANN, K. & MOSER, B. 2005. Professional antigen-presentation function by human gammadelta T Cells. *Science,* 309**,** 264-8.

BREA, D., MEURENS, F., DUBOIS, A. V., GAILLARD, J., CHEVALEYRE, C., JOURDAN, M. L., WINTER, N., ARBEILLE, B., SI-TAHAR, M., GAUTHIER, F. & ATTUCCI, S. 2012. The pig as a model for investigating the role of neutrophil serine proteases in human inflammatory lung diseases. *Biochem J,* 447**,** 363-70.

BROWN, D. M., LEE, S., GARCIA-HERNANDEZ, M. D. L. L. & SWAIN, S. L. 2012. Multifunctional CD4 cells expressing gamma interferon and perforin mediate protection against lethal influenza virus infection. *Journal of virology,* 86**,** 6792-6803.

BUCSAN, A. N., ROUT, N., FOREMAN, T. W., KHADER, S. A., RENGARAJAN, J. & KAUSHAL, D. 2019. Mucosal-activated invariant T cells do not exhibit significant lung recruitment and proliferation profiles in macaques in response to infection with Mycobacterium tuberculosis CDC1551. *Tuberculosis (Edinb),* 116s**,** S11-s18.

CABINIAN, A., SINSIMER, D., TANG, M., ZUMBA, O., MEHTA, H., TOMA, A., SANT'ANGELO, D., LAOUAR, Y. & LAOUAR, A. 2016. Transfer of Maternal Immune Cells by Breastfeeding: Maternal Cytotoxic T Lymphocytes Present in Breast Milk Localize in the Peyer's Patches of the Nursed Infant. *PloS one,* 11**,** e0156762-e0156762.

CALORE, E. E., UIP, D. E. & PEREZ, N. M. 2011. Pathology of the swine-origin influenza A (H1N1) flu. *Pathology - Research and Practice,* 207**,** 86-90.

CAMP, J. V. & JONSSON, C. B. 2017. A Role for Neutrophils in Viral Respiratory Disease. *Front Immunol,* 8**,** 550.

CAROLAN, E., TOBIN, L. M., MANGAN, B. A., CORRIGAN, M., GAOATSWE, G., BYRNE, G., GEOGHEGAN, J., CODY, D., O'CONNELL, J., WINTER, D. C., DOHERTY, D. G., LYNCH, L., O'SHEA, D. & HOGAN, A. E. 2015. Altered distribution and increased IL-17 production by mucosal-associated invariant T cells in adult and childhood obesity. *J Immunol,* 194**,** 5775-80.

CHEN, Z., WANG, H., D'SOUZA, C., SUN, S., KOSTENKO, L., ECKLE, S. B. G., MEEHAN, B. S., JACKSON, D. C., STRUGNELL, R. A., CAO, H., WANG, N., FAIRLIE, D. P., LIU, L., GODFREY, D. I., ROSSJOHN, J.,

MCCLUSKEY, J. & CORBETT, A. J. 2017. Mucosal-associated invariant T-cell activation and accumulation after in vivo infection depends on microbial riboflavin synthesis and co-stimulatory signals. *Mucosal Immunology,* 10**,** 58-68.

CHIEN, Y.-H., MEYER, C. & BONNEVILLE, M. 2014. γδ T Cells: First Line of Defense and Beyond. *Annual Review of Immunology,* 32**,** 121-155.

CHUA, W.-J., KIM, S., MYERS, N., HUANG, S., YU, L., FREMONT, D. H., DIAMOND, M. S. & HANSEN, T. H. 2011. Endogenous MHC-Related Protein 1 Is Transiently Expressed on the Plasma Membrane in a Conformation That Activates Mucosal-Associated Invariant T Cells. *The Journal of Immunology,* 186**,** 4744-4750.

CHUA, W.-J., TRUSCOTT, S. M., EICKHOFF, C. S., BLAZEVIC, A., HOFT, D. F. & HANSEN, T. H. 2012. Polyclonal mucosa-associated invariant T cells have unique innate functions in bacterial infection. *Infection and immunity,* 80**,** 3256-3267.

CONNELLEY, T., AERTS, J., LAW, A. & MORRISON, W. I. 2009. Genomic analysis reveals extensive gene duplication within the bovine TRB locus. *BMC genomics,* 10**,** 192-192.

CONNELLEY, T. K., DEGNAN, K., LONGHI, C. W. & MORRISON, W. I. 2014. Genomic analysis offers insights into the evolution of the bovine TRA/TRD locus. *BMC genomics,* 15**,** 994-994.

CONSTANTINIDES, M. G., LINK, V. M., TAMOUTOUNOUR, S., WONG, A. C., PEREZ-CHAPARRO, P. J., HAN, S.-J., CHEN, Y. E., LI, K., FARHAT, S., WECKEL, A., KRISHNAMURTHY, S. R., VUJKOVIC-CVIJIN, I., LINEHAN, J. L., BOULADOUX, N., MERRILL, E. D., ROY, S., CUA, D. J., ADAMS, E. J., BHANDOOLA, A., SCHARSCHMIDT, T. C., AUBÉ, J., FISCHBACH, M. A. & BELKAID, Y. 2019a. MAIT cells are imprinted by the microbiota in early life and promote tissue repair. *Science,* 366**,** eaax6624.

CONSTANTINIDES, M. G., LINK, V. M., TAMOUTOUNOUR, S., WONG, A. C., PEREZ-CHAPARRO, P. J., HAN, S. J., CHEN, Y. E., LI, K., FARHAT, S., WECKEL, A., KRISHNAMURTHY, S. R., VUJKOVIC-CVIJIN, I., LINEHAN, J. L., BOULADOUX, N., MERRILL, E. D., ROY, S., CUA, D. J., ADAMS, E. J., BHANDOOLA, A., SCHARSCHMIDT, T. C., AUBÉ, J., FISCHBACH, M. A. & BELKAID, Y. 2019b. MAIT cells are imprinted by the microbiota in early life and promote tissue repair. *Science,* 366.

CORBETT, A. J., ECKLE, S. B., BIRKINSHAW, R. W., LIU, L., PATEL, O., MAHONY, J., CHEN, Z., REANTRAGOON, R., MEEHAN, B., CAO, H., WILLIAMSON, N. A., STRUGNELL, R. A., VAN SINDEREN, D., MAK, J. Y., FAIRLIE, D. P., KJER-NIELSEN, L., ROSSJOHN, J. & MCCLUSKEY, J. 2014. T-cell activation by transitory neo-antigens derived from distinct microbial pathways. *Nature,* 509**,** 361-5.

CORBETT, E. L., WATT, C. J., WALKER, N., MAHER, D., WILLIAMS, B. G., RAVIGLIONE, M. C. & DYE, C. 2003. The Growing Burden of Tuberculosis: Global Trends and Interactions With the HIV Epidemic. *Archives of Internal Medicine,* 163**,** 1009-1021.

COSGROVE, C., USSHER, J. E., RAUCH, A., GÄRTNER, K., KURIOKA, A., HÜHN, M. H., ADELMANN, K., KANG, Y.-H., FERGUSSON, J. R., SIMMONDS, P., GOULDER, P., HANSEN, T. H., FOX, J., GÜNTHARD, H. F., KHANNA, N., POWRIE, F., STEEL, A., GAZZARD, B., PHILLIPS, R. E., FRATER, J., UHLIG, H. & KLENERMAN, P. 2013. Early and nonreversible decrease of CD161++ /MAIT cells in HIV infection. *Blood,* 121**,** 951-961.

COUGHLAN, L., SRIDHAR, S., PAYNE, R., EDMANS, M., MILICIC, A., VENKATRAMAN, N., LUGONJA, B., CLIFTON, L., QI, C., FOLEGATTI, P. M., LAWRIE, A. M., ROBERTS, R., DE GRAAF, H., SUKHTANKAR, P., FAUST, S. N., LEWIS, D. J. M., LAMBE, T., HILL, A. & GILBERT, S. C. 2018. Heterologous Two-Dose Vaccination with Simian Adenovirus and Poxvirus Vectors Elicits Long-Lasting Cellular Immunity to Influenza Virus A in Healthy Adults. *EBioMedicine,* 29**,** 146-154.

D'SOUZA, C., CHEN, Z. & CORBETT, A. J. 2018. Revealing the protective and pathogenic potential of MAIT cells. *Mol Immunol,* 103**,** 46-54.

DARRAH, P. A., ZEPPA, J. J., MAIELLO, P., HACKNEY, J. A., WADSWORTH, M. H., HUGHES, T. K., POKKALI, S., SWANSON, P. A., GRANT, N. L., RODGERS, M. A., KAMATH, M., CAUSGROVE, C. M., LADDY, D. J., BONAVIA, A., CASIMIRO, D., LIN, P. L., KLEIN, E., WHITE, A. G., SCANGA, C. A., SHALEK, A.

K., ROEDERER, M., FLYNN, J. L. & SEDER, R. A. 2020. Prevention of tuberculosis in macaques after intravenous BCG immunization. *Nature,* 577**,** 95-102.

DAVEY, M. S., WILLCOX, C. R., JOYCE, S. P., LADELL, K., KASATSKAYA, S. A., MCLAREN, J. E., HUNTER, S., SALIM, M., MOHAMMED, F., PRICE, D. A., CHUDAKOV, D. M. & WILLCOX, B. E. 2017. Clonal selection in the human Vδ1 T cell repertoire indicates γδ TCR-dependent adaptive immune surveillance. *Nat Commun,* 8**,** 14760.

DAVIS, M. M. & BJORKMAN, P. J. 1988. T-cell antigen receptor genes and T-cell recognition. *Nature,* 334**,** 395-402.

DE LIMA MOREIRA, M., SOUTER, M. N. T., CHEN, Z., LOH, L., MCCLUSKEY, J., PELLICCI, D. G. & ECKLE, S. B. G. 2020. Hypersensitivities following allergen antigen recognition by unconventional T cells. *Allergy,* 75**,** 2477-2490.

DI PUCCHIO, T., CHATTERJEE, B., SMED-SORENSEN, A., CLAYTON, S., PALAZZO, A., MONTES, M., XUE, Y., MELLMAN, I., BANCHEREAU, J. & CONNOLLY, J. E. 2008. Direct proteasome-independent cross-presentation of viral antigen by plasmacytoid dendritic cells on major histocompatibility complex class I. *Nat Immunol,* 9**,** 551-7.

DO NASCIMENTO, N. C., GUIMARAES, A. M. S., DOS SANTOS, A. P., CHU, Y., MARQUES, L. M. & MESSICK, J. B. 2018. RNA-Seq based transcriptome of whole blood from immunocompetent pigs (Sus scrofa) experimentally infected with Mycoplasma suis strain Illinois. *Veterinary Research,* 49**,** 49.

DOHERTY, P. C., TOPHAM, D. J., TRIPP, R. A., CARDIN, R. D., BROOKS, J. W. & STEVENSON, P. G. 1997. Effector CD4+ and CD8+ T-cell mechanisms in the control of respiratory virus infections. *Immunol Rev,* 159**,** 105-17.

DONALDSON, L. J., RUTTER, P. D., ELLIS, B. M., GREAVES, F. E. C., MYTTON, O. T., PEBODY, R. G. & YARDLEY, I. E. 2009. Mortality from pandemic A/H1N1 2009 influenza in England: public health surveillance study. *BMJ,* 339**,** b5213.

DOYLE, C. & STROMINGER, J. L. 1987. Interaction between CD4 and class II MHC molecules mediates cell adhesion. *Nature,* 330**,** 256-9.

DUSSEAUX, M., MARTIN, E., SERRIARI, N., PEGUILLET, I., PREMEL, V., LOUIS, D., MILDER, M., LE BOURHIS, L., SOUDAIS, C., TREINER, E. & LANTZ, O. 2011. Human MAIT cells are xenobiotic-resistant, tissue-targeted, CD161hi IL-17-secreting T cells. *Blood,* 117**,** 1250-9.

ECKLE, S. B., BIRKINSHAW, R. W., KOSTENKO, L., CORBETT, A. J., MCWILLIAM, H. E., REANTRAGOON, R., CHEN, Z., GHERARDIN, N. A., BEDDOE, T., LIU, L., PATEL, O., MEEHAN, B., FAIRLIE, D. P., VILLADANGOS, J. A., GODFREY, D. I., KJER-NIELSEN, L., MCCLUSKEY, J. & ROSSJOHN, J. 2014. A molecular basis underpinning the T cell receptor heterogeneity of mucosal-associated invariant T cells. *J Exp Med,* 211**,** 1585-600.

ELLMEIER, W., SAWADA, S. & LITTMAN, D. R. 1999. THE REGULATION OF CD4 AND CD8 CORECEPTOR GENE EXPRESSION DURING T CELL DEVELOPMENT. *Annual Review of Immunology,* 17**,** 523-554.

FONI, E., CHIAPPONI, C., BAIONI, L., ZANNI, I., MERENDA, M., ROSIGNOLI, C., KYRIAKIS, C. S., LUINI, M. V., MANDOLA, M. L., BOLZONI, L., NIGRELLI, A. D. & FACCINI, S. 2017. Influenza D in Italy: towards a better understanding of an emerging viral infection in swine. *Scientific Reports,* 7**,** 11660.

FORBERG, H., HAUGE, A. G., VALHEIM, M., GARCON, F., NUNEZ, A., GERNER, W., MAIR, K. H., GRAHAM, S. P., BROOKES, S. M. & STORSET, A. K. 2014. Early Responses of Natural Killer Cells in Pigs Experimentally Infected with 2009 Pandemic H1N1 Influenza A Virus. *PLOS ONE,* 9**,** e100619.

FOUCHIER, R. A., MUNSTER, V., WALLENSTEN, A., BESTEBROER, T. M., HERFST, S., SMITH, D., RIMMELZWAAN, G. F., OLSEN, B. & OSTERHAUS, A. D. 2005. Characterization of a novel influenza A virus hemagglutinin subtype (H16) obtained from black-headed gulls. *J Virol,* 79**,** 2814-22.

FURIN, J., COX, H. & PAI, M. 2019. Tuberculosis. *The Lancet,* 393**,** 1642-1656.

GALANI, I. E. & ANDREAKOS, E. 2015. Neutrophils in viral infections: Current concepts and caveats. *J Leukoc Biol,* 98**,** 557-64.

GAO, W., SUN, W., QU, B., CARDONA, C. J., POWELL, K., WEGNER, M., SHI, Y. & XING, Z. 2012. Distinct Regulation of Host Responses by ERK and JNK MAP Kinases in Swine Macrophages Infected with Pandemic (H1N1) 2009 Influenza Virus. *PLOS ONE,* 7**,** e30328.

GARNER, L. C., KLENERMAN, P. & PROVINE, N. M. 2018. Insights Into Mucosal-Associated Invariant T Cell Biology From Studies of Invariant Natural Killer T Cells. *Frontiers in Immunology,* 9.

GERHARD, W., MOZDZANOWSKA, K., FURCHNER, M., WASHKO, G. & MAIESE, K. 1997. Role of the B-cell response in recovery of mice from primary influenza virus infection. *Immunological Reviews,* 159**,** 95-103.

GHERARDIN, N. A., KELLER, A. N., WOOLLEY, R. E., LE NOURS, J., RITCHIE, D. S., NEESON, P. J., BIRKINSHAW, R. W., ECKLE, S. B. G., WADDINGTON, J. N., LIU, L., FAIRLIE, D. P., ULDRICH, A. P., PELLICCI, D. G., MCCLUSKEY, J., GODFREY, D. I. & ROSSJOHN, J. 2016. Diversity of T Cells Restricted by the MHC Class I-Related Molecule MR1 Facilitates Differential Antigen Recognition. *Immunity,* 44**,** 32-45.

GHERARDIN, N. A., SOUTER, M. N., KOAY, H. F., MANGAS, K. M., SEEMANN, T., STINEAR, T. P., ECKLE, S. B., BERZINS, S. P., D'UDEKEM, Y., KONSTANTINOV, I. E., FAIRLIE, D. P., RITCHIE, D. S., NEESON, P. J., PELLICCI, D. G., ULDRICH, A. P., MCCLUSKEY, J. & GODFREY, D. I. 2018. Human blood MAIT cell subsets defined using MR1 tetramers. *Immunol Cell Biol,* 96**,** 507-525.

GIBBS, A., LEEANSYAH, E., INTROINI, A., PAQUIN-PROULX, D., HASSELROT, K., ANDERSSON, E., BROLIDEN, K., SANDBERG, J. K. & TJERNLUND, A. 2017. MAIT cells reside in the female genital mucosa and are biased towards IL-17 and IL-22 production in response to bacterial stimulation. *Mucosal immunology,* 10**,** 35-45.

GILBERT, S. C. 2013. Advances in the development of universal influenza vaccines. *Influenza Other Respir Viruses,* 7**,** 750-8.

GOLD, M. C., CERRI, S., SMYK-PEARSON, S., CANSLER, M. E., VOGT, T. M., DELEPINE, J., WINATA, E., SWARBRICK, G. M., CHUA, W.-J., YU, Y. Y. L., LANTZ, O., COOK, M. S., NULL, M. D., JACOBY, D. B., HARRIFF, M. J., LEWINSOHN, D. A., HANSEN, T. H. & LEWINSOHN, D. M. 2010. Human Mucosal Associated Invariant T Cells Detect Bacterially Infected Cells. *PLOS Biology,* 8**,** e1000407.

GOLD, M. C., MCLAREN, J. E., REISTETTER, J. A., SMYK-PEARSON, S., LADELL, K., SWARBRICK, G. M., YU, Y. Y. L., HANSEN, T. H., LUND, O., NIELSEN, M., GERRITSEN, B., KESMIR, C., MILES, J. J., LEWINSOHN, D. A., PRICE, D. A. & LEWINSOHN, D. M. 2014. MR1-restricted MAIT cells display ligand discrimination and pathogen selectivity through distinct T cell receptor usage. *Journal of Experimental Medicine,* 211**,** 1601-1610.

GOLD, M. C., NAPIER, R. J. & LEWINSOHN, D. M. 2015. MR1-restricted mucosal associated invariant T (MAIT) cells in the immune response to Mycobacterium tuberculosis. *Immunological reviews,* 264**,** 154-166.

GOLDFINCH, N., REININK, P., CONNELLEY, T., KOETS, A., MORRISON, I. & VAN RHIJN, I. 2010. Conservation of mucosal associated invariant T (MAIT) cells and the MR1 restriction element in ruminants, and abundance of MAIT cells in spleen. *Veterinary research,* 41**,** 62.

GREENE, J. M., DASH, P., ROY, S., MCMURTREY, C., AWAD, W., REED, J. S., HAMMOND, K. B., ABDULHAQQ, S., WU, H. L., BURWITZ, B. J., ROTH, B. F., MORROW, D. W., FORD, J. C., XU, G., BAE, J. Y., CRANK, H., LEGASSE, A. W., DANG, T. H., GREENAWAY, H. Y., KURNIAWAN, M., GOLD, M. C., HARRIFF, M. J., LEWINSOHN, D. A., PARK, B. S., AXTHELM, M. K., STANTON, J. J., HANSEN, S. G., PICKER, L. J., VENTURI, V., HILDEBRAND, W., THOMAS, P. G., LEWINSOHN, D. M., ADAMS, E. J. & SACHA, J. B. 2016. MR1-restricted mucosal-associated invariant T (MAIT) cells respond to mycobacterial vaccination and infection in nonhuman primates. *Mucosal Immunol*.

GREENE, J. M., DASH, P., ROY, S., MCMURTREY, C., AWAD, W., REED, J. S., HAMMOND, K. B., ABDULHAQQ, S., WU, H. L., BURWITZ, B. J., ROTH, B. F., MORROW, D. W., FORD, J. C., XU, G.,

BAE, J. Y., CRANK, H., LEGASSE, A. W., DANG, T. H., GREENAWAY, H. Y., KURNIAWAN, M., GOLD, M. C., HARRIFF, M. J., LEWINSOHN, D. A., PARK, B. S., AXTHELM, M. K., STANTON, J. J., HANSEN, S. G., PICKER, L. J., VENTURI, V., HILDEBRAND, W., THOMAS, P. G., LEWINSOHN, D. M., ADAMS, E. J. & SACHA, J. B. 2017. MR1-restricted mucosal-associated invariant T (MAIT) cells respond to mycobacterial vaccination and infection in nonhuman primates. *Mucosal immunology,* 10**,** 802-813.

GUILLAMÓN MDE, L. & CLAU, L. B. 2010. [The sheep as a large animal experimental model in respiratory diseases research]. *Arch Bronconeumol,* 46**,** 499-501.

GUTIÉRREZ-MARTÍNEZ, E., PLANÈS, R., ANSELMI, G., REYNOLDS, M., MENEZES, S., ADIKO, A. C., SAVEANU, L. & GUERMONPREZ, P. 2015. Cross-Presentation of Cell-Associated Antigens by MHC Class I in Dendritic Cell Subsets. *Frontiers in immunology,* 6**,** 363-363.

HAMADA, H., GARCIA-HERNANDEZ, M. D. L. L., REOME, J. B., MISRA, S. K., STRUTT, T. M., MCKINSTRY, K. K., COOPER, A. M., SWAIN, S. L. & DUTTON, R. W. 2009. Tc17, a Unique Subset of CD8 T Cells That Can Protect against Lethal Influenza Challenge. *The Journal of Immunology,* 182**,** 3469-3481.

HARP, J. A., WATERS, T. E. & GOFF, J. P. 2004. Lymphocyte subsets and adhesion molecule expression in milk and blood of periparturient dairy cattle. *Veterinary Immunology and Immunopathology,* 102**,** 9-17.

HARRIS, K. A., BROUWER, A., UPTON, P. A., ROMERO GARCIA, M. P., GIBBENS, J. C. & DALE, J. 2018. Bovine TB infection status in Great Britain in 2016. *Veterinary Record,* 182**,** 538-544.

HARTY, J. T., TVINNEREIM, A. R. & WHITE, D. W. 2000. CD8+ T Cell Effector Mechanisms in Resistance to Infection. *Annual Review of Immunology,* 18**,** 275-308.

HASHIMOTO, K., HIRAI, M. & KUROSAWA, Y. 1995. A gene outside the human MHC related to classical HLA class I genes. *Science,* 269**,** 693.

HASHIMOTO, Y., MOKI, T., TAKIZAWA, T., SHIRATSUCHI, A. & NAKANISHI, Y. 2007. Evidence for Phagocytosis of Influenza Virus-Infected, Apoptotic Cells by Neutrophils and Macrophages in Mice. *The Journal of Immunology,* 178**,** 2448.

HAUSE, B. M., COLLIN, E. A., LIU, R., HUANG, B., SHENG, Z., LU, W., WANG, D., NELSON, E. A. & LI, F. 2014. Characterization of a Novel Influenza Virus in Cattle and Swine: Proposal for a New Genus in the Orthomyxoviridae Family. *mBio,* 5**,** e00031-14.

HAUSE, B. M., DUCATEZ, M., COLLIN, E. A., RAN, Z., LIU, R., SHENG, Z., ARMIEN, A., KAPLAN, B., CHAKRAVARTY, S., HOPPE, A. D., WEBBY, R. J., SIMONSON, R. R. & LI, F. 2013. Isolation of a novel swine influenza virus from Oklahoma in 2011 which is distantly related to human influenza C viruses. *PLoS pathogens,* 9**,** e1003176-e1003176.

HAYWARD, A. C., WANG, L., GOONETILLEKE, N., FRAGASZY, E. B., BERMINGHAM, A., COPAS, A., DUKES, O., MILLETT, E. R., NAZARETH, I., NGUYEN-VAN-TAM, J. S., WATSON, J. M., ZAMBON, M., FLU WATCH, G., JOHNSON, A. M. & MCMICHAEL, A. J. 2015. Natural T Cell-mediated Protection against Seasonal and Pandemic Influenza. Results of the Flu Watch Cohort Study. *Am J Respir Crit Care Med,* 191**,** 1422-31.

HEIN, W. R. & MACKAY, C. R. 1991. Prominence of γδ T cells in the ruminant immune system. *Immunology Today,* 12**,** 30-34.

HELD, K., BHONSLE-DEENG, L., SIEWERT, K., SATO, W., BELTRÁN, E., SCHMIDT, S., RÜHL, G., NG, J. K. M., ENGERER, P., MOSER, M., KLINKERT, W. E. F., BABBE, H., MISGELD, T., WEKERLE, H., LAPLAUD, D.-A., HOHLFELD, R. & DORNMAIR, K. 2015. αβ T-cell receptors from multiple sclerosis brain lesions show MAIT cell-related features. *Neurology(R) neuroimmunology & neuroinflammation,* 2**,** e107-e107.

HENGST, J., STRUNZ, B., DETERDING, K., LJUNGGREN, H.-G., LEEANSYAH, E., MANNS, M. P., CORNBERG, M., SANDBERG, J. K., WEDEMEYER, H. & BJÖRKSTRÖM, N. K. 2016. Nonreversible MAIT cell-dysfunction in chronic hepatitis C virus infection despite successful interferon-free therapy. *European Journal of Immunology,* 46**,** 2204-2210.

HEWITT, E. W. 2003. The MHC class I antigen presentation pathway: strategies for viral immune evasion. *Immunology,* 110**,** 163-169.

HINKS, T. S. C., MARCHI, E., JABEEN, M., OLSHANSKY, M., KURIOKA, A., PEDIONGCO, T. J., MEEHAN, B. S., KOSTENKO, L., TURNER, S. J., CORBETT, A. J., CHEN, Z., KLENERMAN, P. & MCCLUSKEY, J. 2019. Activation and In Vivo Evolution of the MAIT Cell Transcriptome in Mice and Humans Reveals Tissue Repair Functionality. *Cell Rep,* 28**,** 3249-3262 e5.

HINKS, T. S. C. & ZHANG, X.-W. 2020. MAIT Cell Activation and Functions. *Frontiers in Immunology,* 11.

HOLZER, B., MARTINI, V., EDMANS, M. & TCHILIAN, E. 2019a. T and B Cell Immune Responses to Influenza Viruses in Pigs. *Frontiers in Immunology,* 10.

HOLZER, B., MORGAN, S. B., MARTINI, V., SHARMA, R., CLARK, B., CHIU, C., SALGUERO, F. J. & TCHILIAN, E. 2019b. Immunogenicity and Protective Efficacy of Seasonal Human Live Attenuated Cold-Adapted Influenza Virus Vaccine in Pigs. *Frontiers in Immunology,* 10.

HOLZER, B., MORGAN, S. B., MATSUOKA, Y., EDMANS, M., SALGUERO, F. J., EVERETT, H., BROOKES, S. M., PORTER, E., MACLOUGHLIN, R., CHARLESTON, B., SUBBARAO, K., TOWNSEND, A. & TCHILIAN, E. 2018a. Comparison of Heterosubtypic Protection in Ferrets and Pigs Induced by a Single-Cycle Influenza Vaccine. *J Immunol,* 200**,** 4068-4077.

HOLZER, B., MORGAN, S. B., MATSUOKA, Y., EDMANS, M., SALGUERO, F. J., EVERETT, H., BROOKES, S. M., PORTER, E., MACLOUGHLIN, R., CHARLESTON, B., SUBBARAO, K., TOWNSEND, A. & TCHILIAN, E. 2018b. Comparison of Heterosubtypic Protection in Ferrets and Pigs Induced by a Single-Cycle Influenza Vaccine. *J Immunol*.

HOLZER, B., MORGAN, S. B., MATSUOKA, Y., EDMANS, M., SALGUERO, F. J., EVERETT, H., BROOKES, S. M., PORTER, E., MACLOUGHLIN, R., CHARLESTON, B., SUBBARAO, K., TOWNSEND, A. & TCHILIAN, E. 2018c. Comparison of Heterosubtypic Protection in Ferrets and Pigs Induced by a Single-Cycle Influenza Vaccine. *The Journal of Immunology,* 200**,** 4068.

HOWSON, L. J., AWAD, W., VON BORSTEL, A., LIM, H. J., MCWILLIAM, H. E. G., SANDOVAL-ROMERO, M. L., MAJUMDAR, S., HAMZEH, A. R., ANDREWS, T. D., MCDERMOTT, D. H., MURPHY, P. M., LE NOURS, J., MAK, J. Y. W., LIU, L., FAIRLIE, D. P., MCCLUSKEY, J., VILLADANGOS, J. A., COOK, M. C., TURNER, S. J., DAVEY, M. S., OJAIMI, S. & ROSSJOHN, J. 2020. Absence of mucosal-associated invariant T cells in a person with a homozygous point mutation in MR1. *Science Immunology,* 5**,** eabc9492.

HUANG, S., GILFILLAN, S., CELLA, M., MILEY, M. J., LANTZ, O., LYBARGER, L., FREMONT, D. H. & HANSEN, T. H. 2005. Evidence for MR1 antigen presentation to mucosal-associated invariant T cells. *J Biol Chem,* 280**,** 21183-93.

HUANG, S., MARTIN, E., KIM, S., YU, L., SOUDAIS, C., FREMONT, D. H., LANTZ, O. & HANSEN, T. H. 2009. MR1 antigen presentation to mucosal-associated invariant T cells was highly conserved in evolution. *Proc Natl Acad Sci U S A,* 106**,** 8290-5.

HUSSELL, T. & BELL, T. J. 2014. Alveolar macrophages: plasticity in a tissue-specific context. *Nat Rev Immunol,* 14**,** 81-93.

HWANG, I., SCOTT, J. M., KAKARLA, T., DURIANCIK, D. M., CHOI, S., CHO, C., LEE, T., PARK, H., FRENCH, A. R., BELI, E., GARDNER, E. & KIM, S. 2013. Activation Mechanisms of Natural Killer Cells during Influenza Virus Infection. *PLOS ONE,* 7**,** e51858.

ICHINOHE, T., YAMAZAKI, T., KOSHIBA, T. & YANAGI, Y. 2013. Mitochondrial protein mitofusin 2 is required for NLRP3 inflammasome activation after RNA virus infection. *Proc Natl Acad Sci U S A,* 110**,** 17963-8.

JAMESON, J., UGARTE, K., CHEN, N., YACHI, P., FUCHS, E., BOISMENU, R. & HAVRAN, W. L. 2002. A role for skin gammadelta T cells in wound repair. *Science,* 296**,** 747-9.

JANKE, B. H. 2014. Influenza A virus infections in swine: pathogenesis and diagnosis. *Vet Pathol,* 51**,** 410-26.

JOSÉ, E. S., BORROTO, A., NIEDERGANG, F., ALCOVER, A. & ALARCÓN, B. 2000. Triggering the TCR Complex Causes the Downregulation of Nonengaged Receptors by a Signal Transduction-Dependent Mechanism. *Immunity,* 12**,** 161-170.

JUNO, J. A., WRAGG, K. M., AMARASENA, T., MEEHAN, B. S., MAK, J. Y. W., LIU, L., FAIRLIE, D. P., MCCLUSKEY, J., ECKLE, S. B. G. & KENT, S. J. 2019. MAIT Cells Upregulate α4β7 in Response to Acute Simian Immunodeficiency Virus/Simian HIV Infection but Are Resistant to Peripheral Depletion in Pigtail Macaques. *The Journal of Immunology,* 202**,** 2105.

KAUFFMAN, K. D., SALLIN, M. A., HOFT, S. G., SAKAI, S., MOORE, R., WILDER-KOFIE, T., MOORE, I. N., SETTE, A., ARLEHAMN, C. S. L. & BARBER, D. L. 2018. Limited Pulmonary Mucosal-Associated Invariant T Cell Accumulation and Activation during Mycobacterium tuberculosis Infection in Rhesus Macaques. *Infection and immunity,* 86**,** e00431-18.

KEANE, O. M. 2019. Symposium review: Intramammary infections-Major pathogens and strain-associated complexity. *J Dairy Sci,* 102**,** 4713-4726.

KELLER, A. N., ECKLE, S. B., XU, W., LIU, L., HUGHES, V. A., MAK, J. Y., MEEHAN, B. S., PEDIONGCO, T., BIRKINSHAW, R. W., CHEN, Z., WANG, H., D'SOUZA, C., KJER-NIELSEN, L., GHERARDIN, N. A., GODFREY, D. I., KOSTENKO, L., CORBETT, A. J., PURCELL, A. W., FAIRLIE, D. P., MCCLUSKEY, J. & ROSSJOHN, J. 2017. Drugs and drug-like molecules can modulate the function of mucosal-associated invariant T cells. *Nat Immunol,* 18**,** 402-411.

KHATRI, M., DWIVEDI, V., KRAKOWKA, S., MANICKAM, C., ALI, A., WANG, L., QIN, Z., RENUKARADHYA, G. J. & LEE, C.-W. 2010. Swine Influenza H1N1 Virus Induces Acute Inflammatory Immune Responses in Pig Lungs: a Potential Animal Model for Human H1N1 Influenza Virus. *Journal of Virology,* 84**,** 11210-11218.

KILLIP, M. J., FODOR, E. & RANDALL, R. E. 2015. Influenza virus activation of the interferon system. *Virus Res,* 209**,** 11-22.

KIM, B., SHIN, J. H., HAN, K., SEO, H. W., OH, Y., KANG, I., PARK, C., LEE, B. H., JANG, J. S., KIM, S. H. & CHAE, C. 2011. Expression of myeloperoxidase in swine influenza virus (SIV)-infected neutrophils in lungs from pigs experimentally infected with SIV subtype H1N2. *Vet Res Commun,* 35**,** 469-75.

KIM, H. M., LEE, Y. W., LEE, K. J., KIM, H. S., CHO, S. W., VAN ROOIJEN, N., GUAN, Y. & SEO, S. H. 2008. Alveolar macrophages are indispensable for controlling influenza viruses in lungs of pigs. *J Virol,* 82**,** 4265-74.

KJER-NIELSEN, L., PATEL, O., CORBETT, A. J., LE NOURS, J., MEEHAN, B., LIU, L., BHATI, M., CHEN, Z., KOSTENKO, L., REANTRAGOON, R., WILLIAMSON, N. A., PURCELL, A. W., DUDEK, N. L., MCCONVILLE, M. J., O'HAIR, R. A. J., KHAIRALLAH, G. N., GODFREY, D. I., FAIRLIE, D. P., ROSSJOHN, J. & MCCLUSKEY, J. 2012. MR1 presents microbial vitamin B metabolites to MAIT cells. *Nature,* 491**,** 717-723.

KOAY, H.-F., GHERARDIN, N. A., ENDERS, A., LOH, L., MACKAY, L. K., ALMEIDA, C. F., RUSS, B. E., NOLD-PETRY, C. A., NOLD, M. F., BEDOUI, S., CHEN, Z., CORBETT, A. J., ECKLE, S. B. G., MEEHAN, B., D'UDEKEM, Y., KONSTANTINOV, I. E., LAPPAS, M., LIU, L., GOODNOW, C. C., FAIRLIE, D. P., ROSSJOHN, J., CHONG, M. M., KEDZIERSKA, K., BERZINS, S. P., BELZ, G. T., MCCLUSKEY, J., ULDRICH, A. P., GODFREY, D. I. & PELLICCI, D. G. 2016a. A three-stage intrathymic development pathway for the mucosal-associated invariant T cell lineage. *Nature Immunology,* 17**,** 1300-1311.

KOAY, H.-F., GODFREY, D. I. & PELLICCI, D. G. 2018. Development of mucosal-associated invariant T cells. *Immunology and Cell Biology,* 96**,** 598-606.

KOAY, H. F., GHERARDIN, N. A., ENDERS, A., LOH, L., MACKAY, L. K., ALMEIDA, C. F., RUSS, B. E., NOLD-PETRY, C. A., NOLD, M. F., BEDOUI, S., CHEN, Z., CORBETT, A. J., ECKLE, S. B., MEEHAN, B., D'UDEKEM, Y., KONSTANTINOV, I. E., LAPPAS, M., LIU, L., GOODNOW, C. C., FAIRLIE, D. P., ROSSJOHN, J., CHONG, M. M., KEDZIERSKA, K., BERZINS, S. P., BELZ, G. T., MCCLUSKEY, J., ULDRICH, A. P., GODFREY, D. I. & PELLICCI, D. G. 2016b. A three-stage intrathymic development pathway for the mucosal-associated invariant T cell lineage. *Nat Immunol,* 17**,** 1300-1311.

KOAY, H. F., GHERARDIN, N. A., XU, C., SENEVIRATNA, R., ZHAO, Z., CHEN, Z., FAIRLIE, D. P., MCCLUSKEY, J., PELLICCI, D. G., ULDRICH, A. P. & GODFREY, D. I. 2019. Diverse MR1-restricted T cells in mice and humans. *Nat Commun,* 10**,** 2243.

KORKMAZ, B., MOREAU, T. & GAUTHIER, F. 2008. Neutrophil elastase, proteinase 3 and cathepsin G: physicochemical properties, activity and physiopathological functions. *Biochimie,* 90**,** 227-42.

KOUTSAKOS, M., ILLING, P. T., NGUYEN, T. H. O., MIFSUD, N. A., CRAWFORD, J. C., RIZZETTO, S., ELTAHLA, A. A., CLEMENS, E. B., SANT, S., CHUA, B. Y., WONG, C. Y., ALLEN, E. K., TENG, D., DASH, P., BOYD, D. F., GRZELAK, L., ZENG, W., HURT, A. C., BARR, I., ROCKMAN, S., JACKSON, D. C., KOTSIMBOS, T. C., CHENG, A. C., RICHARDS, M., WESTALL, G. P., LOUDOVARIS, T., MANNERING, S. I., ELLIOTT, M., TANGYE, S. G., WAKIM, L. M., ROSSJOHN, J., VIJAYKRISHNA, D., LUCIANI, F., THOMAS, P. G., GRAS, S., PURCELL, A. W. & KEDZIERSKA, K. 2019. Human CD8+ T cell cross-reactivity across influenza A, B and C viruses. *Nature Immunology,* 20**,** 613-625.

KRAMMER, F., SMITH, G. J. D., FOUCHIER, R. A. M., PEIRIS, M., KEDZIERSKA, K., DOHERTY, P. C., PALESE, P., SHAW, M. L., TREANOR, J., WEBSTER, R. G. & GARCÍA-SASTRE, A. 2018. Influenza. *Nature Reviews Disease Primers,* 4**,** 3.

KREIJTZ, J. H. C. M., FOUCHIER, R. A. M. & RIMMELZWAAN, G. F. 2011. Immune responses to influenza virus infection. *Virus Research,* 162**,** 19-30.

KÜHL, A. A., PAWLOWSKI, N. N., GROLLICH, K., BLESSENOHL, M., WESTERMANN, J., ZEITZ, M., LODDENKEMPER, C. & HOFFMANN, J. C. 2009. Human peripheral γδ T cells possess regulatory potential. *Immunology,* 128**,** 580-588.

KURIOKA, A., WALKER, L. J., KLENERMAN, P. & WILLBERG, C. B. 2016. MAIT cells: new guardians of the liver. *Clinical & Translational Immunology,* 5**,** e98.

LAIDLAW, B. J., DECMAN, V., ALI, M.-A. A., ABT, M. C., WOLF, A. I., MONTICELLI, L. A., MOZDZANOWSKA, K., ANGELOSANTO, J. M., ARTIS, D., ERIKSON, J. & WHERRY, E. J. 2013. Cooperativity Between CD8+ T Cells, Non-Neutralizing Antibodies, and Alveolar Macrophages Is Important for Heterosubtypic Influenza Virus Immunity. *PLOS Pathogens,* 9**,** e1003207.

LAMICHHANE, R., SCHNEIDER, M., DE LA HARPE, S. M., HARROP, T. W. R., HANNAWAY, R. F., DEARDEN, P. K., KIRMAN, J. R., TYNDALL, J. D. A., VERNALL, A. J. & USSHER, J. E. 2019. TCR- or Cytokine-Activated CD8⁺ Mucosal-Associated Invariant T Cells Are Rapid Polyfunctional Effectors That Can Coordinate Immune Responses. *Cell Reports,* 28**,** 3061-3076.e5.

LAOUAR, A. 2020. Maternal Leukocytes and Infant Immune Programming during Breastfeeding. *Trends in Immunology,* 41**,** 225-239.

LE BOURHIS, L., MARTIN, E., PEGUILLET, I., GUIHOT, A., FROUX, N., CORE, M., LEVY, E., DUSSEAUX, M., MEYSSONNIER, V., PREMEL, V., NGO, C., RITEAU, B., DUBAN, L., ROBERT, D., HUANG, S., ROTTMAN, M., SOUDAIS, C. & LANTZ, O. 2010. Antimicrobial activity of mucosal-associated invariant T cells. *Nat Immunol,* 11**,** 701-8.

LE GOFFIC, R., POTHLICHET, J., VITOUR, D., FUJITA, T., MEURS, E., CHIGNARD, M. & SI-TAHAR, M. 2007. Cutting Edge: Influenza A virus activates TLR3-dependent inflammatory and RIG-I-dependent antiviral responses in human lung epithelial cells. *J Immunol,* 178**,** 3368-72.

LE NOURS, J., GHERARDIN, N. A., RAMARATHINAM, S. H., AWAD, W., WIEDE, F., GULLY, B. S., KHANDOKAR, Y., PRAVEENA, T., WUBBEN, J. M., SANDOW, J. J., WEBB, A. I., VON BORSTEL, A., RICE, M. T., REDMOND, S. J., SENEVIRATNA, R., SANDOVAL-ROMERO, M. L., LI, S., SOUTER, M. N. T., ECKLE, S. B. G., CORBETT, A. J., REID, H. H., LIU, L., FAIRLIE, D. P., GILES, E. M., WESTALL, G. P., TOTHILL, R. W., DAVEY, M. S., BERRY, R., TIGANIS, T., MCCLUSKEY, J., PELLICCI, D. G., PURCELL, A. W., ULDRICH, A. P., GODFREY, D. I. & ROSSJOHN, J. 2019. A class of gammadelta T cell receptors recognize the underside of the antigen-presenting molecule MR1. *Science,* 366**,** 1522-1527.

LEEANSYAH, E., GANESH, A., QUIGLEY, M. F., SÖNNERBORG, A., ANDERSSON, J., HUNT, P. W., SOMSOUK, M., DEEKS, S. G., MARTIN, J. N., MOLL, M., SHACKLETT, B. L. & SANDBERG, J. K. 2013. Activation, exhaustion, and persistent decline of the antimicrobial MR1-restricted MAIT-cell population in chronic HIV-1 infection. *Blood,* 121**,** 1124-1135.

LEFEVRE, E. A., CARR, B. V., INMAN, C. F., PRENTICE, H., BROWN, I. H., BROOKES, S. M., GARCON, F., HILL, M. L., IQBAL, M., ELDERFIELD, R. A., BARCLAY, W. S., GUBBINS, S., BAILEY, M., CHARLESTON, B. & COSI 2012. Immune Responses in Pigs Vaccinated with Adjuvanted and Non-Adjuvanted A(H1N1)pdm/09 Influenza Vaccines Used in Human Immunization Programmes. *PLOS ONE,* 7**,** e32400.

LEMAITRE, B., NICOLAS, E., MICHAUT, L., REICHHART, J. M. & HOFFMANN, J. A. 1996. The dorsoventral regulatory gene cassette spätzle/Toll/cactus controls the potent antifungal response in Drosophila adults. *Cell,* 86**,** 973-83.

LENG, T., AKTHER, H. D., HACKSTEIN, C.-P., POWELL, K., KING, T., FRIEDRICH, M., CHRISTOFORIDOU, Z., MCCUAIG, S., NEYAZI, M., ARANCIBIA-CÁRCAMO, C. V., HAGEL, J., POWRIE, F., PERES, R. S., MILLAR, V., EBNER, D., LAMICHHANE, R., USSHER, J., HINKS, T. S. C., MARCHI, E., WILLBERG, C. & KLENERMAN, P. 2019. TCR and Inflammatory Signals Tune Human MAIT Cells to Exert Specific Tissue Repair and Effector Functions. *Cell Reports,* 28**,** 3077-3091.e5.

LEPORE, M., KALINICHENKO, A., COLONE, A., PALEJA, B., SINGHAL, A., TSCHUMI, A., LEE, B., POIDINGER, M., ZOLEZZI, F., QUAGLIATA, L., SANDER, P., NEWELL, E., BERTOLETTI, A., TERRACCIANO, L., DE LIBERO, G. & MORI, L. 2014. Parallel T-cell cloning and deep sequencing of human MAIT cells reveal stable oligoclonal TCRβ repertoire. *Nat Commun,* 5**,** 3866.

LI, Y., LIU, H., WANG, P., WANG, L., SUN, Y., LIU, G., ZHANG, P., KANG, L., JIANG, S. & JIANG, Y. 2016. RNA-Seq Analysis Reveals Genes Underlying Different Disease Responses to Porcine Circovirus Type 2 in Pigs. *PLoS One,* 11**,** e0155502.

LICHTERFELD, M., YU, X. G., WARING, M. T., MUI, S. K., JOHNSTON, M. N., COHEN, D., ADDO, M. M., ZAUNDERS, J., ALTER, G., PAE, E., STRICK, D., ALLEN, T. M., ROSENBERG, E. S., WALKER, B. D. & ALTFELD, M. 2004. HIV-1–specific cytotoxicity is preferentially mediated by a subset of CD8+ T cells producing both interferon-γ and tumor necrosis factor–α. *Blood,* 104**,** 487-494.

LINEHAN, J. L., HARRISON, O. J., HAN, S.-J., BYRD, A. L., VUJKOVIC-CVIJIN, I., VILLARINO, A. V., SEN, S. K., SHAIK, J., SMELKINSON, M., TAMOUTOUNOUR, S., COLLINS, N., BOULADOUX, N., DZUTSEV, A., ROSSHART, S. P., ARBUCKLE, J. H., WANG, C.-R., KRISTIE, T. M., REHERMANN, B., TRINCHIERI, G., BRENCHLEY, J. M., O'SHEA, J. J. & BELKAID, Y. 2018. Non-classical Immunity Controls Microbiota Impact on Skin Immunity and Tissue Repair. *Cell,* 172**,** 784-796.e18.

LIU, Y., ZHENG, J., LIU, Y., WEN, L., HUANG, L., XIANG, Z., LAM, K. T., LV, A., MAO, H., LAU, Y. L. & TU, W. 2017. Uncompromised NK cell activation is essential for virus-specific CTL activity during acute influenza virus infection. *Cell Mol Immunol*.

LOH, L., WANG, Z. F., SANT, S., KOUTSAKOS, M., JEGASKANDA, S., CORBETT, A. J., LIU, L. G., FAIRLIE, D. P., CROWE, J., ROSSJOHN, J., XU, J. Q., DOHERTY, P. C., MCCLUSKEY, J. & KEDZIERSKA, K. 2016. Human mucosal-associated invariant T cells contribute to antiviral influenza immunity via IL-18-dependent activation. *Proceedings of the National Academy of Sciences of the United States of America,* 113**,** 10133-10138.

LOORINGH VAN BEECK, F. A., REININK, P., HERMSEN, R., ZAJONC, D. M., LAVEN, M. J., FUN, A., TROSKIE, M., SCHOEMAKER, N. J., MORAR, D., LENSTRA, J. A., VERVELDE, L., RUTTEN, V. P., VAN EDEN, W. & VAN RHIJN, I. 2009a. Functional CD1d and/or NKT cell invariant chain transcript in horse, pig, African elephant and guinea pig, but not in ruminants. *Mol Immunol,* 46**,** 1424-31.

LOORINGH VAN BEECK, F. A., REININK, P., HERMSEN, R., ZAJONC, D. M., LAVEN, M. J., FUN, A., TROSKIE, M., SCHOEMAKER, N. J., MORAR, D., LENSTRA, J. A., VERVELDE, L., RUTTEN, V. P. M. G., VAN EDEN, W. & VAN RHIJN, I. 2009b. Functional CD1d and/or NKT cell invariant chain transcript in horse, pig, African elephant and guinea pig, but not in ruminants. *Molecular immunology,* 46**,** 1424-1431.

LOPEZ-SAGASETA, J., DULBERGER, C. L., CROOKS, J. E., PARKS, C. D., LUOMA, A. M., MCFEDRIES, A., VAN RHIJN, I., SAGHATELIAN, A. & ADAMS, E. J. 2013. The molecular basis for Mucosal-Associated Invariant T cell recognition of MR1 proteins. *Proceedings of the National Academy of Sciences of the United States of America,* 110**,** E1771-E1778.

LÓPEZ-SAGASETA, J., DULBERGER, C. L., MCFEDRIES, A., CUSHMAN, M., SAGHATELIAN, A. & ADAMS, E. J. 2013. MAIT Recognition of a Stimulatory Bacterial Antigen Bound to MR1. *The Journal of Immunology*, 1301958.

LUBER, C. A., COX, J., LAUTERBACH, H., FANCKE, B., SELBACH, M., TSCHOPP, J., AKIRA, S., WIEGAND, M., HOCHREIN, H., O'KEEFFE, M. & MANN, M. 2010. Quantitative proteomics reveals subset-specific viral recognition in dendritic cells. *Immunity,* 32**,** 279-89.

MACCARI, G., ROBINSON, J., BALLINGALL, K., GUETHLEIN, L. A., GRIMHOLT, U., KAUFMAN, J., HO, C. S., DE GROOT, N. G., FLICEK, P., BONTROP, R. E., HAMMOND, J. A. & MARSH, S. G. 2017. IPD-MHC 2.0: an improved inter-species database for the study of the major histocompatibility complex. *Nucleic Acids Res,* 45**,** D860-d864.

MAGGI, E. 1998. The TH1/TH2 paradigm in allergy. *Immunotechnology,* 3**,** 233-44.

MAIR, K. H., STADLER, M., TALKER, S. C., FORBERG, H., STORSET, A. K., MULLEBNER, A., DUVIGNEAU, J. C., HAMMER, S. E., SAALMULLER, A. & GERNER, W. 2016. Porcine CD3(+)NKp46(+) Lymphocytes Have NK-Cell Characteristics and Are Present in Increased Frequencies in the Lungs of Influenza-Infected Animals. *Front Immunol,* 7**,** 263.

MAISONNASSE, P., BOUGUYON, E., PITON, G., EZQUERRA, A., URIEN, C., DELOIZY, C., BOURGE, M., LEPLAT, J. J., SIMON, G., CHEVALIER, C., VINCENT-NAULLEAU, S., CRISCI, E., MONTOYA, M., SCHWARTZ-CORNIL, I. & BERTHO, N. 2016. The respiratory DC/macrophage network at steady-state and upon influenza infection in the swine biomedical model. *Mucosal Immunol,* 9**,** 835-49.

MAK, J. Y. W., XU, W., REID, R. C., CORBETT, A. J., MEEHAN, B. S., WANG, H., CHEN, Z., ROSSJOHN, J., MCCLUSKEY, J., LIU, L. & FAIRLIE, D. P. 2017. Stabilizing short-lived Schiff base derivatives of 5-aminouracils that activate mucosal-associated invariant T cells. *Nature communications,* 8**,** 14599-14599.

MALIK, G. & ZHOU, Y. 2020. Innate Immune Sensing of Influenza A Virus. *Viruses,* 12**,** 755.

MANDELBOIM, O., LIEBERMAN, N., LEV, M., PAUL, L., ARNON, T. I., BUSHKIN, Y., DAVIS, D. M., STROMINGER, J. L., YEWDELL, J. W. & PORGADOR, A. 2001. Recognition of haemagglutinins on virus-infected cells by NKp46 activates lysis by human NK cells. *Nature,* 409**,** 1055-60.

MAO, H., TU, W., QIN, G., LAW, H. K., SIA, S. F., CHAN, P. L., LIU, Y., LAM, K. T., ZHENG, J., PEIRIS, M. & LAU, Y. L. 2009. Influenza virus directly infects human natural killer cells and induces cell apoptosis. *J Virol,* 83**,** 9215-22.

MARTIN, E., TREINER, E., DUBAN, L., GUERRI, L., LAUDE, H., TOLY, C., PREMEL, V., DEVYS, A., MOURA, I. C., TILLOY, F., CHERIF, S., VERA, G., LATOUR, S., SOUDAIS, C. & LANTZ, O. 2009. Stepwise Development of MAIT Cells in Mouse and Human. *PLOS Biology,* 7**,** e1000054.

MARTINI, V., PAUDYAL, B., CHRUN, T., MCNEE, A., EDMANS, M., MAZE, E., CLARK, B., NUNEZ, A., DOLTON, G., SEWELL, A., BEVERLEY, P., MACLOUGHLIN, R., TOWNSEND, A. & TCHILIAN, E. 2020. Simultaneous aerosol and intra-muscular immunization with influenza vaccine induces powerful protective local T cell and systemic Ab immune responses in pigs. *bioRxiv*, 2020.09.10.291625.

MATSUZAKI, Y., KATSUSHIMA, N., NAGAI, Y., SHOJI, M., ITAGAKI, T., SAKAMOTO, M., KITAOKA, S., MIZUTA, K. & NISHIMURA, H. 2006. Clinical features of influenza C virus infection in children. *J Infect Dis,* 193**,** 1229-35.

MCGILL, J. L., SACCO, R. E., BALDWIN, C. L., TELFER, J. C., PALMER, M. V. & RAY WATERS, W. 2014. The role of gamma delta T cells in immunity to Mycobacterium bovis infection in cattle. *Veterinary Immunology and Immunopathology,* 159**,** 133-143.

MCKINSTRY, K. K., STRUTT, T. M., KUANG, Y., BROWN, D. M., SELL, S., DUTTON, R. W. & SWAIN, S. L. 2012. Memory CD4+ T cells protect against influenza through multiple synergizing mechanisms. *The Journal of clinical investigation,* 122**,** 2847-2856.

MCMICHAEL, A. J., GOTCH, F. M., NOBLE, G. R. & BEARE, P. A. 1983. Cytotoxic T-cell immunity to influenza. *N Engl J Med,* 309**,** 13-7.

MCWILLIAM, H. E., ECKLE, S. B., THEODOSSIS, A., LIU, L., CHEN, Z., WUBBEN, J. M., FAIRLIE, D. P., STRUGNELL, R. A., MINTERN, J. D., MCCLUSKEY, J., ROSSJOHN, J. & VILLADANGOS, J. A. 2016. The intracellular pathway for the presentation of vitamin B-related antigens by the antigen-presenting molecule MR1. *Nat Immunol,* 17**,** 531-7.

MEDZHITOV, R. & JANEWAY, C. A., JR. 1997. Innate immunity: the virtues of a nonclonal system of recognition. *Cell,* 91**,** 295-8.

MEIEROVICS, A., YANKELEVICH, W.-J. C. & COWLEY, S. C. 2013. MAIT cells are critical for optimal mucosal immune responses during in vivo pulmonary bacterial infection. *Proceedings of the National Academy of Sciences of the United States of America,* 110**,** E3119-E3128.

MENA, I., NELSON, M. I., QUEZADA-MONROY, F., DUTTA, J., CORTES-FERNÁNDEZ, R., LARA-PUENTE, J. H., CASTRO-PERALTA, F., CUNHA, L. F., TROVÃO, N. S., LOZANO-DUBERNARD, B., RAMBAUT, A., VAN BAKEL, H. & GARCÍA-SASTRE, A. 2016. Origins of the 2009 H1N1 influenza pandemic in swine in Mexico. *eLife,* 5**,** e16777.

MEUTER, S., EBERL, M. & MOSER, B. 2010. Prolonged antigen survival and cytosolic export in cross-presenting human γδ T cells. *Proc Natl Acad Sci U S A,* 107**,** 8730-5.

MILEY, M. J., TRUSCOTT, S. M., YU, Y. Y., GILFILLAN, S., FREMONT, D. H., HANSEN, T. H. & LYBARGER, L. 2003. Biochemical features of the MHC-related protein 1 consistent with an immunological function. *J Immunol,* 170**,** 6090-8.

MIOSSEC, P., KORN, T. & KUCHROO, V. K. 2009. Interleukin-17 and Type 17 Helper T Cells. *New England Journal of Medicine,* 361**,** 888-898.

MORGAN, S. B., HEMMINK, J. D., PORTER, E., HARLEY, R., SHELTON, H., ARAMOUNI, M., EVERETT, H. E., BROOKES, S. M., BAILEY, M., TOWNSEND, A. M., CHARLESTON, B. & TCHILIAN, E. 2016. Aerosol Delivery of a Candidate Universal Influenza Vaccine Reduces Viral Load in Pigs Challenged with Pandemic H1N1 Virus. *Journal of Immunology,* 196**,** 5014-5023.

MOZDZANOWSKA, K., FURCHNER, M., MAIESE, K. & GERHARD, W. 1997. CD4+T Cells Are Ineffective in Clearing a Pulmonary Infection with Influenza Type A Virus in the Absence of B Cells. *Virology,* 239**,** 217-225.

MULCAHY, M. E. & MCLOUGHLIN, R. M. 2016. Staphylococcus aureus and Influenza A Virus: Partners in Coinfection. *mBio,* 7**,** e02068-16.

NGUYEN, T. K. A., KOETS, A. P., VORDERMEIER, M., JERVIS, P. J., COX, L. R., GRAHAM, S. P., SANTEMA, W. J., MOODY, D. B., VAN CALENBERGH, S., ZAJONC, D. M., BESRA, G. S. & VAN RHIJN, I. 2013. The bovine CD1D gene has an unusual gene structure and is expressed but cannot present α-galactosylceramide with a C26 fatty acid. *International immunology,* 25**,** 91-98.

OZINSKY, A., UNDERHILL, D. M., FONTENOT, J. D., HAJJAR, A. M., SMITH, K. D., WILSON, C. B., SCHROEDER, L. & ADEREM, A. 2000. The repertoire for pattern recognition of pathogens by the innate immune system is defined by cooperation between toll-like receptors. *Proc Natl Acad Sci U S A,* 97**,** 13766-71.

PAAPE, M. J., BANNERMAN, D. D., ZHAO, X. & LEE, J. W. 2003. The bovine neutrophil: Structure and function in blood and milk. *Vet Res,* 34**,** 597-627.

PANG, I. K. & IWASAKI, A. 2011. Inflammasomes as mediators of immunity against influenza virus. *Trends Immunol,* 32**,** 34-41.

PATEL, O., KJER-NIELSEN, L., LE NOURS, J., ECKLE, S. B., BIRKINSHAW, R., BEDDOE, T., CORBETT, A. J., LIU, L., MILES, J. J., MEEHAN, B., REANTRAGOON, R., SANDOVAL-ROMERO, M. L., SULLIVAN, L. C., BROOKS, A. G., CHEN, Z., FAIRLIE, D. P., MCCLUSKEY, J. & ROSSJOHN, J. 2013. Recognition of vitamin B metabolites by mucosal-associated invariant T cells. *Nat Commun,* 4**,** 2142.

PAUZA, C. D. & CAIRO, C. 2015. Evolution and function of the TCR Vgamma9 chain repertoire: It's good to be public. *Cellular Immunology,* 296**,** 22-30.

PEDERSEN, L. E., BREUM, S. Ø., RIBER, U., LARSEN, L. E. & JUNGERSEN, G. 2014. Identification of swine influenza virus epitopes and analysis of multiple specificities expressed by cytotoxic T cell subsets. *Virology Journal,* 11**,** 163.

PELSMAEKER, S., DEVRIENDT, B., LECLERCQ, G. & FAVOREEL, H. W. 2018. Porcine NK cells display features associated with antigen-presenting cells. *Journal of Leukocyte Biology,* 103**,** 129-140.

PETERSSON-WOLFE, C. S., LESLIE, K. E. & SWARTZ, T. H. 2018. An Update on the Effect of Clinical Mastitis on the Welfare of Dairy Cows and Potential Therapies. *Vet Clin North Am Food Anim Pract,* 34**,** 525-535.

PICHLMAIR, A., SCHULZ, O., TAN, C. P., NASLUND, T. I., LILJESTROM, P., WEBER, F. & REIS E SOUSA, C. 2006. RIG-I-mediated antiviral responses to single-stranded RNA bearing 5'-phosphates. *Science,* 314**,** 997-1001.

POONSUK, K., GIMÉNEZ-LIROLA, L. & ZIMMERMAN, J. J. 2018. A review of foot-and-mouth disease virus (FMDV) testing in livestock with an emphasis on the use of alternative diagnostic specimens. *Animal Health Research Reviews,* 19**,** 100-112.

PORCELLI, S., YOCKEY, C. E., BRENNER, M. B. & BALK, S. P. 1993. Analysis of T cell antigen receptor (TCR) expression by human peripheral blood CD4-8- alpha/beta T cells demonstrates preferential use of several V beta genes and an invariant TCR alpha chain. *J Exp Med,* 178**,** 1-16.

PROVINE, N. M., BINDER, B., FITZPATRICK, M. E. B., SCHUCH, A., GARNER, L. C., WILLIAMSON, K. D., VAN WILGENBURG, B., THIMME, R., KLENERMAN, P. & HOFMANN, M. 2018. Unique and Common Features of Innate-Like Human Vδ2(+) γδT Cells and Mucosal-Associated Invariant T Cells. *Frontiers in immunology,* 9**,** 756-756.

PULENDRAN, B. & MADDUR, M. S. 2015. Innate immune sensing and response to influenza. *Curr Top Microbiol Immunol,* 386**,** 23-71.

QIN, G., MAO, H., ZHENG, J., SIA, S. F., LIU, Y., CHAN, P. L., LAM, K. T., PEIRIS, J. S., LAU, Y. L. & TU, W. 2009. Phosphoantigen-expanded human gammadelta T cells display potent cytotoxicity against monocyte-derived macrophages infected with human and avian influenza viruses. *J Infect Dis,* 200**,** 858-65.

RAHIMPOUR, A., KOAY, H. F., ENDERS, A., CLANCHY, R., ECKLE, S. B. G., MEEHAN, B., CHEN, Z., WHITTLE, B., LIU, L., FAIRLIE, D. P., GOODNOW, C. C., MCCLUSKEY, J., ROSSJOHN, J., ULDRICH, A. P., PELLICCI, D. G. & GODFREY, D. I. 2015. Identification of phenotypically and functionally heterogeneous mouse mucosal-associated invariant T cells using MR1 tetramers. *Journal of Experimental Medicine,* 212**,** 1095-1108.

RAINARD, P. & RIOLLET, C. 2003. Mobilization of neutrophils and defense of the bovine mammary gland. *Reprod Nutr Dev,* 43**,** 439-57.

RAJAO, D. S. & VINCENT, A. L. 2015. Swine as a model for influenza A virus infection and immunity. *ILAR J,* 56**,** 44-52.

REANTRAGOON, R., CORBETT, A. J., SAKALA, I. G., GHERARDIN, N. A., FURNESS, J. B., CHEN, Z., ECKLE, S. B. G., ULDRICH, A. P., BIRKINSHAW, R. W., PATEL, O., KOSTENKO, L., MEEHAN, B., KEDZIERSKA, K., LIU, L., FAIRLIE, D. P., HANSEN, T. H., GODFREY, D. I., ROSSJOHN, J., MCCLUSKEY, J. & KJER-NIELSEN, L. 2013. Antigen-loaded MR1 tetramers define T cell receptor heterogeneity in mucosal-associated invariant T cells. *The Journal of Experimental Medicine,* 210**,** 2305-2320.

REANTRAGOON, R., KJER-NIELSEN, L., PATEL, O., CHEN, Z., ILLING, P. T., BHATI, M., KOSTENKO, L., BHARADWAJ, M., MEEHAN, B., HANSEN, T. H., GODFREY, D. I., ROSSJOHN, J. & MCCLUSKEY, J. 2012. Structural insight into MR1-mediated recognition of the mucosal associated invariant T cell receptor. *The Journal of Experimental Medicine,* 209**,** 761.

REBER, A. J., HIPPEN, A. R. & HURLEY, D. J. 2005. Effects of the ingestion of whole colostrum or cell-free colostrum on the capacity of leukocytes in newborn calves to stimulate or respond in one-way mixed leukocyte cultures. *Am J Vet Res,* 66**,** 1854-60.

RENUKARADHYA, G. J., MANICKAM, C., KHATRI, M., RAUF, A., LI, X., TSUJI, M., RAJASHEKARA, G. & DWIVEDI, V. 2011. Functional Invariant NKT Cells in Pig Lungs Regulate the Airway Hyperreactivity: A Potential Animal Model. *Journal of Clinical Immunology,* 31**,** 228-239.

RINKEVICH 1999. Invertebrates versus Vertebrates Innate Immunity: In the Light of Evolution ('Nothing in biology makes sense except in the light of evolution' T. Dobzhansky, Amer Biol Teacher 1973;35:125–9). *Scandinavian Journal of Immunology,* 50**,** 456-460.

SAEIDI, A., ELLEGARD, R., YONG, Y. K., TAN, H. Y., VELU, V., USSHER, J. E., LARSSON, M. & SHANKAR, E. M. 2016. Functional role of mucosal-associated invariant T cells in HIV infection. *Journal of Leukocyte Biology,* 100**,** 305-314.

SAIJO, Y., LOO, E. P. & YASUDA, S. 2018. Pattern recognition receptors and signaling in plant-microbe interactions. *Plant J,* 93**,** 592-613.

SAKAI, S., KAUFFMAN, K. D., OH, S., NELSON, C. E., BARRY, C. E. & BARBER, D. L. 2020. MAIT cell-directed therapy of Mycobacterium tuberculosis infection. *Mucosal Immunology*.

SALOU, M., LEGOUX, F., GILET, J., DARBOIS, A., DU HALGOUET, A., ALONSO, R., RICHER, W., GOUBET, A.-G., DAVIAUD, C., MENGER, L., PROCOPIO, E., PREMEL, V. & LANTZ, O. 2018. A common transcriptomic program acquired in the thymus defines tissue residency of MAIT and NKT subsets. *Journal of Experimental Medicine,* 216**,** 133-151.

SAMJI, T. 2009. Influenza A: understanding the viral life cycle. *The Yale journal of biology and medicine,* 82**,** 153-159.

SAVAGE, A. K., CONSTANTINIDES, M. G., HAN, J., PICARD, D., MARTIN, E., LI, B., LANTZ, O. & BENDELAC, A. 2008. The transcription factor PLZF directs the effector program of the NKT cell lineage. *Immunity,* 29**,** 391-403.

SCHÄFER, A., HÜHR, J., SCHWAIGER, T., DORHOI, A., METTENLEITER, T. C., BLOME, S., SCHRÖDER, C. & BLOHM, U. 2019. Porcine Invariant Natural Killer T Cells: Functional Profiling and Dynamics in Steady State and Viral Infections. *Frontiers in Immunology,* 10.

SCHROYEN, M. & TUGGLE, C. K. 2015. Current transcriptomics in pig immunity research. *Mammalian Genome,* 26**,** 1-20.

SCHULMAN, J. L. & KILBOURNE, E. D. 1965a. Induction of Partial Specific Heterotypic Immunity in Mice by a Single Infection with Influenza A Virus. *J Bacteriol,* 89**,** 170-4.

SCHULMAN, J. L. & KILBOURNE, E. D. 1965b. INDUCTION OF PARTIAL SPECIFIC HETEROTYPIC IMMUNITY IN MICE BY A SINGLE INFECTION WITH INFLUENZA A VIRUS. *Journal of bacteriology,* 89**,** 170-174.

SCHWAIGER, T., SEHL, J., KARTE, C., SCHÄFER, A., HÜHR, J., METTENLEITER, T. C., SCHRÖDER, C., KÖLLNER, B., ULRICH, R. & BLOHM, U. 2019. Experimental H1N1pdm09 infection in pigs mimics human seasonal influenza infections. *PLoS One,* 14**,** e0222943.

SCHWARTZ, J. C., HEMMINK, J. D., GRAHAM, S. P., TCHILIAN, E., CHARLESTON, B., HAMMER, S. E., HO, C. S. & HAMMOND, J. A. 2018. The major histocompatibility complex homozygous inbred Babraham pig as a resource for veterinary and translational medicine. *HLA,* 92**,** 40-43.

SEDER, R. A., DARRAH, P. A. & ROEDERER, M. 2008. T-cell quality in memory and protection: implications for vaccine design. *Nature Reviews Immunology,* 8**,** 247-258.

SERRIARI, N. E., EOCHE, M., LAMOTTE, L., LION, J., FUMERY, M., MARCELO, P., CHATELAIN, D., BARRE, A., NGUYEN-KHAC, E., LANTZ, O., DUPAS, J. L. & TREINER, E. 2014. Innate mucosal-associated invariant T (MAIT) cells are activated in inflammatory bowel diseases. *Clinical and experimental immunology,* 176**,** 266-274.

SIGNER, E. N., JEFFREYS, A. J., LICENCE, S., MILLER, R., BYRD, P. & BINNS, R. 1999. DNA profiling reveals remarkably low genetic variability in a herd of SLA homozygous pigs. *Research in Veterinary Science,* 67**,** 207-211.

SKEHEL, J. J. & WILEY, D. C. 2000. Receptor Binding and Membrane Fusion in Virus Entry: The Influenza Hemagglutinin. *Annual Review of Biochemistry,* 69**,** 531-569.

SLICHTER, C. K., MCDAVID, A., MILLER, H. W., FINAK, G., SEYMOUR, B. J., MCNEVIN, J. P., DIAZ, G., CZARTOSKI, J. L., MCELRATH, M. J., GOTTARDO, R. & PRLIC, M. 2016. Distinct activation thresholds of human conventional and innate-like memory T cells. *JCI insight,* 1**,** e86292.

SMITH, G. J. D., VIJAYKRISHNA, D., BAHL, J., LYCETT, S. J., WOROBEY, M., PYBUS, O. G., MA, S. K., CHEUNG, C. L., RAGHWANI, J., BHATT, S., PEIRIS, J. S. M., GUAN, Y. & RAMBAUT, A. 2009.

Origins and evolutionary genomics of the 2009 swine-origin H1N1 influenza A epidemic. *Nature,* 459**,** 1122-1125.

SOUTER, M. N. T., LOH, L., LI, S., MEEHAN, B. S., GHERARDIN, N. A., GODFREY, D. I., ROSSJOHN, J., FAIRLIE, D. P., KEDZIERSKA, K., PELLICCI, D. G., CHEN, Z., KJER-NIELSEN, L., CORBETT, A. J., MCCLUSKEY, J. & ECKLE, S. B. G. 2019. Characterization of Human Mucosal-associated Invariant T (MAIT) Cells. *Current Protocols in Immunology,* 127**,** e90.

SPAAN, M., HULLEGIE, S. J., BEUDEKER, B. J. B., KREEFFT, K., VAN OORD, G. W., GROOTHUISMINK, Z. M. A., VAN TILBORG, M., RIJNDERS, B., DE KNEGT, R. J., CLAASSEN, M. A. A. & BOONSTRA, A. 2016. Frequencies of Circulating MAIT Cells Are Diminished in Chronic HCV, HIV and HCV/HIV Co-Infection and Do Not Recover during Therapy. *PloS one,* 11**,** e0159243-e0159243.

SRIDHAR, S. 2016. Heterosubtypic T-Cell Immunity to Influenza in Humans: Challenges for Universal T-Cell Influenza Vaccines. *Frontiers in Immunology,* 7.

SRIDHAR, S., BEGOM, S., BERMINGHAM, A., HOSCHLER, K., ADAMSON, W., CARMAN, W., BEAN, T., BARCLAY, W., DEEKS, J. J. & LALVANI, A. 2013. Cellular immune correlates of protection against symptomatic pandemic influenza. *Nat Med,* 19**,** 1305-12.

STRAIGHT, T. M., OTTOLINI, M. G., PRINCE, G. A. & EICHELBERGER, M. C. 2006. Evidence of a cross-protective immune response to influenza A in the cotton rat model. *Vaccine,* 24**,** 6264-6271.

STRUTT, T. M., MCKINSTRY, K. K., MARSHALL, N. B., VONG, A. M., DUTTON, R. W. & SWAIN, S. L. 2013. Multipronged CD4(+) T-cell effector and memory responses cooperate to provide potent immunity against respiratory virus. *Immunological reviews,* 255**,** 149-164.

SULIMAN, S., MURPHY, M., MUSVOSVI, M., GELA, A., MEERMEIER, E. W., GELDENHUYS, H., HOPLEY, C., TOEFY, A., BILEK, N., VELDSMAN, A., HANEKOM, W. A., JOHNSON, J. L., BOOM, W. H., OBERMOSER, G., HUANG, H., HATHERILL, M., LEWINSOHN, D. M., NEMES, E. & SCRIBA, T. J. 2019. MR1-Independent Activation of Human Mucosal-Associated Invariant T Cells by Mycobacteria. *Journal of immunology (Baltimore, Md. : 1950),* 203**,** 2917-2927.

SUMMERFIELD, A. & MCCULLOUGH, K. C. 2009. The porcine dendritic cell family. *Dev Comp Immunol,* 33**,** 299-309.

SUN, J., MADAN, R., KARP, C. L. & BRACIALE, T. J. 2009. Effector T cells control lung inflammation during acute influenza virus infection by producing IL-10. *Nature Medicine,* 15**,** 277-284.

SURESH, R. & MOSSER, D. M. 2013. Pattern recognition receptors in innate immunity, host defense, and immunopathology. *Advances in physiology education,* 37**,** 284-291.

SWAIN, S. L., AGREWALA, J. N., BROWN, D. M., JELLEY-GIBBS, D. M., GOLECH, S., HUSTON, G., JONES, S. C., KAMPERSCHROER, C., LEE, W.-H., MCKINSTRY, K. K., ROMÁN, E., STRUTT, T. & WENG, N.-P. 2006. CD4+ T-cell memory: generation and multi-faceted roles for CD4+ T cells in protective immunity to influenza. *Immunological reviews,* 211**,** 8-22.

SZABO, S. J., KIM, S. T., COSTA, G. L., ZHANG, X., FATHMAN, C. G. & GLIMCHER, L. H. 2000. A Novel Transcription Factor, T-bet, Directs Th1 Lineage Commitment. *Cell,* 100**,** 655-669.

TAKAMATSU, H. H., DENYER, M. S., STIRLING, C., COX, S., AGGARWAL, N., DASH, P., WILEMAN, T. E. & BARNETT, P. V. 2006. Porcine gammadelta T cells: possible roles on the innate and adaptive immune responses following virus infection. *Vet Immunol Immunopathol,* 112**,** 49-61.

TALKER, S. C., STADLER, M., KOINIG, H. C., MAIR, K. H., RODRIGUEZ-GOMEZ, I. M., GRAAGE, R., ZELL, R., DURRWALD, R., STARICK, E., HARDER, T., WEISSENBOCK, H., LAMP, B., HAMMER, S. E., LADINIG, A., SAALMULLER, A. & GERNER, W. 2016. Influenza A Virus Infection in Pigs Attracts Multifunctional and Cross-Reactive T Cells to the Lung. *J Virol,* 90**,** 9364-82.

TANIUCHI, I. 2018. CD4 Helper and CD8 Cytotoxic T Cell Differentiation. *Annual Review of Immunology,* 36**,** 579-601.

THIERRY, A., ROBIN, A., GIRAUD, S., MINOUFLET, S., BARRA, A., BRIDOUX, F., HAUET, T., TOUCHARD, G., HERBELIN, A. & GOMBERT, J. M. 2012. Identification of invariant natural killer T cells in porcine peripheral blood. *Vet Immunol Immunopathol,* 149**,** 272-9.

TILLOY, F., TREINER, E., PARK, S. H., GARCIA, C., LEMONNIER, F., DE LA SALLE, H., BENDELAC, A., BONNEVILLE, M. & LANTZ, O. 1999. An invariant T cell receptor alpha chain defines a novel

TAP-independent major histocompatibility complex class Ib-restricted alpha/beta T cell subpopulation in mammals. *The Journal of experimental medicine,* 189**,** 1907-1921.

TOMURA, M., MARUO, S., MU, J., ZHOU, X.-Y., AHN, H.-J., HAMAOKA, T., OKAMURA, H., NAKANISHI, K., CLARK, S., KURIMOTO, M. & FUJIWARA, H. 1998. Differential Capacities of CD4⁺, CD8⁺, and CD4[−]CD8[−] T Cell Subsets to Express IL-18 Receptor and Produce IFN-γ in Response to IL-18. *The Journal of Immunology,* 160**,** 3759-3765.

TOPHAM, D. J., TRIPP, R. A. & DOHERTY, P. C. 1997. CD8+ T cells clear influenza virus by perforin or Fas-dependent processes. *J Immunol,* 159**,** 5197-200.

TREINER, E., DUBAN, L., BAHRAM, S., RADOSAVLJEVIC, M., WANNER, V., TILLOY, F., AFFATICATI, P., GILFILLAN, S. & LANTZ, O. 2003. Selection of evolutionarily conserved mucosal-associated invariant T cells by MR1. *Nature,* 422**,** 164-9.

TSUKAMOTO, K., DEAKIN, J. E., GRAVES, J. A. M. & HASHIMOTO, K. 2013. Exceptionally high conservation of the MHC class I-related gene, MR1, among mammals. *Immunogenetics,* 65**,** 115-124.

TUNGATT, K., DOLTON, G., MORGAN, S. B., ATTAF, M., FULLER, A., WHALLEY, T., HEMMINK, J. D., PORTER, E., SZOMOLAY, B., MONTOYA, M., HAMMOND, J. A., MILES, J. J., COLE, D. K., TOWNSEND, A., BAILEY, M., RIZKALLAH, P. J., CHARLESTON, B., TCHILIAN, E. & SEWELL, A. K. 2018. Induction of influenza-specific local CD8 T-cells in the respiratory tract after aerosol delivery of vaccine antigen or virus in the Babraham inbred pig. *PLOS Pathogens,* 14**,** e1007017.

TURNER, J. D., FAULKNER, H., KAMGNO, J., CORMONT, F., VAN SNICK, J., ELSE, K. J., GRENCIS, R. K., BEHNKE, J. M., BOUSSINESQ, M. & BRADLEY, J. E. 2003. Th2 Cytokines Are Associated with Reduced Worm Burdens in a Human Intestinal Helminth Infection. *The Journal of Infectious Diseases,* 188**,** 1768-1775.

USSHER, J. E., BILTON, M., ATTWOD, E., SHADWELL, J., RICHARDSON, R., DE LARA, C., METTKE, E., KURIOKA, A., HANSEN, T. H., KLENERMAN, P. & WILLBERG, C. B. 2014. CD161++ CD8+ T cells, including the MAIT cell subset, are specifically activated by IL-12+IL-18 in a TCR-independent manner. *Eur J Immunol,* 44**,** 195-203.

VAN DEN BORNE, B. H., VAN SCHAIK, G., LAM, T. J. & NIELEN, M. 2010. Variation in herd level mastitis indicators between primi- and multiparae in Dutch dairy herds. *Prev Vet Med,* 96**,** 49-55.

VAN EIJK, M., WHITE, M. R., CROUCH, E. C., BATENBURG, J. J., VAANDRAGER, A. B., VAN GOLDE, L. M. G., HAAGSMAN, H. P. & HARTSHORN, K. L. 2003. Porcine Pulmonary Collectins Show Distinct Interactions with Influenza A Viruses: Role of the N-Linked Oligosaccharides in the Carbohydrate Recognition Domain. *The Journal of Immunology,* 171**,** 1431.

VAN RHIJN, I., GODFREY, D. I., ROSSJOHN, J. & MOODY, D. B. 2015. Lipid and small-molecule display by CD1 and MR1. *Nat Rev Immunol,* 15**,** 643-54.

VAN RHIJN, I., GODFROID, J., MICHEL, A. & RUTTEN, V. 2008. Bovine tuberculosis as a model for human tuberculosis: advantages over small animal models. *Microbes Infect,* 10**,** 711-5.

VAN RHIJN, I. & MOODY, D. B. 2015. Donor Unrestricted T Cells: A Shared Human T Cell Response. *The Journal of Immunology,* 195**,** 1927.

VAN WILGENBURG, B., LOH, L., CHEN, Z., PEDIONGCO, T. J., WANG, H., SHI, M., ZHAO, Z., KOUTSAKOS, M., NUSSING, S., SANT, S., WANG, Z., D'SOUZA, C., JIA, X., ALMEIDA, C. F., KOSTENKO, L., ECKLE, S. B. G., MEEHAN, B. S., KALLIES, A., GODFREY, D. I., READING, P. C., CORBETT, A. J., MCCLUSKEY, J., KLENERMAN, P., KEDZIERSKA, K. & HINKS, T. S. C. 2018. MAIT cells contribute to protection against lethal influenza infection in vivo. *Nat Commun,* 9**,** 4706.

VAN WILGENBURG, B., SCHERWITZL, I., HUTCHINSON, E. C., LENG, T. Q., KURIOKA, A., KULICKE, C., DE LARA, C., COLE, S., VASANAWATHANA, S., LIMPITIKUL, W., MALASIT, P., YOUNG, D. C., DENNEY, L., MOORE, M. D., FABRIS, P., GIORDANI, M. T., OO, Y. H., LAIDLAW, S. M., DUSTIN, L. B., HO, L. P., THOMPSON, F. M., RAMAMURTHY, N., MONGKOLSAPAYA, J., WILLBERG, C. B.,

SCREATON, G. R., KLENERMAN, P. & CONSORTIUM, S.-H. 2016. MAIT cells are activated during human viral infections. *Nature Communications,* 7**,** 11.

VANTOUROUT, P. & HAYDAY, A. 2013. Six-of-the-best: unique contributions of gammadelta T cells to immunology. *Nat Rev Immunol,* 13**,** 88-100.

VINTON, C., WU, F., ROSSJOHN, J., MATSUDA, K., MCCLUSKEY, J., HIRSCH, V., PRICE, D. A. & BRENCHLEY, J. M. 2016. Mucosa-Associated Invariant T Cells Are Systemically Depleted in Simian Immunodeficiency Virus-Infected Rhesus Macaques. *Journal of Virology,* 90**,** 4520-4529.

VOILLET, V., BUGGERT, M., SLICHTER, C. K., BERKSON, J. D., MAIR, F., ADDISON, M. M., DORI, Y., NADOLSKI, G., ITKIN, M. G., GOTTARDO, R., BETTS, M. R. & PRLIC, M. 2018. Human MAIT cells exit peripheral tissues and recirculate via lymph in steady state conditions. *JCI Insight,* 3.

VORKAS, C. K., WIPPERMAN, M. F., LI, K., BEAN, J., BHATTARAI, S. K., ADAMOW, M., WONG, P., AUBÉ, J., JUSTE, M. A. J., BUCCI, V., FITZGERALD, D. W. & GLICKMAN, M. S. 2018. Mucosal-associated invariant and γδ T cell subsets respond to initial Mycobacterium tuberculosis infection. *JCI insight,* 3**,** e121899.

WADDINGTON, C. S., WALKER, W. T., OESER, C., REINER, A., JOHN, T., WILKINS, S., CASEY, M., ECCLESTON, P. E., ALLEN, R. J., OKIKE, I., LADHANI, S., SHEASBY, E., HOSCHLER, K., ANDREWS, N., WAIGHT, P., COLLINSON, A. C., HEATH, P. T., FINN, A., FAUST, S. N., SNAPE, M. D., MILLER, E. & POLLARD, A. J. 2010. Safety and immunogenicity of AS03_B adjuvanted split virion versus non-adjuvanted whole virion H1N1 influenza vaccine in UK children aged 6 months-12 years: open label, randomised, parallel group, multicentre study. *BMJ,* 340.

WALKER, L. J., KANG, Y. H., SMITH, M. O., THARMALINGHAM, H., RAMAMURTHY, N., FLEMING, V. M., SAHGAL, N., LESLIE, A., OO, Y., GEREMIA, A., SCRIBA, T. J., HANEKOM, W. A., LAUER, G. M., LANTZ, O., ADAMS, D. H., POWRIE, F., BARNES, E. & KLENERMAN, P. 2012. Human MAIT and CD8αα cells develop from a pool of type-17 precommitted CD8+ T cells. *Blood,* 119**,** 422-33.

WAN, Y. Y. & FLAVELL, R. A. 2009. How diverse--CD4 effector T cells and their functions. *J Mol Cell Biol,* 1**,** 20-36.

WANG, H., D'SOUZA, C., LIM, X. Y., KOSTENKO, L., PEDIONGCO, T. J., ECKLE, S. B. G., MEEHAN, B. S., SHI, M., WANG, N., LI, S., LIU, L., MAK, J. Y. W., FAIRLIE, D. P., IWAKURA, Y., GUNNERSEN, J. M., STENT, A. W., GODFREY, D. I., ROSSJOHN, J., WESTALL, G. P., KJER-NIELSEN, L., STRUGNELL, R. A., MCCLUSKEY, J., CORBETT, A. J., HINKS, T. S. C. & CHEN, Z. 2018. MAIT cells protect against pulmonary Legionella longbeachae infection. *Nature Communications,* 9**,** 3350.

WANG, J., GUILLAUME, J., PAUWELS, N., VAN CALENBERGH, S., VAN RHIJN, I. & ZAJONC, D. M. 2012. Crystal structures of bovine CD1d reveal altered αGalCer presentation and a restricted A' pocket unable to bind long-chain glycolipids. *PloS one,* 7**,** e47989-e47989.

WANG, Z., WAN, Y., QIU, C., QUIÑONES-PARRA, S., ZHU, Z., LOH, L., TIAN, D., REN, Y., HU, Y., ZHANG, X., THOMAS, P. G., INOUYE, M., DOHERTY, P. C., KEDZIERSKA, K. & XU, J. 2015. Recovery from severe H7N9 disease is associated with diverse response mechanisms dominated by CD8+ T cells. *Nature Communications,* 6**,** 6833.

WATERS, W. R., PALMER, M. V., THACKER, T. C., DAVIS, W. C., SREEVATSAN, S., COUSSENS, P., MEADE, K. G., HOPE, J. C. & ESTES, D. M. 2011. Tuberculosis immunity: opportunities from studies with cattle. *Clinical & developmental immunology,* 2011**,** 768542-768542.

WEINFURTER, J. T., BRUNNER, K., CAPUANO, S. V., 3RD, LI, C., BROMAN, K. W., KAWAOKA, Y. & FRIEDRICH, T. C. 2011. Cross-reactive T cells are involved in rapid clearance of 2009 pandemic H1N1 influenza virus in nonhuman primates. *PLoS pathogens,* 7**,** e1002381-e1002381.

WENCKER, M., TURCHINOVICH, G., DI MARCO BARROS, R., DEBAN, L., JANDKE, A., COPE, A. & HAYDAY, A. C. 2014. Innate-like T cells straddle innate and adaptive immunity by altering antigen-receptor responsiveness. *Nat Immunol,* 15**,** 80-7.

WILGENBURG, B. V., LOH, L., CHEN, Z., PEDIONGCO, T. J., WANG, H., SHI, M., ZHAO, Z., KOUTSAKOS, M., NUSSING, S., SANT, S., WANG, Z., D'SOUZA, C., JIA, X., ALMEIDA, C. F., KOSTENKO, L., ECKLE, S. B. G., MEEHAN, B. S., KALLIES, A., GODFREY, D. I., READING, P. C., CORBETT, A. J.,

MCCLUSKEY, J., KLENERMAN, P., KEDZIERSKA, K. & HINKS, T. S. C. 2018. MAIT cells contribute to protection against lethal influenza infection in vivo. *Nat Commun,* 9**,** 4706.

WILKINSON, T. M., LI, C. K., CHUI, C. S., HUANG, A. K., PERKINS, M., LIEBNER, J. C., LAMBKIN-WILLIAMS, R., GILBERT, A., OXFORD, J., NICHOLAS, B., STAPLES, K. J., DONG, T., DOUEK, D. C., MCMICHAEL, A. J. & XU, X. N. 2012. Preexisting influenza-specific CD4+ T cells correlate with disease protection against influenza challenge in humans. *Nat Med,* 18**,** 274-80.

WONG, P. & PAMER, E. G. 2003. CD8 T Cell Responses to Infectious Pathogens. *Annual Review of Immunology,* 21**,** 29-70.

XIAO, X., LI, K., MA, X., LIU, B., HE, X., YANG, S., WANG, W., JIANG, B. & CAI, J. 2019a. Mucosal-Associated Invariant T Cells Expressing the TRAV1-TRAJ33 Chain Are Present in Pigs. *Frontiers in Immunology,* 10.

XIAO, X., LIU, B., MA, X., YANG, S. & CAI, J. 2019b. Molecular cloning and characterization of the pig MHC class Ⅰ-related MR1 gene. *Developmental & Comparative Immunology,* 96**,** 58-67.

YAMAGUCHI, H., HIRAI, M., KUROSAWA, Y. & HASHIMOTO, K. 1997. A highly conserved major histocompatibility complex class I-related gene in mammals. *Biochem Biophys Res Commun,* 238**,** 697-702.

YAMAMOTO, K., MIYOSHI-KOSHIO, T., UTSUKI, Y., MIZUNO, S. & SUZUKI, K. 1991. Virucidal activity and viral protein modification by myeloperoxidase: a candidate for defense factor of human polymorphonuclear leukocytes against influenza virus infection. *J Infect Dis,* 164**,** 8-14.

YANG, G., RICHT, J. & DRIVER, J. 2018. Harnessing Invariant NKT Cells to Improve Influenza Vaccines: A Pig Perspective. *International Journal of Molecular Sciences,* 19**,** 68.

YAP, K. L., ADA, G. L. & MCKENZIE, I. F. C. 1978. Transfer of specific cytotoxic T lymphocytes protects mice inoculated with influenza virus. *Nature,* 273**,** 238-239.

YETTER, R. A., BARBER, W. H. & SMALL, P. A., JR. 1980. Heterotypic immunity to influenza in ferrets. *Infection and immunity,* 29**,** 650-653.

YU, H., YANG, A., DERRICK, S., MAK, J. Y. W., LIU, L., FAIRLIE, D. P. & COWLEY, S. 2020. Artificially induced MAIT cells inhibit M. bovis BCG but not M. tuberculosis during in vivo pulmonary infection. *Scientific Reports,* 10**,** 13579.

ZHAO, Y., ZHANG, Y. H., DENNEY, L., YOUNG, D., POWELL, T. J., PENG, Y. C., LI, N., YAN, H. P., WANG, D. Y., SHU, Y. L., KENDRICK, Y., MCMICHAEL, A. J., HO, L. P. & DONG, T. 2012. High levels of virus-specific CD4+ T cells predict severe pandemic influenza A virus infection. *Am J Respir Crit Care Med,* 186**,** 1292-7.

ZHENG, J., LIU, Y., LAU, Y.-L. & TU, W. 2013. [ggr][dgr]-T cells: an unpolished sword in human anti-infection immunity. *Cell Mol Immunol,* 10**,** 50-57.

Chapter 7 Appendices

7.1 Peptides for Epitope identification

Table 7.1 H1N1pdm09 Nuclear protein peptides.

Pool	Denomination	Sequence	Length
P 1	HNP1	MASQGTKRSYEQMETGGE	18
	HNP2	KRSYEQMETGGERQDATE	18
	HNP3	METGGERQDATEIRASVG	18
	HNP4	RQDATEIRASVGRMIGGI	18
	HNP5	IRASVGRMIGGIGRFYIQ	18
	HNP6	RMIGGIGRFYIQMCTELK	18
	HNP7	GRFYIQMCTELKLSDYDG	18
	HNP8	MCTELKLSDYDGRLIQNS	18
	HNP9	LSDYDGRLIQNSITIERM	18
	HNP10	RLIQNSITIERMVLSAFD	18
P 2	HNP11	ITIERMVLSAFDERRNKY	18
	HNP12	VLSAFDERRNKYLEEHPS	18
	HNP13	ERRNKYLEEHPSAGKDPK	18
	HNP14	LEEHPSAGKDPKKTGGPI	18
	HNP15	AGKDPKKTGGPIYRRIGG	18
	HNP16	KTGGPIYRRIGGKWMREL	18
	HNP17	YRRIGGKWMRELILYDKE	18
	HNP18	KWMRELILYDKEEIRRVW	18
	HNP19	ILYDKEEIRRVWRQANNG	18
	HNP20	EIRRVWRQANNGEDATAG	18
P 3	HNP21	RQANNGEDATAGLTHIMI	18
	HNP22	EDATAGLTHIMIWHSNLN	18
	HNP23	LTHIMIWHSNLNDATYQR	18
	HNP24	WHSNLNDATYQRTRALVR	18
	HNP25	DATYQRTRALVRTGMDPR	18
	HNP26	TRALVRTGMDPRMCSLMQ	18
	HNP27	TGMDPRMCSLMQGSTLPR	18
	HNP28	MCSLMQGSTLPRRSGAAG	18
	HNP29	GSTLPRRSGAAGAAVKGV	18
	HNP30	RSGAAGAAVKGVGTIAME	18
P 4	HNP31	AAVKGVGTIAMELIRMIK	18
	HNP32	GTIAMELIRMIKRGINDR	18
	HNP33	LIRMIKRGINDRNFWRGE	18
	HNP34	RGINDRNFWRGENGRRTR	18

Pool	Denomination	Sequence	Length
	HNP35	NFWRGENGRRTRVAYERM	18
	HNP36	NGRRTRVAYERMCNILKG	18
	HNP37	VAYERMCNILKGKFQTAA	18
	HNP38	CNILKGKFQTAAQRAMMD	18
	HNP39	KFQTAAQRAMMDQVRESR	18
	HNP40	QRAMMDQVRESRNPGNAE	18
P 5	HNP41	QVRESRNPGNAEIEDLIF	18
	HNP42	NPGNAEIEDLIFLARSAL	18
	HNP43	IEDLIFLARSALILRGSV	18
	HNP44	LARSALILRGSVAHKSCL	18
	HNP45	ILRGSVAHKSCLPACVYG	18
	HNP46	AHKSCLPACVYGLAVASG	18
	HNP47	PACVYGLAVASGHDFERE	18
	HNP48	LAVASGHDFEREGYSLVG	18
	HNP49	HDFEREGYSLVGVDPFKL	18
	HNP50	GYSLVGVDPFKLLQNSQV	18
P 6	HNP51	VDPFKLLQNSQVVSLMRP	18
	HNP52	LQNSQVVSLMRPNENPAH	18
	HNP53	VSLMRPNENPAHKSQLVW	18
	HNP54	NENPAHKSQLVWMACHSA	18
	HNP55	KSQLVWMACHSAAFEDLR	18
	HNP56	MACHSAAFEDLRVSSFIR	18
	HNP57	AFEDLRVSSFIRGKKVIP	18
	HNP58	VSSFIRGKKVIPRGKLST	18
	HNP59	GKKVIPRGKLSTRGVQIA	18
	HNP60	RGKLSTRGVQIASNENVE	18
P7	HNP61	RGVQIASNENVETMDSNT	18
	HNP62	SNENVETMDSNTLELRSR	18
	HNP63	TMDSNTLELRSRYWAIRT	18
	HNP64	LELRSRYWAIRTRSGGNT	18
	HNP65	YWAIRTRSGGNTNQQKAS	18
	HNP66	RSGGNTNQQKASAGQISV	18
	HNP67	NQQKASAGQISVQPTFSV	18
	HNP68	AGQISVQPTFSVQRNLPF	18
	HNP69	QPTFSVQRNLPFERATVM	18
	HNP70	QRNLPFERATVMAAFSGN	18
P 8	HNP71	ERATVMAAFSGNNEGRTS	18
	HNP72	AAFSGNNEGRTSDMRTEV	18
	HNP73	NEGRTSDMRTEVIRMMES	18
	HNP74	DMRTEVIRMMESAKPEDL	18
	HNP75	IRMMESAKPEDLSFQGRG	18
	HNP76	AKPEDLSFQGRGVFELSD	18
	HNP77	SFQGRGVFELSDEKATNP	18

Pool	Denomination	Sequence	Length
	HNP78	VFELSDEKATNPIVPSFD	18
	HNP79	EKATNPIVPSFDMSNEGS	18
	HNP80	IVPSFDMSNEGSYFFGDN	18
	HNP81	MSNEGSYFFGDNAEEYDS	18

Table 7.2 H1N1pdm09 Matrix 1 peptides.

Pool	Denomination	Sequence	Length
Pool 1	HM1	MSLLTEVETYVLSIIPSG	18
	HM2	VETYVLSIIPSGPLKAEI	18
	HM3	SIIPSGPLKAEIAQRLES	18
	HM4	PLKAEIAQRLESVFAGKN	18
	HM5	AQRLESVFAGKNTDLEAL	18
	HM6	VFAGKNTDLEALMEWLKT	18
	HM7	TDLEALMEWLKTRPILSP	18
	HM8	MEWLKTRPILSPLTKGIL	18
	HM9	RPILSPLTKGILGFVFTL	18
	HM10	LTKGILGFVFTLTVPSER	18
Pool 2	HM11	GFVFTLTVPSERGLQRRR	18
	HM12	TVPSERGLQRRRFVQNAL	18
	HM13	GLQRRRFVQNALNGNGDP	18
	HM14	FVQNALNGNGDPNNMDRA	18
	HM15	NGNGDPNNMDRAVKLYKK	18
	HM16	NNMDRAVKLYKKLKREIT	18
	HM17	VKLYKKLKREITFHGAKE	18
	HM18	LKREITFHGAKEVSLSYS	18
	HM19	FHGAKEVSLSYSTGALAS	18
	HM20	VSLSYSTGALASCMGLIY	18
Pool 3	HM21	TGALASCMGLIYNRMGTV	18
	HM22	CMGLIYNRMGTVTTEAAF	18
	HM23	NRMGTVTTEAAFGLVCAT	18
	HM24	TTEAAFGLVCATCEQIAD	18
	HM25	GLVCATCEQIADSQHRSH	18
	HM26	CEQIADSQHRSHRQMATT	18
	HM27	SQHRSHRQMATTTNPLIR	18
	HM28	RQMATTTNPLIRHENRMV	18
	HM29	TNPLIRHENRMVLASTTA	18
	HM30	HENRMVLASTTAKAMEQM	18
Pool 4	HM31	LASTTAKAMEQMAGSSEQ	18
	HM32	KAMEQMAGSSEQAAEAME	18

Pool	Denomination	Sequence	Length
	HM33	AGSSEQAAEAMEVANQTR	18
	HM34	AAEAMEVANQTRQMVHAM	18
	HM35	VANQTRQMVHAMRTIGTH	18
	HM36	QMVHAMRTIGTHPSSSAG	18
	HM37	RTIGTHPSSSAGLKDDLL	18
	HM38	PSSSAGLKDDLLENLQAY	18
	HM39	LKDDLLENLQAYQKRMGV	18
	HM40	ENLQAYQKRMGVQMQRFK	18

Table 7.3 H1N1pdm09 Haemagglutinin peptides.

Pool	Denomination	Sequence	Length
Pool 1	HA. 1	MKAILIVLLYTFATANAD	18
	HA. 2	LIVLLYTFATANADTLCI	18
	HA. 3	LYTFATANADTLCIGYHA	18
	HA. 4	ATANADTLCIGYHANNST	18
	HA. 5	ADTLCIGYHANNSTDTVD	18
	HA. 6	CIGYHANNSTDTVDTVLE	18
	HA. 7	HANNSTDTVDTVLEKNVT	18
	HA. 8	STDTVDTVLEKNVTVTHS	18
	HA. 9	VDTVLEKNVTVTHSVNLL	18
	HA. 10	LEKNVTVTHSVNLLEDKH	18
Pool 2	HA. 11	VTVTHSVNLLEDKHNGKL	18
	HA. 12	HSVNLLEDKHNGKLCKLR	18
	HA. 13	LLEDKHNGKLCKLRGVAP	18
	HA. 14	KHNGKLCKLRGVAPLHLG	18
	HA. 15	KLCKLRGVAPLHLGKCNI	18
	HA. 16	LRGVAPLHLGKCNIAGWI	18
	HA. 17	APLHLGKCNIAGWILGNP	18
	HA. 18	LGKCNIAGWILGNPECES	18
	HA. 19	NIAGWILGNPECESLSTA	18
	HA. 20	WILGNPECESLSTASSWS	18
Pool 3	HA. 21	NPECESLSTASSWSYIVE	18
	HA. 22	ESLSTASSWSYIVETSSS	18
	HA. 23	TASSWSYIVETSSSDNGT	18
	HA. 24	WSYIVETSSSDNGTCYPG	18
	HA. 25	VETSSSDNGTCYPGDFID	18
	HA. 26	SSDNGTCYPGDFIDYEEL	18
	HA. 27	GTCYPGDFIDYEELREQL	18
	HA. 28	PGDFIDYEELREQLSSVS	18
	HA. 29	IDYEELREQLSSVSSFER	18
	HA. 30	ELREQLSSVSSFERFEIF	18

Pool	Denomination	Sequence	Length
Pool 4	HA. 31	QLSSVSSFERFEIFPKTS	18
	HA. 32	VSSFERFEIFPKTSSWPN	18
	HA. 33	ERFEIFPKTSSWPNHDSN	18
	HA. 34	IFPKTSSWPNHDSNKGVT	18
	HA. 35	TSSWPNHDSNKGVTAACP	18
	HA. 36	PNHDSNKGVTAACPHAGA	18
	HA. 37	SNKGVTAACPHAGAKSFY	18
	HA. 38	VTAACPHAGAKSFYKNLI	18
	HA. 39	CPHAGAKSFYKNLIWLVK	18
	HA. 40	GAKSFYKNLIWLVKKGNS	18
Pool 5	HA. 41	FYKNLIWLVKKGNSYPKL	18
	HA. 42	LIWLVKKGNSYPKLSKSY	18
	HA. 43	VKKGNSYPKLSKSYINDK	18
	HA. 44	NSYPKLSKSYINDKGKEV	18
	HA. 45	KLSKSYINDKGKEVLVLW	18
	HA. 46	SYINDKGKEVLVLWGIHH	18
	HA. 47	DKGKEVLVLWGIHHPSTS	18
	HA. 48	EVLVLWGIHHPSTSADQQ	18
	HA. 49	LWGIHHPSTSADQQSLYQ	18
	HA. 50	HHPSTSADQQSLYQNADA	18
Pool 6	HA. 51	TSADQQSLYQNADAYVFV	18
	HA. 52	QQSLYQNADAYVFVGTSR	18
	HA. 53	YQNADAYVFVGTSRYSKK	18
	HA. 54	DAYVFVGTSRYSKKFKPE	18
	HA. 55	FVGTSRYSKKFKPEIAIR	18
	HA. 56	SRYSKKFKPEIAIRPKVR	18
	HA. 57	KKFKPEIAIRPKVRGQEG	18
	HA. 58	PEIAIRPKVRGQEGRMNY	18
	HA. 59	IRPKVRGQEGRMNYYWTL	18
	HA. 60	VRGQEGRMNYYWTLVEPG	18
	HA. 61	EGRMNYYWTLVEPGDKIT	18
Pool 7	HA. 62	NYYWTLVEPGDKITFEAT	18
	HA. 63	TLVEPGDKITFEATGNLV	18
	HA. 64	PGDKITFEATGNLVVPRY	18
	HA. 65	ITFEATGNLVVPRYAFAM	18
	HA. 66	ATGNLVVPRYAFAMERNA	18
	HA. 67	LVVPRYAFAMERNAGSGI	18
	HA. 68	RYAFAMERNAGSGIIISD	18
	HA. 69	AMERNAGSGIIISDTPVH	18
	HA. 70	NAGSGIIISDTPVHDCNT	18
	HA. 71	GIIISDTPVHDCNTTCQT	18
	HA. 72	SDTPVHDCNTTCQTPKGA	18
Pool 8	HA. 73	VHDCNTTCQTPKGAINTS	18

Pool	Denomination	Sequence	Length
	HA. 74	NTTCQTPKGAINTSLPFQ	18
	HA. 75	QTPKGAINTSLPFQNIHP	18
	HA. 76	GAINTSLPFQNIHPITIG	18
	HA. 77	TSLPFQNIHPITIGKCPK	18
	HA. 78	FQNIHPITIGKCPKYVKS	18
	HA. 79	HPITIGKCPKYVKSTKLR	18
	HA. 80	IGKCPKYVKSTKLRLATG	18
	HA. 81	PKYVKSTKLRLATGLRNV	18
	HA. 82	KSTKLRLATGLRNVPSIQ	18
	HA. 83	LRLATGLRNVPSIQSRGL	18
Pool 9	HA. 84	TGLRNVPSIQSRGLFGAI	18
	HA. 85	NVPSIQSRGLFGAIAGFI	18
	HA. 86	IQSRGLFGAIAGFIEGGW	18
	HA. 87	GLFGAIAGFIEGGWTGMV	18
	HA. 88	AIAGFIEGGWTGMVDGWY	18
	HA. 89	FIEGGWTGMVDGWYGYHH	18
	HA. 90	GWTGMVDGWYGYHHQNEQ	18
	HA. 91	MVDGWYGYHHQNEQGSGY	18
	HA. 92	WYGYHHQNEQGSGYAADL	18
	HA. 93	HHQNEQGSGYAADLKSTQ	18
	HA. 94	EQGSGYAADLKSTQNAID	18
Pool 10	HA. 95	GYAADLKSTQNAIDEITN	18
	HA. 96	DLKSTQNAIDEITNKVNS	18
	HA. 97	TQNAIDEITNKVNSVIEK	18
	HA. 98	IDEITNKVNSVIEKMNTQ	18
	HA. 99	TNKVNSVIEKMNTQFTAV	18
	HA. 100	NSVIEKMNTQFTAVGKEF	18
	HA. 101	EKMNTQFTAVGKEFNHLE	18
	HA. 102	TQFTAVGKEFNHLEKRIE	18
	HA. 103	AVGKEFNHLEKRIENLNK	18
	HA. 104	EFNHLEKRIENLNKKVDD	18
	HA. 105	LEKRIENLNKKVDDGFLD	18
Pool 11	HA. 106	IENLNKKVDDGFLDIWTY	18
	HA. 107	NKKVDDGFLDIWTYNAEL	18
	HA. 108	DDGFLDIWTYNAELLVLL	18
	HA. 109	LDIWTYNAELLVLLENER	18
	HA. 110	TYNAELLVLLENERTLDY	18
	HA. 111	ELLVLLENERTLDYHDSN	18
	HA. 112	LLENERTLDYHDSNVKNL	18
	HA. 113	ERTLDYHDSNVKNLYEKV	18
	HA. 114	DYHDSNVKNLYEKVRSQL	18
	HA. 115	SNVKNLYEKVRSQLKNNA	18
	HA. 116	NLYEKVRSQLKNNAKEIG	18

Pool	Denomination	Sequence	Length
Pool 12	HA. 117	KVRSQLKNNAKEIGNGCF	18
	HA. 118	QLKNNAKEIGNGCFEFYH	18
	HA. 119	NAKEIGNGCFEFYHKCDN	18
	HA. 120	IGNGCFEFYHKCDNTCME	18
	HA. 121	CFEFYHKCDNTCMESVKN	18
	HA. 122	YHKCDNTCMESVKNGTYD	18
	HA. 123	DNTCMESVKNGTYDYPKY	18
	HA. 124	MESVKNGTYDYPKYSEEA	18
	HA. 125	KNGTYDYPKYSEEAKLNR	18
	HA. 126	YDYPKYSEEAKLNREEID	18
	HA. 127	KYSEEAKLNREEIDGVKL	18
Pool 13	HA. 128	EAKLNREEIDGVKLESTR	18
	HA. 129	NREEIDGVKLESTRIYQI	18
	HA. 130	IDGVKLESTRIYQILAIY	18
	HA. 131	KLESTRIYQILAIYSTVA	18
	HA. 132	TRIYQILAIYSTVASSLV	18
	HA. 133	QILAIYSTVASSLVLVVS	18
	HA. 134	IYSTVASSLVLVVSLGAI	18
	HA. 135	VASSLVLVVSLGAISFWM	18
	HA. 136	LVLVVSLGAISFWMCSNG	18
	HA. 137	VSLGAISFWMCSNGSLQC	18
	HA. 138	AISFWMCSNGSLQCRICI	18

Table 7.4 H1N1pdm09 Neuraminidase peptides.

Pool	Denomination	Sequence	Length
Pool 1	NA. 1	MNPNQKIITIGSVCMTIG	18
	NA. 2	QKIITIGSVCMTIGMANL	18
	NA. 3	TIGSVCMTIGMANLILQI	18
	NA. 4	VCMTIGMANLILQIGNII	18
	NA. 5	IGMANLILQIGNIISIWI	18
	NA. 6	NLILQIGNIISIWISHSI	18
	NA. 7	QIGNIISIWISHSIQLGN	18
	NA. 8	IISIWISHSIQLGNQNQI	18
Pool 2	NA. 9	WISHSIQLGNQNQIETCN	18
	NA. 10	SIQLGNQNQIETCNQSVI	18
	NA. 11	GNQNQIETCNQSVITYEN	18
	NA. 12	QIETCNQSVITYENNTWV	18
	NA. 13	CNQSVITYENNTWVNQTY	18
	NA. 14	VITYENNTWVNQTYVNIS	18
	NA. 15	ENNTWVNQTYVNISNTNF	18
	NA. 16	WVNQTYVNISNTNFAAGQ	18

Pool	Denomination	Sequence	Length
Pool 3	NA. 17	TYVNISNTNFAAGQSVVS	18
	NA. 18	ISNTNFAAGQSVVSVKLA	18
	NA. 19	NFAAGQSVVSVKLAGNSS	18
	NA. 20	GQSVVSVKLAGNSSLCPV	18
	NA. 21	VSVKLAGNSSLCPVSGWA	18
	NA. 22	LAGNSSLCPVSGWAIYSK	18
	NA. 23	SSLCPVSGWAIYSKDNSI	18
	NA. 24	PVSGWAIYSKDNSIRIGS	18
Pool 4	NA. 25	WAIYSKDNSIRIGSKGDV	18
	NA. 26	SKDNSIRIGSKGDVFVIR	18
	NA. 27	SIRIGSKGDVFVIREPFI	18
	NA. 28	GSKGDVFVIREPFISCSP	18
	NA. 29	DVFVIREPFISCSPLECR	18
	NA. 30	IREPFISCSPLECRTFFL	18
	NA. 31	FISCSPLECRTFFLTQGA	18
	NA. 32	SPLECRTFFLTQGALLND	18
	NA. 33	CRTFFLTQGALLNDKHSN	18
Pool 5	NA. 34	FLTQGALLNDKHSNGTIK	18
	NA. 35	GALLNDKHSNGTIKDRSP	18
	NA. 36	NDKHSNGTIKDRSPYRTL	18
	NA. 37	SNGTIKDRSPYRTLMSCP	18
	NA. 38	IKDRSPYRTLMSCPIGEV	18
	NA. 39	SPYRTLMSCPIGEVPSPY	18
	NA. 40	TLMSCPIGEVPSPYNSRF	18
	NA. 41	CPIGEVPSPYNSRFESVA	18
	NA. 42	EVPSPYNSRFESVAWSAS	18
Pool 6	NA. 43	PYNSRFESVAWSASACHD	18
	NA. 44	RFESVAWSASACHDGINW	18
	NA. 45	VAWSASACHDGINWLTIG	18
	NA. 46	ASACHDGINWLTIGISGP	18
	NA. 47	HDGINWLTIGISGPDNGA	18
	NA. 48	NWLTIGISGPDNGAVAVL	18
	NA. 49	IGISGPDNGAVAVLKYNG	18
	NA. 50	GPDNGAVAVLKYNGIITD	18
	NA. 51	GAVAVLKYNGIITDTIKS	18
Pool 7	NA. 52	VLKYNGIITDTIKSWRNN	18
	NA. 53	NGIITDTIKSWRNNILRT	18
	NA. 54	TDTIKSWRNNILRTQESE	18
	NA. 55	KSWRNNILRTQESECACV	18
	NA. 56	NNILRTQESECACVNGSC	18
	NA. 57	RTQESECACVNGSCFTVM	18
	NA. 58	SECACVNGSCFTVMTDGP	18
	NA. 59	CVNGSCFTVMTDGPSDGQ	18

Pool	Denomination	Sequence	Length
	NA. 60	SCFTVMTDGPSDGQASYK	18
Pool 8	NA. 61	VMTDGPSDGQASYKIFRI	18
	NA. 62	GPSDGQASYKIFRIEKGK	18
	NA. 63	GQASYKIFRIEKGKIVKS	18
	NA. 64	YKIFRIEKGKIVKSVEMN	18
	NA. 65	RIEKGKIVKSVEMNAPNY	18
	NA. 66	GKIVKSVEMNAPNYHYEE	18
	NA. 67	KSVEMNAPNYHYEECSCY	18
	NA. 68	MNAPNYHYEECSCYPDSS	18
	NA. 69	NYHYEECSCYPDSSEITC	18
Pool 9	NA. 70	EECSCYPDSSEITCVCRD	18
	NA. 71	CYPDSSEITCVCRDNWHG	18
	NA. 72	SSEITCVCRDNWHGSNRP	18
	NA. 73	TCVCRDNWHGSNRPWVSF	18
	NA. 74	RDNWHGSNRPWVSFNQNL	18
	NA. 75	HGSNRPWVSFNQNLEYQI	18
	NA. 76	RPWVSFNQNLEYQIGYIC	18
	NA. 77	SFNQNLEYQIGYICSGIF	18
	NA. 78	NLEYQIGYICSGIFGDNP	18
Pool 10	NA. 79	QIGYICSGIFGDNPRPND	18
	NA. 80	ICSGIFGDNPRPNDKTGS	18
	NA. 81	IFGDNPRPNDKTGSCGPV	18
	NA. 82	NPRPNDKTGSCGPVSSNG	18
	NA. 83	NDKTGSCGPVSSNGANGV	18
	NA. 84	GSCGPVSSNGANGVKGFS	18
	NA. 85	PVSSNGANGVKGFSFKYG	18
	NA. 86	NGANGVKGFSFKYGNGVW	18
	NA. 87	GVKGFSFKYGNGVWIGRT	18
Pool 11	NA. 88	FSFKYGNGVWIGRTKSIS	18
	NA. 89	YGNGVWIGRTKSISSRNG	18
	NA. 90	VWIGRTKSISSRNGFEMI	18
	NA. 91	RTKSISSRNGFEMIWDPN	18
	NA. 92	ISSRNGFEMIWDPNGWTG	18
	NA. 93	NGFEMIWDPNGWTGTDNN	18
	NA. 94	MIWDPNGWTGTDNNFSIK	18
	NA. 95	PNGWTGTDNNFSIKQDII	18
	NA. 96	TGTDNNFSIKQDIIGINE	18
Pool 12	NA. 97	NNFSIKQDIIGINEWSGY	18
	NA. 98	IKQDIIGINEWSGYSGSF	18
	NA. 99	IIGINEWSGYSGSFVQHP	18
	NA. 100	NEWSGYSGSFVQHPELTG	18
	NA. 101	GYSGSFVQHPELTGLDCI	18
	NA. 102	SFVQHPELTGLDCIRPCF	18

Pool	Denomination	Sequence	Length
	NA. 103	HPELTGLDCIRPCFWVEL	18
	NA. 104	TGLDCIRPCFWVELIRGR	18
	NA. 105	CIRPCFWVELIRGRPKEN	18
Pool 13	NA. 106	CFWVELIRGRPKENTIWT	18
	NA. 107	ELIRGRPKENTIWTSGSS	18
	NA. 108	GRPKENTIWTSGSSISFC	18
	NA. 109	ENTIWTSGSSISFCGVNS	18
	NA. 110	WTSGSSISFCGVNSDTVG	18
	NA. 111	SSISFCGVNSDTVGWSWP	18
	NA. 112	FCGVNSDTVGWSWPDGAE	18
	NA. 113	NSDTVGWSWPDGAELPFT	18
	NA. 114	VGWSWPDGAELPFTIDK	17

7.2 TCR sequencing TRAV chain rearrangements 5-OP-RU MR1 tetramer+ T cells

Table 7.5 Top 50 TCR rearrangements Cow 1

clone count	% of clones	V gene hit with best score	aaSeqCDR3	J gene hit with best score
27683	40.15113058	TRAV1a	CVVMDGNYQWIW	TRAJ33
14858	21.54988614	TRAV1a	CVVIDGNYQWIW	TRAJ33
790	1.145807649	TRAV12f	CVVSAGGGNRLIF	TRAJ45
673	0.976112086	TRAV29b	CAASWSAGNYKYVF	TRAJ40
460	0.667179138	TRAVXaa	CALSDWGGGNKLIF	TRAJ10
426	0.617865897	TRAV2b	CALTQDYKYVF	TRAJ40
277	0.401757872	TRAVXq	CALWMA_YQWIW	TRAJ33
275	0.398857093	TRAV8l	CAL*Q_DKLIF	TRAJ34
258	0.374200473	TRAV14e	CALTP_RFYF	TRAJ21
251	0.364047747	TRAV9k	CALWGVF	TRAJ15
244	0.353895021	TRAV1a	CVVINAGYALHF	TRAJ41
243	0.352444631	TRAVYa	CVVDNKYRGSSLGRFYF	TRAJ18
242	0.350994242	TRAV22p	CAVGRPQSGGANQLVF	TRAJ36
232	0.336490348	TRAV1a	CVVLHKLMF	TRAJ50
225	0.326337622	TRAV28a	CAVEIWQ_AGQKLVF	TRAJ54
222	0.321986453	TRAV22o	CAVRLIR_TDKLNF	TRAJ3
214	0.310383338	TRAV2b	CALTR_GKLIF	TRAJ23
208	0.301681001	TRAV1a	CVVNNAGNMFTF	TRAJ39

clone count	% of clones	V gene hit with best score	aaSeqCDR3	J gene hit with best score
203	0.294429054	TRAV2f	CAPTKASSGWQLTF	TRAJ22
195	0.282825939	TRAV1a	CVVIDGNYKYVF	TRAJ40
193	0.27992516	TRAV22t	CAVEYGGAANQLIF	TRAJ32
185	0.268322044	TRAV26b	RILILE_FKFVF	TRAJ9
179	0.259619708	TRAV22h	CAANNNAGNMFTF	TRAJ39
177	0.256718929	TRAVYd	CVVEEGTNRFYF	TRAJ21
173	0.250917371	TRAV4a	CIVRDSGNTGRLTF	TRAJ37
170	0.246566203	TRAV1a	CVDNNNNNLRF	TRAJ43
169	0.245115814	TRAV3b	CAVKDN*_GWGKLNF	TRAJ24
164	0.237863866	TRAVXz	CALSFL*_SGWQLTF	TRAJ22
163	0.236413477	TRAV22aa	CAVLE_FKFVF	TRAJ9
160	0.232062309	TRAV22l	CAVRGSSLGRFYF	TRAJ18
153	0.221909583	TRAV38a	CAYSGSGDRLTF	TRAJ46
150	0.217558414	TRAV14c	CALNVYQGGNALVF	TRAJ15
149	0.216108025	TRAV38b	CA*G*V_GQKLVF	TRAJ54
147	0.213207246	TRAV38d	CAYSGVG_GSYQLTF	TRAJ28
146	0.211756857	TRAV38b	CAYSPYGGAANQLIF	TRAJ32
144	0.208856078	TRAVXk	CALSAR_SRTLTF	TRAJ5
136	0.197252962	TRAV25p	CAGLTA_GKLNF	TRAJ24
133	0.192901794	TRAV38b	CAPEGQGFSIVF	TRAJ25
132	0.191451405	TRAV22o	CASTDGWGKLNF	TRAJ24
129	0.187100236	TRAV13b	GTDNTRIFF	TRAJ31
127	0.184199458	TRAV3e	CAVMDWGGGNKLIF	TRAJ10
126	0.182749068	TRAV38a	CAYSGGGAGQKLVF	TRAJ54
125	0.181298679	TRAV38c	CAYSGPNPNYKLTF	TRAJ20
124	0.179848289	TRAV2b	CALSGSSGWQLTF	TRAJ22
123	0.1783979	TRAV9g	CALMYSK_NYKLTF	TRAJ20
121	0.175497121	TRAV22t	CAVQLT_WGKLNF	TRAJ24
119	0.172596342	TRAV26aj	CVLRGTNAGYALHF	TRAJ41
117	0.169695563	TRAV19a	CAHRGSSLGRFYF	TRAJ18
Clone sum				
68947				

Table 7.6 Top 50 TCR rearrangements Cow 2.

clone count	% of clones	V gene hit with best score	aaSeqCDR3	J gene hit with best score
19794	57.6	TRAV1a	CVVMDGNYQWIW	TRAJ33
6212	18.1	TRAV1a	CVVIDGNYQWIW	TRAJ33
1202	3.5	TRAV21d	CAVRL_ALHF	TRAJ41
963	2.8	TRAV1a	CVDNNNNNLRF	TRAJ43
640	1.9	TRAV14e	CALREPRSSGVYNKLTF	TRAJ4

clone count	% of clones	V gene hit with best score	aaSeqCDR3	J gene hit with best score
431	1.3	TRAV38b	CAFNTNRFYF	TRAJ21
365	1.1	TRAV2d	VL*GGGAANQLIF	TRAJ32
358	1.0	TRAV22n	CAVQLNNYKLTF	TRAJ20
327	1.0	TRAV22n	CAVPGR_NALVF	TRAJ15
283	0.8	TRAV27a	CAG*PG_GKLIF	TRAJ23
236	0.7	TRDV1ah	CTLSIGE_GNKLIF	TRAJ10
192	0.6	TRAVXab	CALNQV_QKLVF	TRAJ16
176	0.5	TRAV25u	CTEHQ_RFYF	TRAJ21
150	0.4	TRAV3d	CAVSEH_NRFYF	TRAJ21
145	0.4	TRAV12f	CAVFKW_QKLVF	TRAJ16
141	0.4	TRAVYc	CAVEAGR_GNKLIF	TRAJ10
140	0.4	TRAVXp	CALSDAYYNQGGKLIF	TRAJ23
138	0.4	TRAV12b	CAVSYQ_RDKLIF	TRAJ34
132	0.4	TRAVXn	CALSDR_RFKFVF	TRAJ9
122	0.4	TRAV22q	CAVGHR_TGKLTF	TRAJ27
110	0.3	TRAV9g	CVLRASL*_QGGKLIF	TRAJ23
98	0.3	TRAVYa	CVVGYRR_AIGKLTF	TRAJ2
98	0.3	TRAV1a	CVVTPV_GKLTF	TRAJ27
95	0.3	TRAV12b	CAVSPL*_SGWQLTF	TRAJ22
94	0.3	TRAV22h	CAVQH_NRFYF	TRAJ21
87	0.3	TRDV1as	CVLRA*_TNRFYF	TRAJ21
84	0.2	TRAVXp	CALSDLYYNQGGKLIF	TRAJ23
84	0.2	TRAV29b	CAGCLLV_YNKLTF	TRAJ4
81	0.2	TRAV22h	CAVLPGTGSYQLTF	TRAJ28
78	0.2	TRAV25k	CAEA*RER_SSLGRFYF	TRAJ18
76	0.2	TRAV13b	CAASIWC_YNKLTF	TRAJ4
73	0.2	TRAVYd	CVEHRY_GKLTF	TRAJ27
70	0.2	TRAVYg	CAVRTLNNYKLTF	TRAJ20
65	0.2	TRAVXw	CALIYW_GFKFVF	TRAJ9
63	0.2	TRAV1a	CVVLDGNYQWIW	TRAJ33
57	0.2	TRAV13j	CAAL*IQ_YNTLTF	TRAJ11
57	0.2	TRAV8f	CAPRPL_NVLHL	TRAJ35
56	0.2	TRAV4b	CIVGLGSRTLTF	TRAJ5
53	0.2	TRAV25u	CTGQGGNALVF	TRAJ15
47	0.1	TRAV26ah	CVPTQE_TGRLTF	TRAJ37
41	0.1	TRAV14c	CALNEPAP_GAIGKLTF	TRAJ2
40	0.1	TRAV21d	CAGRL_ALHF	TRAJ41
39	0.1	TRAV16a	CALGQH_NRFYF	TRAJ21
39	0.1	TRAV20b	CAVPP_RFYF	TRAJ21
37	0.1	TRAVXz	CALSEGQGFSLVF	TRAJ25
36	0.1	TRAVXac	CALSDRSW_NNRKLIW	TRAJ38
35	0.1	TRAV1a	CVVLDGNYQWIW	TRAJ33

clone count	% of clones	V gene hit with best score	aaSeqCDR3	J gene hit with best score
33	0.1	TRAV3d	CAVSPFQ_GQKLVF	TRAJ16
Clone sum				
34336				

Table 7.7 Top 50 TCR rearrangements Cow 3.

clone count	% of clones	V gene hit with best score	aaSeqCDR3	J gene hit with best score
14038	44.1	TRAV1a	CVVMDGNYQWIW	TRAJ33
8529	26.8	TRAV1a	CVVIDGNYQWIW	TRAJ33
1124	3.5	TRAV1a	CVVMDGNYQWIW	TRAJ33
1102	3.5	TRAV1a	CVAQDGNYQWIW	TRAJ33
927	2.9	TRAV26am	CILRDGEGQGFSIVF	TRAJ25
742	2.3	TRAV16a	CALVRSTDNSRIFF	TRAJ31
482	1.5	TRAV22q	CAVQHR_SRTLTF	TRAJ5
285	0.9	TRAV9g	CALIQEE_IGKLTF	TRAJ2
264	0.8	TRAV22x	CAVQESYR_GAIGKLTF	TRAJ2
225	0.7	TRAV13f	CAAKVGL_GNVLHL	TRAJ35
217	0.7	TRAV1a	CVAVDGNYQWIW	TRAJ33
162	0.5	TRAVXe	CALRDLQ_RDKLIF	TRAJ34
152	0.5	TRAV17a	CAPVDQGGNALVF	TRAJ15
137	0.4	TRAV1a	CVVLDGNYQWIW	TRAJ33
129	0.4	TRAV2a	CALSEHWGGGNKLIF	TRAJ10
121	0.4	TRAV1a	CVVIDGNYQWIW	TRAJ33
115	0.4	TRAV22t	CAVQLTP_TGKLTF	TRAJ27
111	0.3	TRAV25b	CAPQ*C_GNMFTF	TRAJ39
105	0.3	TRAV2b	CALR*WGGGNKLIF	TRAJ10
100	0.3	TRAV18h	CALIPGE_GNKLIF	TRAJ10
99	0.3	TRAV21b	CAVKGTLTF	TRAJ11
96	0.3	TRAV12f	CAVR*HR_TGKLTF	TRAJ27
95	0.3	TRAV28b	CAVDGNYQWIW	TRAJ33
90	0.3	TRAVYg	CAVEPTSGWQLTF	TRAJ22
87	0.3	TRAVXr	CALSDSGWQLTF	TRAJ22
86	0.3	TRAV22q	CAVL*V_QKLVF	TRAJ16
84	0.3	TRAV22w	CAVQLRPIGGAIGKLTF	TRAJ2
82	0.3	TRAV10d	CVVGE*_VYWLTF	TRAJ20
80	0.3	TRAV5b	CATGKLTF	TRAJ27
75	0.2	TRAVYa	CVVEA*P_GGKLIF	TRAJ23
74	0.2	TRAV25b	CAGEVAL_NTRIFF	TRAJ31
72	0.2	TRAV26u	CVLREDNTGTGKLTF	TRAJ27

clone count	% of clones	V gene hit with best score	aaSeqCDR3	J gene hit with best score
72	0.2	TRAVXp	CALPEIR_TDKLNF	TRAJ3
72	0.2	TRAV1a	CVVRDGNYQWIW	TRAJ33
70	0.2	TRAV26u	CVLREASGTGSYQLTF	TRAJ28
66	0.2	TRAVYa	CVVEAGL_NSRIFF	TRAJ31
63	0.2	TRAV1a	CVVNDGNYQWIW	TRAJ33
63	0.2	TRDV1aj	CALEKGGKLIF	TRAJ23
62	0.2	TRAV2f	CALMGT_GRLTF	TRAJ37
62	0.2	TRAV26u	CVPDRQ_RTLTF	TRAJ5
61	0.2	TRAV26ai	CVLREASLDSGYNTLTF	TRAJ11
60	0.2	TRAV26u	CVLIIGRF_SGQKLVF	TRAJ16
57	0.2	TRAV18h	CALSDGE_GNKLIF	TRAJ10
52	0.2	TRAV1a	CVVIEGNYQWIW	TRAJ33
50	0.2	TRAV17a	CAPDTTDGWGKLNF	TRAJ24
49	0.2	TRAV25v	CAEF**A_GYQKFVF	TRAJ8-1
49	0.2	TRAV26u	CVLREFR_YNTLTF	TRAJ11
47	0.1	TRAV10b	CVVVLIT_GTGKLTF	TRAJ27
Clone sum				
31828				

Table 7.8 Top 50 TCR rearrangements Cow 4.

clone count	% of clones	V gene hit with best score	aaSeqCDR3	J gene hit with best score
20519	43.8	TRAV1a	CVVMDGNYQWIW	TRAJ33
9887	21.1	TRAV1a	CVVIDGNYQWIW	TRAJ33
684	1.5	TRAV22b	CAVQLQGLFSNRDKLIF	TRAJ34
664	1.4	TRAV22n	RIQH_PTF	TRAJ11
559	1.2	TRAV3b	CAGWDW_SYQLTF	TRAJ28
507	1.1	TRAV1a	CVVIEGNYQWIW	TRAJ33
504	1.1	TRAV38b	CA*WVI_GWQLTF	TRAJ22
490	1.0	TRAV1a	CVLTSGANQLVF	TRAJ36
339	0.7	TRAV2g	CAQTSGANQLVF	TRAJ36
305	0.7	TRAVXb	CALSLL*_NYKLTF	TRAJ20
247	0.5	TRAV22o	CAVQLDGGGFKFVF	TRAJ9
237	0.5	TRAV2b	CAPGLT_SRIFF	TRAJ31
222	0.5	TRAV38a	CAYSEV_QKLVF	TRAJ16
202	0.4	TRAV1a	CVISNRDKLIF	TRAJ34
183	0.4	TRAV22w	CAVQLDRD_GSYQLTF	TRAJ28
182	0.4	TRAV26ai	CVLREAGMTTDGWGKLNF	TRAJ24
180	0.4	TRAV26ah	CVLGLPGTGSYQLTF	TRAJ28

clone count	% of clones	V gene hit with best score	aaSeqCDR3	J gene hit with best score
164	0.4	TRAV26ah	CVPRAYSGTGSYQLTF	TRAJ28
163	0.3	TRAV1a	CVVVNGNYQWIW	TRAJ33
160	0.3	TRAV22x	CASRMGV_ANQLIF	TRAJ32
146	0.3	TRAV22d	CAVQL_YKLTF	TRAJ20
138	0.3	TRAV12f	CAVSFK_GQKLVF	TRAJ16
138	0.3	TRAV1a	CVVTNGNYQWIW	TRAJ33
137	0.3	TRAVXp	CALGGPGAIGKLTF	TRAJ2
136	0.3	TRAV1a	CVVIDGNYKYVF	TRAJ40
135	0.3	TRAV29b	CAATSGGNYQWIW	TRAJ33
132	0.3	TRAV20e	CAVQTEH_GYQKFVF	TRAJ8-1
124	0.3	TRAVXaa	CASFSSGQKLVF	TRAJ16
123	0.3	TRAV25v	CAEKTARR_SSLGRFYF	TRAJ18
120	0.3	TRAV18b	CALSGASGVYNKLTF	TRAJ4
117	0.3	TRAV1a	CVVSDGNYQWIW	TRAJ33
116	0.2	TRAVXk	CALPLLMNTGSRTLTF	TRAJ5
115	0.2	TRAV9g	CALRRT_NRFYF	TRAJ21
112	0.2	TRAVXb	CALISGQKLVF	TRAJ16
111	0.2	TRAV25u	CTA_RI	TRAJ20
102	0.2	TRAVYd	CVHSWGENYKYVF	TRAJ40
102	0.2	TRAV25v	CAEASY_TNRFYF	TRAJ21
99	0.2	TRAV38b	CAYSVPWWW_SAYGKLMF	TRAJ52
99	0.2	TRAV22h	CAVLDGNYQWIW	TRAJ33
99	0.2	TRAV14e	CALTA_GKLNF	TRAJ24
98	0.2	TRAV22n	CAVPRHR_SRTLTF	TRAJ5
98	0.2	TRAV10b	CVVQNSGYNTPTF	TRAJ11
97	0.2	TRAVXg	CALSDRQGGSERLLF	TRAJ57
97	0.2	TRAV22ab	CAVQLDTGRLTF	TRAJ37
97	0.2	TRAV22o	CAVQL_ENLRF	TRAJ43
95	0.2	TRAV27a	CAGEE_YKYVF	TRAJ40
93	0.2	TRAV12c	CAVTQGGSERLLF	TRAJ57
92	0.2	TRAV10b	CVVGASYNQGGKLIF	TRAJ23

Clone sum	
46797	